# CHEMISTRY AND PHYSIOLOGY OF FEEDING DETERRENT PRODUCTION BY THE MARINE DIATOM PHAEODACTYLUM TRICORNUTUM

by

# BARBARA ANN SHAW

B.Sc., The University of British Columbia, 1988

A THESIS SUBMITTED IN PARTIAL FULFILLMENT OF

THE REQUIREMENTS FOR THE DEGREE OF

DOCTOR OF PHILOSOPHY

in

THE FACULTY OF GRADUATE STUDIES

Department of Oceanography

We accept this thesis as conforming to the required standard

# THE UNIVERSITY OF BRITISH COLUMBIA

March 1994

© Barbara Ann Shaw, 1994

In presenting this thesis in partial fulfilment of the requirements for an advanced degree at the University of British Columbia, I agree that the Library shall make it freely available for reference and study. I further agree that permission for extensive copying of this thesis for scholarly purposes may be granted by the head of my department or by his or her representatives. It is understood that copying or publication of this thesis for financial gain shall not be allowed without my written permission.

(Signature)

Department of Occanography

The University of British Columbia Vancouver, Canada

Date <u>April 5 /94</u>

#### **Abstract**

It has been proposed that some marine phytoplankton use chemical feeding deterrents to reduce or inhibit zooplankton grazing. While a number of studies have shown that certain phytoplankton reduce zooplankton feeding, few studies have dealt with both the chemistry (isolation and identification) and the physiology of production of feeding deterrents.

A bioassay to detect feeding deterrents was developed. This bioassay measured the rate of fecal pellet production of the harpacticoid copepod *Tigriopus californicus* when fed a diet of the diatom *Thalassiosira pseudonana* in the presence of dissolved feeding deterrents. Using this bioassay, the cellular extracts of several species of phytoplankton were screened. The diatom *Phaeodactylum tricornutum* and the dinoflagellate *Gonyaulax grindleyi* were found to deter feeding.

Bioassay-guided chemical fractionation was used to isolate the compounds responsible for the feeding deterrent activity of *Phaeodactylum tricornutum*. Spectroscopic techniques identified four of these compounds as apo-10'-fucoxanthinal, apo-12'-fucoxanthinal, and apo-13'-fucoxanthinone. The IC<sub>50</sub> (concentration of compound at which feeding was inhibited by 50%) values ranged from 1.8 to 20 ppm, while the LC<sub>50</sub> (concentration of compound at which there was a 50% mortality rate in the test population) ranged between 37 and 340 ppm.

Preliminary studies on the physiology of production of these feeding deterrents were performed. In order to carry out these studies, an analytical HPLC method was developed to measure the apo-fucoxanthinoid concentrations in crude cell extracts. Detailed analysis of HPLC data collected on *Phaeodactylum tricornutum* cell extracts identified another potential feeding deterrent compound, apo-10-fucoxanthinal.

Production of apo-fucoxanthinoids during the growth cycle of *Phaeodactylum* tricornutum and *Thalassiosira pseudonana* was tracked using HPLC and quantitative

bioassays. Although apo-fucoxanthinoids were produced enzymatically from fucoxanthin by both diatoms, *P. tricornutum* produced much greater amounts of these compounds than *T. pseudonana*. Thus the degree of production appears to be speciesspecific. The production of total intracellular apo-fucoxanthinoids increased with the culture age and the degree of phosphate limitation experienced by the culture. The concentration of total intracellular apo-fucoxanthinoids in *P. tricornutum* was calculated to be 1000 times higher than the amount required to produce a 50% inhibition of fecal pellet production in the copepod *Tigriopus californicus*.

# **Table of Contents**

Abstract ii
Table of Contentsiv
List of Tables
List of Figures xiv
Acknowledgments
Dedicationxxiv
Chapter 1: General Introduction  i. Antibiotic, Antifungal, and Cytotoxic Compounds  ii. Toxins  Paralytic Shellfish Poisoning (PSP)  Diarrhetic Shellfish Poisoning (DSP)  Amnesic Shellfish Poisoning (ASP)  Ciguatera  Brevetoxin  Other Toxins from Marine Phytoplankton  Cyanobacterial Toxins  iii. Allelopathic Compounds  iv. Bacterial Attractants  11  v. Feeding Deterrents  12  Feeding Deterrent Effects on Copepods  12  Feeding Deterrent Effects on Other Zooplankton  15  vi. Thesis Objectives  18
Chapter 2: Evaluation of the Copepod Tigriopus californicus as a Bioassay Organism for the Detection of Chemical Feeding Deterrents Produced by Marine Phytoplankton
28

C. Results and Discussion	28
i. Phytoplankton Cultures	28
ii. Egestion Rate Experiments	
iii. Bioassay Method Using Feeding Deterrents Adsorbed onto Gi Fish Food	round
iv. Bioassay Method Using Dissolved Feeding Deterrents	
v. Bioassay Method Using Feeding Deterrents Produced by Live	Cells
D. General Discussion and Conclusions	
Chapter 3: Isolation and Structure Determination of Chemical Feeding Deterren	
the Diatom Phaeodactylum tricornutum	
A. Introduction	
i. Chromatographic Techniques	
Column Chromatography	
Detection Methods	47
ii. Spectroscopic Techniques	
Ultraviolet-Visible Spectroscopy (UV-vis)	49
Infrared Spectroscopy (IR)	52
Nuclear Magnetic Resonance Spectroscopy (nmr)	54
Mass Spectrometry	60
B. Materials and Methods	63
i. Phytoplankton Cultures	63
ii. Chromatography	63
iii. Feeding Deterrent Bioassays for Bioassay-guided Chemical	
Fractionation	65
iv. Semi-synthetic Procedure	65
v. Spectroscopy	66
C. Results and Discussion	66
i. Chromatography	66
ii. Spectroscopy	70
Natural Compounds	70
Semi-synthetic Compounds	72
a) Apo-10'-fucoxanthinal (1)	
b) Apo-12'-fucoxanthinal (2)	91
c) Apo-12-fucoxanthinal (3)	97
d) Apo-13'-fucoxanthinone (4)	106
iii. Bioassay Results for Semi-synthetic Compounds	
D. General Discussion and Conclusions	
Chapter 4: Observations on Lethal and Sub-lethal Effects of Apo-fucoxanthinoid	
the Copepod Tigriopus californicus	
A. Introduction	
B. Materials and Methods	119

C. Results and Discussion	120
i. Fecal Pellet Volume	120
ii. Fecal Pellet Count	121
iii. Total Fecal Pellet Volume	124
iv. Lethal Concentrations	127
D. General Discussion and Conclusions	129
Chapter 5: Development of an High Performance Liquid Chromatography Tech	inique
for Quantitative Analyses of Apo-fucoxanthinoids	
A. Introduction	
B. Materials and Methods	133
i. Sample Preparation	
ii. HPLC Method	
C. Results and Discussion	135
i. Standards	135
ii. Analysis of Crude Cellular Extract from Phaeodactylum tricon	rnutum
***************************************	141
D. General Discussion and Conclusions	142
Detecting Apo-fucoxanthinoid Feeding Deterrents - A Preliminary Study Biotic and Abiotic Apo-fucoxanthinoid Production	144
A. Introduction	
B. Materials and Methods	
i. Phytoplankton Cultures	
ii. Bioassay Procedure	
iii. HPLC Analysis	
iv. Fucoxanthin Incubation Experiment	
C. Results and Discussion	
i. Phytoplankton Cultures	
ii. Comparison of Quantitative Bioassays and HPLC Analysis	
iii. Quantitative Feeding Deterrent Bioassays	
iv. HPLC Analysis of Intracellular Apo-fucoxanthinoids	
v. HPLC Analysis of Extracellular Apo-fucoxanthinoids	
v. Fucoxanthin Incubation Experiment	
D. General Discussion and Conclusions	165
Chapter 7: General Discussion, Conclusions, and Future Directions	
A. Conclusions	
B. General Discussion	
i. Ecological Implications	
ii. Commercial Applications	
C. Future Research Questions	172

Literature Cited.	174
Appendix A. A Model Demonstrating the Use of Total Fecal Production as a Measur of Fecal Pellet Production Rate	
Appendix B. Growth of Phytoplankton Cultures	189
Appendix C. Raw Data and Statistical Analysis for Feeding Deterrent Bioassays in Chapter 2	190
Appendix D. Fecal Pellet Volume Measurements	202
Appendix E. Spectroscopic Data for Apo-fucoxanthinoids	203
Appendix F. Raw Data for Calculation of IC50 and LC50 Values in Chapter 42	229
Appendix G. PROBIT Method for Calculating IC50 and LC50 Values	235
Appendix H. Growth of Phytoplankton Cultures2	238
Appendix I. Calculation of Cell Volumes	241
Appendix J. Results from Feeding Deterrent Bioassays of Samples from a <i>Thalassios pseudonana</i> Culture (#1) and Two <i>Phaeodactylum tricornutum</i> Cultures (#2 at #3)	nd
Appendix K. Results from the HPLC Analysis of Samples from a <i>Thalassiosira</i> pseudonana Culture (#1) and Two Phaeodactylum tricornutum Cultures (#2 at #3)	
Appendix L. Comparison of the Results of the Quantitative Bioassays and the HPLC Method for Detecting Feeding Deterrents	
Appendix M. Fucoxanthin Incubation Experiments	256

# **List of Tables**

Table 1. Feeding of <i>Tigriopus californicus</i> on fluorescently stained <i>Thalassiosira</i> pseudonana cells. Copepods treated with antibiotics prior to experiment.  Observations made on copepods preserved in formalin
Table 2. Desorption chemical ionization mass spectrometry data for the four feeding deterrent compounds. Note that the molecular ion is [M+H] <sup>+</sup> for DCI-MS. An high resolution DCI-MS was not obtained for compound (3) as the sample decomposed before the spectrum could be taken. This is not surprising, as Bonnett <i>et al.</i> (1969) reported this compound as unstable.
Table 3. Comparison of proton nmr shifts (in ppm relative to internal TMS) for four feeding deterrent compounds with literature values from Bonnett et al. (1969). Peak multiplicity abbreviations: s = singlet; d = doublet; dd = doublet of doublets; m = multiplet
<b>Table 4.</b> Chemical shifts and coupling constants for the four semi-synthetic apofucoxanthinoids. Peak multiplicity abbreviations: s = singlet; d = doublet; dd = doublet of doublets; m = multiplet
Table 5. Comparison of UV-vis data for the four semi-synthetic compounds with literature values from Bonnett et al. (1969). Note that UV-vis spectra for this research were not run in CHCl <sub>3</sub> as several of the semi-synthetic compounds decomposed in this solvent.
Table 6. Comparison of IR data for the four semi-synthetic compounds with literature values from Bonnett et al. (1969)
<b>Table 7.</b> Comparison of proton chemical shifts of the all trans and 13-cis forms of apo-12-fucoxanthinal and $\beta$ -apo-12'-carotenal (Vetter <i>et al.</i> , 1971)104
<b>Table 8.</b> Constants for the equation $F = F_m * e^{-kc^a}$ when fitted to the data sets for each of the four apo-fucoxanthinoid compounds
Table 9. IC <sub>50</sub> values and standard deviations calculated from the fecal pellet production rate data for the four apo-fucoxanthinoids using the PROBIT method. a, b = calculated parameters from the PROBIT method (Appendix G); r <sup>2</sup> = coefficient of determination (a measure of how well the data fits the PROBIT line).
<b>Table 10.</b> Constants for the equation $F = F_m * e^{-kc^a}$ when fitted to the data sets for each of the four apo-fucoxanthinoid compounds

Table	11. IC <sub>50</sub> values and standard deviations calculated from the fecal volume production rate data for the four apo-fucoxanthinoids using the PROBIT method. a, b = calculated parameters from the PROBIT method (Appendix G); r <sup>2</sup> = coefficient of determination (a measure of how well the data fits the PROBIT line)
Table	12. Constants for the equation $S = 100 * e^{-kc^a}$ when fitted to the data sets for the two apo-fucoxanthinoid compounds tested for lethal effects
Table	13. LC <sub>50</sub> values and standard deviations calculated for apo-10'-fucoxanthinal and apo-12'-fucoxanthinal using the PROBIT method. a, b = calculated parameters from the PROBIT method (Appendix G); r2 = coefficient of determination (a measure of how well the data fits the PROBIT line)129
Table	14. Program for the HPLC solvent system gradient used for quantifying apofucoxanthinoids
Table	15. Data on apo-fucoxanthinoid standards for quantitative HPLC assays. V = volts; s = seconds; V s = volt seconds = peak area as given by the photo-diode array detector
Table	16. Comparison of HPLC data from apo-fucoxanthinoids in a crude cellular extract from <i>Phaeodactylum tricornutum</i> with HPLC data from standards142
Table	<b>B1.</b> Growth of <i>Phaeodactylum tricornutum</i> , <i>Thalassiosira pseudonana</i> , and <i>Gonyaulax grindleyi</i> cultures at 19 °C with continuous irradiance of approximately 70 μmol m <sup>-2</sup> s <sup>-1</sup>
Table	C1. Raw data for the fecal pellet production rate of <i>Tigriopus californicus</i> over two different time intervals when presented with a diet of ground fish food191
Table	C2. Statistical analysis of raw data from Table C1
Table <sup>(</sup>	C3. Raw data for the fecal pellet production rate of both untreated and antibiotic-treated <i>Tigriopus californicus</i> when presented with varying concentrations of <i>Thalassiosira pseudonana</i> cells. Each replicate consisted of two copepods incubated for 24 h
Table (	C4. Statistical analysis of raw data from Table C3

Table C5. Raw data for the egestion rate of <i>Tigriopus californicus</i> in response to treatments of copepods with antibiotics and treatments of ground fish food with cellular extracts from <i>Gonyaulax grindleyi</i> . The coated fish food was ≈ 20-23% cellular extract by weight. UU = untreated copepods fed uncoated fish food; UC = untreated copepods fed fish food coated with <i>G. grindleyi</i> cellular extract; AU = antibiotic-treated copepods fed uncoated fish food; AC = antibiotic-treated copepods fed fish food coated with <i>G. grindleyi</i> cellular extract
Table C6.    Statistical analysis of raw data from Table C5    195
Table C7. Raw data for the egestion rate of <i>Tigriopus californicus</i> in response to treatments of copepods with antibiotics and treatments of ground fish food with cellular extracts from <i>Thalassiosira pseudonana</i> . The coated fish food was ≈ 28% cellular extract by weight. UU = untreated copepods fed uncoated fish food; UC = untreated copepods fed fish food coated with <i>T. pseudonana</i> cellular extract; AU = antibiotic-treated copepods fed uncoated fish food; AC = antibiotic-treated copepods fed fish food coated with <i>T. pseudonana</i> cellular extract
Table C8. Statistical analysis of raw data from Table C7.    197
<b>Table C9.</b> Raw data for the egestion rate of <i>Tigriopus californicus</i> in response to a diet of ground fish food coated with cellular extracts from <i>Thalassiosira</i> pseudonana and <i>Phaeodactylum tricornutum</i> . The coated fish food was $\approx 20\%$ cellular extract by weight. ATP = antibiotic-treated copepods fed fish food coated with <i>T. pseudonana</i> cellular extract; APT = antibiotic-treated copepods fed fish food coated with <i>P. tricornutum</i> cellular extract
Table C10. Statistical analysis of raw data from Table C9.   198
Table C11. Raw data for the egestion rate of <i>Tigriopus californicus</i> when presented with a diet of live phytoplankton cells. ADTP = antibiotic-treated copepods fed live <i>Thalassiosira pseudonana</i> cells suspended in dissolved cellular extract from <i>T. pseudonana</i> ; ADPT = antibiotic-treated copepods fed fed live <i>T. pseudonana</i> cells suspended in dissolved cellular extract from <i>Phaeodactylum tricornutum</i> .
Table C12. Statistical analysis of raw data from Table C11

Table C13. Raw data for the egestion rate of Tigriopus californicus when presented with a diet of live phytoplankton cells. ALTP = antibiotic-treated copepods fed live Thalassiosira pseudonana cells; ALPT = antibiotic-treated copepods fed fed live Phaeodactylum tricornutum cells. The cells were presented to the copepods at a density of 6 x 10 <sup>5</sup> cells ml <sup>-1</sup> . Replicate 2 of the T. pseudonana series was anomalous (copepods were unhealthy) and was not used for data analysis
Table C14. Statistical analysis of raw data from Table C13201
Table D1. Measurements of diameter and length of fecal pellets from <i>Tigriopus</i> californicus on a diet of ground fish food. Pellet volume is calculated using the volume equation for a cylinder, $V = \pi r^2 h$ .
Table F1. Measurements of fecal pellet volume ( $10^5 \mu m^3$ ) for Tigriopus californicus feeding on Thalassiosira pseudonana in the presence of various concentrations of apo-10'-fucoxanthinal or apo-12'-fucoxanthinal
Table F2. Measurements of fecal pellet volume (10 <sup>5</sup> μm <sup>3</sup> ) for <i>Tigriopus californicus</i> feeding on <i>Thalassiosira pseudonana</i> in the presence of various concentrations of apo-12-fucoxanthinal or apo-13'-fucoxanthinane
<b>Table F3.</b> Measurement of fecal pellet production rate (pellets h <sup>-1</sup> copepod <sup>-1</sup> ) for <i>Tigriopus californicus</i> feeding on <i>Thalassiosira pseudonana</i> in the presence of various concentrations of apo-10'-fucoxanthinal or apo-12'-fucoxanthinal232
<b>Table F4.</b> Measurements of fecal pellet production rate (pellets h <sup>-1</sup> copepod <sup>-1</sup> ) for <i>Tigriopus californicus</i> feeding on <i>Thalassiosira pseudonana</i> in the presence of various concentrations of apo-12-fucoxanthinal or apo-13'-fucoxanthinone233
Table F5. Measurement of fecal volume production rate (10 <sup>5</sup> μm <sup>3</sup> h <sup>-1</sup> copepod <sup>-1</sup> ) for <i>Tigriopus californicus</i> feeding on <i>Thalassiosira pseudonana</i> in the presence of various concentrations of apo-10'-fucoxanthinal or apo-12'-fucoxanthinal233
Table F6. Measurements of fecal volume production rate ( $10^5 \mu m^3 h^{-1}$ copepod <sup>-1</sup> ) for <i>Tigriopus californicus</i> feeding on <i>Thalassiosira pseudonana</i> in the presence of various concentrations of apo-12-fucoxanthinal or apo-13'-fucoxanthinone.234
<b>Table F7.</b> Percentage of <i>Tigriopus californicus</i> which survived at the end of 24 h when feeding on <i>Thalassiosira pseudonana</i> in the presence of various concentrations of apo-10'-fucoxanthinal or apo-12'-fucoxanthinal234
Table H1. Growth of <i>Thalassiosira pseudonana</i> (culture #1) at 19°C with continuous irradiance of 224 μmol m <sup>-2</sup> s <sup>-1</sup> . Errors are ± 1 SD238

<b>Table H2.</b> Growth of <i>Phaeodactylum tricornutum</i> (culture #2) at 19°C with continuous irradiance of 224 $\mu$ mol m <sup>-2</sup> s <sup>-1</sup> . Errors are $\pm$ 1 SD.
239
<b>Table H3.</b> Growth of <i>Phaeodactylum tricornutum</i> (culture #3) at 19°C with continuous irradiance of 224 $\mu$ mol m <sup>-2</sup> s <sup>-1</sup> . Errors are $\pm$ 1 SD.
Table H4. Calculated growth constants from the data in Tables H1 - H3 for         Phaeodactylum tricornutum and Thalassiosira pseudonana.       240
Table I1. Cell dimensions for <i>Phaeodactylum tricornutum</i> and <i>Thalassiosira</i> pseudonana as measured with a microsope (n = 10). Errors shown are ± 1  SD
Table J1. Raw data from quantitative bioassays of samples from cultures #1, #2, and #3.    244
Table J2. Calculated values for the relative concentration of apo-12'-fucoxanthinal in the bioassay medium and in the intracellular fluid of the cell. The error values shown are estimates based on the variability of the bioassay results244
Table J3. Pairwise comparisons of the fecal pellet production rates for samples from cultures #1, #2, and #3. As the sample variances were significantly different, an ANOVA analysis could not be applied to the entire data set. Each pair of samples was compared using an ANOVA on the raw, untransformed data (AU), an ANOVA on the log transformed raw data (AL), or a Mann-Whitney U test (MW), depending on the normality and variances of the sample data sets. S = samples were significantly the same; D = samples were significantly different.
<b>Table J4.</b> Comparison of the average relative intracellular apo-12'-fucoxanthinal concentrations for the two <i>Phaeodactylum tricornutum</i> cultures (#2 and #3) with the control (Cc = 0) and with the <i>Thalassiosira pseudonana</i> culture (#1)247
Table K1. Raw data from analysis of culture samples for apo-fucoxanthinoids using the HPLC/PDA system
Table K2. Retention times and absorbance maxima wavelengths for compounds of interest eluting from the HPLC
Table K3. Amounts of fucoxanthin and apo-fucoxanthinoids in the volume of sample injected onto the HPLC column.       249
Table K4. Intracellular concentrations of fucoxanthin and apo-fucoxanthinoids based on the results from the HPLC analysis

Table K5. Comparison of the average intracellular concentrations of fucoxanthin and the apo-fucoxanthinoids for the two <i>Phaeodactylum tricornutum</i> cultures (#2 and #3) with the control (Cc = 0) and with the <i>Thalassiosira pseudonana</i> culture (#1).
Table K6. Amounts of fucoxanthin present in the extracellular medium, expressed as amount "leaked" per cell.       251
Table L1. Comparison of the fecal pellet production rate calculated from the HPLC results (Fp) with the fecal pellet production rate measured by the quantitative bioassay (Fb). For this comparison, $a=2.87/20.00$ (from IC <sub>50</sub> calculations, Chapter 4) and $b=0$ . At $\alpha=0.05$ and $n=6$ , $ t_{crit}(two-tailed) =2.571$ .
<b>Table L2.</b> Model used to explain underestimation of the feeding inhibition of the crude cellular extracts by the HPLC results. Optimization produced $a=11.0$ and $b=0.225$ . At $\alpha=0.05$ and $n=6$ , $ t_{crit}(two-tailed) =2.571254$
<b>Table L3.</b> Comparison of the average relative intracellular concentrations of apo-12'-fucoxanthinal for the two <i>Phaeodactylum tricornutum</i> cultures (#2 and #3) with the control ( $Cc = 0$ ) and with the <i>Thalassiosira pseudonana</i> culture (#1)255
Table M1. Changes in peak areas ( $\mu$ V s = $\mu$ Volt seconds) over time for samples from a 500 ml solution of fucoxanthin incubated in ES enriched (Harrison et al., 1980) seawater at 19°C with continuous irradiance of $\approx 224 \ \mu$ mol m <sup>-2</sup> s <sup>-1</sup> . Absorbance was measured at 446 nm. No apo-10'-fucoxanthinal, apo-12'-fucoxanthinal, apo-12-fucoxanthinal, apo-13'-fucoxanthinone, or unknown #1 was present in these samples. Peaks #1, #2, and #3 are unidentified breakdown products of fucoxanthin. Peak #5 is probably a cis-trans isomer of fucoxanthin.
Table M2. Peak areas of the fucoxanthin breakdown products measured as a percentage of the fucoxanthin peak area.
Table M3. HPLC data for five peaks observed during analysis of samples from the fucoxanthin incubation experiment

# **List of Figures**

Fig.	1.	Some examples of antibiotic, antifungal, and cytotoxic compounds isolated from phytoplankton.
Fig.	2.	Some examples of toxins isolated from marine phytoplankton6
Fig.	3.	Some examples of toxins isolated from cyanobacteria9
Fig.	4.	Feeding response, as measured by egestion rate, for untreated and antibiotic-treated <i>Tigriopus californicus</i> feeding on <i>Thalassiosira pseudonana</i>
Fig.		Feeding responses, as measured by egestion rate, of <i>Tigriopus californicus</i> to treatment of copepods with antibiotics and treatment of ground fish food with cellular extracts from three phytoplankton species. Set A: UU = untreated copepods fed uncoated fish food; UC = untreated copepods fed fish food coated with <i>Gonyaulax grindleyi</i> cellular extract; AU = antibiotic-treated copepods fed uncoated fish food; AC = antibiotic-treated copepods fed fish food coated with <i>G. grindleyi</i> cellular extract. Set B: UU = untreated copepods fed uncoated fish food; UC = untreated copepods fed fish food coated with <i>Thalassiosira pseudonana</i> cellular extract; AU = antibiotic-treated copepods fed uncoated fish food; AC = antibiotic-treated copepods fed fish food coated with <i>T. pseudonana</i> cellular extract. Set C: ATP = antibiotic-treated copepods fed fish food coated with <i>T. pseudonana</i> cellular extract; APT = antibiotic-treated copepods fed fish food coated with <i>T. pseudonana</i> cellular extract; APT = antibiotic-treated copepods fed fish food coated with <i>Phaeodactylum tricornutum</i> cellular extract. Error bars are ± 1 SD (n = 6)
	7.	Feeding responses, as measured by egestion rate, of <i>Tigriopus californicus</i> when presented with a diet of live phytoplankton cells. Set A: ADTP = antibiotic-treated copepods fed live <i>Thalassiosira pseudonana</i> cells suspended in dissolved cellular extract from <i>T. pseudonana</i> ; ADPT = antibiotic-treated copepods fed live <i>T. pseudonana</i> cells suspended in dissolved cellular extract from <i>Phaeodactylum tricornutum</i> . Set B: ALTP = antibiotic-treated copepods fed live <i>T. pseudonana</i> cells; ALPT = antibiotic-treated copepods fed live <i>P. tricornutum</i> cells. Error bars are $\pm 1$ SD (n = 6)
_		solute concentration in the mobile phase $(C_M)$ . Line A is for partition chromatography and line B is for absorption chromatography44
Fig.		An example of a chromatogram. t1, t2, and t3 are the retention times for components 1, 2, and 3 respectively

energy states and transitions from a ground state to an electronic excited state.  PE = potential energy; internuclear distance = distance between the two nuclei of the molecule; E = emitted energy; A = absorbed energy
Fig. 10. An example of a typical spectrum generated by the absorption of energy by a molecule
Fig. 11. A portion of the electromagnetic spectrum showing regions which provide important spectroscopic information about the structure of a molecule 50
Fig. 12. Molecular orbitals involved in electronic transitions in organic molecules 50
Fig. 13. Schematic representation of the electronic energy levels of molecular orbitals in organic molecules
Fig. 14. The approximate regions where various types bonds absorb (stretching vibrations only). Note that frequency is given in wavenumbers ( $\overline{\nu} = 1/\lambda$ in cm <sup>-1</sup> ).
Fig. 15. Orientations of spin states for a nucleus with I = 1/2 in a external magnetic field. E = energy of spin states; H = magnetic field of spinning nucleus; H <sub>0</sub> = applied magnetic field.
Fig. 16. A proton nmr spectrum for the compound ethyl acetate. The numbers on the structural model of ethyl acetate represent the protons at those positions in the molecule. The numbers associated with peaks in the spectrum indicate which protons are responsible for each peak. Note that protons at position 1 in the molecule produce a signal which has three lines (2 neighbors + 1 = triplet), the protons at position 2 produce a signal which has four lines (3 neighbors + 1 = quartet), and the protons at position 5 produce a signal with no splitting (0 neighbors + 1 = singlet). The areas under the signals in the spectrum have the ratio 3:2:3 for position 1 protons: position 2 protons: position 5 protons. Protons at position 5, which are in close proximity to an oxygen atom, are deshielded relative to protons at position 1, and have a chemical shift which is further downfield.
Fig. 17. A <sup>1</sup> H- <sup>1</sup> H COSY spectrum for ethyl acetate. Note the cross-peaks which indicate coupling between protons at positions 1 and 2. This coupling is represented by an arrow in the structural model of ethyl acetate. All cross peaks are reflected across the diagonal in a COSY, so that there are two cross peaks for any given coupling, and the COSY spectrum is symmetrical about the diagonal.
Fig. 18. A schematic of a simple mass spectrometer. V = voltage across accelerator plates; H = applied magnetic field

_	solvent extractions and acid-base properties of molecules. B indicates points in the scheme where bioassays were performed. (+) = feeding deterrent activity; (-) = no feeding deterrent activity
	1. Isolation scheme for feeding deterrent compounds (1) and (2). B indicates points in the scheme where bioassays were performed. (+) = feeding deterrent activity; (-) = no feeding deterrent activity
_	Isolation scheme for feeding deterrent compounds (3) and (4). B indicates points in the scheme where bioassays were performed. (+) = feeding deterrent activity; (-) = no feeding deterrent activity
Fig. 22	2. Structure and numbering scheme for the carotenoid fucoxanthin
Fig. 23	3. Structure and numbering scheme for apo-10'-fucoxanthinal (1)
_	Low resolution DCI mass spectrum of semi-synthetic apo-10'-fucoxanthinal (1) using NH <sub>3</sub> as the reagent gas
	Fragmentation pattern ( $\alpha$ -cleavage) of apo-10'-fucoxanthinal (1), explaining the peak at 197 in the DCI mass spectrum
	in C <sub>6</sub> D <sub>6</sub> . * denotes minor grease impurities
	Lexpansion of the proton nmr (500 MHz) spectrum of semi-synthetic apo-10'-fucoxanthinal (1) in C <sub>6</sub> D <sub>6</sub> showing resonances from the methyl groups. * denotes minor impurities
;	• Expansion of the proton nmr (500 MHz) spectrum of semi-synthetic apo-10'-fucoxanthinal (1) in C <sub>6</sub> D <sub>6</sub> showing protons at positions 3, 4, and 7. * denotes minor impurities
	Expansion of the proton nmr (500 MHz) spectrum of semi-synthetic apo-10'-fucoxanthinal (1) in C <sub>6</sub> D <sub>6</sub> showing the olefinic protons and the aldehyde proton. * denotes minor impurities
	• 1H-1H COSY (500 MHz) spectrum of semi-synthetic apo-10'-fucoxanthinal (1) in C <sub>6</sub> D <sub>6</sub> .
	Expansion of the <sup>1</sup> H- <sup>1</sup> H COSY (500 MHz) spectrum of semi-synthetic apo- 10'-fucoxanthinal (1) in C <sub>6</sub> D <sub>6</sub> showing couplings between ring protons and geminal methylene couplings in the chain.

Fig. 3	32. Expansion of the <sup>1</sup> H- <sup>1</sup> H COSY (500 MHz) spectrum of semi-synthetic apo- 10'-fucoxanthinal (1) in C <sub>6</sub> D <sub>6</sub> showing couplings between olefinic protons.
Fig. 3	33. Expansion of the <sup>1</sup> H- <sup>1</sup> H COSY (500 MHz) spectrum of semi-synthetic apo- 10'-fucoxanthinal (1) in C <sub>6</sub> D <sub>6</sub> showing couplings between the olefinic protons and aldehyde proton
Fig. 3	34. Expansion of the <sup>1</sup> H- <sup>1</sup> H COSY (500 MHz) spectrum of semi-synthetic apo- 10'-fucoxanthinal (1) in C <sub>6</sub> D <sub>6</sub> showing allylic couplings
Fig. 3	35. Structure and numbering scheme for apo-12'-fucoxanthinal (2)
Fig. 3	36. Low resolution DCI mass spectrum of semi-synthetic apo-12'-fucoxanthinal (2) using NH <sub>3</sub> as the reagent gas
Fig. 3	37. Fragmentation pattern ( $\alpha$ -cleavage) of apo-12'-fucoxanthinal (2), explaining the peak at 197 in the DCI mass spectrum
Fig. 3	38. Proton nmr (400 MHz) spectrum of semi-synthetic apo-12'-fucoxanthinal (2) in C <sub>6</sub> D <sub>6</sub> . * denotes impurities. 94
Fig. 3	<b>89.</b> Expansion of the proton nmr (400 MHz) spectrum of semi-synthetic apo-12'-fucoxanthinal (2) in C <sub>6</sub> D <sub>6</sub> showing resonances from the methyl groups and the aldehyde proton. * denotes impurities
Fig. 4	10. Expansion of the proton nmr (400 MHz) spectrum of semi-synthetic apo-12'-fucoxanthinal (2) in C <sub>6</sub> D <sub>6</sub> showing olefinic protons
Fig. 4	11. Structure and numbering scheme for apo-12-fucoxanthinal (3)
Fig. 4	2. Low resolution DCI mass spectrum of semi-synthetic apo-12-fucoxanthinal (3) using NH <sub>3</sub> as the reagent gas
Fig. 4	3. Fragmentation pattern of apo-12-fucoxanthinal (3), explaining the peak at 347 in the DCI mass spectrum
Fig. 4	4. Proton nmr (500 MHz) spectrum of semi-synthetic apo-12-fucoxanthinal (3) in CD <sub>2</sub> Cl <sub>2</sub> . * denotes impurities
Fig. 4	5. Expansion of the proton nmr (500 MHz) spectrum of semi-synthetic apo-12-fucoxanthinal (3) in CD <sub>2</sub> Cl <sub>2</sub> showing resonances from the methyl groups. * denotes minor impurities. Note the doubling of the methyl peaks due to the presence of the cis isomer.

Fig. 46. Expansion of the proton nmr (500 MHz) spectrum of semi-synthetic apo-12-fucoxanthinal (3) in CD <sub>2</sub> Cl <sub>2</sub> showing olefinic protons. * denotes impurities (probably cis-trans isomers of compound (3)); t = resonances from the all transcompound; c = resonances from the major mono-cis compound (probably 13 cis)	ns
Fig. 47. Expansion of the proton nmr (500 MHz) spectrum of semi-synthetic apo-12-fucoxanthinal (3) in CD <sub>2</sub> Cl <sub>2</sub> showing the aldehyde proton. * denotes impuriti (probably cis-trans isomers of compound (3)); t = resonances from the all transcompound; c = resonances from the major mono-cis compound (probably 13 cis).	ies ns
Fig. 48. Structure and numbering scheme for apo-13'-fucoxanthinone (4)	06
Fig. 49. Low resolution DCI mass spectrum of semi-synthetic apo-13'-fucoxanthinor (4) using NH <sub>3</sub> as the reagent gas	
Fig. 50. Fragmentation pattern of apo-13'-fucoxanthinone (4), explaining the peak at 255 in the DCI mass spectrum	
Fig. 51. Proton nmr (500 MHz) spectrum of semi-synthetic apo-13'-fucoxanthinone (4) in CD <sub>2</sub> Cl <sub>2</sub> . * denotes minor grease impurities	09
Fig. 52. Expansion of the proton nmr (500 MHz) spectrum of semi-synthetic apo-13 fucoxanthinone (4) in CD <sub>2</sub> Cl <sub>2</sub> showing resonances from the methyl groups.	
Fig. 53. Expansion of the proton nmr (500 MHz) spectrum of semi-synthetic apo-13 fucoxanthinone (4) in CD <sub>2</sub> Cl <sub>2</sub> showing olefinic protons	
Fig. 54. <sup>1</sup> H- <sup>1</sup> H COSY (500 MHz) spectrum of semi-synthetic apo-13'-fucoxanthinor (4) in CD <sub>2</sub> Cl <sub>2</sub> showing couplings between olefinic protons and couplings between ring protons.	
Fig. 55. <sup>1</sup> H- <sup>1</sup> H COSY (500 MHz) spectrum of semi-synthetic apo-13'-fucoxanthinor (4) in CD <sub>2</sub> Cl <sub>2</sub> showing allylic couplings	
Fig. 56. Comparison of the structures of apo-13'-fucoxanthinone (4) and grasshopper ketone (Meinwald et al., 1968).	
Fig. 57. Decrease in fecal pellet volume of the copepod <i>Tigriopus californicus</i> when given increasing amounts of the compound apo-12'-fucoxanthinal. Error bars = ± 1 SD.	

Fig. :	58. Decrease in fecal pellet production rate of the copepod <i>Tigriopus californicus</i> when given increasing amounts of the compound apo-12'-fucoxanthinal. The IC <sub>50</sub> value, as calculated by the PROBIT method, is shown
Fig. 5	59. Decrease in fecal volume production rate of the copepod <i>Tigriopus</i> californicus when given increasing amounts of the compound apo-12'-fucoxanthinal. The IC <sub>50</sub> value, as calculated by the PROBIT method, is shown.
Fig. (	50. Increased mortality of the copepod <i>Tigriopus californicus</i> when given increasing amounts of the compound apo-12'-fucoxanthinal. The LC <sub>50</sub> value, as calculated by the PROBIT method, is shown
Fig. (	51. Data generated by the HPLC/photodiode array detector system for the apo- 10'-fucoxanthinal standard. A. Contour plot. B. Chromatogram at 418 nm showing peak at 9.045 min. C. UV-vis spectrum of peak at 9.045 min136
Fig. 6	52. Data generated by the HPLC/photodiode array detector system for the apo- 12'-fucoxanthinal standard. A. Contour plot. B. Chromatogram at 393 nm showing peak at 7.710 min. C. UV-vis spectrum of peak at 7.710 min137
Fig. 6	63. Data generated by the HPLC/photodiode array detector system for the apo- 12-fucoxanthinal standard. A. Contour plot. B. Chromatogram at 407 nm showing peak at 12.970 min. C. UV-vis spectrum of peak at 12.970 min138
Fig. 6	64. Data generated by the HPLC/photodiode array detector system for the apo- 13'-fucoxanthinone standard. A. Contour plot. B. Chromatogram at 329 nm showing peak at 5.245 min. C. UV-vis spectrum of peak at 5.245 min139
Fig. 6	55. Data from HPLC/photodiode array detector for crude cellular extract from <i>Phaeodactylum tricornutum</i> . Shaded areas indicate two peaks identified as apo-13'-fucoxanthinone (at 5.240 min) and apo-12'-fucoxanthinal (at 7.307 min) respectively
Fig. 6	indicates the time at which the culture changed from logarithmic growth to senescence phase. The culture was harvested three times for analysis as shown.  M = mid-log phase; L = late log/early senescence phase; S = senescence phase.

Fig. 67. Comparison of predicted fecal pellet production rates (Fp) from HPLC analysis of samples with observed fecal pellet production rates (Fb) from the bioassay. Comparisons are shown for 3 cultures (1, 2, 3) at 3 times (M, L, S). Culture 1 was Thalassiosira pseudonana and cultures 2 and 3 were Phaeodactylum tricornutum. M = mid-log phase; L = late log/early senescence phase; S = senescence phase. Error bars are ± 1 SD (n=6) from bioassay replicates
Fig. 68. Comparison of predicted fecal pellet production rates (Fp), calculated using a model (described in Appendix L) and the results from HPLC analysis of samples, with observed fecal pellet production rates (Fb) from the bioassay. Comparisons are shown for 3 cultures (1, 2, 3) at 3 times (M, L, S). Culture 1 was Thalassiosira pseudonana and cultures 2 and 3 were Phaeodactylum tricornutum. M = mid-log phase; L = late log/early senescence phase; S = senescence phase. Error bars are ± 1 SD (n=6) from bioassay replicates156
Fig. 69. Comparison of the average relative intracellular apo-12'-fucoxanthinal concentrations from <i>Phaeodactylum tricornutum</i> and <i>Thalassiosira pseudonana</i> . Error bars are $\pm$ 1 SD. No error bars are shown on data from the <i>T. pseudonana</i> culture as it was not replicated.
Fig. 70. Comparison of the average relative intracellular apo-12'-fucoxanthinal concentrations for the two <i>Phaeodactylum tricornutum</i> cultures. Error bars are estimated from the relative error in the bioassays as there was no replication of these samples.
Fig. 71. Comparison of the average intracellular concentrations of fucoxanthin, apo-10-fucoxanthinal, apo-12'-fucoxanthinal, and apo-13'-fucoxanthinone from <i>Phaeodactylum tricornutum</i> (filled circles) and <i>Thalassiosira pseudonana</i> (open circles). Error bars are ± 1 SD. No error bars are shown on data from the <i>T. pseudonana</i> culture as it was not replicated
Fig. 72. Comparison of the average relative intracellular apo-12'-fucoxanthinal concentration from <i>Phaeodactylum tricornutum</i> (filled circles) and <i>Thalassiosira pseudonana</i> (open circles). Error bars are $\pm$ 1 SD. No error bars are shown on data from the <i>T. pseudonana</i> culture as it was not replicated
Fig. 73. Degradation of fucoxanthin incubated in seawater at 19°C with continuous irradiance of $\approx 224 \ \mu \text{mol m}^{-2} \text{ s}^{-1}$ .

Fig.	A1. Model for fecal pellet production rate. For simplicity, $F_{max}$ and the total elapsed time are both equal to 1 unit. Graph A represents the control (no feeding deterrent), with $b=5$ (from equation for total number of fecal pellets). Graph B represents the affect of a feeding deterrent, with $b=1$ . The area under the curve, from $t_1=0$ to $t_2=1$ (vertical line), is the total number of fecal pellets. The average fecal pellet production rate over this time interval is shown by the horizontal dotted line.
Fig.	E1. Low resolution DCI mass spectrum of natural apo-10'-fucoxanthinal (1) using NH <sub>3</sub> as the reagent gas
Fig.	E2. Low resolution DCI mass spectrum of natural apo-12'-fucoxanthinal (2) using NH <sub>3</sub> as the reagent gas
Fig.	E3. Low resolution DCI mass spectrum of natural apo-12-fucoxanthinal (3) using NH <sub>3</sub> as the reagent gas
Fig.	E4. Low resolution DCI mass spectrum of natural apo-13'-fucoxanthinone (4) using NH <sub>3</sub> as the reagent gas
Fig.	E5. Proton nmr (500 MHz) spectrum of natural apo-10'-fucoxanthinal (1) in C <sub>6</sub> D <sub>6</sub> . * denotes impurities, probably grease or fatty acids
Fig.	E6. Expansion of the proton nmr (500 MHz) spectrum of natural apo-10'-fucoxanthinal (1) in C <sub>6</sub> D <sub>6</sub> showing resonances from the methyl groups. * denotes impurities, probably grease or fatty acids
Fig.	E7. Expansion of the proton nmr (500 MHz) spectrum of natural apo-10'-fucoxanthinal (1) in C <sub>6</sub> D <sub>6</sub> showing methylene protons at position 7. * denotes minor impurities.
Fig.	E8. Expansion of the proton nmr (500 MHz) spectrum of natural apo-10'-fucoxanthinal (1) in C <sub>6</sub> D <sub>6</sub> showing the olefinic protons and the aldehyde proton.
Fig.	E9. Proton nmr (500 MHz) spectrum of natural apo-12'-fucoxanthinal (2) in C <sub>6</sub> D <sub>6</sub> . * denotes impurities, probably grease or fatty acids
Fig.	E10. Expansion of the proton nmr (500 MHz) spectrum of natural apo-12'-fucoxanthinal (2) in C <sub>6</sub> D <sub>6</sub> showing resonances from the methyl groups. * denotes impurities, probably grease or fatty acids
Fig.	E11. Expansion of the proton nmr (500 MHz) spectrum of natural apo-12'- fucoxanthinal (2) in C <sub>6</sub> D <sub>6</sub> showing the methylene protons as position 7. * denotes impurities.

Fig.	fuc	Expansion of the proton nmr (500 MHz) spectrum of natural apo-12'- coxanthinal (2) in C <sub>6</sub> D <sub>6</sub> showing the olefinic protons and the aldehyde oton
Fig.		Proton nmr (500 MHz) spectrum of natural apo-12-fucoxanthinal (3) in O <sub>2</sub> Cl <sub>2</sub> . * denotes impurities, probably grease or fatty acids
Fig.	fuc	Expansion of the proton nmr (500 MHz) spectrum of natural apo-12-coxanthinal (3) in CD <sub>2</sub> Cl <sub>2</sub> showing resonances from the methyl groups. * notes minor impurities, probably grease or fatty acids
Fig.	fuc	Expansion of the proton nmr (500 MHz) spectrum of natural apo-12-coxanthinal (3) in CD <sub>2</sub> Cl <sub>2</sub> showing olefinic protons. * denotes impurities ostly cis-trans isomers of compound (3))
Fig.		Expansion of the proton nmr (500 MHz) spectrum of natural apo-12-coxanthinal (3) in CD <sub>2</sub> Cl <sub>2</sub> showing the aldehyde proton
Fig.		Proton nmr (500 MHz) spectrum of natural apo-13'-fucoxanthinone (4) in O <sub>2</sub> Cl <sub>2</sub> . * denotes impurities, probably grease or fatty acids
Fig.		Ultraviolet-visible spectrum of semi-synthetic apo-10'-fucoxanthinal (1) in thanol
Fig.		Ultraviolet-visible spectrum of semi-synthetic apo-12'-fucoxanthinal (2) in thanol
Fig.		Ultraviolet-visible spectrum of semi-synthetic apo-12-fucoxanthinal (3) in thanol
Fig.		Ultraviolet-visible spectrum of semi-synthetic apo-13'-fucoxanthinone (4) in thanol
Fig.	E22.	Infrared spectrum of semi-synthetic apo-10'-fucoxanthinal (1) (film)225
Fig.	E23.	Infrared spectrum of semi-synthetic apo-12'-fucoxanthinal (2) (film)226
Fig.	E24.	Infrared spectrum of semi-synthetic apo-12-fucoxanthinal (3) (film)227
Fig.	E25.	Infrared spectrum of semi-synthetic apo-13'-fucoxanthinone (4) (film)228

#### **Acknowledgments**

It is with greatest pleasure that I acknowledge the many people who have contributed to the research and work which has gone into this thesis. As with any interdisciplinary work, this project has been as much a group effort as the product of a single author. To my supervisors Drs. Raymond Andersen and Paul Harrison, I express my deep gratitude. Together, the three of us bridged the interdisciplinary gap between chemistry and biology, and made sense of this work. Without their support and encouragement, and their combined expertise in their fields, this project would have never gone to completion.

Throughout this work, I have had tremendous support from members of the Andersen lab and the extended "Harrison" lab. John Berges and David Montagnes have given me advice on computers, bailed me out of stats problems, proof-read papers, and have been sounding boards for new ideas. Jana Pika, Eric Dumdei, Dave Burgoyne, Shichang Miao, and Judy Needham, the senior (and now graduated) group of the Andersen lab, deserve many thanks for help in solving chemistry problems, coffee breaks, and good times.

I wish to thank the entire UBC Oceanography department for answering a thousand questions. The following people have been especially helpful, both for advice and technical help. Dr. Al Lewis provided the "Tig 1" culture which was used throughout this work, in addition to much advice and culturing expertise. Elaine Simons, as curator of the North-East Pacific Culture Collection, provided the phytoplankton cultures. Dr. "Max" Taylor helped to bring me up to date on my phytoplankton species names, provided slides of the critters I was working with, let me use his video camera for filming "Tig", and gave advice and support as a member of my committee. Mike LeBlanc was responsible for giving me a green thumb, and especially deserves my thanks for those early mornings at the wall, without which I would have gone crazy during my thesis write-up. The UBC Oceanography office staff have been terrific. Chris Mewis has seen me through numerous struggles with bureaucratic red tape, and Olive Lau and Carol Leven have kindly put up with my take over of their office space during the preparation of this thesis.

This research was supported by a strategic grant from the Natural Sciences and Engineering Research Council (NSERC) of Canada. Personal funding was provided by an NSERC Postgraduate Scholarship and an I.W. Killam Predoctoral Fellowship.

Finally (but not lastly), I would like thank my husband Ken for his love and support, and his ability to endure with me even when the going got rough.



For anyone who has ever gazed with child-like wonder into a tidepool

"There are good things to see in tidepools and there are exciting and interesting thoughts to be generated from the seeing. Every new eye applied to the peep hole which looks out at the world may fish in some new beauty and some new pattern, and the world of the human mind must be enriched by such fishing."

John Steinbeck, in the foreword from Between Pacific Tides (Edward F. Ricketts and Jack Calvin, 1948)

#### Chapter 1

#### **General Introduction**

Phytoplankton, the microscopic plants inhabiting the upper reaches of the world's oceans, are the base of all oceanic food webs. These photosynthetic organisms convert light energy from the sun into chemical energy in the form of various chemical compounds. These compounds, when ingested, provide energy to other organisms further along the food chain. However, phytoplankton are not simply convenient packages of energy to be consumed at random by grazers. Various species of phytoplankton can produce "protective" compounds - chemicals which can inhibit grazing, reduce bacterial numbers, eliminate competition for space and inorganic nutrients from other species of phytoplankton, or even produce lethal effects in other organisms. Studies on the interaction of phytoplankton with other organisms via these compounds can increase our basic understanding of the transfer of energy through marine food webs.

The production of bioactive compounds by phytoplankton has been a topic of research for a number of years. Algae secrete a wide variety of compounds into their environment, including substances such as vitamins, amino acids, fatty acids, siderophores, pigments, and simple carbohydrates. To explain the interaction of phytoplankton with other organisms in their environment, Bell and Mitchell (1972) introduced the concept of the "phycosphere", a zone surrounding each phytoplankton cell composed of a high concentration of these algal exudates. These compounds may be actively secreted into the environment, or they may be released passively upon death and lysis of the phytoplankton. In addition, phytoplankton may have compounds closely associated with the cell surface, or contained in an external sheath of mucus, which can be detected during the filtering/handling process by which grazers ingest these cells. Compounds within the phytoplankton cells can also be released when the

cells are broken during ingestion. These substances can have a number of effects on organisms coexisting with the phytoplankton. They may act as antibiotic or antifungal compounds, toxins, allelopathic compounds, bacterial attractants, or compounds which reduce or inhibit feeding of potential grazers.

#### i. Antibiotic, Antifungal, and Cytotoxic Compounds

It has long been known that certain species of phytoplankton are more resistant to bacterial colonization than others. Living marine diatoms were found to exhibit some resistance to bacterial attack (Waksman et al., 1938). Later, actively growing populations of the diatom *Skeletonema costatum* were also shown to have low levels of bacterial colonization (Droop and Elsen, 1966). These observations led to the belief that some phytoplankton must be producing antimicrobial compounds.

The first partly identified antibiotic to be isolated from phytoplankton was a substance called chlorellin, which was obtained from the green alga, *Chlorella*. This substance was composed of peroxides of unsaturated fatty acids (Pratt *et al.*, 1944; Spoehr *et al.*, 1949; Scutt, 1964). The first positively identified extracellular antibacterial compound was isolated by Sieburth, who determined that the antibacterial properties of the haptophyte *Phaeocystis pouchetii* were due to the presence of acrylic acid (Sieburth, 1959a, 1959b, 1960, 1961, 1965, 1968; Guillard and Hellebust, 1971; Fig. 1). Eicosapentaenoic acid, a simple unsaturated fatty acid, was found to be an intracellular antibiotic in the diatom *Asterionella glacialis* (= *japonica*; Pesando, 1972; Fig. 1). More recently,  $\beta$ -diketone, another low molecular weight compound with antibiotic properties, was isolated from the extracellular filtrates of the dinoflagellate *Prorocentrum minimum* (Andersen *et al.*, 1980; Fig. 1). Antibiotic compounds have been isolated from every class of phytoplankton. However, the vast majority of these compounds were isolated from intracellular extracts, and little is known about

Fig. 1. Some examples of antibiotic, antifungal, and cytotoxic compounds isolated from phytoplankton.

extracellular antibiotic production. These antibiotics belong to a wide range of chemical classes, such as carbohydrates, proteins, or terpenoids, but few chemical structures have been determined.

Some phytoplankton produce compounds which have potent antifungal activity. Goniodomin A (Fig. 1), isolated from the cell extract of the dinoflagellate *Goniodoma pseudogoniaulax*, has a strong antifungal activity, but little or no activity against bacteria (Sharma *et al.*, 1968; Murakami *et al.*, 1988). Another group of antifungal compounds, the gambieric acids (Fig. 1), have recently been isolated from the dinoflagellate *Gambierdiscus toxicus* (Nagai *et al.*, 1992a, 1992b). These compounds inhibited the growth of the fungi *Aspergillus niger*, and were present both intracellularly and in the culture medium.

Many species of phytoplankton have been screened for biologically active natural products in the search for "drugs from the sea". Extracts from these phytoplankton are tested for antibacterial, antifungal, and antiviral activity against organisms which cause diseases in humans, and for antitumor activity to find drugs which can combat cancer. The amphidinolides (Fig. 1), a group of antineoplastic (antitumor) compounds isolated from the dinoflagellate *Amphidinium* sp. are an example of biologically active compounds isolated from phytoplankton by this approach (Kobayashi *et al.*, 1986; Ishibashi *et al.*, 1987; Kobayashi *et al.*, 1988). These compounds are potent cytotoxins, and probably play a protective role in the natural environment.

#### ii. Toxins

To date, the vast majority of research on compounds produced by phytoplankton has been focused on toxins which have human impacts. These toxins cause human poisoning when fish or shellfish which have ingested the phytoplankton are eaten by

humans. The effects of these toxins on humans have been well studied, but the effects on other marine organisms are only poorly understood. In freshwater systems, livestock mortality due to toxins produced by cyanobacteria has received a great deal of attention (Carmichael, 1986).

#### Paralytic Shellfish Poisoning (PSP)

Saxitoxin (Fig. 2) was first isolated from toxic Alaska butter clams, Saxidomus giganteus, (Schantz, et al., 1957; Schantz, 1960) and was later discovered to be produced by the dinoflagellate Alexandrium (= Gonyaulax) catenella (Schantz et al., 1966). The structure of this toxin was elucidated by Schantz et al. (1975). At this time, there are at least 18 forms of saxitoxin which have been isolated and identified (Taylor, 1990) from a number of different species of dinoflagellates. Ogata et al. (1990) suggested that the PSP toxicity in Alexandrium tamarense (= Protogonyaulax tamarensis), Alexandrium (= Protogonyaulax) catenella, Alexandrium (= Protogonyaulax) cohorticula, Gymnodinium catenatum, Fragilidium sp., and Alexandrium sp. may in fact be due to intracellular bacteria (Moraxella sp.) which produce the saxitoxins.

### Diarrhetic Shellfish Poisoning (DSP)

At least 12 toxins have been isolated so far which are responsible for DSP. These toxins can be separated into three groups according to their basic skeletons (Fig. 2). The first group includes okadaic acid and compounds based on okadaic acid. The structure of okadaic acid was first determined by Tachibana *et al.* (1981). The second group consists of the pectenotoxins, which are polyether macrolides. The structures of these compounds were elucidated by Yasumoto *et al.* (1985) and Murata *et al.* (1986). The third group is based on the structure of yessotoxin, isolated and identified by Murata *et al.* (1987). These toxins are produced by a number of *Dinophysis* sp., and also by *Prorocentrum lima* (Yasumoto, 1990).

Fig. 2. Some examples of toxins isolated from marine phytoplankton.

#### Amnesic Shellfish Poisoning (ASP)

ASP (also known as domoic acid poisoning) is caused by the excitatory amino-acid and neurotoxin, domoic acid (Fig. 2). Until recently, it was only known to be present in two species of red algae (*Chondria armata* and *Alsidium corallinum*) of the family Rhodomelaceae (Fattorusso and Piattelli, 1980; Ohfune and Tomita, 1982). In 1987, cultivated blue mussels (*Mytilus edulis*) in eastern Prince Edward Island became toxic, and it was determined that the pennate diatom *Pseudonitzschia* (= *Nitzschia*) pungens was responsible for the toxin production (Wright et al., 1989). Another group of compounds isolated from *P. pungens*, the bacillariolides (Fig. 2), was also implicated as possible agents in the outbreak of amnesic shellfish poisoning (Wang and Shimizu, 1990).

#### Ciguatera

The epiphytic dinoflagellate *Gambierdiscus toxicus* produces ciguatoxin (Fig. 2), which causes ciguatera poisoning in coral reef fish (Yasumoto *et al.*, 1977; Murata *et al.*, 1989). Two other toxins, maitotoxin (Fig. 2) and gambierol (Fig. 2), have also been isolated from this species (Yokoyama *et al.*, 1988; Murata *et al.*, 1993; Satake *et al.*, 1993).

#### **Brevetoxin**

The marine dinoflagellate Gymnodinium breve (= Ptychodiscus brevis) produces at least 9 lipid-soluble neurotoxins called brevetoxins (Baden, 1989; Schulman et al., 1990). These toxins are responsible for Florida's red tides and cause both fish kills and human illness (neurotoxic shellfish poisoning, NSP). The toxins are based on one of two different backbones of polyether trans-fused lactone-containing ring structures (Fig. 2).

## Other Toxins from Marine Phytoplankton

The benthic dinoflagellate *Prorocentrum lima* has been found to produce okadaic acid and its esters. In addition to these previously identified compounds, *P*.

lima also produces prorocentrolide (Fig. 2), a toxic, nitrogen-containing macrocycle (Torigoe et al., 1988). This compound may play a role in shellfish poisoning.

Some phytoplankton produce ichthyotoxins (toxins affecting fish), resulting in massive fish kills and damage to marine ecosystems. The flagellate *Chrysochromulina* polylepis and the dinoflagellate *Gyrodinium aureolum* both produce ichthyotoxins which are also potent hemolysins (lyse blood cells). The structures of several of these hemolysins (Fig. 2) have been determined (Yasumoto et al., 1990).

Fig. 3. Some examples of toxins isolated from cyanobacteria.

## Cyanobacterial Toxins

The alkaloid neurotoxin anatoxin-a (Fig. 3) is produced by strains of Anabaena flos-aquae (Huber, 1972; Devlin et al., 1977). Poisoning of animals by this toxin can occur after drinking water containing whole or lysed cells. Microcystis aeroginosa, M. viridis, Anabaena flos-aquae, and Oscillatoria agardhii produce microcystins (Fig. 3),

hepatotoxins which are also responsible for animal poisoning (Hughes et al., 1958; Carmichael and Gorham, 1981; Carmichael and Mahmood, 1984; Carmichael et al., 1988a). Microcystin-LR has also been found in the marine environment. It has been detected in mussels from the Northeastern Pacific Ocean, Eastern Canada, and Europe (Chen et al., 1993), and has also been linked to a severe liver disease (netpen liver disease, NLD) that occurs in Atlantic salmon which are net-pen reared in British Columbia (Andersen et al., 1993). The organisms responsible for microcystin-LR production in marine environments have not yet been identified. A compound similar in structure to the microcystins, nodularin (Fig. 3), is produced by Nodularia spumigena (Carmichael et al., 1988b, Rinehart et al., 1988). Cyanobacteria also produce PSP toxins. Saxitoxin and some related compounds have been isolated from Aphanizomenon flos-aquae (Carmichael, 1986).

#### iii. Allelopathic Compounds

Some algal exudates appear to play an allelopathic role. A rapid change in phytoplankton populations over two days was observed in Brest Bay, France in July, 1987. The population shifted from domination by *Chaetoceros* sp. to domination by *Gyrodinium* cf. *aureolum*. Filtered water taken from Brest Bay at this time decreased the growth of cultures of the diatom *Chaetoceros gracile* (Gentien and Arzul, 1990a). The dinoflagellate *G*. cf. *aureolum* was shown to release an exotoxin into its environment which decreased the growth of other algae (*Chaetoceros gracile*, *Dunaliella tertiolecta*, *Isochrysis galbana*, *Skeletonema costatum*, and *Tetraselmis suecica*) in culture (Gentien and Arzul, 1990b). This production of exotoxins probably plays an important role in bloom development. An extracellular autoinhibitor was produced by the diatom *Skeletonema costatum* as it entered senescence. In addition to autoinhibition, this compound also inhibited growth of a number of other diatoms and

the flagellate *Chattonella*, but had no inhibitory effect on the growth of dinoflagellates (Imada *et al.*, 1991). Thus *S. costatum* not only contributes to cessation of its own bloom, it may prevent bloom formation by other diatoms.

#### iv. Bacterial Attractants

Algal exudates can also act as bacterial attractants. Four marine bacteria isolates showed chemotactic responses towards filtrates from cultures of the diatoms *Skeletonema costatum* and *Thalassiosira pseudonana* (= Cyclotella nana) and the green alga *Dunaliella tertiolecta* (Bell and Mitchell, 1972). Jones and Cannon (1986) suggested that heterotrophic bacteria utilize these algal exudates for growth.

## v. Feeding Deterrents

Phytoplankton produce compounds which can reduce or inhibit the grazing of various herbivorous zooplankton. For the purpose of this thesis, a "feeding deterrent" will be broadly defined as any substance which inhibits or decreases the normal feeding of an organism on a preferred food, without causing death. Feeding deterrents produced by phytoplankton may be:

- 1) a toxin which, in sub-lethal doses, causes a physiological response in the organism which decreases feeding (e.g. a neurotoxin),
- 2) any non-toxic compound which causes a physiological response in the organism such that feeding is reduced or inhibited (e.g. a compound causing regurgitation),
- 3) any compound which an organism can detect using its sensory apparatus and which causes it to reduce or cease feeding, either through an instinctive or learned response.

# Feeding Deterrent Effects on Copepods

Much research has been done on the behavior of copepods feeding on a number of phytoplankton species, ranging from laboratory feeding studies to field observations. Originally, it was believed that consumption of phytoplankton was dependent only on the physical attributes of the phytoplankton, particularly abundance and size. At low concentrations, phytoplankton cells are ingested in direct proportion to their abundance, while at higher concentrations, the functional response becomes saturated and the ingestion rate remains constant or declines (Mullin, 1963; Parsons *et al.*, 1967; Frost, 1972). Large cells are ingested with greater efficiency than small cells (Mullin, 1963; Frost, 1977; Runge, 1980; Harris, 1982).

This model was unable to explain certain selective feeding behaviors of copepods. In the field, the calanoid copepods *Calanus pacificus* collected from a dinoflagellate bloom of *Gymnodinium flavum* had emptier guts than those collected outside the bloom (Huntley, 1982). In laboratory experiments, *C. pacificus* preferred a smaller diatom, *Thalassiosira weissflogii* ( $\approx 17~\mu m$ ), over *G. flavum* ( $\approx 35~\mu m$ ). In another field study, the effects of a *Phaeocystis* sp. bloom in the English Channel were observed (Bautista *et al.*, 1992). Three copepod size fractions (dominated by the species *Calanus helgolandicus*, *Pseudocalanus elongatus*, and *Oithona* sp.) showed lower gut pigment contents, ingestion rates and copepod abundances during the *Phaeocystis* bloom when compared with the previous period of diatom dominance. *Phaeocystis* appeared to produce a compound which had a negative effect on the copepods, and this compound indirectly contributed to the development of the *Phaeocystis* bloom by reducing grazing pressure. These results suggest that factors other than size and concentration of cells affect copepod feeding.

To determine if copepod feeding rates varied with dinoflagellate species, a number of laboratory experiments were conducted using *Calanus pacificus* (Huntley *et al.*, 1986). The feeding rates of *C. pacificus* on various dinoflagellates were compared

to the feeding rate on plastic beads of similar size. Plastic beads were known to be rejected as food by copepods (Huntley et al., 1983). The dinoflagellates Alexandrium (= Gonyaulax) acatenella, Alexandrium (= Gonyaulax) catenella, Gonyaulax polyedra, Gyrodinium dorsum, Gyrodinium resplendens, and Peridinium foliaceum were consumed at rates higher than plastic beads of the same size, while the species Alexandrium tamarense (= Gonyaulax tamarensis), Gonyaulax grindleyi (= Protoceratium reticulatum), Gymnodinium breve (= Ptychodiscus brevis) and Scrippsiella trochoidea were consumed at rates lower than plastic beads of the same size. Furthermore, filtrate from exponentially growing G. grindleyi caused a decrease in feeding upon the normally palatable G. resplendens, while the cell homogenate of G. grindleyi did not alter the filtration rate. This suggested that G. grindleyi was producing and secreting a compound which inhibited feeding. Huntley (1986) proposed that the production of feeding deterrents allowed slow growing species (e.g. dinoflagellates) to attain bloom concentrations.

The feeding deterrents produced by some dinoflagellates caused marked behavioral changes in *Calanus pacificus*. In order to determine the mechanisms by which feeding was inhibited, a video system was used to observe and record the behavior of restrained copepods when presented with dinoflagellates producing feeding deterrents (Sykes and Huntley, 1987). Copepods presented with *Gonyaulax grindleyi* failed to maintain full guts, and often regurgitated after 45-120 min. In the presence of *Gymnodinium breve*, copepods exhibited rapid heart rate and loss of motor control. Copepods fed *Scrippsiella trochoidea* occasionally displayed mouth part twitching or failure to maintain gut fullness. Thus, these feeding deterrents appeared to work by reducing the efficiency with which the copepod could filter and absorb food particles.

A number of other researchers have found evidence for food selectivity by copepods. Mullin (1963) showed that the grazing rates of four *Calanus* spp. decreased as the concentration of phytoplankton cells of the species *Ditylum brightwellii*,

Gonyaulax polyedra, Asterionella glacialis (= japonica), and Thalassiosira weissflogii (= fluviatilis) increased. Mullin proposed that these effects could be attributed to the presence of an inhibitory substance. Furthermore, Mullin showed that grazing rates decreased as the age of the phytoplankton culture increased, suggesting that the inhibitory substance was produced in greater quantities in senescent cells. Van Alstyne (1986) showed that cellular extracts from the dinoflagellate Scrippsiella trochoidea and the raphidophyte Heterosigma carterae (incorrectly identified as Olisthodiscus luteus) and filtrate from cultures of H. carterae appeared to have an inhibitory effect on the feeding rate of the copepod Centropages hamatus. The toxic dinoflagellate Alexandrium tamarense (= Protogonyaulax tamarensis) was demonstrated to decrease the ingestion rate of *Pseudocalanus* spp. by physiological incapacitation following assimilation of the toxins (Ives, 1987). Gill and Harris (1987) designed experiments which quantified the response of copepods to certain diets by measuring the beat frequency of the first maxilla (a component of the copepod filtering apparatus). The copepod Calanus helgolandicus showed strong decreases in beat frequency on diets of the dinoflagellates S. trochoidea and Gyrodinium aureolum when compared to a diet of the diatom *Thalassiosira weissflogii*. Decreases in beat frequency were also shown for the copepod Temora longicornis on diets of S. trochoidea, A. tamarense (= Protogonyaulax tamarensis), and G. aureolum. More recent experiments using the inshore marine copepods *Pseudodiaptomus marinus* and *Acartia omorii* have shown that the filtrates of the dinoflagellate Gymnodinium nagasakiense and the raphidophyte H. carterae also contain deterrent compounds which reduce feeding on Heterocapsa triquetra, a normally edible species (Uye and Takamatsu, 1990).

# Feeding Deterrent Effects on Other Zooplankton

Work has also been done on the effects of feeding deterrents on other zooplankton species. The tintinnid Favella ehrenbergii showed decreased feeding on the dinoflagellate Amphidinium carterae (Stoecker et al., 1981). Amphidinium carterae is known to produce a choline-like substance (Wangersky and Guillard, 1960; Thurburg and Sasner, 1973; Taylor et al., 1974), and it is believed that this substance may be acting as a feeding deterrent. Heterosigma caterae has been shown to produce both reduced growth rates and lethal effects on two species of tintinnids, Tintinnopsis tubulosoides and Favella sp. (Verity and Stoecker, 1982). It was postulated that these effects were due either to cellular toxicity, induced by ingestion or direct contact with H. carterae cells, or to exposure to a short-lived exudate. Exudates in the culture medium from the PSP-producing dinoflagellate Alexandrium tamarense caused the tintinnid F. ehrenbergii to undergo ciliary reversals, resulting in continuous backwards swimming, followed by swelling and subsequent lysis (Hansen, 1989). The toxicity of the medium depended on the growth phase of the dinoflagellate. The highest level of toxicity was found in the period following exponential growth, suggesting that the cells exude toxins when growth becomes limited. Another PSP-producing dinoflagellate, Alexandrium ostenfeldii, showed a similar effect on F. ehrenbergii (Hansen et al., 1992). In both cases, indirect evidence suggested that the effect on the ciliate was caused by PSP toxins. The toxic prymnesiophyte Chrysochromulina polylepis negatively affected both the growth and ingestion rates of F. ehrenbergii (Carlsson et al., 1990). Carlsson suggested that this limitation of grazing may contribute to bloom formation.

Brachionus plicatilis, a marine rotifer, showed a lower ingestion rate when it was fed Heterosigma sp. than for Chlamydomonas sp. (Chotiyaputta and Hirayama, 1978). Since Heterosigma sp. is larger than Chlamydomonas sp., this preference is not food-size selectivity. A second marine rotifer, Synchaeta cecilia, showed feeding

inhibition when given a mixture of an acceptable food species and low concentrations of *Heterosigma carterae* (Egloff, 1986). It was proposed that contact with *H. caterae* cells was required for inhibition of feeding and growth. Mucilage production by *H. carterae* (Leadbeater, 1969) may mediate grazer inhibition.

Decreased filtration rates in molluscs have been attributed to inhibitory compounds. The bivalve Hiatella arctica was found to have a lower filtration rate on Isochrysis galbana than on Phaeodactylum tricornutum (Ali, 1970). This reduced filtration rate was due to an inhibitory factor released into the medium by I. galbana. The effects of phytoplankton exudates on the feeding behavior of the blue mussel Mytilus edulis have been observed (Ward and Targett, 1989). The filtration rates of mussels presented with polystyrene beads suspended in filtrates from six phytoplankton species, I. galbana, Heterosigma carterae, Dunaliella tertiolecta, Tetraselmis suecica, Thalassiosira weissflogii, and T. pseudonana, were measured. Filtration rates were found to be reduced for the species H. carterae and D. tertiolecta. Aureococcus anophagefferens, a brown-tide chrysophyte, was found to inhibit the lateral ciliary activity in isolated gills of the bivalves Mercenaria mercenaria and M. edulis, but did not inhibit the lateral ciliary activity of the bivalves Mya arenaria, Geukensia demissa, and Argopecten irradians (Draper et al., 1990). The lateral cilia of species that were unaffected by Aureococcus were also unaffected by the neurotransmitter dopamine, while the lateral cilia of the species inhibited by Aureococcus were also inhibited by dopamine. It was suggested that Aureococcus may be releasing a dopamine antagonist. A detailed review on the effects of algal blooms on shellfish has been done by Shumway (1990).

In the freshwater environment, the daphnid *Daphnia pulicaria* showed feeding inhibition in the presence of the toxic cyanobacteria *Microcystis* sp., and in the presence of the purified toxin, microcystin-LR (DeMott *et al.*, 1991). DeMott

suggested that this feeding inhibition response was a physiological and behavioral adaptation which allowed the daphnid to coexist with toxic cyanobacteria.

Feeding deterrents have both commercial and ecological significance. Phytoplankton are an important food source in mariculture. They are an essential component in the diet of marine bivalve molluscs (e.g. oysters, clams, scallops, and mussels), the larvae of some marine gastropods (e.g. abalone), larvae of salt-water shrimp (*Penaeus* and *Metapenaeus*), some fish species (e.g. *Tilapia*, silvercarp, milkfish), and zooplankters. Zooplankters, in turn, can be used as live food for rearing larvae of numerous freshwater and marine fish and crustaceans (prawns, shrimp, crabs, and lobsters). Commonly used zooplankters are rotifers (Brachionus), copepods (Tigriopus), cladocerans (Daphnia, Moina), and brine shrimp (Artemia). Today, more than 40 different species of phytoplankton are being used in mariculture. The most frequently used species are the diatoms Skeletonema costatum, Thalassiosira pseudonana, Phaeodactylum tricornutum, Chaetoceros calcitrans, the flagellates Isochrysis galbana, Pavlova lutheri, Tetraselmis suecica, Dunaliella spp., and the chlorococcalean Chlorella spp. (DePauw and Persoone, 1988). Production of feeding deterrents by such species may decrease growth rates or increase mortality in mariculture species (e.g. oysters). Identification of deterrent producing species will improve mariculture practices. In the natural environment, production of feeding deterrents may control grazing and determine which species will bloom and how long the bloom will persist.

Although it has been known for the last three decades that certain phytoplankton produce feeding deterrents, very little research has been done on the chemistry of these compounds. This thesis attempts to combine studies on both the biology and chemistry (isolation and structural characterization) of a few feeding deterrent compounds.

# vi. Thesis Objectives

The objectives of this thesis were as follows:

- 1) To develop a simple, rapid, cost-efficient, reliable, and accurate bioassay to detect feeding deterrents from marine phytoplankton.
- 2) To isolate and characterize the structure of a feeding deterrent compound produced by a marine phytoplankton.
- 3) To determine the effects of various concentrations of the isolated feeding deterrent on the zooplankton used in the bioassay.
- 4) To develop an HPLC method for the quantitative measurement of the isolated feeding deterrent.
- 5) To determine when during the life cycle of the phytoplankton the isolated feeding deterrent was produced.

### **Chapter 2**

Evaluation of the Copepod *Tigriopus californicus* as a Bioassay Organism for the Detection of Chemical Feeding Deterrents Produced by Marine Phytoplankton

#### A. Introduction

In order to screen phytoplankton species for feeding deterrent production and to isolate and identify deterrent compounds, one needs to find a biological system which responds to feeding deterrents. Such a system, when used to detect and quantify deterrent compounds, is referred to as a feeding deterrent bioassay. This bioassay must be simple, rapid, cost-efficient, reliable, and accurate, as it will be used to guide the chemical fractionation of phytoplankton extracts necessary to isolate deterrent compounds. A number of criteria were considered when selecting an organism to use in this bioassay:

- the organism must be capable of responding to feeding deterrents and must react to the presence of these deterrents with a response which can be easily measured in the laboratory.
- 2) the organism must have a short life cycle. As many samples must be bioassayed in order to isolate a single deterrent compound, a bioassay turnover time of hours or days would be preferable. Organisms which require months to rear would mean that the waiting time for results would be too long.
- 3) the organism must be easily cultured in the laboratory. Researchers requiring this bioassay may not have the time or skill needed to grow sensitive, difficult to culture organisms. Also, organisms grown in the lab can be reared under controlled conditions and thus have known life histories, while

- organisms collected from nature may have undergone prior stresses which will alter their responses in the bioassay.
- 4) the organism must be ecologically relevant. Test results from marine feeding deterrents bioassayed using non-marine organisms cannot be ecologically interpreted. The bioassay organism should be one which would be expected to encounter phytoplankton feeding deterrents in nature.

Based on the above criteria, some candidates for this bioassay were the rotifer *Brachionus plicatilis*, larvae of the oyster *Crassostrea gigas*, and the harpacticoid copepod *Tigriopus californicus*. *T. californicus* was selected as best fulfilling the requirements of the bioassay.

Tigriopus californicus is a small marine harpacticoid copepod which inhabits supralittoral splash pools. This copepod is easily cultured in the laboratory, and has a life cycle of approximately 24 days. It is an extremely tolerant organism (Burton et al., 1979; Dethier, 1980), capable of surviving long periods of starvation. It is possible that compounds which would deter the feeding of a less tolerant copepod will have little or no affect on T. californicus. However, if a compound elicits a deterrent response from T. californicus, that compound may completely inhibit the feeding of a less tolerant species. Thus feeding deterrents detected by T. californicus would certainly be of ecological significance.

Feeding rate, measured by fecal pellet production, was used to assess the sublethal responses of *Tigriopus californicus* to feeding deterrents. There are two methods for observing a decrease in feeding rate: measuring ingestion rate or egestion rate. Ingestion rate is defined as particles consumed per hour per animal. To get ingestion rate, one can either measure the decrease of food particles from the medium over time, using a device such as a Coulter Counter, or one can measure the increase in food particles in the gut over time, using fluorescent beads or fluorescently labeled prey as food particles and an epifluorescent microscope. Egestion rate is defined as fecal

pellets produced per hour per animal. Egestion rate is obtained by measuring the increase in number of fecal pellets in the medium over time. This is done simply by settling the pellets out of the medium and counting them using an inverted microscope. It was decided to use egestion rate for this work. The initial start-up costs for this procedure are low, as the only instrument required is an inverted microscope. Furthermore, fecal pellets are large, easily identified objects that require little training in microscopy to be able to enumerate. Egestion rate has been shown to be proportional to ingestion rate for the copepods T. californicus (Wootton, 1989) and Calanus pacificus (Huntley et al., 1983). As well, Ayukai and Nishizawa (1986) found a linear relationship between ingestion and egestion rates for Calanus pacificus feeding on the diatom Thalassiosira decipiens, as did Tsuda and Nemoto (1990) for Pseudocalanus newmani feeding on the diatom Phaeodactylum tricornutum. Tsuda and Nemoto (1990) recommended the use of fecal pellets as an indicator of ingestion rates of copepods. Fecal pellet production rate has also been shown to be an indicator of sub-lethal toxic stress in marine copepods (Reeve et al., 1977). Furthermore, the total number of fecal pellets produced over a given time can be used to determine if there was a decrease in fecal pellet production rate during that time interval (Appendix A).

The bioassay was evaluated using the dinoflagellate Gonyaulax grindleyi, a known producer of feeding deterrents, and the diatom Phaeodactylum tricornutum, a suspected producer of feeding deterrents. Huntley et al. (1986) showed that G. grindleyi caused decreased feeding in the copepod Calanus pacificus, and that the material producing this response was extracellular. Phaeodactylum tricornutum is an easily grown species which is commonly used in mariculture. Epifanio et al. (1981) suspected that this species might produce a feeding deterrent based on the results of their oyster larvae feeding experiments.

The diatom *Thalassiosira pseudonana* was used as the control for this research. It is also used in mariculture, and is frequently used for laboratory experiments. Based

on previous studies (Chapter 1), there is no indication that *T. pseudonana* produces a feeding deterrent.

#### **B.** Materials and Methods

#### i. Phytoplankton Cultures

Cultures of the diatoms *Thalassiosira pseudonana* and *Phaeodactylum* tricornutum, and the dinoflagellate Gonyaulax grindleyi were grown and harvested to yield cellular extracts suitable for testing in the feeding deterrent bioassay. Unialgal cultures of *P. tricornutum* Bohlin (NEPCC #640), *T. pseudonana* (Hustedt) Hasle and Heimdal clone 3H (NEPCC #58), and *G. grindleyi* (NEPCC #535) were obtained from the Northeast Pacific Culture Collection (NEPCC), Department of Oceanography, University of British Columbia. Natural seawater (salinity  $\approx 28^{\text{O}/\text{OO}}$ ) was collected from West Vancouver, British Columbia at a site 100 m from shore and 15 m depth. Seawater used for culturing was filtered through activated charcoal to remove organics (Craigie and McLachlan, 1964), and then filtered through a 0.8  $\mu$ m Millipore filter to remove particulates. The seawater was sterilized by autoclaving. All cultures were grown using full ES enriched natural seawater (Harrison *et al.*, 1980) at 19°C under continuous irradiance ( $\approx 70 \mu$ mol m<sup>-2</sup> s<sup>-1</sup>) with stirring at  $\approx 60 \text{ rpm}$ .

Culture growth was measured by *in vivo* fluorescence. The growth rate  $(\mu)$  was calculated by plotting the natural logarithm of the fluorescence values against the culture age (days). The time during which the cells were in log phase was estimated, and a straight line was fitted to the data points in this phase using the least squares method. The slope of this line was the growth rate. Cell densities of *Thalassiosira* pseudonana were determined using either a Coulter Counter (model TAII) or an inverted compound microscope (400x power). Cell densities of *Phaeodactylum* tricornutum and Gonyaulax grindleyi were only determined microscopically.

Cultures were harvested in late log or early senescence phase. Phytoplankton cells were collected by a series of gentle filtration (<50 mm Hg) techniques. Initially, the cultures were filtered through a 30  $\mu$ m (nominal size) Nitex screen to remove large cell clumps, followed by filtration through a 5  $\mu$ m (nominal size) Nitex screen. Cells were rinsed from both screens with methanol and collected in a grinding tube. The filtrate which passed through the screens was then filtered through a GF/F glass fiber filter and this filter was added to the grinding tube. Cellular extracts of the phytoplankton cells were obtained by grinding the harvested cells in methanol and rinsing the cell debris repeatedly in methanol until all pigments were removed. This methanolic extract was filtered through a GF/F glass fiber filter to remove remaining cell debris. The methanolic extract then underwent rotary evaporation to yield a dry solid which was used in the bioassay procedures.

Heat-killed *Thalassiosira pseudonana* cells were fluorescently stained with 5-(4,6-dichlorotriazin-2-yl) aminofluorescein (DTAF) using the methodology developed by Sherr *et al.* (1991). The stained cells were resuspended in filtered natural seawater and sonicated (1 min in bath sonicator at 60 Hz) to remove clumps. The density of fluorescent cells was determined using the Coulter Counter. These resuspended cells were then used as fluorescently labeled prey in feeding experiments.

# ii. Copepod Cultures

A culture of the harpacticoid copepod *Tigriopus californicus* was maintained to provide a continuous supply of organisms for the bioassay. *Tigriopus californicus* (Tig-1) was originally isolated from splash pools on the West Coast of Vancouver Island by Dr. A.G. Lewis, University of British Columbia, in 1966 (Sullivan and Bisalputra, 1980). Copepods used for the bioassay were maintained in filtered natural seawater in 1 L Pyrex flasks at 18°C at an irradiance of  $\approx 100 \,\mu$ mol m<sup>-2</sup> s<sup>-1</sup> and a L:D cycle of 18:6 h. The copepods were fed either a diet of ground fish food (Wardley's

Basic Fish Food for Tropical Fish) or a diet of the diatom *Thalassiosira pseudonana*. To reduce variability in the bioassay due to differences in the sex or life stage of the copepods, only the adult (C6) male copepods were used.

Copepods with reduced bacterial contaminants were prepared by soaking the copepods in a solution of 800 mg penicillin-G, 180 mg dihydrostreptomycin, 8 mg chloramphenical, and 20 mg dextrose in 100 ml of filtered, autoclaved natural seawater for 48 h (adapted from Wootton, 1989). Both antibiotic-treated and untreated copepods were then placed in autoclaved seawater without food for 24 h before being used in a bioassay.

Differences in grazing rates were determined by measuring fecal pellet production. The water in which the copepods were incubated was quantitatively transferred to a 10 ml cylindrical settling chamber, the contents were settled for 30 min, and fecal pellets were counted at low power (100x) using an inverted compound microscope.

#### iii. Egestion Rate Experiments

The suitability of fecal pellet production rate as a measure of ingestion rate in *Tigriopus californicus* was tested in a preliminary experiment. Copepods were preconditioned on a diet of ground fish food prior to the experiment. One male C6 copepod was added to a well (volume  $\approx 15$  ml) of a tissue culture plate and given an excess of ground fish food. Two experiments with 5 replicates in each were done The copepods were incubated at 18°C at an irradiance of  $\approx 100 \, \mu$ mol m<sup>-2</sup> s<sup>-1</sup> and a L:D cycle of 18:6 h. In the first experiment the incubation time was 50.5 h, and in the second experiment it was 137 h. The fecal pellet production rate of the copepods was then measured, and the condition of the fecal pellets was examined microscopically.

A second preliminary experiment was used to determine if *Tigriopus* californicus would feed on the diatom *Thalassiosira pseudonana*, and what the time

course of fecal pellets production was on this diet. The copepods were preconditioned for 24 h without food prior to the experiment. One antibiotic-treated male C6 copepod was added to a well (volume  $\approx 15$  ml) of a tissue culture plate and given an excess of heat-killed, fluorescently stained *T. pseudonana* cells (Sherr *et al.*, 1991). Six experiments were done. The copepods were incubated at 18°C at an irradiance of  $\approx 100 \ \mu \text{mol m}^{-2} \text{ s}^{-1}$  and a L:D cycle of 18:6 h. At various time intervals, each experiment was terminated by the addition of formalin. The number of fecal pellets in each experiment was enumerated, and the formalin-treated copepods were examined under fluorescent microscopy.

Using egestion as an index of feeding, an experiment was designed to determine the feeding response of *Tigriopus californicus* to *Thalassiosira pseudonana* cells and to determine the concentration of *T. pseudonana* cells required to saturate the egestion rate of *T. californicus*. Based on the results of the two preliminary experiments (Results and Discussion), a convenient incubation period of 24 h was selected, as this time was long enough to ensure a constant rate of pellet production.

Various concentrations of *Thalassiosira pseudonana* cells were placed in the wells (volume  $\approx 15$  ml) of a tissue culture plate and two male C6 copepods were added to each well. The animals were incubated for 24 h at 18°C at an irradiance of  $\approx 100$   $\mu$ mol m<sup>-2</sup> s<sup>-1</sup> and a L:D cycle of 18:6 h. The fecal pellet production rate of the copepods was then measured. To determine if treatment of copepods with antibiotics had any effects, this experiment was repeated twice, once with untreated copepods and once with antibiotic-treated copepods. The change in fecal pellet production rate with food concentration fitted the equation:

$$F = (F_{max} * c)/(K_C + c)$$

where F = the fecal pellet production rate (fecal pellets  $h^{-1}$  copepod<sup>-1</sup>),  $F_{max}$  = the maximum fecal pellet production rate, c = the concentration of T. pseudonana cells,

and  $K_C$  = the concentration of T. pseudonana cells required to reach the half-saturation fecal pellet production rate.

## iv. Bioassay Method Using Feeding Deterrents Adsorbed onto Ground Fish Food

Extracts from phytoplankton cells were adsorbed onto ground fish food (Wardley's Basic Fish Food for Tropical Fish), and this treated fish food was presented as a food source to copepods to determine if the presence of a feeding deterrent on the surface of a normally palatable food particle would produce a decrease in feeding. Fish food particles are very lipophilic, and were expected to behave in a manner similar to the reverse phase microparticles used by Ward and Targett (1989) to adsorb dissolved ectocrines. A weighed sample of the dry methanolic cell extract was dissolved in methanol and added to autoclaved ground fish food. The fish food was dried under vacuum to remove the methanol, then reground. The treated fish food contained 20-28% cellular extract by weight. Two mg of this treated fish food was suspended in 10 ml of autoclaved seawater. This mixture was placed in a single well (volume  $\approx 15$  ml) of a tissue culture plate with one male C6 copepod and incubated for  $\approx 65-75$  h at 18°C at an irradiance of ≈ 100  $\mu$ mol m<sup>-2</sup> s<sup>-1</sup> and a L:D cycle of 18:6 h. Fecal pellets were settled and counted at the end of the bioassay. Untreated ground fish food was used as the control. Six replicates were done. To observe if the antibiotic treatment had an effect, the experiment was performed twice, once with untreated copepods and once with antibiotic-treated copepods.

### v. Bioassay Method Using Dissolved Feeding Deterrents

Extracts from phytoplankton cells were dissolved in seawater and mixed with live *Thalassiosira pseudonana* cells to determine if the presence of a dissolved feeding deterrent would produce a decrease in feeding by copepods on a normally palatable phytoplankton species. Two mg of the dried methanolic cell extract to be bioassayed was dissolved in 5 ml of autoclaved seawater and sonicated (1 min in bath sonicator at 60 Hz) to facilitate mixing. If the extract to be tested was not soluble in seawater, it was dispersed using 4 drops of dimethylsulfoxide (DMSO). When DMSO was used to dissolve the extract, it was also added to the control.

Five ml of an exponentially growing culture of *Thalassiosira pseudonana* was added to the dissolved cell extract. If the cell cultures were clumped, cell clumps were broken up using sonification (1 min in bath sonicator at 60 Hz) and filtration (forced through a 200  $\mu$ m screen at a rate of  $\approx 50$  ml min<sup>-1</sup> using a syringe; repeated 4 times). Microscopic observations indicated that these procedures did not lyse the *T. pseudonana* cells. The final concentration of *T. pseudonana* cells was kept at or above the level required for saturation of the egestion rate of *Tigriopus californicus* (Results and Discussion), so decreases in fecal pellet production would not be due to decreased food levels.

The mixture of dissolved cell extract and live *Thalassiosira pseudonana* cells was placed in one well (volume  $\approx 15$  ml) of a tissue culture plate and 2 male C6 copepods were added. The assay was incubated for  $\approx 20$  h at  $18^{\circ}$ C at an irradiance of  $\approx 100 \ \mu \text{mol m}^{-2} \text{ s}^{-1}$  and a L:D cycle of 18:6 h. Copepods were pretreated with antibiotics and preconditioned in autoclaved seawater without food for 24 h prior to the bioassay. Fecal pellets were settled and counted at the end of the bioassay. Six replicates were done. A control was conducted using the cell extract from the diatom *T. pseudonana* which had no feeding deterrent activity when bioassayed using the ground fish food assay (Results and Discussion).

# vi. Bioassay Method Using Feeding Deterrents Produced by Live Cells

To determine if live cells produced feeding deterrents in concentrations sufficient to inhibit feeding, copepods were presented with live cell cultures at a density of 6 x  $10^5$  cells ml<sup>-1</sup>. Cell clumps in 10 ml of exponentially growing *Phaeodactylum tricornutum* cell culture were broken up using sonification (1 min in bath sonicator at 60 Hz) and filtration (forced through a 200  $\mu$ m screen at a rate of  $\approx 50$  ml min<sup>-1</sup> using a syringe; repeated 4 times). The cell culture was placed in one well (volume  $\approx 15$  ml) of a tissue culture plate and 2 male C6 copepods were added. The assay was incubated for  $\approx 20$  h at  $18^{\circ}$ C at an irradiance of  $\approx 100$   $\mu$ mol m<sup>-2</sup> s<sup>-1</sup> and a L:D cycle of 18:6 h. Copepods were pretreated with antibiotics and preconditioned in autoclaved seawater without food for 24 h prior to the bioassay. Fecal pellets were settled and counted at the end of the bioassay. Six replicates were conducted. A control was run using *Thalassiosira pseudonana* cell culture at a density of 6 x  $10^5$  cells ml<sup>-1</sup>, as this diatom did not produce a feeding deterrent (Results and Discussion).

#### C. Results and Discussion

#### i. Phytoplankton Cultures

Typical data on the growth of *Phaeodactylum tricornutum*, *Thalassiosira* pseudonana, and Gonyaulax grindleyi are listed in Appendix B. The growth rates of 1.57 d<sup>-1</sup> for *T. pseudonana* and 0.825 d<sup>-1</sup> for *P. tricornutum* agree reasonably well with published results of 1.59 d<sup>-1</sup> for *T. pseudonana* and 1.11 d<sup>-1</sup> for *P. tricornutum* under conditions of 17.5 °C and 44 μmol m<sup>-2</sup> s<sup>-1</sup> (Thompson *et al.*, 1990). Huntley *et al.* (1986) gave a growth rate of 0.131 d<sup>-1</sup> for *G. grindleyi*. This concurs with the value 0.271 d<sup>-1</sup> obtained for this research, even though Huntley's culture conditions (17 °C, 15 klux, and *Gonyaulax polyedra* medium from Loeblich (1975)) were quite different from those used in this work.

#### ii. Egestion Rate Experiments

When fed a diet of ground fish food, fecal pellet production of *Tigriopus* californicus was constant over time (Appendix C, Tables C1 and C2). Both the short term experiment (50.5 h) and the long term experiment (137 h) yielded an average fecal pellet production rate of 1.1 pellets h-1 (n=5, F=0.0036,  $\alpha$ =0.999). Since the copepods were preconditioned on a diet of ground fish food prior to the experiment, they were not expected to have a lag period in fecal pellet production. Microscopic examination of the fecal pellets showed no signs of coprorhexy (the breaking up of the fecal pellet by the copepod in order to remove and ingest the membrane which surrounds the pellet; Lampitt *et al.*, 1990) or fecal pellet degradation over the time frame of the experiment. Therefore, it was assumed that fecal pellet production was constant over at least 100 h.

pseudonana cells, the copepod was fed heat-killed, fluorescently stained *T. pseudonana* cells, and the ingestion of these cells was observed over time. These observations are recorded in Table 1. From these results, it was apparent that the copepods were able to ingest the *T. pseudonana* cells and produce fecal pellets on this diet. The first stained fecal pellet was produced within 30 min of the addition of the food source, and fecal pellet production had reached a constant rate within 4 h. The general staining observed on the head and thorax appeared to be from breakage of cells during ingestion, thus counting intact cells in the gut would not give a good approximation of ingestion rate. For future experiments, an incubation time of 24 h was selected based on the results of this preliminary experiment, as this would be a long enough time interval to ensure a constant fecal pellet production rate had been reached.

**Table 1.** Feeding of *Tigriopus californicus* on fluorescently stained *Thalassiosira* pseudonana cells. Copepods treated with antibiotics prior to experiment. Observations made on copepods preserved in formalin.

Time (min)	Observations	Fecal pellets
5	cell clusters on first pair of legs and feeding apparatus	0
10	cell clumps on first pair of legs and feeding apparatus (10-15 cells)	0
30	approximately 9 cells on feeding limbs and 5 cells in first section of gut	2
60	general staining of head and thorax region including first three pairs of legs; small clump of cells in mid-gut region	1
240	cells found throughout the gut; heavy staining of the thorax and first three pair of legs; 9 cells in mid-gut; 7 cells in hind-gut	9
480	entire digestive tract stained; all legs stained; clump of heavy staining near anus	23

The egestion rate response of *Tigriopus californicus* to varied concentrations of *Thalassiosira pseudonana* cells is shown in Figure 4 (raw data and statistical analysis in Appendix C, Tables C3 and C4). The data were analyzed using the Wilkinson method for estimating the parameters of a Michaelis-Menten type equation  $(F = (F_{max}*c)/(K_c+c); Wilkinson, 1961)$ . Untreated copepods had a maximum fecal pellet production rate  $(F_{max})$  of 1.6 fecal pellets  $h^{-1}$  (S.E. = 0.1) and a half-saturation constant  $(K_c)$  of 2 x 10<sup>4</sup> cells ml<sup>-1</sup> (S.E. = 1 x 10<sup>4</sup>). Antibiotic treated copepods had a  $F_{max}$  of 1.9 fecal pellets  $h^{-1}$  (S.E. = 0.2) and a  $K_c$  of 2 x 10<sup>4</sup> cells ml<sup>-1</sup> (S.E. = 1 x 10<sup>4</sup>). Using a two-tailed t-test, the maximum fecal pellet production rates (n=18, t=1.4,  $\alpha$ =0.09) and the half-saturation constants (n=18, t=0.21,  $\alpha$ =0.25) of treated and untreated copepods were not significantly different. It appears that the antibiotic treatment does not affect the feeding behavior of the copepods. For both treatments, a cell density of greater than 1 x 10<sup>5</sup> cells ml<sup>-1</sup> produced a saturated egestion rate

response in *T. californicus*. Therefore, all bioassays using *T. pseudonana* were run with cell densities at or above this concentration.

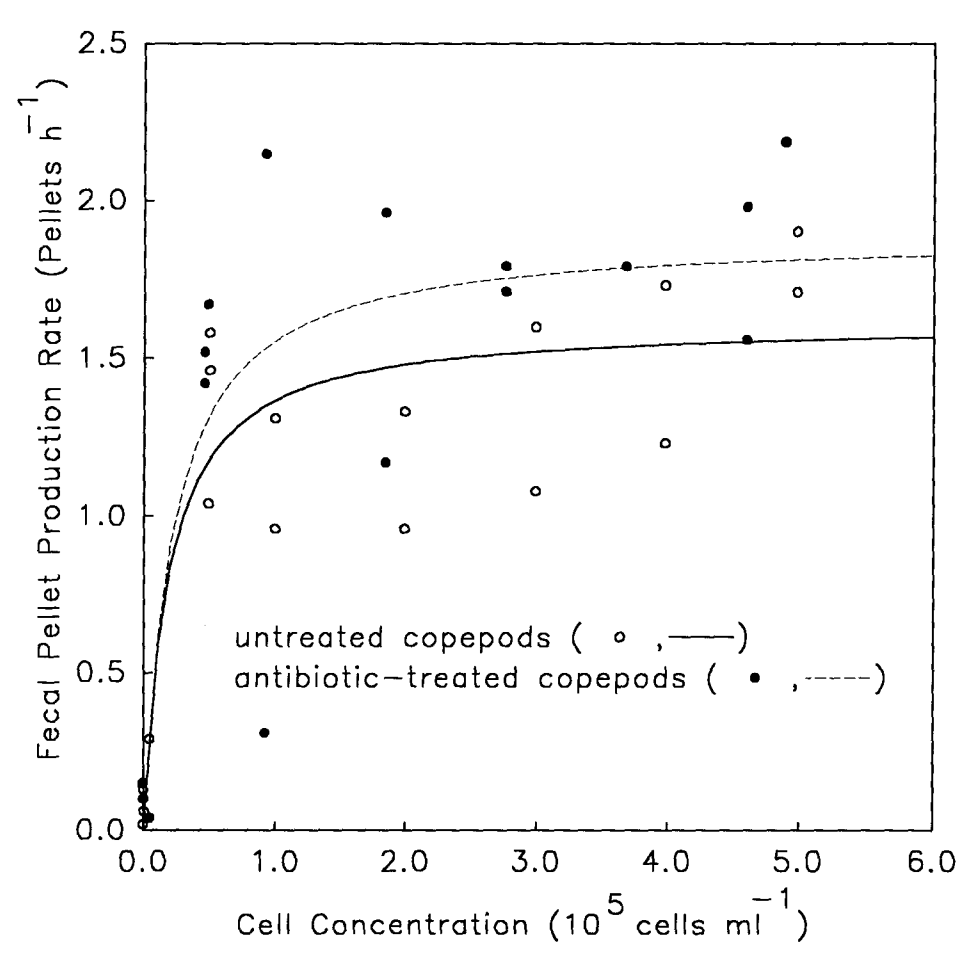


Fig. 4. Feeding response, as measured by egestion rate, for untreated and antibiotic-treated *Tigriopus californicus* feeding on *Thalassiosira pseudonana*.

Tsuda and Nemoto (1990) found similar results during feeding experiments using the marine planktonic copepod *Pseudocalanus newmani* and the diatom *Phaeodactylum tricornutum*. They gave an  $F_{max}$  of 3.48 x  $10^5~\mu m^3~h^{-1}$  copepod<sup>-1</sup> and a  $K_c$  of 5.95 x  $10^5~\mu m^3~ml^{-1}$ . Using an average volume of 2.26 x  $10^5~\mu m^3$  for fecal pellets produced by *Tigriopus californicus* (experimentally measured; Appendix D, Table D1) and an average volume of 35  $\mu m^3$  for *Thalassiosira pseudonana* cells (Rublee *et al.*, 1989), the  $F_{max}$  is 3.7 x  $10^5~\mu m^3~h^{-1}$  copepod<sup>-1</sup> (S.E. = 3 x  $10^4$ ) and

the  $K_c$  is 6 x 10<sup>5</sup>  $\mu$ m<sup>3</sup> ml<sup>-1</sup> (S.E. = 4 x 10<sup>5</sup>) for untreated copepods. Given the degree of approximation involved in the conversions of the results from this research, and the fact that different species were used in each work, the comparison of the results is very good.

### iii. Bioassay Method Using Feeding Deterrents Adsorbed onto Ground Fish Food

A cellular extract from Gonyaulax grindleyi was tested for feeding deterrents by adsorbing this extract onto ground fish food. The data from this experiment were arranged into 4 blocks (untreated copepods fed fish food with no adsorbed cell extract, antibiotic-treated copepods fed fish food with no adsorbed cell extract, untreated copepods fed fish food with adsorbed G. grindleyi cell extract, and antibiotic treated copepods fed fish food with adsorbed G. grindleyi cell extract) and analyzed using twofactor analysis of variance (Fig. 5A; raw data and statistical analysis in Appendix C, Tables C5 and C6). There was significant interaction between the 2 treatments (treatment of copepods with antibiotics; treatment of fish food with cell extracts)  $(n=24, F=9.8, \alpha=0.005)$ . Protected two-tailed t-tests showed that there were significant differences between antibiotic-treated copepods and untreated copepods and between fish food with no adsorbed cell extract and fish food with adsorbed cell extract. One-factor ANOVA showed that the antibiotic-treated copepods produced significantly fewer fecal pellets on a diet of fish food with adsorbed cell extract than on a diet of fish food with no adsorbed cell extract (n=6, F=15,  $\alpha$ =0.004). This indicates that G. grindleyi does produce an extractable cellular feeding deterrent. These results correlated with work done by Huntley (1986), who also showed that G. grindleyi inhibited feeding. However, Huntley showed that the feeding deterrent from G. grindleyi was extracellular not intracellular. The deterrent compound may be produced and stored intracellularly and released extracellularly only at certain times

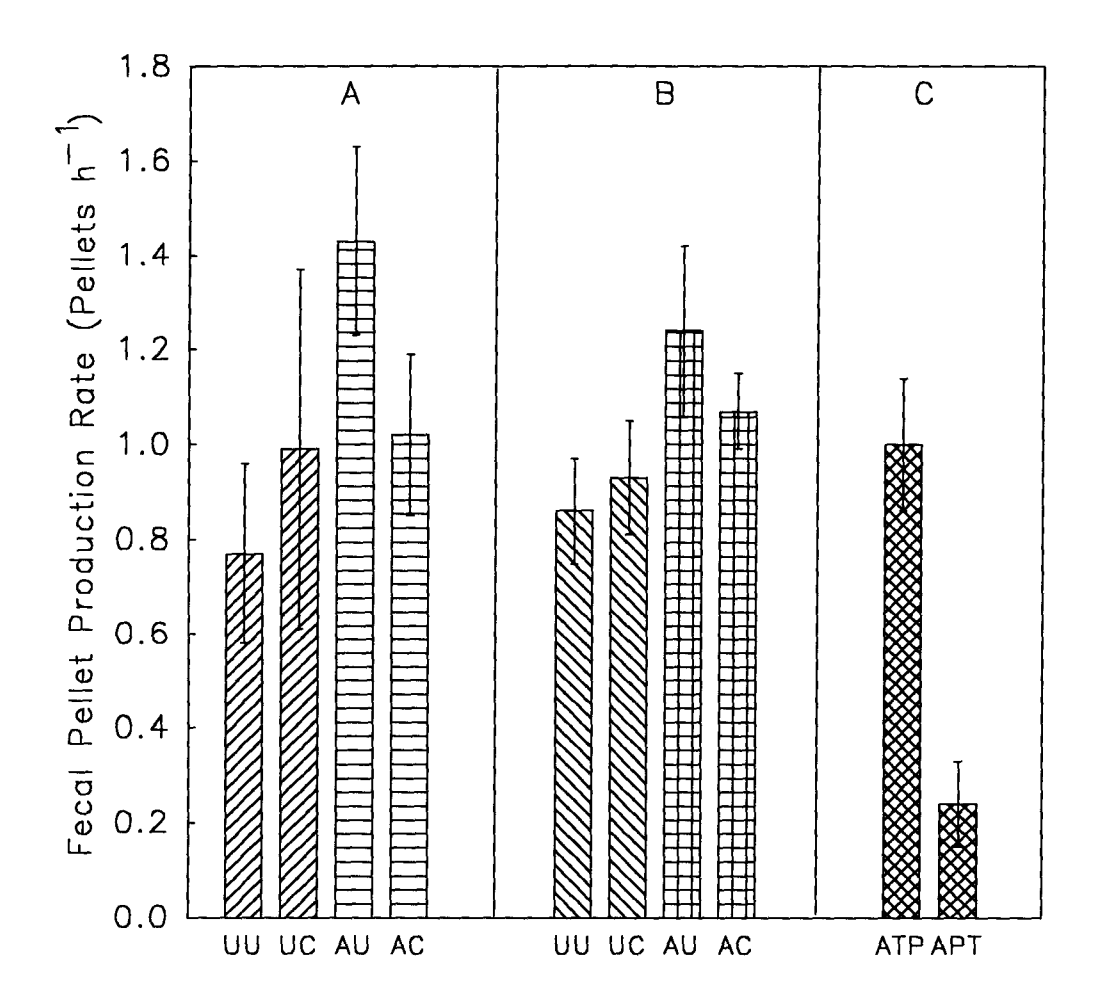


Fig. 5. Feeding responses, as measured by egestion rate, of *Tigriopus californicus* to treatment of copepods with antibiotics and treatment of ground fish food with cellular extracts from three phytoplankton species. Set A: UU = untreated copepods fed uncoated fish food; UC = untreated copepods fed fish food coated with *Gonyaulax grindleyi* cellular extract; AU = antibiotic-treated copepods fed uncoated fish food; AC = antibiotic-treated copepods fed fish food coated with *G. grindleyi* cellular extract. Set B: UU = untreated copepods fed uncoated fish food; UC = untreated copepods fed fish food coated with *Thalassiosira pseudonana* cellular extract; AU = antibiotic-treated copepods fed fish food coated with *T. pseudonana* cellular extract. Set C: ATP = antibiotic-treated copepods fed fish food coated with *T. pseudonana* cellular extract.

APT = antibiotic-treated copepods fed fish food coated with *Phaeodactylum tricornutum* cellular extract. Error bars are ± 1 SD (n = 6).

during the cell growth cycle. Thus, these conflicting results may be due to the fact that the feeding deterrent is present intracellularly at some times and extracellularly at others. Untreated copepods did not show a significantly different response between the two diets (n=6, F=1.7,  $\alpha=0.23$ ), suggesting that the bioassay is affected by bacteria on the copepods or in the medium.

A cellular extract from *Thalassiosira pseudonana* was bioassayed for feeding deterrents. The data were arranged into 4 blocks, as in the previous experiment, and analyzed using two-factor analysis of variance (Fig. 5B; raw data and statistical analysis in Appendix C, Tables C7 and C8). There was no significant interaction between the 2 treatments (treatment of copepods with antibiotics; treatment of fish food with cell extracts) (n=24, F=3.8,  $\alpha$ =0.07). Data from both groups fed fish food with no adsorbed cell extract and both groups fed fish food with adsorbed *T. pseudonana* cell extract were combined and analyzed by one-factor ANOVA. There was no significantly different response between a diet of fish food treated with *T. pseudonana* cell extract and a diet of untreated fish food (n=12, F=1.1,  $\alpha$ =0.31). It appears that *T. pseudonana* does not produce any cellular feeding deterrents that affect this copepod. ANOVA also showed that antibiotic-treated copepods produced more fecal pellets than untreated copepods (n=12, F=20,  $\alpha$ <0.001), indicating that bacterial contaminants have a significant effect on the copepods.

In both of the above experiments, antibiotic-treated copepods produced significantly more fecal pellets than untreated copepods. As bacteria affect the feeding of *Tigriopus californicus* on ground fish food, future bioassays were performed with antibiotic-treated copepods to decrease this effect.

A cellular extract from *Phaeodactylum tricornutum* was bioassayed for feeding deterrents (Fig. 5C; raw data and statistical analysis in Appendix C, Tables C9 and C10). A cellular extract from *Thalassiosira pseudonana* was used as the control.

ANOVA showed that copepods on a diet of *P. tricornutum* treated fish food produced

significantly fewer fecal pellets than copepods on a diet of T. pseudonana treated fish food (n=6, F=130,  $\alpha$ <0.001). Therefore, P. tricornutum produced a cellular substance which was a feeding deterrent.

By adsorbing cell extracts onto ground fish food, the bioassay simulated the situation where an algal cell has various compounds attached to or closely associated with the cell surface (similar to the "phycosphere" concept proposed by Bell and Mitchell (1972)). The copepod was then able to handle the food particle and accept or reject it on the basis of its surface properties. This was a more realistic model than simply dissolving the cell extracts in the medium, and provided some information on the mechanisms involved (e.g. the copepods detected the feeding deterrent when handling the food particles). Using cell extracts eliminated feeding preferences based on size, shape, and texture of the algal cell. However, many of the fish food particles were of a similar size and shape as the fecal pellets. This made counting fecal pellets slow and subjective, since fecal pellets were difficult to distinguish from fish food particles. Therefore, adsorbing cell extracts onto fish food was not a suitable method for bioassay-guided chemical fractionation.

#### iv. Bioassay Method Using Dissolved Feeding Deterrents

A cellular extract from *Phaeodactylum tricornutum* was tested for feeding deterrents by presenting the copepods with the extract dissolved in seawater and mixed with live *Thalassiosira pseudonana* cells as the food source (Fig. 6A; raw data and statistical analysis in Appendix C, Tables C11 and C12). Copepods produced significantly fewer fecal pellets when presented with live *T. pseudonana* cells mixed with dissolved cellular extract from *P. tricornutum* cells than when presented with live *T. pseudonana* cells mixed with dissolved cellular extract from *T. pseudonana* cells  $(n=6, F=61, \alpha < 0.001)$ . The feeding deterrent produced by *P. tricornutum* affects *Tigriopus californicus* when dissolved in seawater.

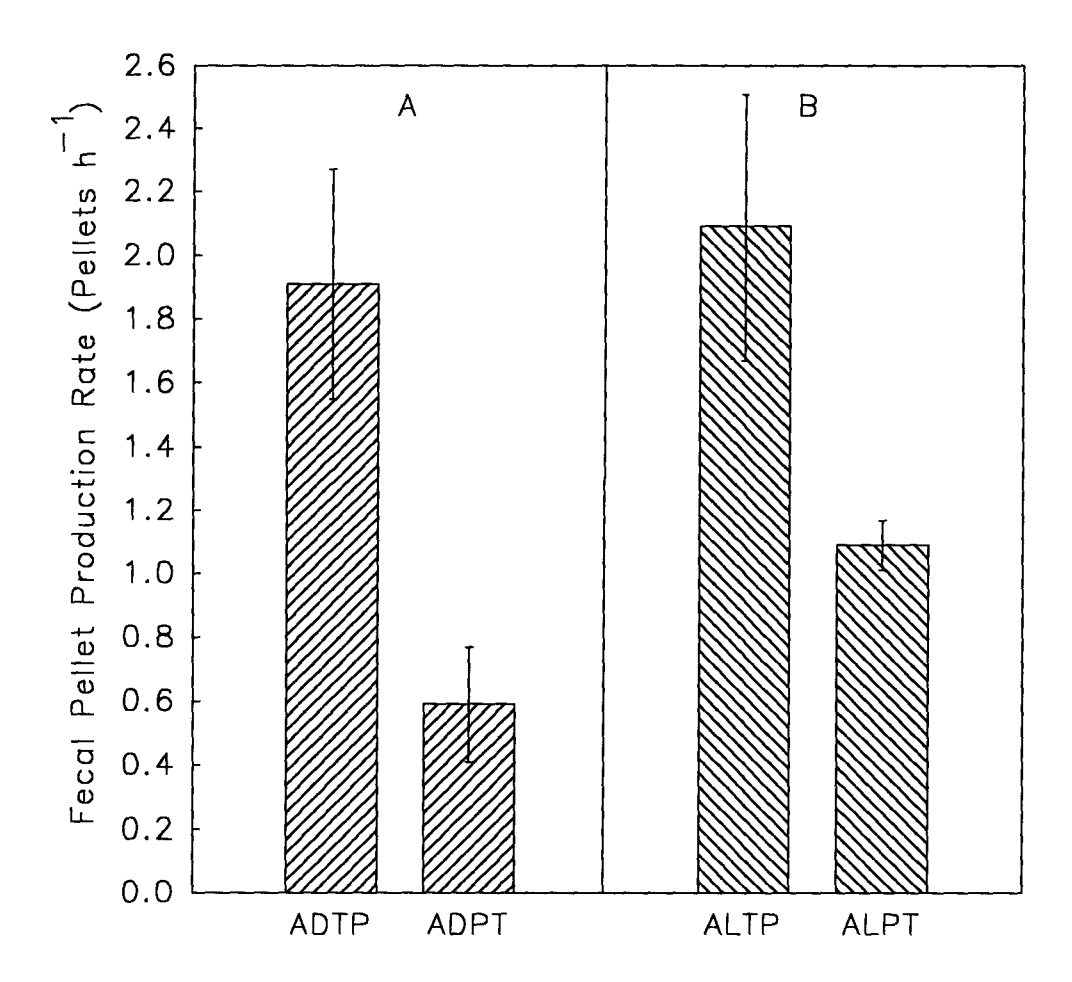


Fig. 6. Feeding responses, as measured by egestion rate, of *Tigriopus californicus* when presented with a diet of live phytoplankton cells. Set A: ADTP = antibiotic-treated copepods fed live *Thalassiosira pseudonana* cells suspended in dissolved cellular extract from *T. pseudonana*; ADPT = antibiotic-treated copepods fed live *T. pseudonana* cells suspended in dissolved cellular extract from *Phaeodactylum tricornutum*. Set B: ALTP = antibiotic-treated copepods fed live *T. pseudonana* cells; ALPT = antibiotic-treated copepods fed live *P. tricornutum* cells. Error bars are  $\pm$  1 SD (n = 6).

The fecal pellets were more easily and quickly counted when the feeding deterrent was presented to the copepods as a dissolved material in the presence of live phytoplankton cells than when the copepods were provided with ground fish food onto which the feeding deterrent was adsorbed. There was no confusion in distinguishing fecal pellets from phytoplankton cells. This removed the subjective bias found in the

ground fish food method resulting from the difficulty in correctly identifying food particles from fecal pellets. The speed and ease of performing this method made it suitable for bioassay-guided chemical fractionation. As in the previous method, using cell extracts eliminated feeding preferences based on size, shape, and texture of the algal cell. However, presenting the feeding deterrent in a dissolved form may be unrealistic, especially if the feeding deterrent is actually intracellular or closely associated with the cell surface. In these cases, the feeding deterrent response in the natural environment may be different.

#### v. Bioassay Method Using Feeding Deterrents Produced by Live Cells

To determine if feeding deterrents produced by *Phaeodactylum tricornutum* could be detected in live cultures, *Tigriopus californicus* was exposed to both *Thalassiosira pseudonana* and *P. tricornutum* live cells (Fig. 6B; raw data and statistical analysis in Appendix C, Tables C13 and C14). Copepods fed live *P. tricornutum* cells produced significantly fewer fecal pellets than copepods fed live *T. pseudonana* cells (n=5, F=32,  $\alpha<0.005$  for both ANOVA and Mann-Whitney U tests). Thus, a feeding deterrent can be detected from live *P. tricornutum* cells.

Presenting live phytoplankton cells to the copepods allowed the bioassay to simulate the natural environment. The copepod was able to detect the feeding deterrent at concentrations produced by live cells. Whether the feeding deterrent was present as a component of the cell's "phycosphere", as a dissolved exudate, or intracellularly was not determined from this method. In addition, this method did not control for changes in feeding due to differences in the size, shape, and texture of the phytoplankton cells.

#### D. General Discussion and Conclusions

Many species of marine phytoplankton reduce or completely inhibit feeding in various zooplankton (Ali, 1970; Chotiyaputta and Hirayama, 1978; Huntley, 1982; Verity and Stoecker, 1982; Egloff, 1986; Huntley et al., 1986; Sykes and Huntley, 1987; Ward and Targett, 1989; Uye and Takamatsu, 1990). The known PSP toxins, saxitoxin and its derivatives, have been shown to be feeding deterrents to both copepods and tintinnids (Ives, 1987; Hansen, 1989; Hansen et al., 1992). Toxins from freshwater cyanobacteria (microcystin-LR, nodularin) have also been found to be feeding deterrents (DeMott et al., 1991). However, no feeding deterrent compound has been isolated and structurally characterized from a marine phytoplankton using a bioassay specifically designed to detect feeding deterrents. Isolation of an active compound from a crude extract requires bioassay-guided chemical fractionation of the crude extract to be performed. Therefore, a fast and reliable bioassay is needed, since many samples must be bioassayed to isolate one active compound. Most feeding deterrent bioassays presently in use are tedious, require expensive and specialized equipment and supplies, or demand high levels of skill in culturing or collecting delicate bioassay organisms (Huntley et al., 1986; Sykes and Huntley, 1987).

In previous work, feeding deterrents have been detected by measuring ingestion rate (Huntley et al., 1986). This approach is often tedious and time consuming (e.g. cell/bead counts). As fecal pellet production rate (egestion) has been correlated with ingestion rate for copepods (Huntley et al., 1983; Ayukai and Nishizawa, 1986; Tsuda and Nemoto, 1990), this approach was used. Counting fecal pellets is rapid, easy, and requires little skill. As egestion rate is an indirect measure of feeding, it is not always tightly coupled to ingestion rate, and a bioassay using egestion rate may have decreased accuracy. In practice, however, this does not appear to be a problem.

Bacteria associated with Tigriopus californicus or the culture medium reduced the feeding of the copepod on ground fish food. When T. californicus was treated with antibiotics, the egestion rate increased, and the copepods were more responsive to the presence of a feeding deterrent. Bacteria may be harmful to the copepods (decreasing egestion rate), may be producing their own feeding deterrent compounds (decreasing egestion rate), may be breaking down the feeding deterrent being bioassayed (decreasing sensitivity of the bioassay), or may be providing an additional food source for the copepods (decreasing sensitivity of the bioassay). Antibiotic treatment had a much greater effect on copepods fed ground fish food than copepods fed live Thalassiosira pseudonana cells. This may be due to the fact that ground fish food contains large amounts of organics which may become dissolved in the medium during the bioassay, while healthy diatom cells leak only a small amount of organics (as compared with ground fish food) into the medium. As these dissolved organics provide a good source of nutrients for any bacteria present, ground fish food would tend to stimulate bacterial growth more than live diatom cells. Treatment of copepods with antibiotics would greatly decrease the number of bacteria present at the start of the bioassay, and prevent the formation of a large bacterial population even when ground fish food is used as the food source. Antibiotic treatment is recommended for copepods with heavy bacterial contamination.

The type of food source used in the bioassay is important. Food sources with large particle sizes, such as ground fish food, make fecal pellet counts difficult, while food sources with small particle sizes, such as diatom cells, produce a background against which fecal pellets are easily counted. For greatest accuracy, small phytoplankton ( $<20 \ \mu m$ ) should be used.

For bioassay-guided chemical fractionation of crude phytoplankton extracts, the bioassay method using dissolved extracts is recommended. This is the most rapid and simple of the three bioassay procedures examined.

Using *Tigriopus californicus* as the indicator organism, a feeding deterrent was detected in the cell extracts from both the diatom *Phaeodactylum tricornutum* and the dinoflagellate *Gonyaulax grindleyi*. This is in agreement with recent work (in collaboration with this author) done on the grazing rates of larval oysters (Thompson *et al.*, 1993) which showed a decrease in grazing rates when filtrates from *P. tricornutum* or *G. grindleyi* were present. Therefore, it appears that the production of feeding deterrents is not limited to dinoflagellates (marine) or cyanobacteria (freshwater), and it is possible that many classes of phytoplankton produce these compounds. Further screening of other phytoplankton is required.

Huntley et al. (1986) showed that Gonyaulax grindleyi produced an extracellular feeding deterrent during logarithmic growth and that cellular extracts had no activity. However, this research shows that the cellular extract does have feeding deterrent activity. The cultures used for this work were harvested during late exponential phase/early senescence. It is possible that the difference in results is due to the growth phase in which the culture was harvested. Trick et al. (1981) and Hansen (1989) showed that the release of extracellular materials by phytoplankton is dependent upon their growth phase.

This work showed that *Phaeodactylum tricornutum* at a density of 6 x 10<sup>5</sup> cell ml<sup>-1</sup> was capable of producing feeding inhibition in *Tigriopus californicus*. Although this density is too high for a normal ecological system, further studies of feeding inhibition by *P. tricornutum* at lower cell densities are merited. If phytoplankton which produce feeding deterrents are found in bloom concentrations in nature, these blooms could deter predators. Thus, feeding deterrents may control which phytoplankton species are palatable and assimilated by zooplankton. This, in turn, may initiate or extend blooms of non-palatable species. Ultimately, feeding deterrents may control transfer of energy along some paths in the food web.

A new, rapid, and reliable bioassay for feeding deterrents has been developed. This bioassay is capable of detecting deterrent compounds from both live cells and cell extracts, and should provide a valuable tool in screening other phytoplankton for the production of feeding deterrent compounds and determining the chemical nature of these compounds.

#### Chapter 3

# <u>Isolation and Structure Determination of Chemical Feeding Deterrents from the</u> <u>Diatom Phaeodactylum tricornutum</u>

#### A. Introduction

The second objective of this research was to isolate and characterize the structure of a feeding deterrent produced by a marine phytoplankter using chromatographic and spectroscopic techniques. The development of a feeding deterrent bioassay (Chapter 2) made it possible to carry out bioassay-guided chemical fractionation in order to isolate active feeding deterrent compounds. Using this bioassay, chemical feeding deterrents were isolated from the marine diatom *Phaeodactylum tricornutum*.

This introduction will give a brief description of the principles involved in the chromatographic and spectroscopic techniques used in this research. The theories behind these principles will not be dealt with in detail, however references will be given for those who wish to pursue these subjects in more depth.

### i. Chromatographic Techniques

The science of chromatography encompasses a wide range of separation methods which allow scientists to isolate and identify related components from complex mixtures. The one common element for these methods is the use of a stationary phase and a mobile phase. Components in a mixture are carried through the stationary phase by the flow of the mobile one. Separations are based on the differences in migration rates among the various components.

Several types of column chromatography have been used in this research to isolate feeding deterrent compounds. In column chromatography, the stationary phase is held in a narrow tube through which mobile phase is forced under pressure or by gravity. If the mobile phase is a liquid, then this is referred to as liquid chromatography. Liquid-solid chromatography (LSC) has a liquid mobile phase and a solid stationary phase. Migration of components through the column is controlled by an equilibrium between adsorption of the components on the solid stationary phase and dissolution of the components in the liquid mobile phase. Liquid-bonded phase chromatography (LBC) has a liquid mobile phase and an organic species bonded to a solid surface as the stationary phase. Migration of components through the column is controlled not only by an adsorption equilibrium, but also by an equilibrium between dissolution in the mobile phase and dissolution in the bonded phase. This second equilibrium is termed a partition equilibrium (Skoog, 1985).

Chromatographic separations are based upon differences in the extent to which solutes are partitioned between the mobile and stationary phases. This equilibrium can be described quantitatively by the equation  $K = C_S/C_M$ , where K is the partition coefficient,  $C_S$  is the concentration of the solute in the stationary phase, and  $C_M$  is the concentration of the solute in the mobile phase. If one plots  $C_S$  against  $C_M$ , then ideally this is a linear function (since  $C_S = K*C_M$ ) (Fig. 7, line A). A chromatographic method which satisfies this ideal is referred to as linear or partition chromatography. However, if the solute is adsorbed onto the stationary phase, then one gets a curve similar to line B in Figure 7. This curve is described by the equation  $C_S = K*C_M^n$ , where n is a constant. A chromatography (Skoog, 1985).

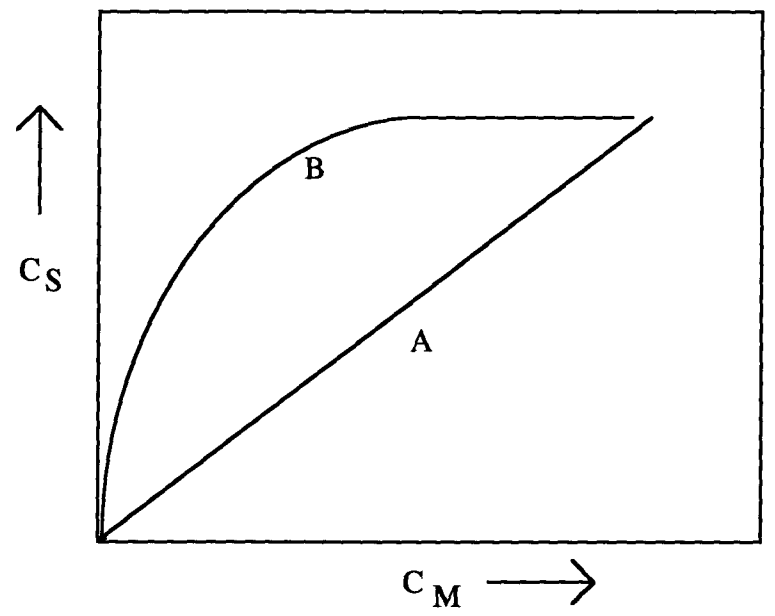


Fig. 7. Theoretical plots of solute concentration in the stationary phase  $(C_S)$  against solute concentration in the mobile phase  $(C_M)$ . Line A is for partition chromatography and line B is for absorption chromatography.

Separation of components in column chromatography is carried out through a process termed elution, whereby a solute is washed through a column by additions of fresh solvent. A single portion of a sample, dissolved in the mobile phase, is introduced at the head of the column at time = t<sub>0</sub>, at which time the components of the sample distribute themselves between the mobile and stationary phases. Addition of mobile phase (eluent) at the head of the column forces the sample down the column, where further partitioning takes place. Since solute movement can only occur in the mobile phase, the average rate at which a solute migrates depends on the fraction of time it spends in the mobile phase. Thus, if K is small, the solute spends a large amount of time in the mobile phase and elutes quickly. Differences in the K's for different components in a mixture allow components to separate into bands located along the length of the column. Isolation of components in these separated bands is then accomplished by passing sufficient eluent through the column to cause the

individual bands to pass out the end, where they can be collected (time =  $t_n$ ) (Skoog, 1985).

If a detector that responds to solute concentration is placed at the end of the column, and its signal is plotted as a function of time, one can obtain a chromatogram (Fig. 8). This plot, which consists of a series of symmetric peaks, contains two valuable pieces of information:

- 1) retention time the time at which the component elutes. This can be used to identify components in a sample.
- 2) area under the peak this is a quantitative measure of the amount of each component (Skoog, 1985).

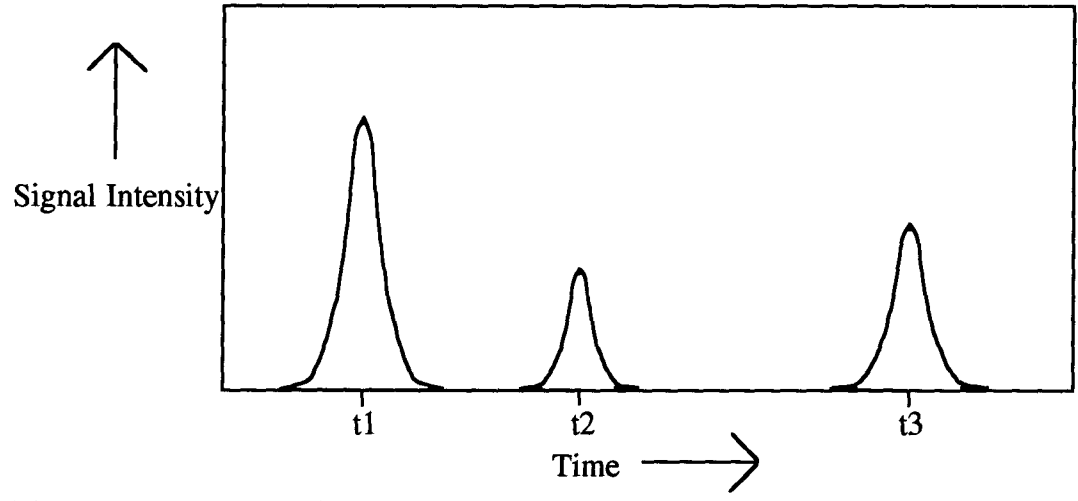


Fig. 8. An example of a chromatogram. t1, t2, and t3 are the retention times for components 1, 2, and 3 respectively.

### Column Chromatography

The types of column chromatography used in this research were:

a) alumina chromatography

This is a type of adsorption chromatography. Retention of components is a function of interaction with the surface hydroxyls of the alumina stationary phase through the formation of hydrogen bonds and dipole-dipole

interactions. Polar compounds are more strongly adsorbed than nonpolar compounds. The mobile phase is generally an organic solvent lower in polarity than the stationary phase.

# b) normal phase silica chromatography

This is a type of adsorption chromatography. Normal phase refers to chromatography in which the stationary phase is more polar than the mobile phase. Retention of components is a function of interaction with the surface silanols (Si-OH groups) of the silica gel stationary phase through the formation of hydrogen bonds and dipole-dipole interactions. Polar compounds are more strongly adsorbed than nonpolar compounds. Silica gel has a lower adsorbing power than alumina.

# c) reverse phase C-18 bonded silica chromatography

Migration of compounds through this type of column is controlled mainly by the partition equilibrium. Reverse phase refers to chromatography in which the stationary phase is more hydrophobic than the mobile phase. In C-18 bonded silica chromatography, long alkyl groups (C-18) are bonded to the silanol groups of the silica gel. Retention of components is a function of hydrophobic interactions with the surface alkyl groups of the stationary phase. Nonpolar compounds are more strongly adsorbed than polar compounds.

# d) high performance liquid chromatography (HPLC)

HPLC is a form of column chromatography in which the column efficiency (the ability of the column to resolve separate components in a mixture) and speed have been increased by packing the column with particles of stationary phase material as small as 5  $\mu$ m and pumping mobile phase through the column using a high pressure pump. The packing material used in HPLC columns is the same as for normal column chromatography.

#### **Detection Methods**

Two methods for detecting feeding deterrents in eluent from various columns were used:

# a) feeding deterrent bioassay

As bands elute from the column, they are collected, and a portion of this collected material is simply bioassayed as described in Chapter 2. This allows the fraction containing the active feeding deterrent compounds to be identified.

### b) photo-diode array (PDA) detector

This is a detector unit which consists of an array of photo-diodes. Each diode measures light intensity at a given wavelength of light. Thus, at any given time, the array is capable of measuring light intensities at a number of wavelengths. The output of this unit is a plot of absorbance (amount of light absorbed by a sample passing through the unit =  $\log(I_0/I)$ , where  $I_0$  is the intensity of incident light and I is the intensity of emergent light) against wavelength. This is referred to as an absorption spectrum. When attached to a column, this detector gives an absorption spectrum for each component eluting from the column which has a light absorbing chromophore. The absorption spectrum can be used to both identify and quantify the component.

#### ii. Spectroscopic Techniques

Spectroscopy is the study of the quantized interaction of energy (typically electromagnetic) with matter. Molecular spectroscopy deals with the spectroscopy of atoms bound together to form molecules. Electrons within molecules can move, and molecules themselves can vibrate and rotate. All these motions are quantized (Fig. 9).

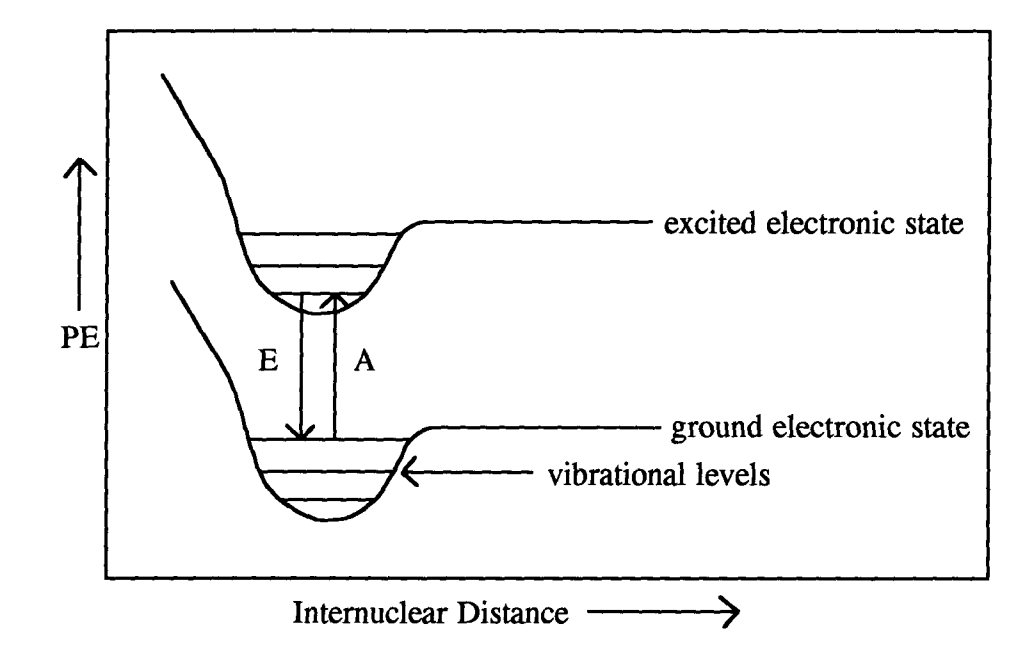


Fig. 9. Potential energy curves (schematic) of a diatomic molecule showing quantized energy states and transitions from a ground state to an electronic excited state. PE = potential energy; internuclear distance = distance between the two nuclei of the molecule; E = emitted energy; A = absorbed energy.

A photon of energy may be absorbed by a molecule, causing the molecule to be excited from one quantized energy level to a higher energy level, if  $\Delta E$ , the energy difference between the two levels, corresponds exactly to the energy of the photon. Since  $\Delta E = h\nu$  (Planck-Einstein equation; h = Planck's constant;  $\nu = frequency$  of absorbed radiation) and  $c = \lambda\nu$  (c = speed of light;  $\lambda = wavelength$  of absorbed radiation), then the equation  $\Delta E = hc/\lambda$  can be derived. Therefore, the greater the energy of the absorbed photon, the shorter the wavelength of absorption. A typical spectrum is a plot of the absorption or emission of energy by a molecule against the wavelength ( $\lambda$ ) or frequency ( $\nu$ ) of that energy (Fig. 10). An absorption peak in a spectrum can be characterized by the wavelength of maximum absorption ( $\lambda_{max}$ ) and the intensity of the absorption at this wavelength (Forbes, 1965).

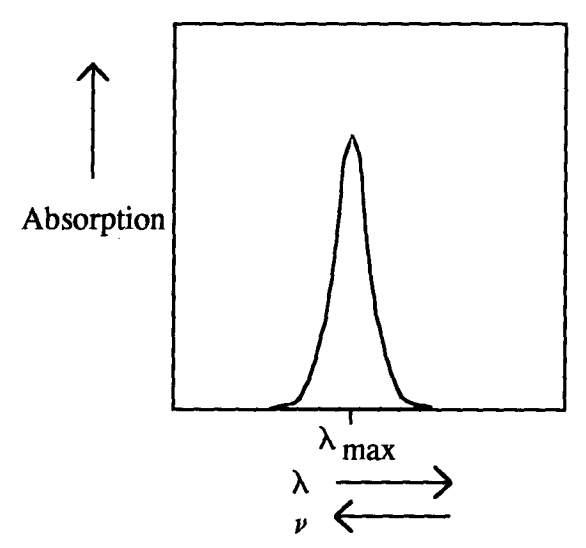
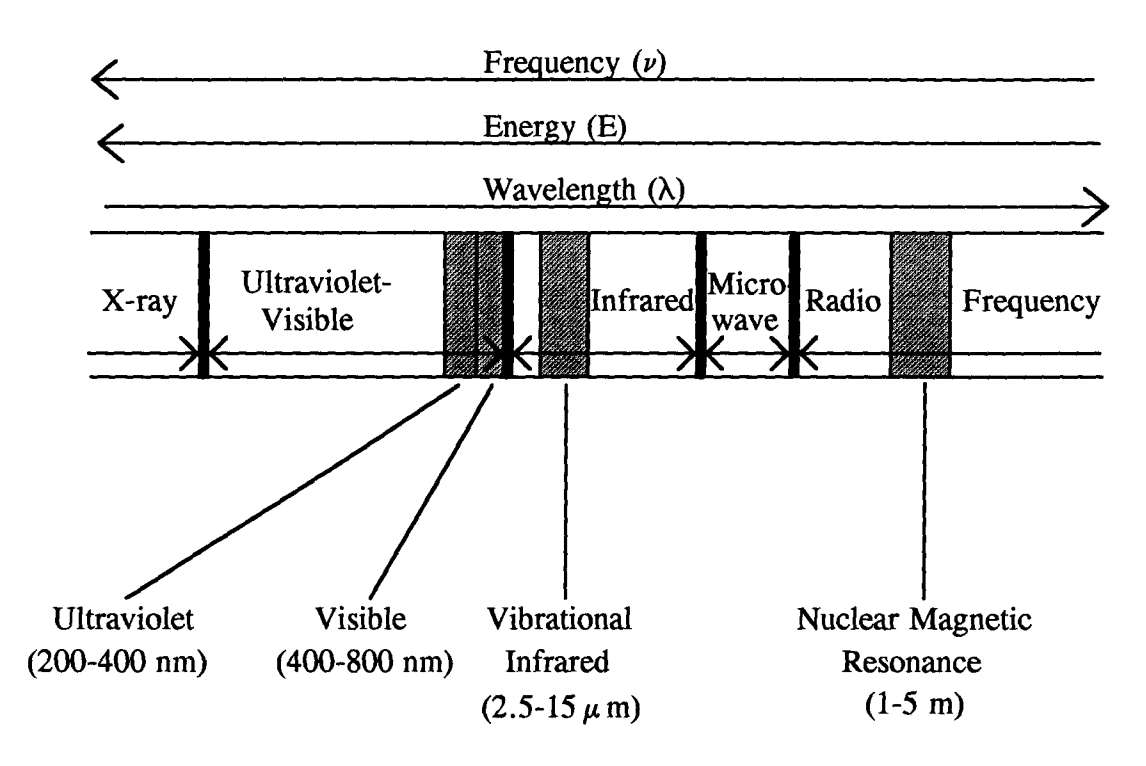


Fig. 10. An example of a typical spectrum generated by the absorption of energy by a molecule.

The absorption of a photon of energy of a particular wavelength by a molecule is a result of the structural features in that molecule which are capable of absorbing that specific energy package. Thus, the wavelength of the absorbed energy can be used as an indication of structural features of a molecule. Energy from several regions of the electromagnetic spectrum give vital information about the structure of organic molecules (Fig. 11; Pavia *et al.*, 1979).

## <u>Ultraviolet-Visible Spectroscopy (UV-vis)</u>

Ultraviolet-visible spectroscopy is the study of absorption of ultraviolet or visible light (200 - 800 nm) by electrons in a molecule. This absorbed energy excites the electrons from bonding to antibonding molecular orbitals in a process referred to as an electronic transition. Molecular orbitals which are important in UV-vis spectroscopy are shown in Figure 12 (Pavia *et al.*, 1979).



**Fig. 11.** A portion of the electromagnetic spectrum showing regions which provide important spectroscopic information about the structure of a molecule.

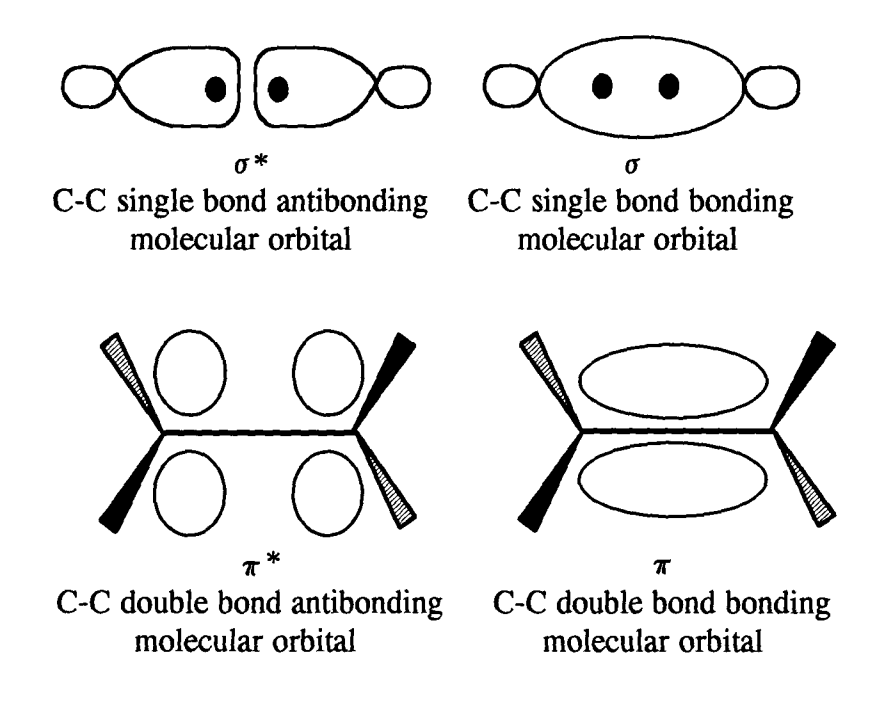
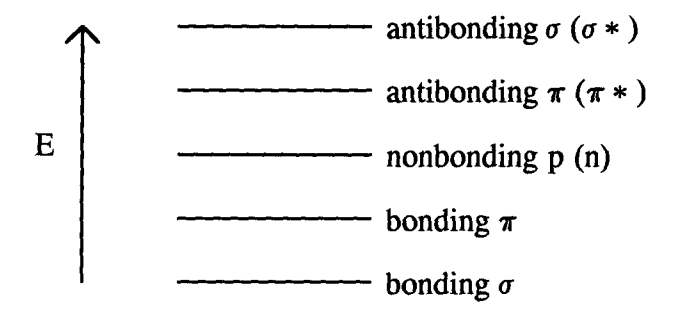


Fig. 12. Molecular orbitals involved in electronic transitions in organic molecules.

It is possible to have the following electronic transitions:  $\sigma \to \sigma^*$ ;  $\pi \to \pi^*$ ;  $n \to \pi^*$  and  $n \to \sigma^*$  (Fig. 13). The  $\pi \to \pi^*$  transition is of particular interest in molecules containing conjugated double bonds. As the number of p orbitals making up the conjugated system is increased, the transition from the highest occupied molecular orbital (HOMO) to the lowest unoccupied antibonding molecular orbital (LUMO) has progressively lower energy. In practical terms, as conjugation increases, the wavelength of absorbed light energy becomes longer. In polyenes with cis double bonds (trans double bond =  $\frac{1}{2}$ ; cis double bond =  $\frac{1}{2}$ ), a second, more energetic  $\pi \to \pi^*$  transition is allowed, resulting in a "cis band" at a shorter wavelength than the main  $\pi \to \pi^*$  transition (Pavia *et al.*, 1979).



**Fig. 13.** Schematic representation of the electronic energy levels of molecular orbitals in organic molecules.

The  $\lambda_{\text{max}}$  for  $\pi \to \pi^*$  transitions can be calculated empirically by various sets of empirical rules depending on the type of molecule (Woodward-Fieser rules for dienes; Fieser-Kuhn rules for polyenes; Woodward's rules for enones; Nielsen's rules for  $\alpha,\beta$ -unsaturated acids and esters). Therefore, for these types of compounds, one can deduce the structure of the chromophore (a group of atoms responsible for the absorption of a specific wavelength of energy by the molecule) from the  $\lambda_{\text{max}}$  (Pavia et al., 1979).

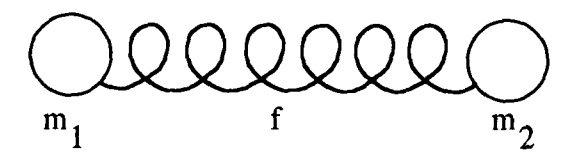
The intensity of the absorption of light at  $\lambda_{max}$  is expressed as an extinction coefficient,  $\epsilon$  (molar extinction coefficient or molar absorptivity). Absorbance and molar absorptivity are related by the Beer-Lambert law:

$$A = \log (I_0/I) = \varepsilon cd$$
 where 
$$A = absorbance$$
 
$$I_0 = intensity of incident light$$
 
$$I = intensity of emergent light$$
 
$$c = concentration of compound (M)$$
 
$$d = length of cell holding sample (cm)$$
 
$$\varepsilon = molar absorptivity.$$

# Infrared Spectroscopy (IR)

Infrared spectroscopy is the study of the absorption of IR radiation (2.5 -  $15 \mu m$ ) by a molecule. This absorption of radiation causes the molecule to undergo a transition from one vibrational energy state to a higher vibrational energy state. Radiation in this energy range corresponds to the stretching and bending vibrational frequencies of bonds in most covalent molecules. Only bonds which have a dipole moment (polar bonds) are capable of absorbing IR radiation, as there must be an oscillating dipole moment in order for energy transfer from incoming radiation to occur. Therefore, bonds which are symmetrically substituted will not produce a signal in an IR spectrum.

The stretching vibration of a bond in a molecule can be compared to two balls at the end of a spring:



This vibration can be described by the equation:

$$\nu = k\sqrt{\frac{f(m_1 + m_2)}{m_1 m_2}}$$
  
where  $\nu = \text{vibration frequency}$   
 $k = \text{constant}$   
 $m_1$  and  $m_2 = \text{masses of atoms in the bond}$   
 $f = \text{force constant of bond} \approx \text{bond strength.}$ 

Therefore, stronger bonds absorb IR radiation of higher frequencies. Carbon-carbon bonds have vibrational frequencies such that:

Infrared spectroscopy provides two useful types of information: (1) IR spectra act as "fingerprints" to identify molecules, since no two molecules produce identical IR spectra; (2) IR spectra give structural information about functional groups in a molecule, as specific functional groups give specific IR absorptions (Fig. 14; Pavia et al., 1979).

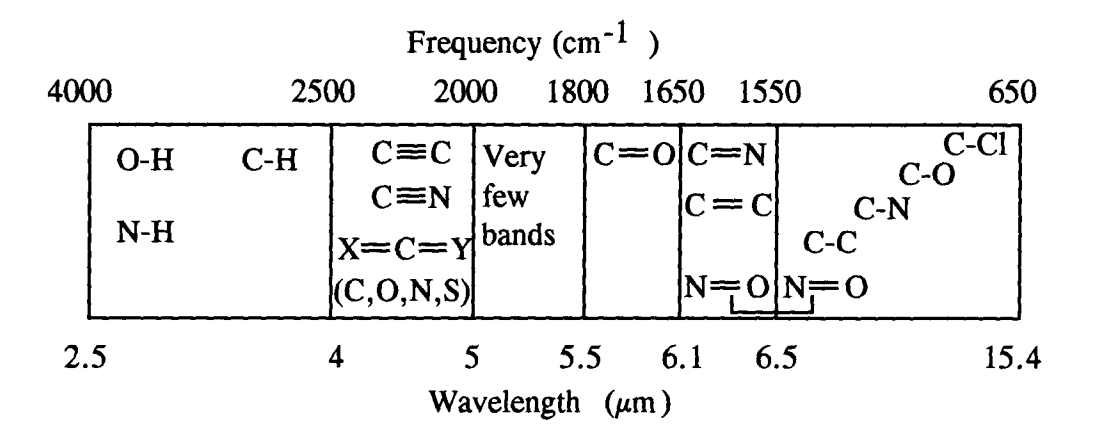


Fig. 14. The approximate regions where various types bonds absorb (stretching vibrations only). Note that frequency is given in wavenumbers  $(\bar{\nu} = 1/\lambda)$  in cm<sup>-1</sup>.

## Nuclear Magnetic Resonance Spectroscopy (nmr)

All nuclei have charge by virtue of containing protons, and behave as though they were spinning. A spinning charge generates a magnetic field, H, and has a magnetic dipole. Nuclear magnetic resonance spectroscopy is the study of the absorption of photons of suitable frequency (radiowave frequency = RF) by certain nuclei when placed in an external magnetic field, resulting in the excitation of their spin states. Spin (I) is a quantized value (I =  $\pm 1/2$ ,  $\pm 1$ ,  $\pm 3/2$ , ...). The simplest nmr spectra are given by nuclei with spin values of 1/2. Therefore, in organic molecules, nmr spectroscopy measures the absorption of energy by  $^{1}$ H,  $^{13}$ C, and  $^{31}$ P nuclei, which all have I = 1/2. An nmr spectrum records increasing magnetic field along the x-axis and increasing intensity of energy absorption along the y-axis. In proton nmr, which only measures absorbances due to protons, every proton in the molecule will generate a peak in the spectrum (Kemp, 1986).

The energy difference between two spin states of a nucleus is dependent upon the applied external magnetic field ( $H_0$ ) and the magnetogyric ratio ( $\gamma$ , a unique property of the nucleus). This relationship is described by the following equation:

$$\Delta E = \gamma (h/2\pi) H_0 = h\nu$$

where  $\nu$  = frequency of absorbed energy/frequency of spinning nucleus h = Planck's constant

Therefore, the frequency of the absorbed energy is  $\nu = (\gamma/2\pi)H_0$ . When the spin of the nucleus is oriented parallel to the applied magnetic field,  $H_0$ , the energy of the spin state is lowest. When the spin is oriented opposite to the applied magnetic field, the energy of the spin state is highest (Fig. 15; Kemp, 1986).

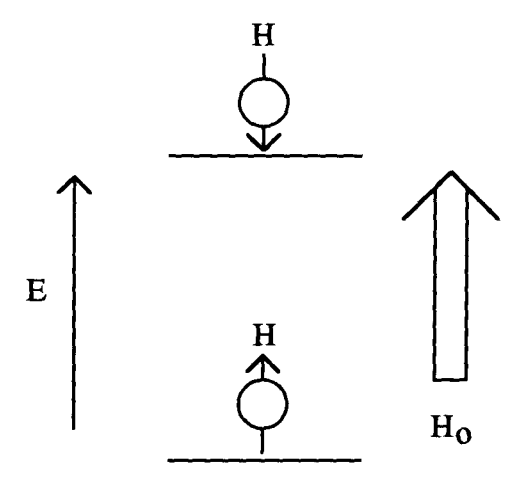


Fig. 15. Orientations of spin states for a nucleus with I = 1/2 in a external magnetic field. E = energy of spin states; H = magnetic field of spinning nucleus;  $H_O = \text{applied magnetic field}$ .

The atoms surrounding a nucleus in a molecule have electrons which can generate induced local magnetic fields that enhance or oppose the applied magnetic field,  $H_0$ , such that the nucleus actually experiences a magnetic field,  $H_i$ , which is different from  $H_0$ . These "shielding" and "deshielding" effects are unique for each molecule, and each proton in the molecule will experience a different  $H_i$ . Therefore, all protons will resonate (precess) at different frequencies and absorb photons of different energies (since  $\nu = (\gamma/2\pi)H_i$ ). This resonance frequency ( $\nu_r$ ) is expressed in terms of its chemical shift in ppm from the resonance frequency of a standard peak ( $\nu_s$ ) (Stevens, 1987):

chemical shift = 
$$\frac{(v_r - v_s)x10^6}{v_s}$$

This explanation of nmr spectroscopy is somewhat simplified. The actual acquisition of an nmr spectrum is quite complex, and a detailed explanation is not within the scope of this introduction.

# a) proton nmr

The most basic nmr experiment, in which resonances due to all the protons in the molecule are observed, is called a proton nmr (Fig. 16). A proton nmr provides three important pieces of information which can be used to determine the structure of a molecule (Bose, 1965):

## 1) chemical shift of a peak

The chemical shift of a peak is characteristic of the electronic and magnetic environment of the proton corresponding to it. Protons attached to oxygen containing groups are "deshielded" and resonate at a higher magnetic field (resulting in a downfield shift towards larger ppm values). Protons attached to groups containing only carbon and hydrogen are "shielded" and resonate at a lower magnetic field (resulting in an upfield shift towards smaller ppm values). Thus, the environment of a proton can be determined by its chemical shift. Chemical shifts for protons in various environments have been determined empirically and have been published in chemical shift tables.

## 2) area under a peak (peak integration)

The area under a peak is proportional to the number of protons responsible for that signal. Therefore, a proton spectrum can be used to calculate the total number of protons in a molecule.

### 3) spin-spin coupling

A nucleus can "sense" the energy state of another nucleus via the agency of the electrons in the chemical bonds separating them. This "coupling" of nuclei is formally called electron-coupled spin-spin interaction. This spin-spin coupling is generally observable only if four or less bonds separate the two interacting nuclei. Spin-spin coupling produces splitting in the peak produced by a proton. For simple systems, the resonance of a given proton

will be split into n+1 lines, where n is the number of neighboring protons. The spacing between the lines in a multiplet will be equal to the coupling constant (J) between the interacting protons. Therefore, the number of near neighbors a proton has can be determined from the splitting patterns in an nmr spectrum.

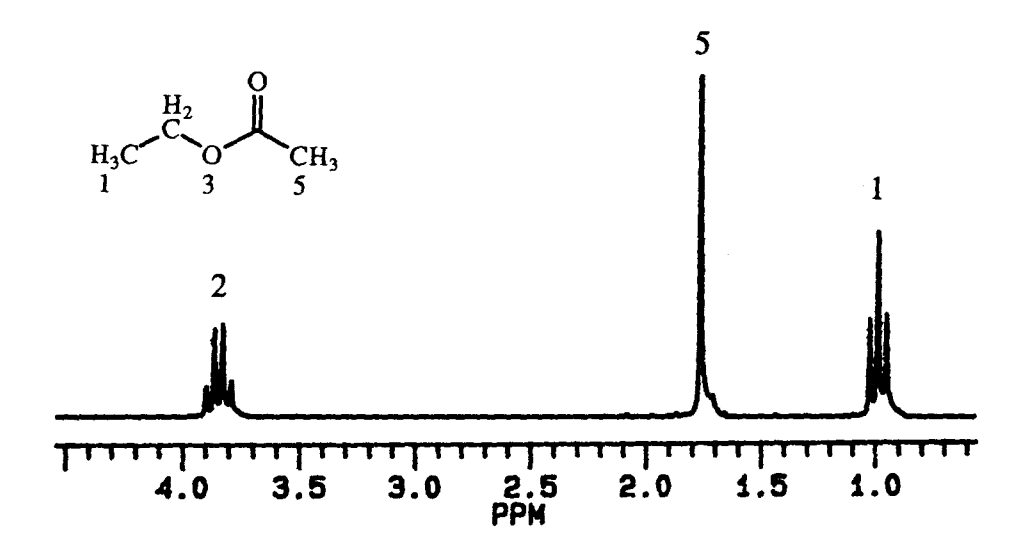


Fig. 16. A proton nmr spectrum for the compound ethyl acetate. The numbers on the structural model of ethyl acetate represent the protons at those positions in the molecule. The numbers associated with peaks in the spectrum indicate which protons are responsible for each peak. Note that protons at position 1 in the molecule produce a signal which has three lines (2 neighbors + 1 = triplet), the protons at position 2 produce a signal which has four lines (3 neighbors + 1 = quartet), and the protons at position 5 produce a signal with no splitting (0 neighbors + 1 = singlet). The areas under the signals in the spectrum have the ratio 3: 2: 3 for position 1 protons: position 2 protons: position 5 protons. Protons at position 5, which are in close proximity to an oxygen atom, are deshielded relative to protons at position 1, and have a chemical shift which is further downfield.

# b) <sup>1</sup>H - <sup>1</sup>H COSY (homonuclear <u>correlation spectroscopy</u>)

In a complex proton nmr spectrum, it is often quite difficult to observe and interpret the spin-spin coupling between protons, as peaks may be overlapping or coupled systems may not obey the n+1 rule. To obtain more information on proton

coupling, additional nmr experiments must be performed. The simplest of these is called a double irradiation experiment. In this experiment, there is a selective irradiation of a particular proton in the molecule with an RF (radio frequency) field at the same frequency at which that proton resonates. The resulting effects of this irradiation on the rest of the protons in the molecule are observed. In this type of experiment, the spin-spin couplings due to the irradiated proton disappear from all other resonances in the spectrum. By comparing the coupling patterns in the irradiated spectrum with the patterns in a nonirradiated spectrum, one can determine which protons are coupled to the irradiated proton. An irradiation experiment is termed a one-dimensional (1-D) nmr. If one wanted to determine all the proton couplings in a molecule, one could perform an irradiation experiment on every proton in the molecule. This would generate a data set in which the independent variable would be the proton being irradiated (given as a chemical shift, ppm) and the dependent variable would be the protons coupled to the irradiated proton (given as chemical shifts, ppm). However, such a series of experiments requires a great deal of time and work, and the results may be ambiguous if there is overlap in the proton signals (Wüthrich, 1986).

A 2-D COSY (<sup>1</sup>H -<sup>1</sup>H COSY) is basically equivalent to a series of 1-D irradiation experiments for each proton in the spectrum, although the process by which the data is acquired is much different. Two-dimensional nmr experiments rely on pulsing the nuclei with a series of RF pulses at specific angles to the applied magnetic field, Ho, and at specific time intervals to generate the data set. Instead of performing a number of separate experiments, all the data is collected in one experiment by varying a single experimental parameter throughout the experiment (for more information on the acquisition of 2-D nmr spectra, refer to Benn and Gunther, 1983). Chemical shift information is contained in the positions of the peaks ("diagonal peaks" shown by contour lines) along the diagonal from the upper right to the lower left. Couplings between individual peaks are manifested by "cross-peaks" located at the

intersection of straight lines parallel to the x and y-axes through the diagonal peaks. A COSY spectrum allows one to "walk" through all the couplings in a spin system (a group of coupled protons) simply by connecting the cross peaks to the diagonal peaks (Fig. 17; Wüthrich, 1985).

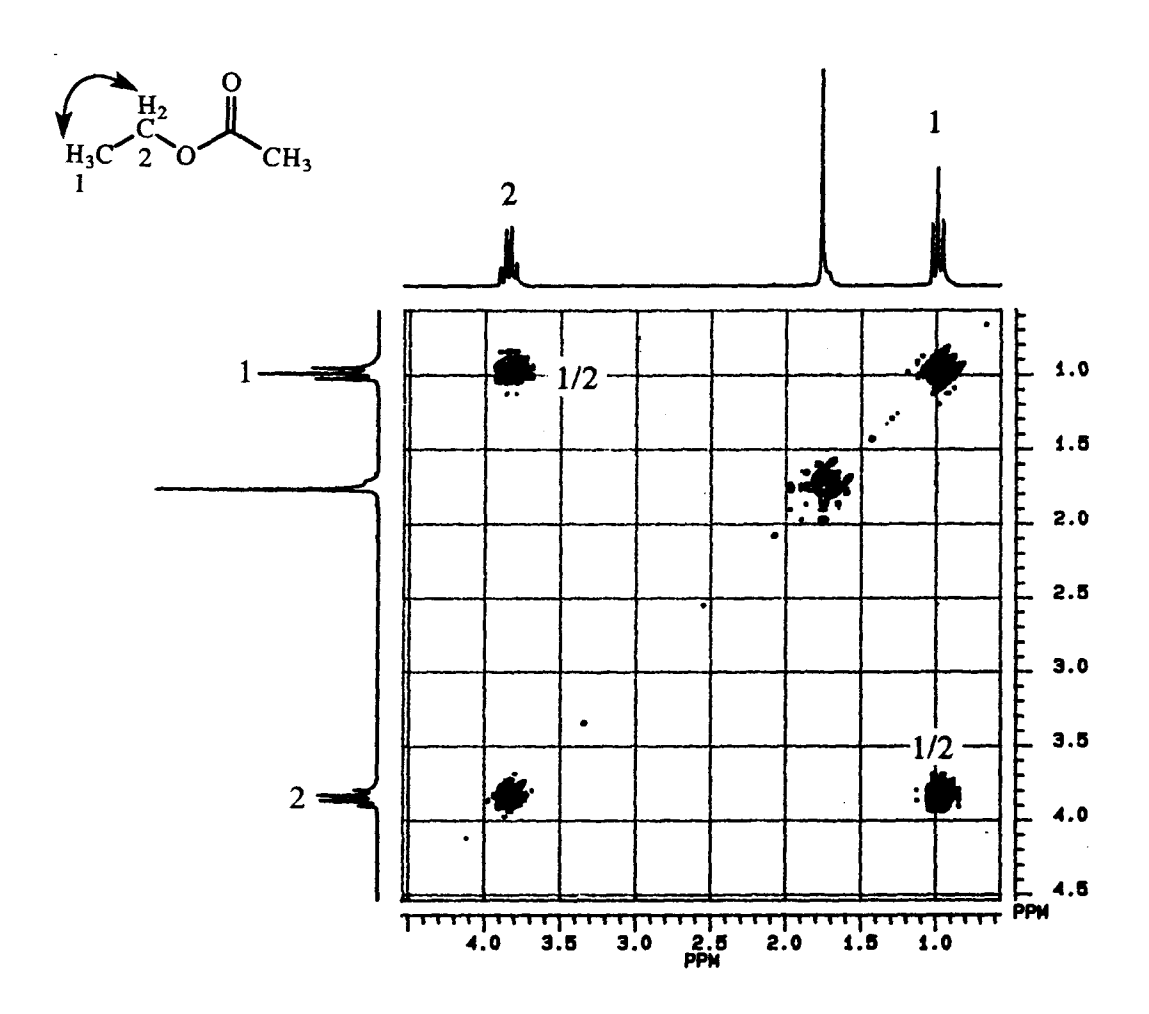


Fig. 17. A <sup>1</sup>H-<sup>1</sup>H COSY spectrum for ethyl acetate. Note the cross-peaks which indicate coupling between protons at positions 1 and 2. This coupling is represented by an arrow in the structural model of ethyl acetate. All cross peaks are reflected across the diagonal in a COSY, so that there are two cross peaks for any given coupling, and the COSY spectrum is symmetrical about the diagonal.

## **Mass Spectrometry**

Mass spectrometry is based on the principle that it is possible to obtain the mass-to-charge ratio (m/e or m/z) of an ion in gas phase. Since multicharged ions are much less abundant than those with a single electronic charge, then, in practice, m/e is equal to the mass of the ion, M. A mass spectrometer performs three essential functions (Fig. 18; Pavia et al., 1979):

- 1) it converts molecules into ions and accelerates these ions in an electric field.
- 2) it separates the accelerated ions according to m/e ratio in a magnetic or electric field.
- 3) it detects ions with a particular m/e ratio using a device which is able to count the number of ions which strike it. The output from this detector is amplified and fed to a recorder which produces a graph with the number of particles detected as a function of the m/e ratio. This graph is the mass spectrum.

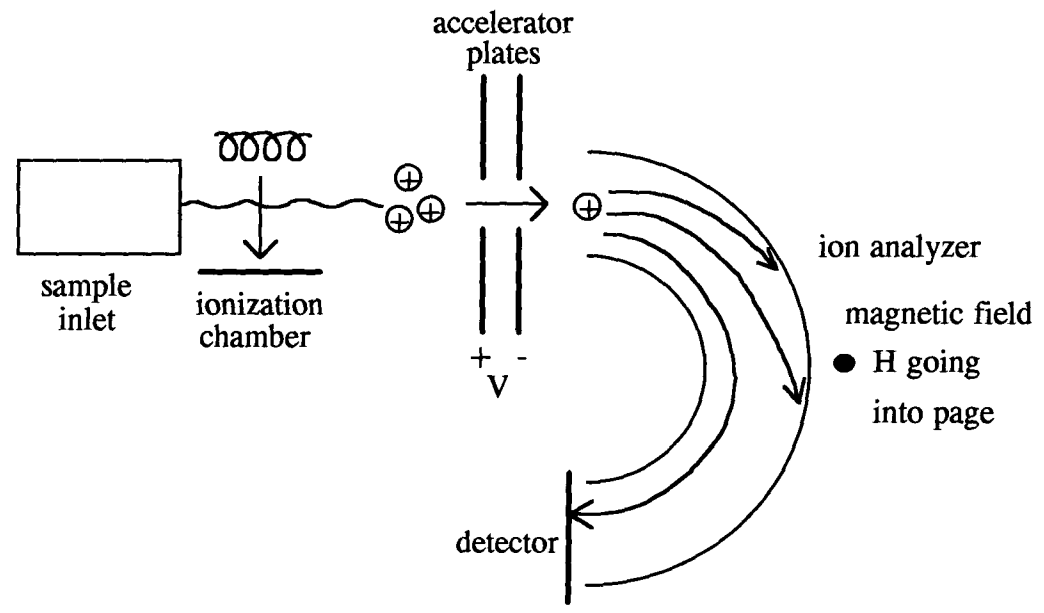


Fig. 18. A schematic of a simple mass spectrometer. V = voltage across accelerator plates; H = applied magnetic field.

## a) ion source

In this research, desorption chemical ionization (DCI) was used to ionize the sample. Positive ions are generated by electron bombardment of an excess of reagent gas, usually methane (CH<sub>4</sub>) or ammonia (NH<sub>3</sub>). The sample is applied to a suitable probe which is inserted directly into the reagent ion plasma. A programmed heating current is used to "distill" the sample from the probe, and sample molecules are ionized by collision with the positive ions from the reagent gas (Harrison, 1992). DCI is considered a "gentle" ionization technique, and weak bonds are left intact. Therefore, the primary peak in the mass spectrum is usually [M+H]+ (where M+ is the molecular ion). Using NH<sub>3</sub> as the reagent gas, the following reactions occur:

- 1) NH<sub>3</sub> + e<sup>-</sup> → NH<sub>3</sub><sup>+</sup> · + 2e<sup>-</sup>
   (an electron is removed from the reagent gas molecule by high energy electron bombardment)
- 2)  $NH_3^+ \cdot + NH_3 \rightarrow NH_4^+ + NH_2 \cdot$  (stabilization of the reagent gas ion)
- 3)  $NH_4^+ + M \rightarrow NH_3 + MH^+$

(proton exchange between the sample molecule and the ionized reagent gas)

## b) ion analyzer

The most common ion analyzer uses the principle that a magnetic field causes ions to be deflected along curved paths defined by the m/e ratio and kinetic energy (KE) of the ion. The KE of an ion is defined:

$$KE = eV = \frac{1}{2}mv^2$$
  
where  $KE = \text{kinetic energy of ion}$   
 $e = \text{charge on ion}$   
 $m = \text{mass of ion}$ 

v = velocity of ion

V = accelerating voltage

Thus,  $v = \sqrt{\frac{2eV}{m}}$ . To get the ion to travel in a curved path within the ion analyzer chamber, centripetal and centrifugal forces must be equal:

$$\frac{\text{mv}^2}{\text{r}} = \text{HeV}$$

where r = radius of curve

H = magnetic field strength

Therefore, for an ion analyzer using magnetic deflection,  $\frac{m}{e} = \frac{H^2 r^2}{2V}$ . Either the accelerating voltage (V) or the magnetic field strength (H) is continuously varied in order to detect all of the ions produced in the ionization chamber (Pavia *et al.*, 1979).

A mass spectrum gives the following information for a molecule:

- 1) the molecular weight of the molecule.
- 2) parts of the molecular structure. The ionized sample molecule may be unstable and can break up or fragment during the ionization process. These "fragments" can be used as clues to determine the chemical structure of a compound, as fragmentation patterns are typical of certain structural features in a molecule.

#### **B.** Materials and Methods

#### i. Phytoplankton Cultures

The source and maintenance of stock unialgal cultures of *Phaeodactylum* tricornutum Bohlin (NEPCC #640) were described in Chapter 2. Culturing conditions were the same as described in Chapter 2, with the following changes. Seawater used for culturing was filter sterilized using a 0.45  $\mu$ m Millipore filter. Cultures were grown in 120 L plastic bags at an irradiance of  $\approx 100 \ \mu$ mol m<sup>-2</sup> s<sup>-1</sup> with a L:D cycle of 18:6 h and at a temperature of 18°C. The cultures were aerated vigorously with air filtered through a GF/F filter. Cultures were harvested in late log or early senescence phase.

Cell culture (360 L) was harvested by gentle filtration through a 5  $\mu$ m Nitex screen. The cells were rinsed from the screen with methanol and collected in a grinding tube. Cellular extracts of the phytoplankton cells were obtained by grinding the harvested cells in methanol and rinsing the cell debris repeatedly in methanol until all the pigments were removed. This methanolic extract was filtered through a GF/F glass fiber filter to remove remaining cell debris. The methanolic extract then underwent rotary evaporation to produce a gummy oil.

### ii. Chromatography

The methanolic extract yielded 20.4 g of a dark green oil. This oil was divided into 3 portions, and each portion processed as follows. The oil was dissolved in 10 ml of 0.05 M sulfuric acid and extracted with 50 ml of diethyl ether. The organic phase was dried, dissolved in 25 ml of 80% ethanol and extracted with 4 x 25 ml n-hexane. The ethanolic phase was dried, dissolved in 20 ml of 0.45 M sodium hydroxide and extracted with 50 ml diethyl ether. The organic phase was dried to give a brown gum. The three portions of brown gum were combined (1.88 g).

A portion (630 mg) of the brown gum was dissolved in 20% ethanol and applied to two C-18 sep-paks (in series). The sep-paks were rinsed with 20% ethanol and the active material was eluted with ethyl acetate (yield 360 mg). This material was chromatographed on a silica gel short column (Taber, 1982) with ethyl acetate/dichloromethane (1:1) to give 4 fractions: A (green), B (yellow), C (orangered), D (blue-green). Fraction B (230 mg) was active. Further purification was carried out on a 1 g silica gel short column in chloroform giving fractions B1 (yellow, active) and B2 (orange-red). Final purification of B1 was carried out by HPLC (Econosil C-18, 5  $\mu$ m column, 1 = 250 mm, I.D. = 4.6 mm; gradient system #1: methanol/water/ethyl acetate (40:50:10 to 35:45:20), 0.7 ml/min, 90 min run). Yield of pure apo-10'-fucoxanthinal (1) and apo-12'-fucoxanthinal (2) was  $\approx$  1 mg each.

A second portion (1.25 g) of the brown gum was chromatographed on a 10 g silica gel (TLC grade) vacuum column packed in a buchner funnel using dichloromethane/ethyl acetate/acetic acid (25:25:1) to yield 3 fractions: X (green), Y (active, red-orange), Z (blue-green). Fraction Y was dried and pumped under vacuum to remove the acetic acid, and applied to a 10 g silica gel short column and eluted with dichloromethane/ethyl acetate (1:1) to give 4 fractions: Y1 (green), Y2 (active, yelloworange), Y3 (red-orange), Y4 (blue-green). Y2 was further purified on an alumina (grade IV) column using 5% acetone in hexane to give 3 fractions: Y21 (active, yellow), Y22 (orange), Y23 (orange-red). Final purification of Y21 was carried out by HPLC (Econosil C-18, 5  $\mu$ m column, 1 = 250 mm, I.D. = 4.6 mm; gradient system #2 (for apo-12-fucoxanthinal (3)): methanol/water/ethyl acetate (65:25:10 to 65:0:35), 0.7 ml/min, 60 min run; gradient system #3 (for apo-13'-fucoxanthinone (4)): methanol/water/ethyl acetate (40:50:10 to 0:0:100), 0.7 ml/min, 80 min run). Yield of pure apo-12-fucoxanthinal (3) and apo-13'-fucoxanthinone (4) was < 1 mg each.

## iii. Feeding Deterrent Bioassays for Bioassay-guided Chemical Fractionation

A weighed amount of dried material to be bioassayed was dissolved in 5 ml of autoclaved seawater and sonicated (1 min in bath sonicator at 60 Hz) to facilitate mixing. If the material to be tested was not soluble in seawater, it was dispersed using 4 drops of dimethylsulfoxide (DMSO). When DMSO was used to dissolve the extract, it was also added to the control. Five ml of an exponentially growing culture of the diatom Thalassiosira pseudonana was added to the dissolved cell extract. If the cell cultures were clumped, cell clumps were broken up using mild sonification (1 min in bath sonicator at 60 Hz) and filtration (forced through a 200  $\mu$ m screen at a rate of  $\approx$ 50 ml min<sup>-1</sup> using a syringe; repeated 4 times). This mixture was placed in one well (volume ≈ 15 ml) of a tissue culture plate and two male C6 copepods (Tigriopus californicus) were added. The assay was incubated for ≈20 h at 18°C with an irradiance of  $\approx 100 \,\mu\text{mol m}^{-2}\,\text{s}^{-1}$  and a L:D cycle of 18:6. Copepods were preconditioned in autoclaved seawater without food for 24 h prior to the bioassay. Copepods were pretreated with antibiotics if they were heavily contaminated with bacteria. Degree of feeding inhibition was measured by counting fecal pellets. Six replicates were done. A control was done using a cell extract from T. pseudonana (which has no feeding deterrent effects on T. californicus). Data were analyzed by analysis of variance (ANOVA) to determine statistical significance.

#### iv. Semi-synthetic Procedure

Fucoxanthin was isolated by the method described by Haugen and Liaaen-Jensen (1989) from the brown seaweed *Fucus distichus* collected from Copper Cove, West Vancouver, British Columbia on March 6, 1993. Zinc permanganate (Zn(MnO<sub>4</sub>)<sub>2</sub>) was prepared based on the methodology by Lux (1965) and Wolfe and Ingold (1983). The fucoxanthin (1.2 g) was oxidized with Zn(MnO<sub>4</sub>)<sub>2</sub> based on the method described by Bonnett *et al.* (1969). The reaction mixture was chromatographed on an alumina

(grade IV) column using 5% acetone in hexane to give 3 fractions: E (pale yellow), F (orange), G (dark orange), H (red-orange). Fraction G (12.9 mg) was purified on HPLC (system #1) to give 1.6 mg apo-10'-fucoxanthinal (1) and 1.8 mg apo-12'-fucoxanthinal (2). Fraction F (18.3 mg) was purified on HPLC (systems #2 and #3) to give 0.2 mg each of apo-12-fucoxanthinal (3) and apo-13'-fucoxanthinone (4).

## v. Spectroscopy

<sup>1</sup>H 1-D NMR and 2-D COSY experiments were carried out on either a 400 MHz or a 500 MHz Bruker instrument. Mass spectra were obtained by desorption chemical ionization using either a Nermag R10-10C (for low resolution spectra) or a Kratos MS80RFA (for high resolution spectra) mass spectrometer. Infrared spectroscopy was done on a Perkin-Elmer 1600 Series Fourier Transform IR spectrometer. Ultraviolet-visible spectroscopy was done on an LKB Ultraspec II spectrophotometer (Berges and Virtanen, 1993).

#### C. Results and Discussion

## i. Chromatography

Crude methanolic extracts of the diatom *Phaeodactylum tricornutum* were found to have feeding deterrent activity against adult C6 males of the copepod *Tigriopus* californicus (Chapter 2). In order to determine which compounds in the crude extract were responsible for this activity, various chromatographic methods were employed to isolate these active compounds. Results from the feeding deterrent bioassay were used to guide the chemical fractionation and isolation of the active components. Figures 19, 20, and 21 illustrate the various chromatographic techniques used to isolate the feeding deterrent compounds, and the use of the bioassay to track feeding deterrent activity through the fractionation scheme. Four active feeding deterrents were isolated in trace

(< 1 mg) amounts. These compounds tended to track with the orange-yellow carotenoid pigments throughout most of the isolation procedures, and compounds (1),</li>
(2), and (3) were a yellow color. All four compounds contained impurities. However, with such trace amounts, further chromatographic purification was not practical.

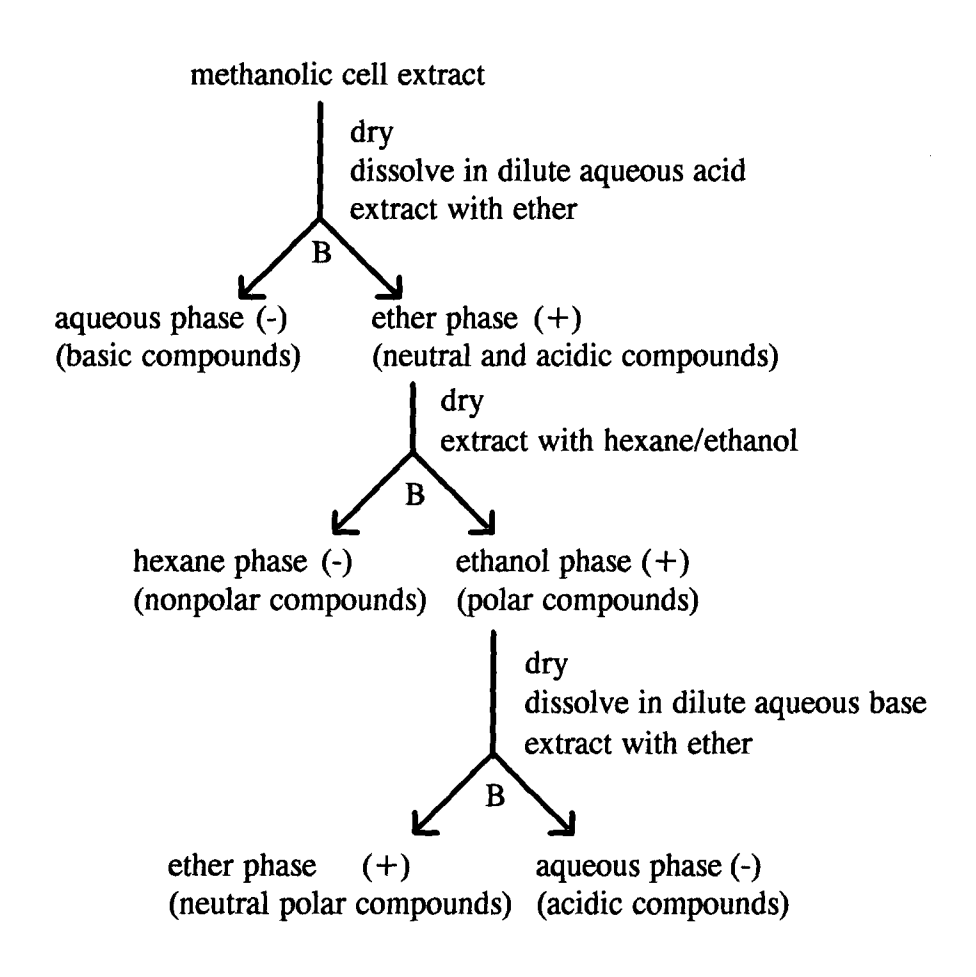


Fig. 19. Preliminary isolation scheme for feeding deterrent compounds using solvent-solvent extractions and acid-base properties of molecules. B indicates points in the scheme where bioassays were performed. (+) = feeding deterrent activity; (-) = no feeding deterrent activity.

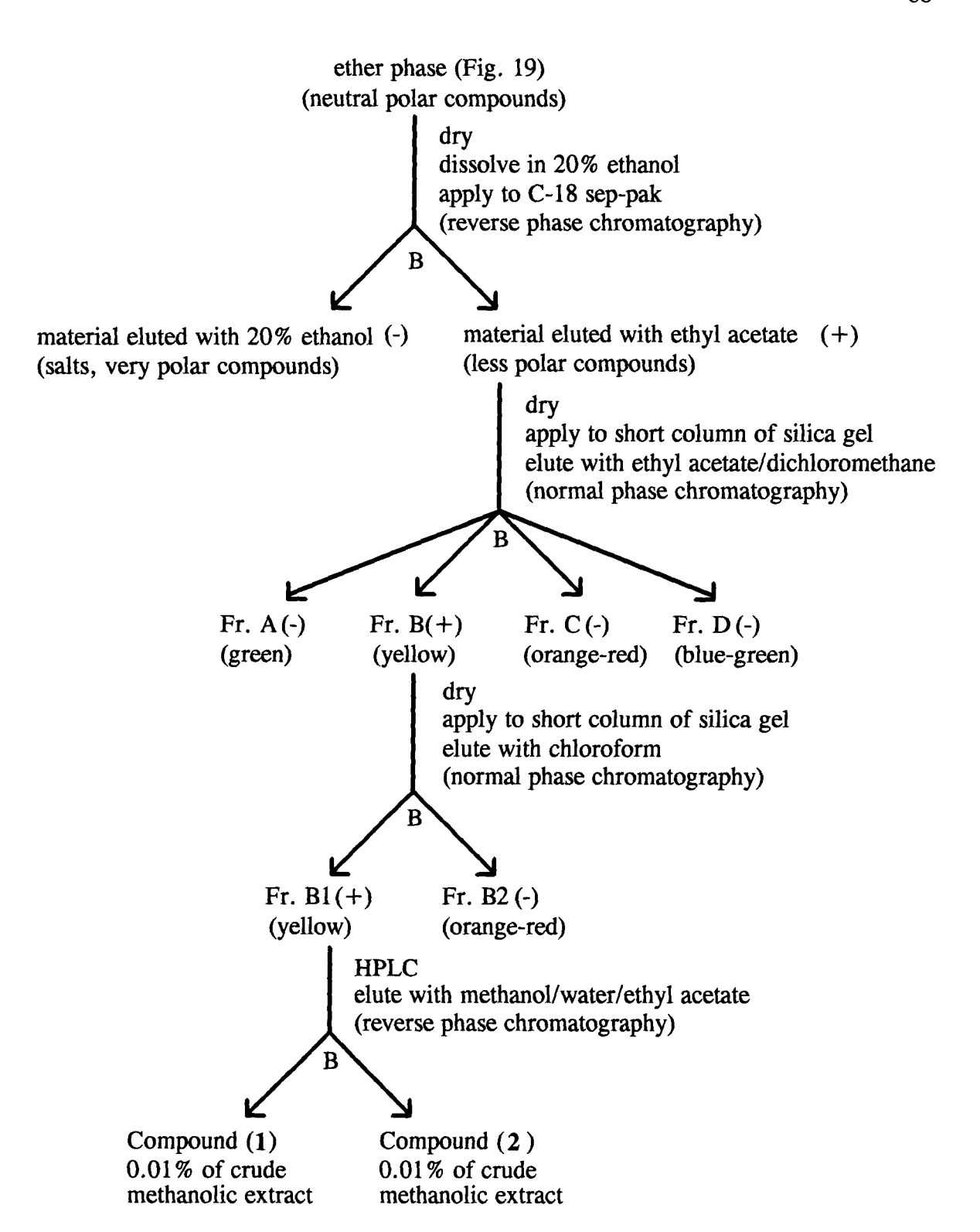


Fig. 20. Isolation scheme for feeding deterrent compounds (1) and (2). B indicates points in the scheme where bioassays were performed. (+) = feeding deterrent activity; (-) = no feeding deterrent activity.

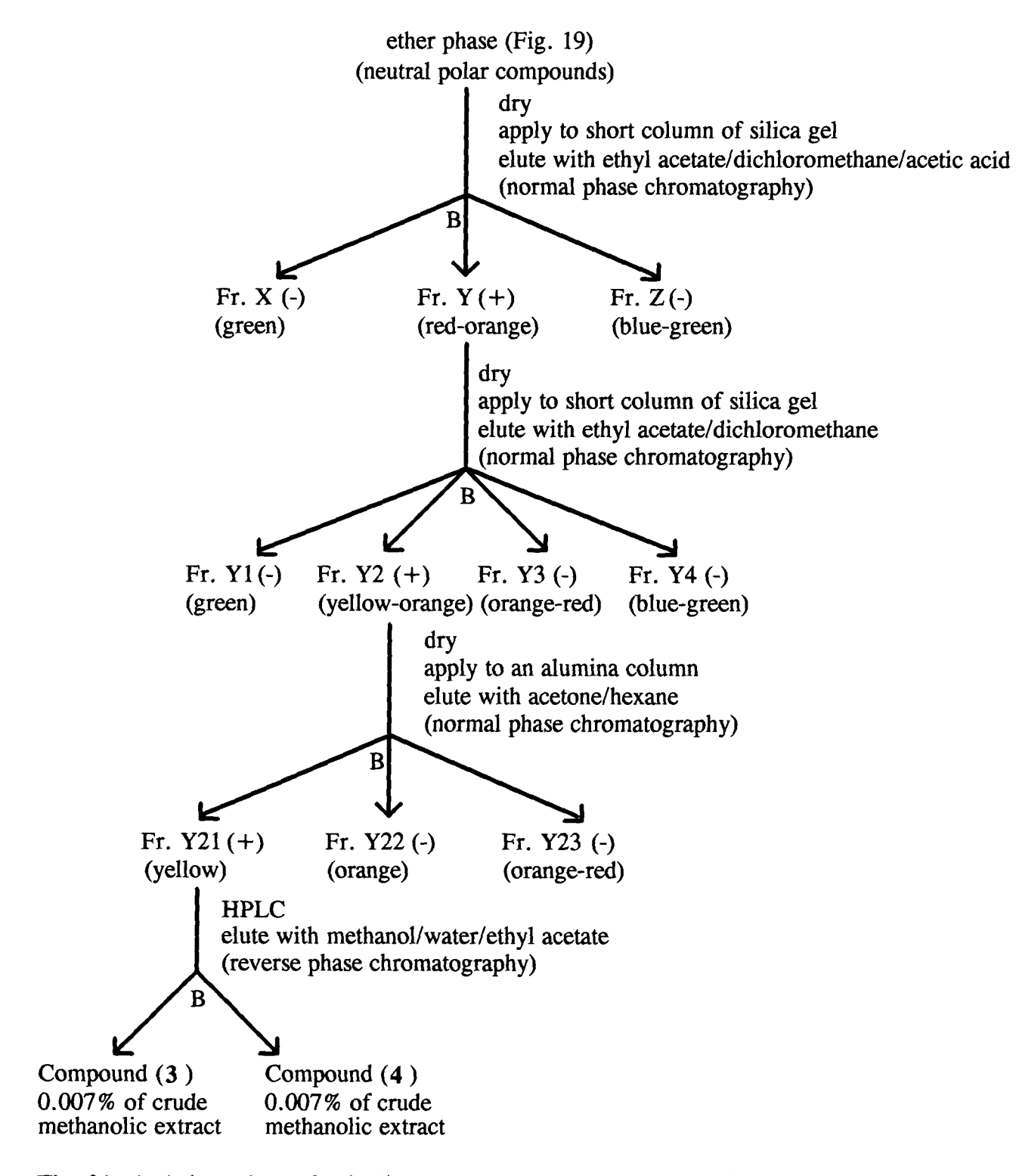


Fig. 21. Isolation scheme for feeding deterrent compounds (3) and (4). B indicates points in the scheme where bioassays were performed. (+) = feeding deterrent activity; (-) = no feeding deterrent activity.

## ii. Spectroscopy

Four compounds with feeding deterrent activity were isolated from the crude cellular extracts of the diatom *Phaeodactylum tricornutum*. In order to determine the chemical structures of these four compounds, several spectroscopic methods were used to provide information about structural aspects of the molecules. These methods were mass spectrometry, ultraviolet-visible spectroscopy, infrared spectroscopy, and nuclear magnetic resonance spectroscopy.

## Natural Compounds

The compounds isolated from *Phaeodactylum tricornutum* cell extract (which will be referred to as the "natural" compounds) were present in very small quantities. This made analysis by spectroscopic methods difficult. However, it was possible to obtain a low resolution DCI mass spectrum for all four compounds (Appendix E, Figs. E1 - E4), a high resolution DCI mass spectrum for three of the four compounds, and a proton nmr spectrum for all the compounds (Appendix E, Figs. E5 - E17). As three of the compounds were yellow in color, it was believed that the compounds were xanthophylls. Comparison of the mass spectrometry and nmr data obtained for these compounds with that given by Bonnett *et al.* (1969), tentatively identified three of the four compounds as apo-10'-fucoxanthinal (1), apo-12'-fucoxanthinal (2), and apo-12-fucoxanthinal (3) (Tables 2 and 3). By extrapolation, the fourth compound was suspected to be apo-13'-fucoxanthinone (4). However, impurities present made it unclear as to whether the biological activity was due to these identified compounds or the impurities.

Table 2. Desorption chemical ionization mass spectrometry data for the four isolated feeding deterrent compounds. Note that the molecular ion is [M+H]<sup>+</sup> for DCI-MS. An high resolution DCI-MS was not obtained for compound (3) as the sample decomposed before the spectrum could be taken. This is not surprising, as Bonnett *et al.* (1969) reported this compound as unstable.

Compound	Low resolution DCI-MS (MH+)	High resolution DCI-MS (MH+)	Deviation (ΔM) (ppm)
Apo-10'-fucoxanthinal (1)	425	425.2694	0.3
Apo-12'-fucoxanthinal (2)	399	399.2560	2.5
Apo-12-fucoxanthinal (3)	425	-	-
Apo-13'-fucoxanthinone (4)	333	333.2050	-1.6

**Table 3.** Comparison of proton nmr chemical shifts (in ppm relative to internal TMS) for four feeding deterrent compounds with literature values from Bonnett *et al.* (1969). Peak multiplicity abbreviations: s = singlet; d = doublet; dd = doublet of doublets; m = multiplet.

Position	Apo-12-fucoxanthinal (3)		Apo-13'-fucoxanthinone (4)	
	Measured, ppm	Literature,	Measured, ppm	Literature,
	in CD <sub>2</sub> Cl <sub>2</sub>	ppm in CDCl <sub>3</sub>	in CD <sub>2</sub> Cl <sub>2</sub>	ppm in CDCl <sub>3</sub>
16'-CH <sub>3</sub>	1.34 (s)	1.33 (s)	1.35 (s)	unknown
17'-CH <sub>3</sub>	1.08 (s)	1.08 (s)	1.08 (s)	unknown
CH <sub>3</sub> (OAc)	2.01 (s)	1.97 (s)	2.01 (s)	unknown
18'-CH <sub>3</sub>	1.36 (s)	1.33 (s)	1.37 (s)	unknown
19'-CH <sub>3</sub>	1.84 (s)	1.83 (s)	1.91 (s)	unknown
20'-CH <sub>3</sub>	2.04 (s)	2.04 (s)	2.25 (s)	unknown
20-CH <sub>3</sub>	1.86 (s)	1.83 (s)	NA	NA
2'-CH <sub>2</sub>	-,-	-,-	-,-	unknown
4'-CH <sub>2</sub>	-,-	-,-	-,-	unknown
3'-CH	-	-	-	unknown
8'-CH	6.08 (s)	-	6.10 (s)	unknown
10'-CH	$\sim 6.15 \text{ (d)}$	-	6.12 (d)	unknown
11'-CH	$\sim 6.74 \text{ (dd)}$	-	7.46 (dd)	unknown
12'-CH	6.38 (d)	-	6.17 (d)	unknown
14'-CH	6.32 (d)	-	NA	NA
15'-CH	7.06 (dd)	-	NA	NA
15-CH	$\sim 6.66 \text{ (dd)}$	-	NA	NA
14-CH	6.96 (d)	-	NA	NA
12-CH	9.43 (s)	9.48 (s)	NA	NA

Table 3. Continued.

Position	Apo-10'-fucoxanthinal (1)		Apo-12'-fucoxanthinal (2)	
	Measured, ppm in		Measured, ppm	Literature,
	$C_6D_6$	in CDCl <sub>3</sub>	in $C_6D_6$	ppm in CDCl <sub>3</sub>
16-CH <sub>3</sub>	1.09 (s)	1.04 (s)	1.09 (s)	1.04 (s)
17-CH <sub>3</sub>	1.01 (s)	0.96 (s)	1.00 (s)	0.96 (s)
18-CH <sub>3</sub>	1.24 (s)	1.22 (s)	1.24 (s)	1.22 (s)
19-CH <sub>3</sub>	1.72 (s)	1.95 (s)	1.78 (s)	1.95 (s)
20-CH <sub>3</sub>	1.48 (s)	1.99 (s)	1.67 (s)	1.87 (s)
20'-CH <sub>3</sub>	1.91 (s)	1.96 (s)	1.91 (s)	1.91 (s)
2-CH <sub>2</sub>	-,-	-,-	-,-	-,-
4-CH <sub>2</sub>	-,2.22 (dd)	-,-	-,-	-,-
7-CH <sub>2</sub>	2.63 (d), 3.53 (d)	2.60 (d), -	2.63 (d), 3.52 (d)	2.57 (d), -
3-CH	3.80 (m)	-	3.80 (m)	-
10-CH	6.24 (d)	-	6.14 (d)	-
11-CH	6.60 (dd)	-	6.56 (dd)	-
12-CH	6.45 (d)	-	6.44 (d)	-
14-CH	6.12 (d)	-	6.40 (d)	-
15-CH	6.43 (dd)	-	-	-
15'-CH	6.52 (dd)	-	6.42 (dd)	-
14'-CH	-	-	6.53 (d)	-
12'-CH	6.62 (d)	-	9.43 (s)	9.45 (s)
11'-CH	6.12 (dd)	-	NA	NA
10'-CH	9.55 (d)	9.62 (d)	NA	NA

# Semi-synthetic Compounds

In order to confirm the spectroscopic identification of the four feeding deterrent compounds, and to resolve the problems with impurities in the natural compounds, the four compounds were prepared semi-synthetically from fucoxanthin, as these compounds are clearly related to fucoxanthin. Fucoxanthin (Fig. 22) is a major carotenoid pigment in both diatoms and macroscopic brown algae. However, brown algae and diatoms are otherwise quite unrelated. Therefore, compounds produced semi-synthetically from fucoxanthin isolated from a brown seaweed, *Fucus distichus*, should contain impurities which are different from the ones associated with compounds derived naturally from fucoxanthin in the diatom *Phaeodactylum tricornutum*. Using

this rationale, the four feeding deterrent compounds were prepared semi-synthetically by oxidative cleavage of fucoxanthin using zinc permanganate. This reaction is non-specific, and produced a number of cleavage products in addition to the four desired ones. As a result, yields were low ( $\approx 0.1\%$  for compounds (1) and (2) and  $\approx 0.01\%$  for compounds (3) and (4)). These compounds were isolated and purified using a chromatographic scheme similar to the ones described previously.

Fig. 22. Structure and numbering scheme for the carotenoid fucoxanthin.

# a) Apo-10'-fucoxanthinal (Fig. 23)

Fig. 23. Structure and numbering scheme for apo-10'-fucoxanthinal (1).

A low resolution DCI mass spectrum of the semi-synthetic apo-10'-fucoxanthinal gave an  $[M+H]^+$  peak at 425 (Fig. 24). High resolution DCI mass spectrometry gave a value for  $[M+H]^+$  of 425.2683 (deviation = -2.2 ppm). These

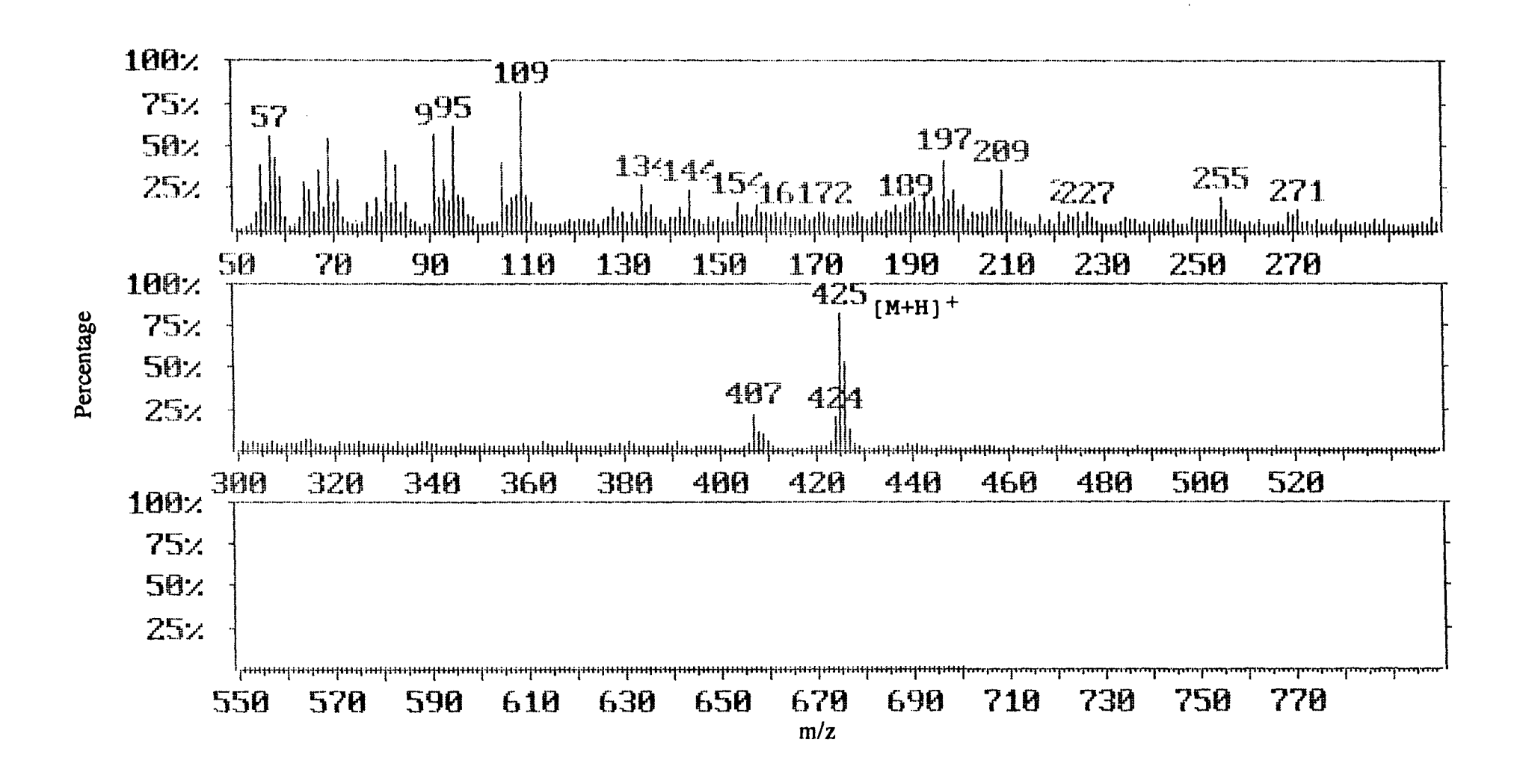


Fig. 24. Low resolution DCI mass spectrum of semi-synthetic apo-10'-fucoxanthinal (1) using NH3 as the reagent gas.

results are in good agreement with the mass spectrometry results for the natural apo10'-fucoxanthinal (Appendix E, Fig. E1; Table 2), indicating that the natural and semisynthetic materials are indeed the same compounds. In both of these materials, one of
the major fragment ions shown in the low resolution DCI mass spectrum was at an m/z
value of 197. This peak can be explained by the loss of the long carbon chain from the
molecule, as shown in Figure 25.

Fig. 25. Fragmentation pattern ( $\alpha$ -cleavage) of apo-10'-fucoxanthinal (1), explaining the peak at 197 in the DCI mass spectrum.

The proton nmr spectrum of apo-10'-fucoxanthinal indicated that there were six methyl groups, nine olefinic protons, one aldehyde proton, one methine proton, and six methylene protons (Figs. 26 - 29; Table 4). The chemical shift values for these protons match those for the natural apo-10'-fucoxanthinal (Tables 3 and 4). The relationships between these protons were established by a  ${}^{1}H^{-1}H$  COSY nmr experiment (Figs. 30 - 34). The olefinic proton H-11' correlated with the olefinic proton H-12' and the

aldehyde proton H-10', forming an AMX coupling pattern (a spin system containing three protons, A, M, and X, which are separated by large chemical shifts [Δppm > J/50]). A second AMX pattern was formed by H-11 coupling with H-10 and H-12. A four proton spin system was observed with the protons H-14, H-15, H-15', and H-14'. This was an AMNX spin system, with M and N separated by a small chemical shift (Δppm < J/50) and A and M and N and X separated by large chemical shifts. The methylene protons, H-2a and H-2b, were geminally coupled (coupling between protons on the same carbon atom), and coupled to the methine proton, H-3. The geminally coupled methylene protons, H-4a and H-4b, were also coupled to H-3. The isolated methylene protons, H-7a and H-7b, showed geminal coupling as well. Allylic coupling of olefinic protons with methyl protons was seen between the H-20' methyl and the H-14' methine protons, between the H-19 methyl and the H-10 methine protons, and between the H-20 methyl and the H-14 methine protons.

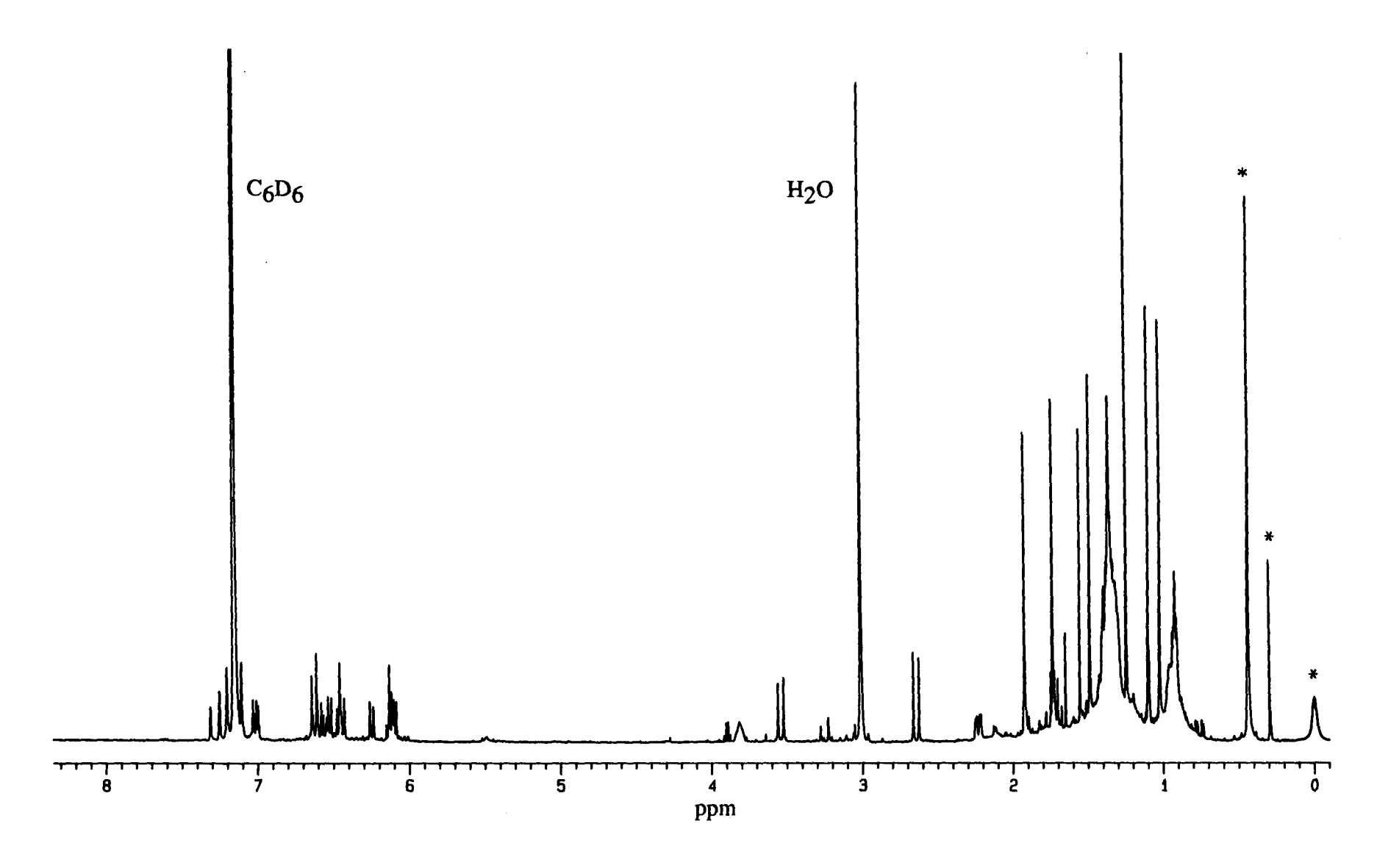


Fig. 26. Proton nmr (500 MHz) spectrum of semi-synthetic apo-10'-fucoxanthinal (1) in C<sub>6</sub>D<sub>6</sub>. \* denotes minor grease impurities.

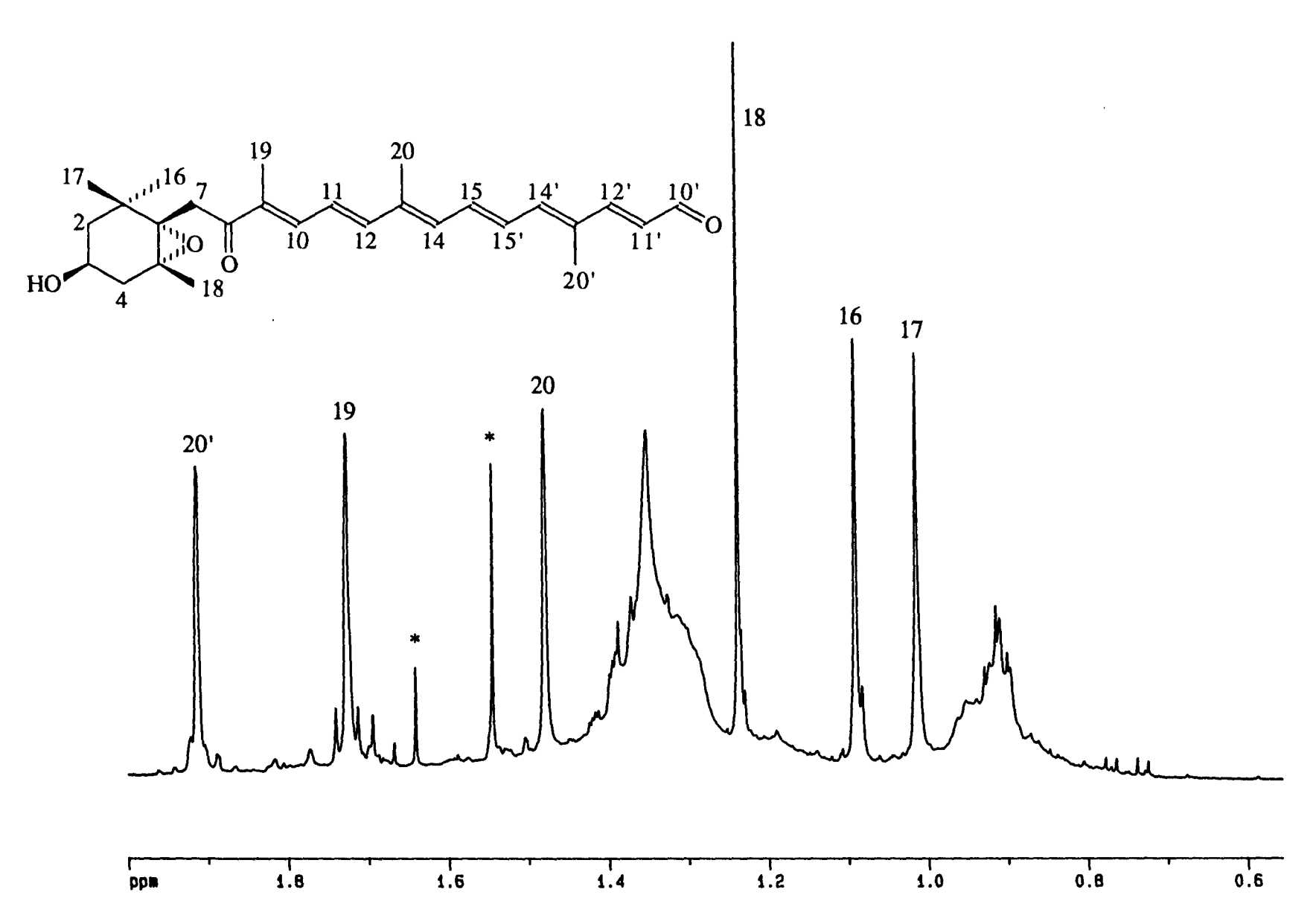


Fig. 27. Expansion of the proton nmr (500 MHz) spectrum of semi-synthetic apo-10'-fucoxanthinal (1) in C<sub>6</sub>D<sub>6</sub> showing the resonances from the methyl groups. \* denotes minor impurities.

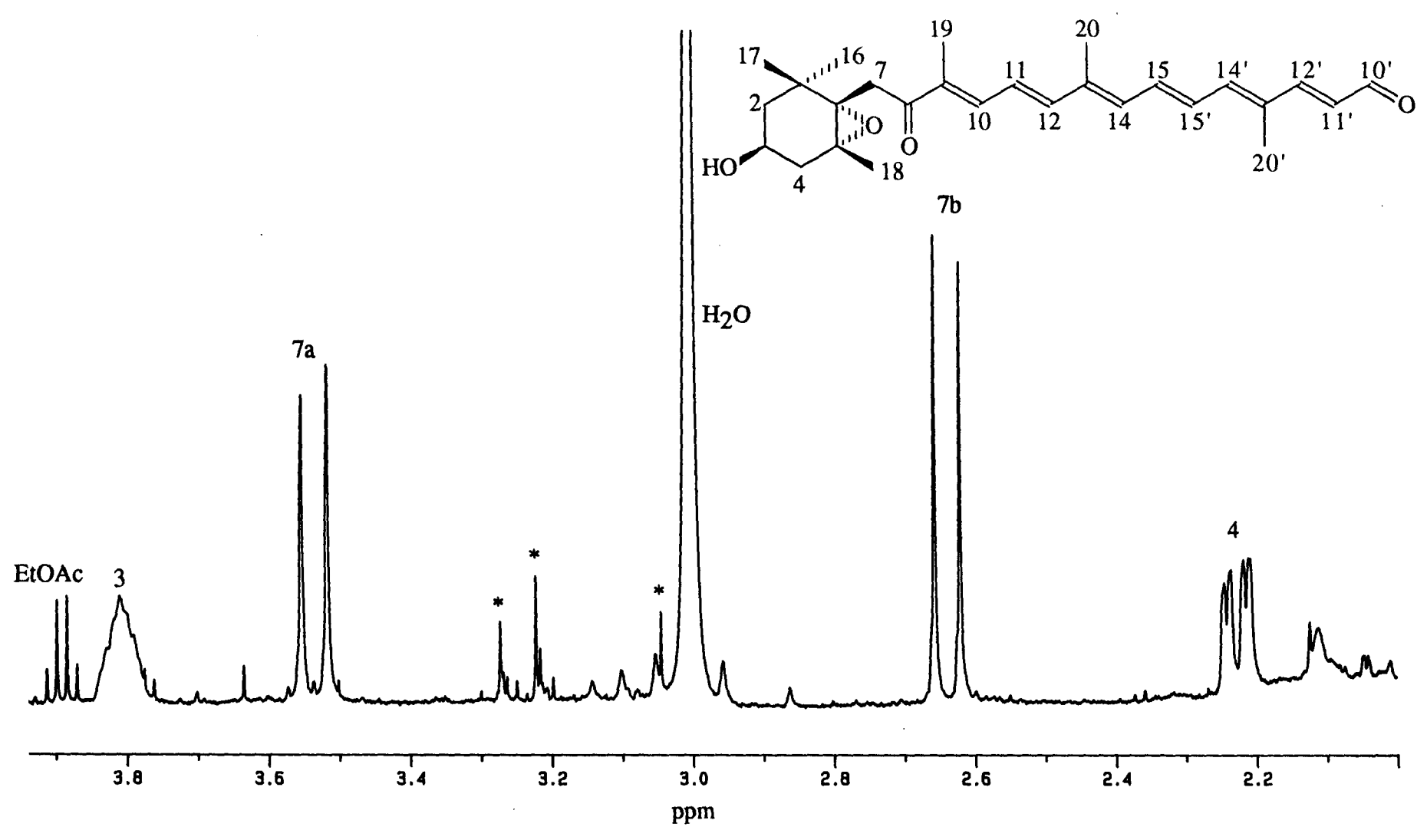


Fig. 28. Expansion of the proton nmr (500 MHz) spectrum of semi-synthetic apo-10'-fucoxanthinal (1) in C<sub>6</sub>D<sub>6</sub> showing protons at positions 3, 4, and 7. \* denotes minor impurities.

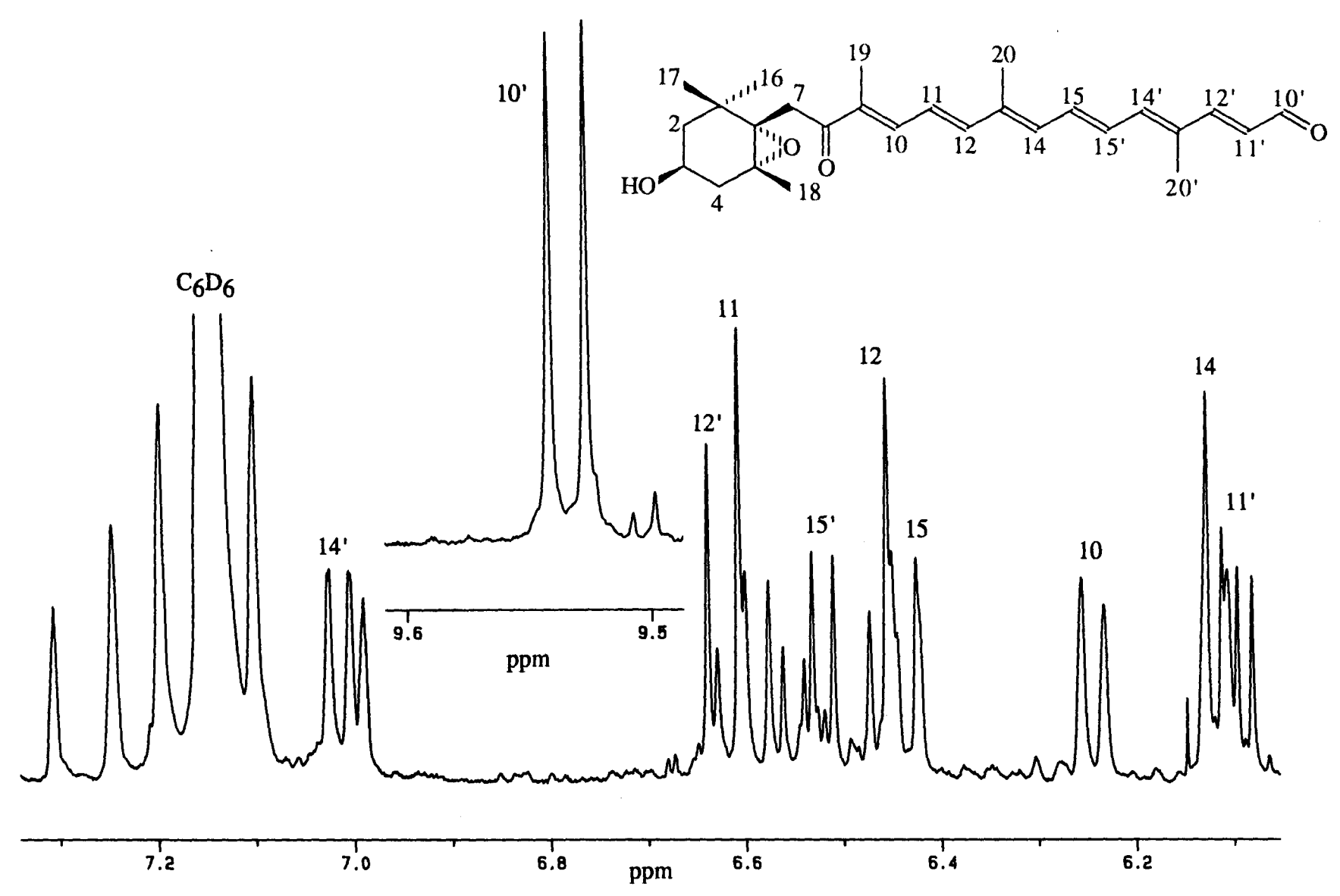


Fig. 29. Expansion of the proton nmr (500 MHz) spectrum of semi-synthetic apo-10'-fucoxanthinal (1) in C<sub>6</sub>D<sub>6</sub> showing the olefinic protons and the aldehyde proton. \* denotes minor impurities.

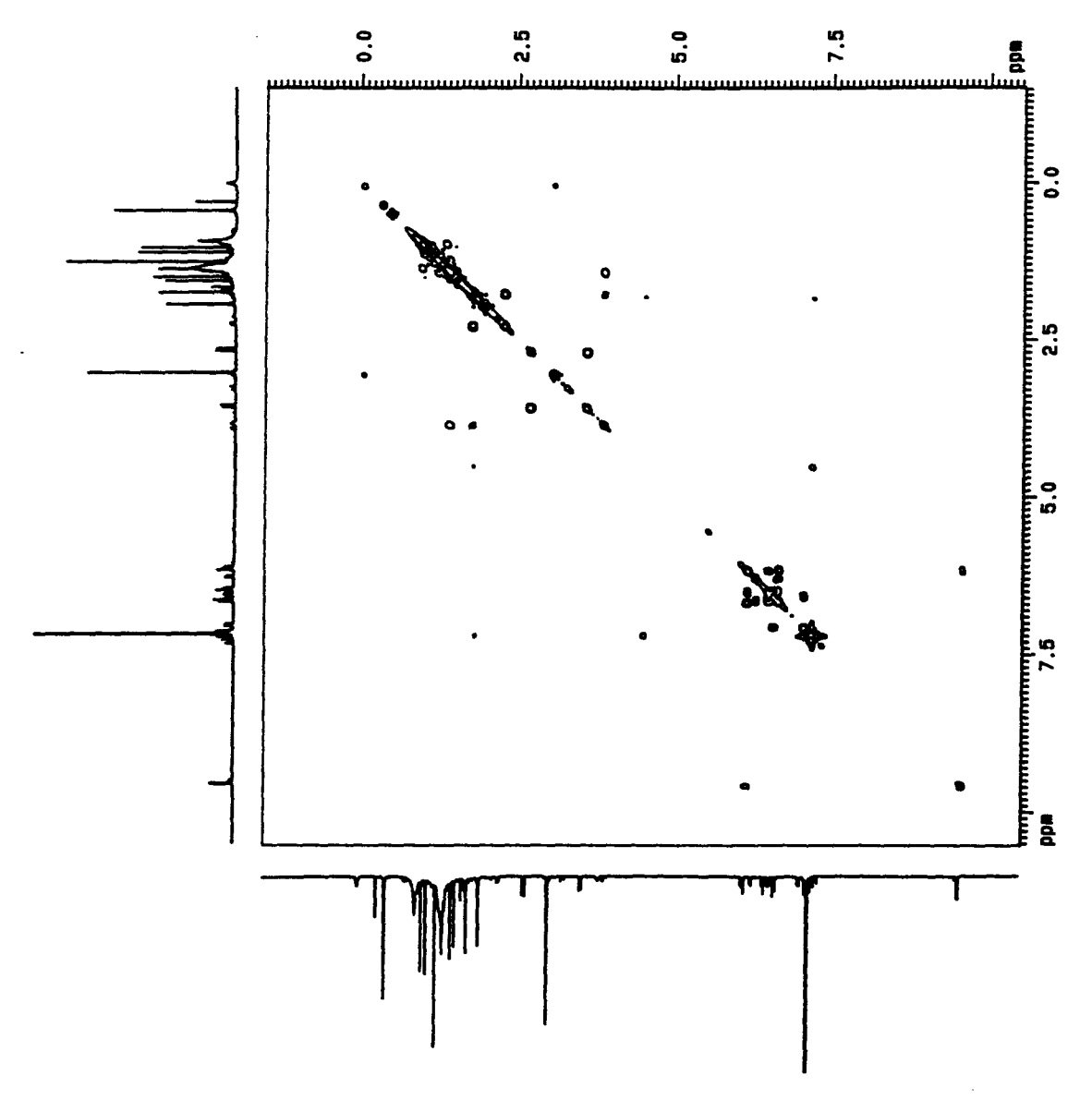


Fig. 30. <sup>1</sup>H-<sup>1</sup>H COSY (500 MHz) spectrum of semi-synthetic apo-10'-fucoxanthinal (1) in C<sub>6</sub>D<sub>6</sub>.

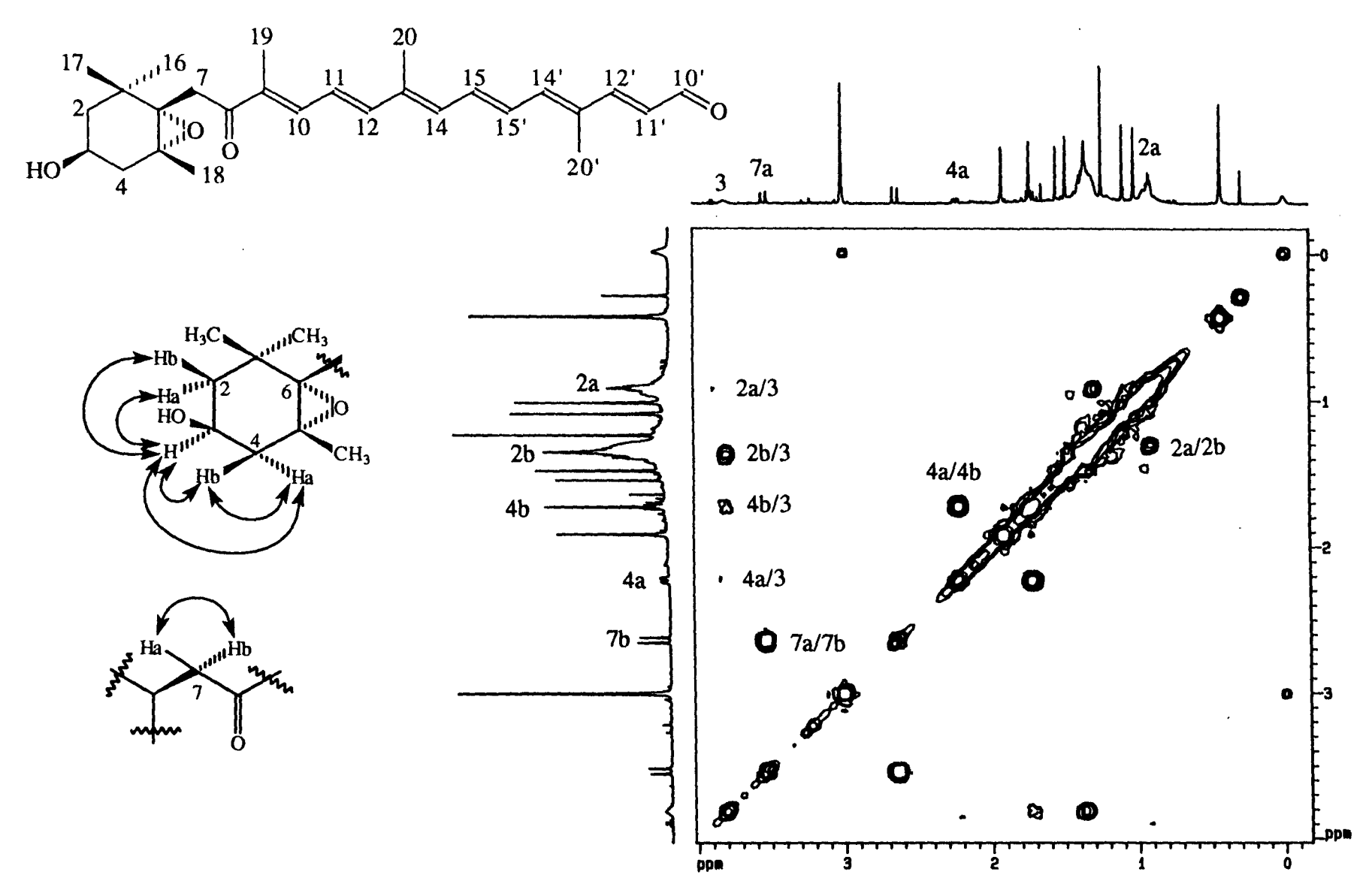


Fig. 31. Expansion of the <sup>1</sup>H-<sup>1</sup>H COSY (500 MHz) spectrum of semi-synthetic apo-10'-fucoxanthinal (1) in C<sub>6</sub>D<sub>6</sub> showing couplings between ring protons and geminal methylene couplings in the chain.

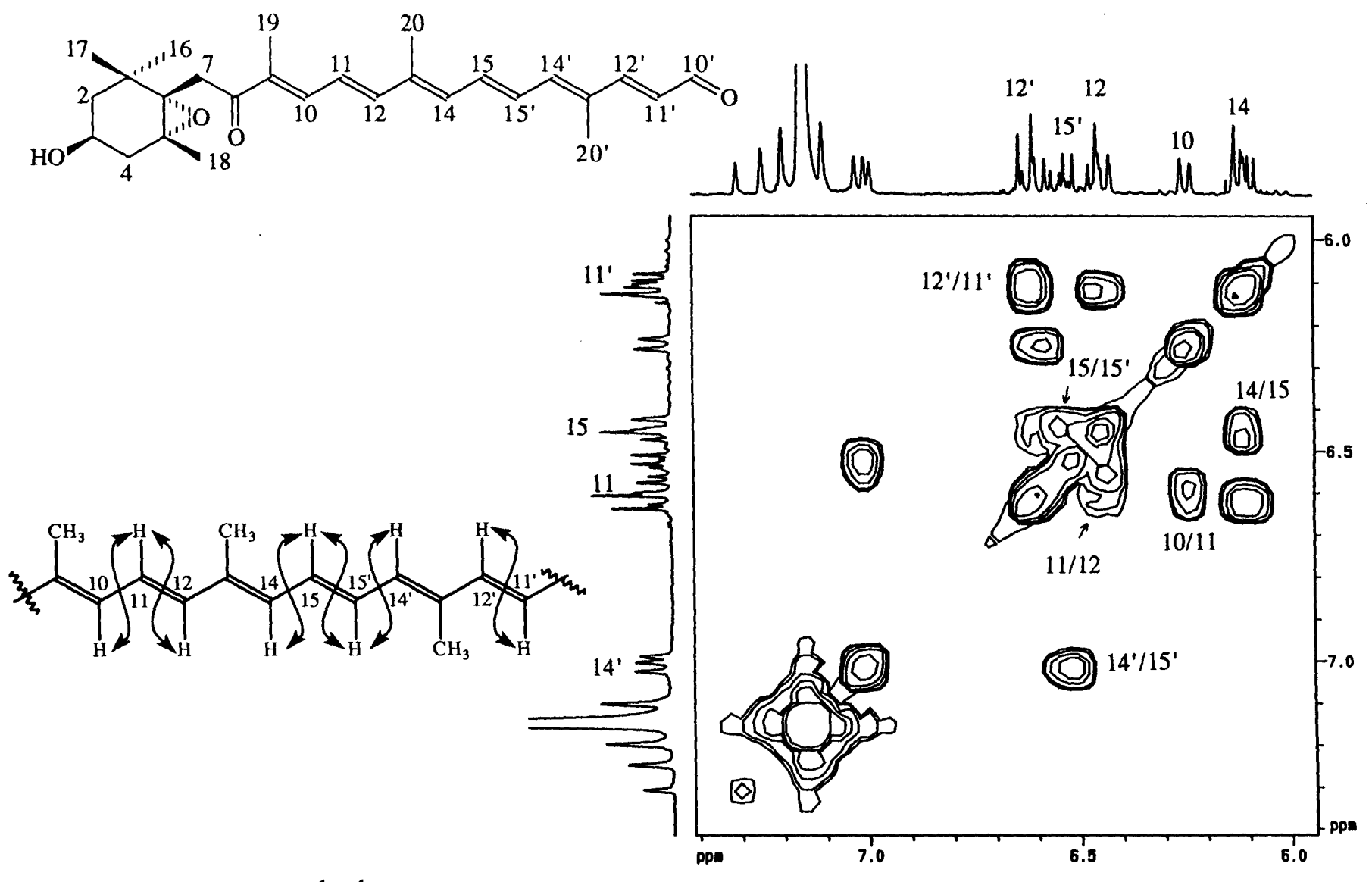


Fig. 32. Expansion of the <sup>1</sup>H-<sup>1</sup>H COSY (500 MHz) spectrum of semi-synthetic apo-10'-fucoxanthinal (1) in C<sub>6</sub>D<sub>6</sub> showing couplings between olefinic protons.

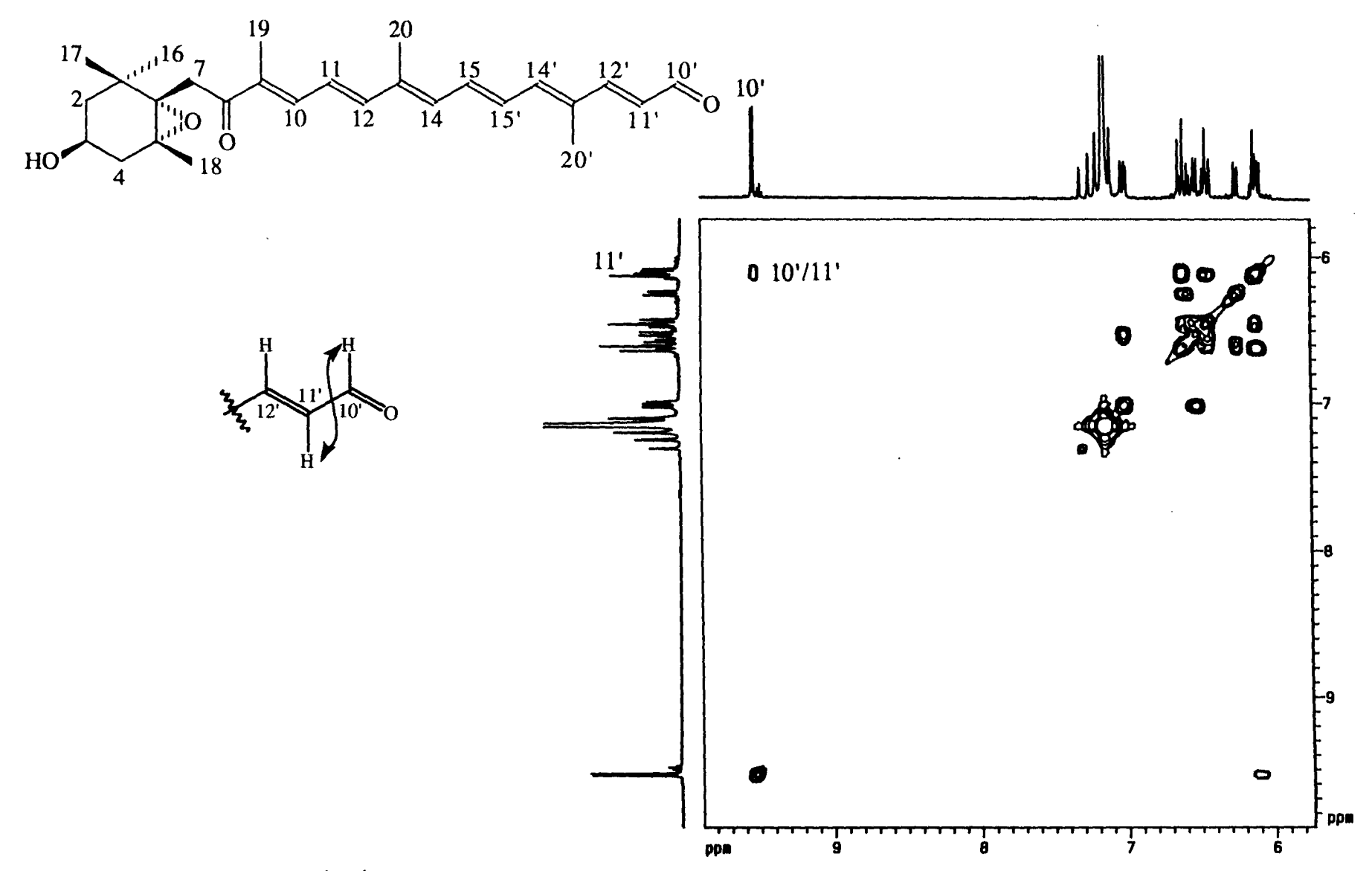


Fig. 33. Expansion of the <sup>1</sup>H-<sup>1</sup>H COSY (500 MHz) spectrum of semi-synthetic apo-10'-fucoxanthinal (1) in C<sub>6</sub>D<sub>6</sub> showing couplings between the olefinic protons and aldehyde proton.

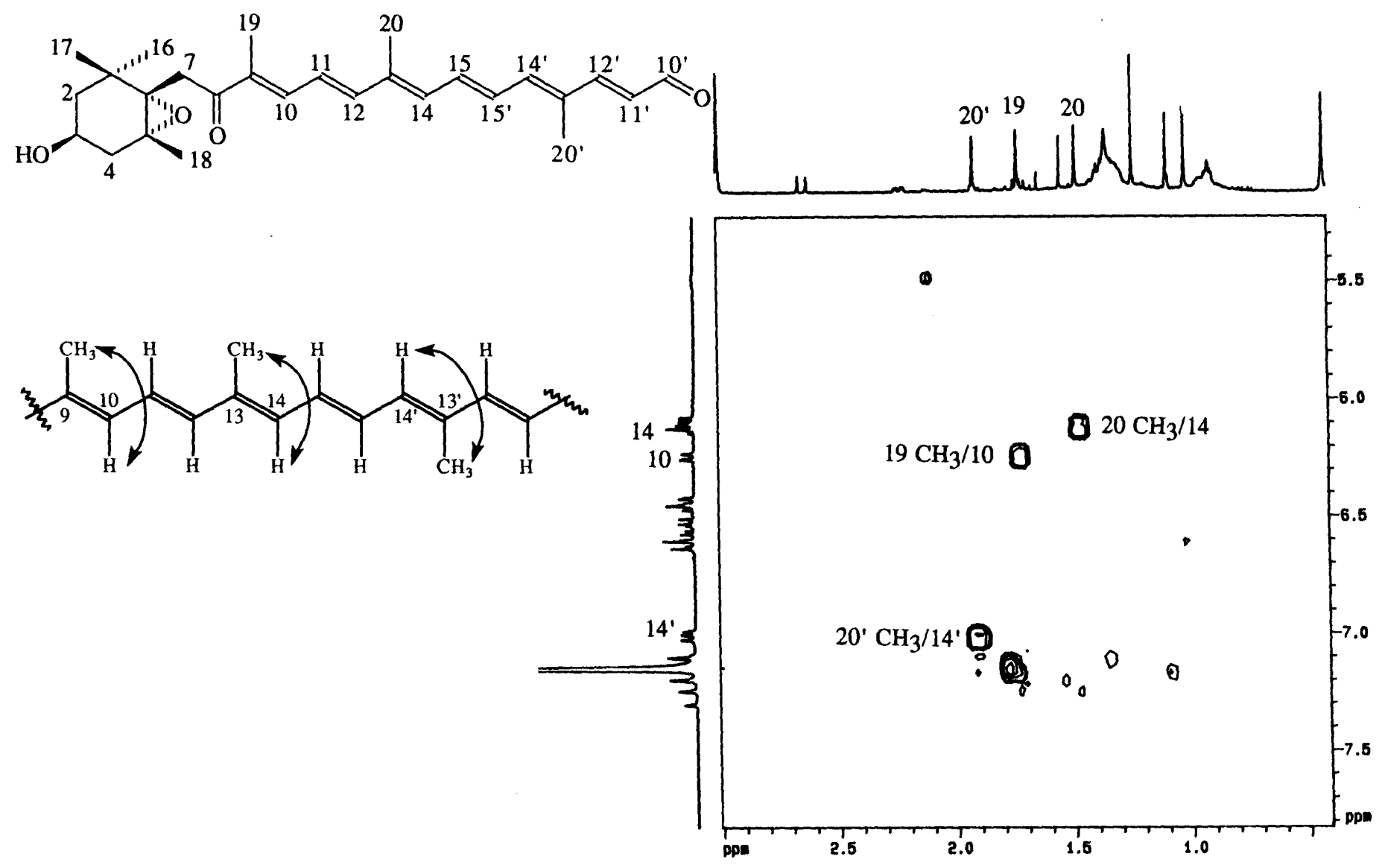


Fig. 34. Expansion of the <sup>1</sup>H-<sup>1</sup>H COSY (500 MHz) spectrum of semi-synthetic apo-10'-fucoxanthinal (1) in C<sub>6</sub>D<sub>6</sub> showing allylic couplings.

**Table 4.** Chemical shifts and coupling constants for the four semi-synthetic apofucoxanthinoids. Peak multiplicity abbreviations: s = singlet; d = doublet; dd = doublet of doublets; m = multiplet.

Position	Apo-10'-fucoxanthinal (1)		Apo-12'-fuco	xanthinal (2)	
	Chemical shift,	Coupling	Chemical shift,	Coupling	
	ppm in C <sub>6</sub> D <sub>6</sub>	constant (Hz)	ppm in C <sub>6</sub> D <sub>6</sub>	constant (Hz)	
16-CH <sub>3</sub>	1.09 (s)	NA	1.10 (s)	NA	
17-CH <sub>3</sub>	1.01 (s)	NA	1.01 (s)	NA	
18-CH <sub>3</sub>	1.25 (s)	NA	1.24 (s)	NA	
19-CH <sub>3</sub>	1.71 (s)	NA	1.78 (s)	NA	
20-CH <sub>3</sub>	1.49 (s)	NA	1.68 (s)	NA	
20'-CH <sub>3</sub>	1.92 (s)	NA	1.91 (s)	NA	
2a-CH <sub>2</sub>	0.91 (dd)	5.3, 19	-	-	
2b-CH <sub>2</sub>	1.36 (dd)	8.8, 19	-	-	
$4a-CH_2$	2.22 (dd)	4.1, 14	2.23 (dd)	-	
$4b-CH_2$	1.71 (dd)	8.8, 14	-	-	
7a-CH <sub>2</sub>	3.53 (d)	19	3.53 (d)	-	
$7b-CH_2$	2.64 (d)	19	2.62 (d)	-	
3-CH	3.80 (m)	~	3.80 (m)	-	
10-CH	6.24 (d)	13	6.16 (d)	-	
11-CH	6.60 (dd)	7.4, 13	6.56 (dd)	-	
12-CH	6.44 (d)	7.4	6.44 (d)	-	
14-CH	6.11 (d)	12	6.42 (d)	-	
15-CH	6.43 (dd)	12, 13	7.01 (dd)	-	
15'-CH	6.51 (dd)	12, 13	6.43 (dd)	-	
14'-CH	7.01 (d)	12	6.55 (d)	-	
12'-CH	6.61 (d)	16	9.44 (s)	NA	
11'-CH	6.10 (dd)	7.6, 16	NA	NA	
10'-CH	9.53 (d)	7.6	NA	NA	

Table 4. Continued.

Position	Apo-12-fucoxanthinal (3)		Apo-13'-fucox	anthinone (4)
1 Osition	Chemical shift, Coupling		Chemical shift,	Coupling
	ppm in CD <sub>2</sub> Cl <sub>2</sub>	constant (Hz)	ppm in CD <sub>2</sub> Cl <sub>2</sub>	constant (Hz)
161 CII.		<del></del>		<del></del>
16'-CH <sub>3</sub>	1.34 (s)	NA	1.34 (s)	NA
17'-CH <sub>3</sub>	1.08 (s)	NA	1.08 (s)	NA
18'-CH <sub>3</sub>	1.36 (s)	NA	1.37 (s)	NA
19'-CH <sub>3</sub>	1.84 (s)	NA	1.91 (s)	NA
20'-CH <sub>3</sub>	2.04 (s)	NA	2.25 (s)	NA
20-CH <sub>3</sub>	1.86 (s)	NA	NA	NA
CH <sub>3</sub> (OAc)	2.01 (s)	NA	2.01 (s)	NA
2'a-CH <sub>2</sub>	-	-	1.42 (dd)	-
2'b-CH <sub>2</sub>	-	~	2.00 (dd)	-
4'a-CH <sub>2</sub>	-	-	2.21 (dd)	-
4'b-CH <sub>2</sub>	-	-	1.48 (dd)	-
3'-CH	-	-	5.31 (m)	-
8'-CH	6.08 (s)	NA	6.10 (s)	NA
10'-CH	$\approx 6.15$ (d)	-	6.12 (d)	16
11'-CH	$\approx 6.74 \text{ (dd)}$	-	7.46 (dd)	12, 16
12'-CH	6.38 (d)	-	6.17 (d)	12
14'-CH	6.32 (d)	-	NA	NA
15'-CH	7.06 (dd)	-	NA	NA
15-CH	$\approx 6.66 \text{ (dd)}$	-	NA	NA
14-CH	6.97 (d)	-	NA	NA
12-CH	9.44 (s)	NA	NA	NA

416.2 nm

The UV-vis spectrum of this compound gave a  $\lambda_{max}$  of 418 nm in methanol (Appendix E, Fig. E18) and 409 nm in ether. These values compare reasonably well with literature values (Table 5). Using the Fieser-Kuhn rules for calculating the  $\lambda_{max}$  of polyenes (Pavia *et al.*, 1979), the following values were calculated:

	114 nm
8*(48.0 - (1.7*8))	275.2 nm
4*5	<u>20 nm</u>
	409.2 nm
nol:	

+7 nm

These values agree very well with the observed values. Note the "cis band" at 313 nm (Appendix E, Fig. E18), which indicates the presence of one or more cis isomers of apo-10'-fucoxanthinal in the sample. These cis isomers form rapidly from the trans compound in the presence of light. The formation of these cis isomers was difficult to prevent during the isolation procedures, and, once present, the cis isomers were very difficult to separate from the trans compound. In addition, the cis isomers are capable of transforming back into the trans compound in the presence of light, hence an equilibrium is established between cis and trans isomers in light. As light is present in the marine environment, these transformations probably occur once these compounds are released from the phytoplankton cells during grazing. Therefore, since the cis isomers did not interfere with structure determination and are probably present in the natural environment, no further effort was made to isolate or remove them from the semi-synthetic material.

**Table 5.** Comparison of UV-vis data for the four semi-synthetic compounds with literature values from Bonnett *et al.* (1969). Note that UV-vis spectra for this research were not run in CHCl<sub>3</sub> as several of the semi-synthetic compounds decomposed in this solvent.

Compound	UV-vis, observed $\lambda_{\text{max}}$ (nm) $\epsilon$ (M <sup>-1</sup> cm <sup>-1</sup> )	UV-vis, literature $\lambda_{\text{max}}$ (nm) $\epsilon$ (M <sup>-1</sup> cm <sup>-1</sup> )
Apo-10'-fucoxanthinal (1)	methanol: 418 (41.7 x 10 <sup>3</sup> ε) ether: 409	CHCl <sub>3</sub> : 426 (100.9 x $10^3 \varepsilon$ ) light petroleum: 410
Apo-12'-fucoxanthinal (2)	methanol: 393 (33.9 x $10^3 \epsilon$ ) ether: 383	CHCl <sub>3</sub> : 400 (75.0 x 10 <sup>3</sup> ε) light petroleum: 384
Apo-12-fucoxanthinal (3)	methanol: $407 (16.0 \times 10^3 \epsilon)$	light petroleum: 407
Apo-13'-fucoxanthinone (4)	methanol: 329 (15.4 x $10^3 \varepsilon$ )	-

The IR spectrum of apo-10'-fucoxanthinal (Appendix E, Fig. E22) showed stretching vibrations characteristic of an  $\alpha,\beta$ -unsaturated ketone, an  $\alpha,\beta$ -unsaturated aldehyde, and a hydroxyl group, which corresponds to the proposed structure. These vibrational frequencies were compared with data from Bonnett *et al.* (1969) and were in good agreement with his results (Table 6).

**Table 6.** Comparison of IR data for the four semi-synthetic compounds with literature values from Bonnett *et al.* (1969).

Compound	IR, observed	IR, literature	Functional group
	(cm <sup>-1</sup> )	ν (cm <sup>-1</sup> )	
	film	solid	
Apo-10'-fucoxanthinal (1)	3448	3450	OH
ripo to tuonamma (1)	1662	1660	$\alpha,\beta$ -unsaturated ketone
	-	1640	$\alpha,\beta$ -unsaturated aldehyde
	1585	1585	conjugated C=C
	1127	1125	C-O
	971	975	С-Н
Apo-12'-fucoxanthinal (2)	3453	3450	ОН
	1660	1660	$\alpha,\beta$ -unsaturated ketone +
			$\alpha,\beta$ -unsaturated aldehyde
	1604	1605	conjugated C=C
	1015	1015	C-O
	969	975	С-Н
Apo-12-fucoxanthinal (3)	3437	3550	ОН
	2933	2900	C-H
	1927	1935	C=C=C
	1721	1720	Acetate $C=O$
	1662	1670	$\alpha,\beta$ -unsaturated aldehyde
	1609	1610	conjugated C=C
	1017	1020	C-O
	966	975	С-Н
Apo-13'-fucoxanthinone (4)	3442	-	ОН
	2964	-	С-Н
	2926	-	C-H
	1931	-	C=C=C
	1732	-	Acetate $C=O$
	1661	-	$\alpha,\beta$ -unsaturated aldehyde
	1597	-	conjugated C=C

## b) Apo-12'-fucoxanthinal (Fig. 35)

Fig. 35. Structure and numbering scheme for apo-12'-fucoxanthinal (2).

A low resolution DCI mass spectrum of the semi-synthetic apo-12'-fucoxanthinal gave an [M+H]<sup>+</sup> peak at 399 (Fig. 36). Using high resolution DCI mass spectrometry, a value of 399.2535 (deviation = -0.02 ppm) was obtained for [M+H]<sup>+</sup>. This agrees well with the mass spectrometry results for the natural apo-12'-fucoxanthinal (Appendix E, Fig. E2; Table 2). A major fragment ion shown in the low resolution DCI mass spectrum at an m/z value of 197 can be explained by the loss of the long carbon chain from the molecule, as shown in Figure 37.

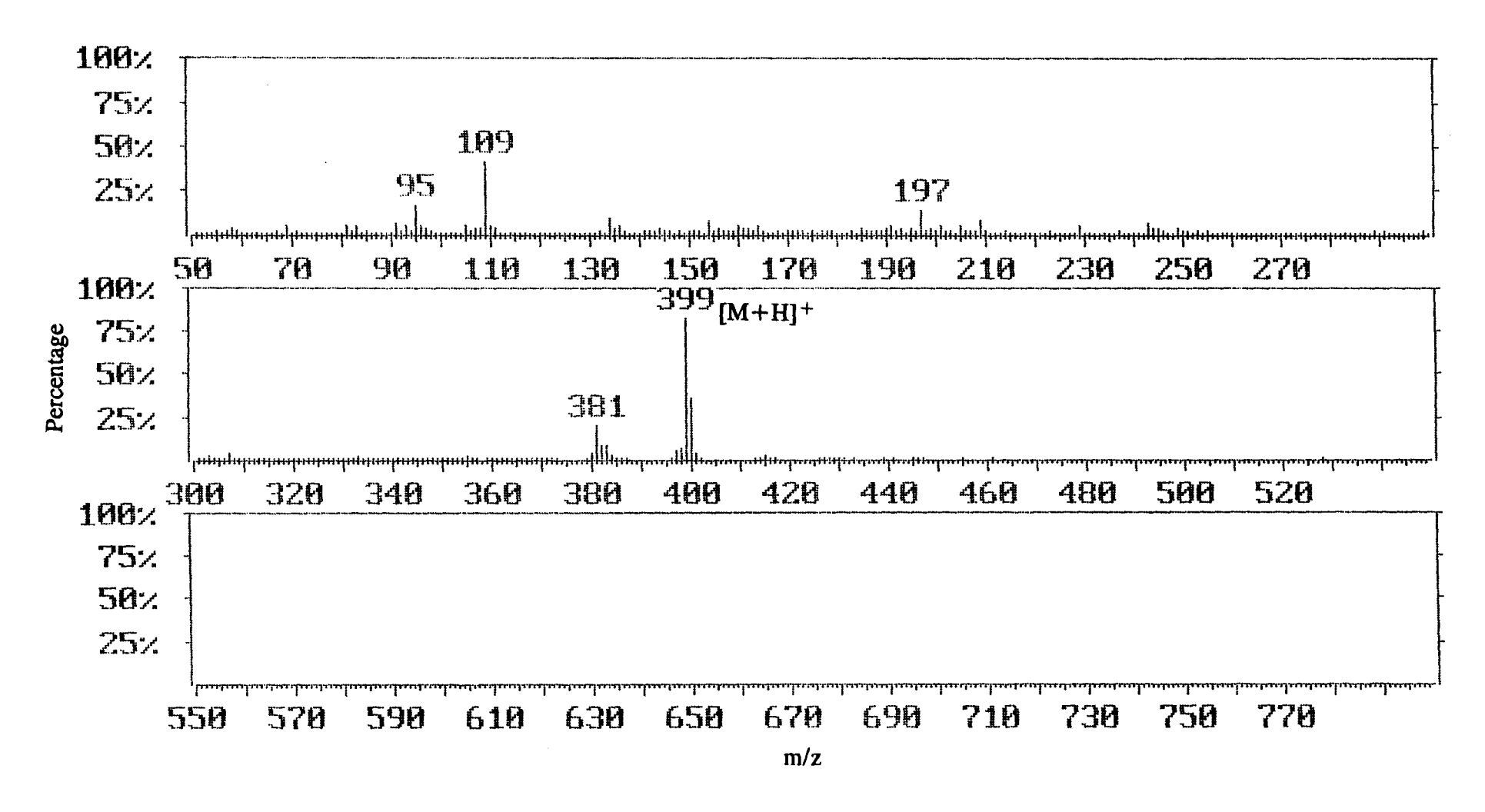


Fig. 36. Low resolution DCI mass spectrum of semi-synthetic apo-12'-fucoxanthinal (2) using NH3 as the reagent gas.

Fig. 37. Fragmentation pattern ( $\alpha$ -cleavage) of apo-12'-fucoxanthinal (2), explaining the peak at 197 in the DCI mass spectrum.

The proton nmr spectrum of apo-12'-fucoxanthinal indicated that there were six methyl groups, seven olefinic protons, one aldehyde proton, one methine proton, and six methylene protons (Figs. 38 - 40; Table 4). These signals were assigned to positions in the molecule by comparison with the chemical shifts from apo-10'-fucoxanthinal. The chemical shift values for these protons match those for the natural apo-12'-fucoxanthinal (Tables 3 and 4).

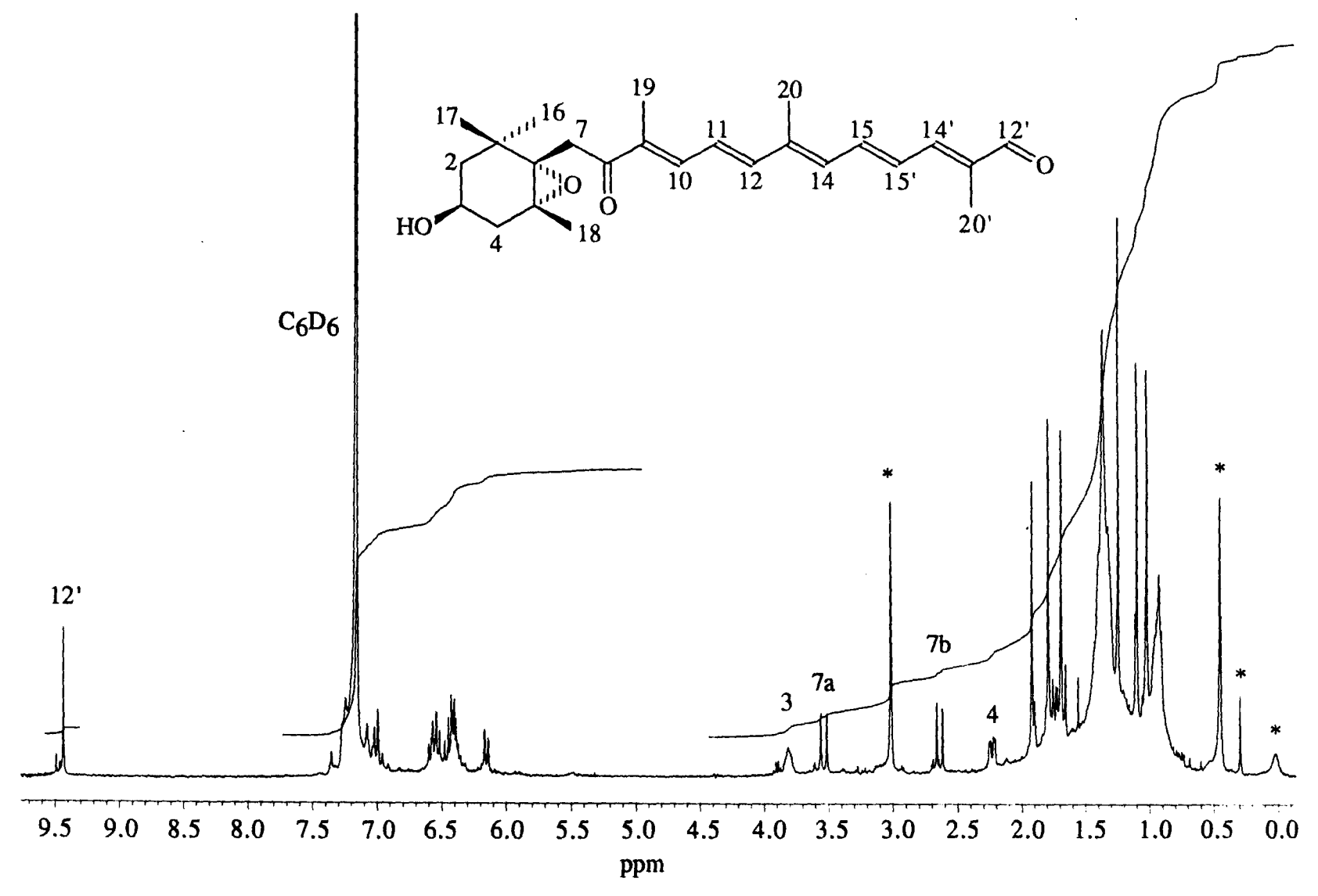


Fig. 38. Proton nmr (400 MHz) spectrum of semi-synthetic apo-12'-fucoxanthinal (2) in C<sub>6</sub>D<sub>6</sub>. \* denotes impurities.

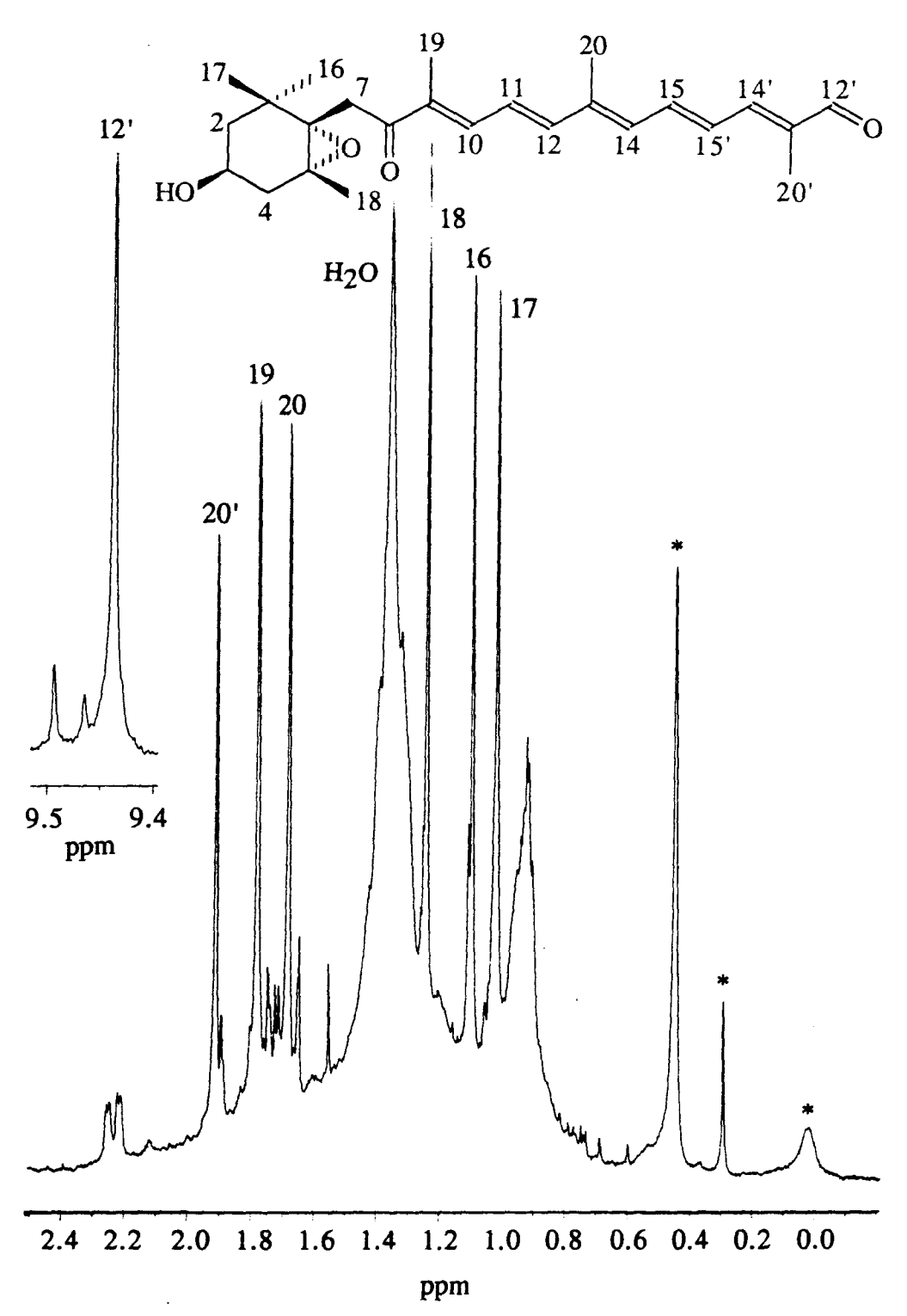


Fig. 39. Expansion of the proton nmr (400 MHz) spectrum of semi-synthetic apo-12'-fucoxanthinal (2) in C<sub>6</sub>D<sub>6</sub> showing resonances from the methyl groups and the aldehyde proton. \* denotes impurities.

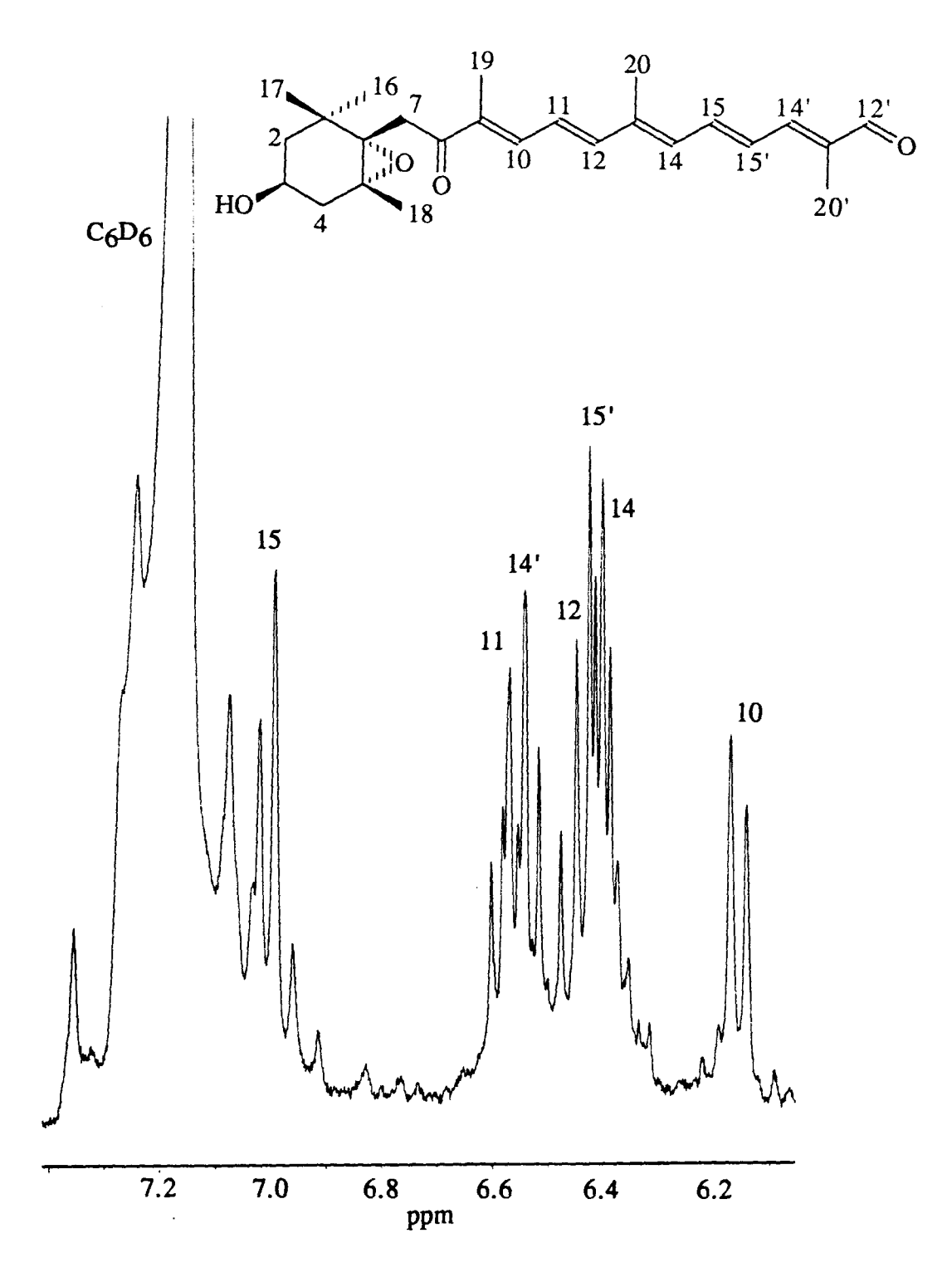


Fig. 40. Expansion of the proton nmr (400 MHz) spectrum of semi-synthetic apo-12'-fucoxanthinal (2) in C<sub>6</sub>D<sub>6</sub> showing olefinic protons.

The UV-vis spectrum of this compound gave a  $\lambda_{max}$  of 393 nm in methanol (Appendix E, Fig. E19) and 383 nm in ether. These values are in good agreement with the literature values (Table 5). The  $\lambda_{max}$  was calculated as follows:

base value:		114 nm
7 conjugated double bonds	:	
	7*(48.0 - (1.7*7))	252.7 nm
4 alkyl substituents:		
	4*5	<u>20 nm</u>
total (in hexane):		386.7 nm
solvent correction for meth	anol:	
	+7 nm	393.7 nm

These calculated values agree very well with the observed values. As before, there is a "cis band" at 290 nm (Appendix E, Fig. E19), indicating the presence of cis isomer impurities.

The IR spectrum of apo-12'-fucoxanthinal (Appendix E, Fig. E23) showed stretching vibrations for an  $\alpha,\beta$ -unsaturated ketone, an  $\alpha,\beta$ -unsaturated aldehyde, and a hydroxyl group. These vibrational frequencies corresponded well to results from Bonnett *et al.* (1969; Table 6).

# c) Apo-12-fucoxanthinal (Fig. 41)

Fig. 41. Structure and numbering scheme for apo-12-fucoxanthinal (3).

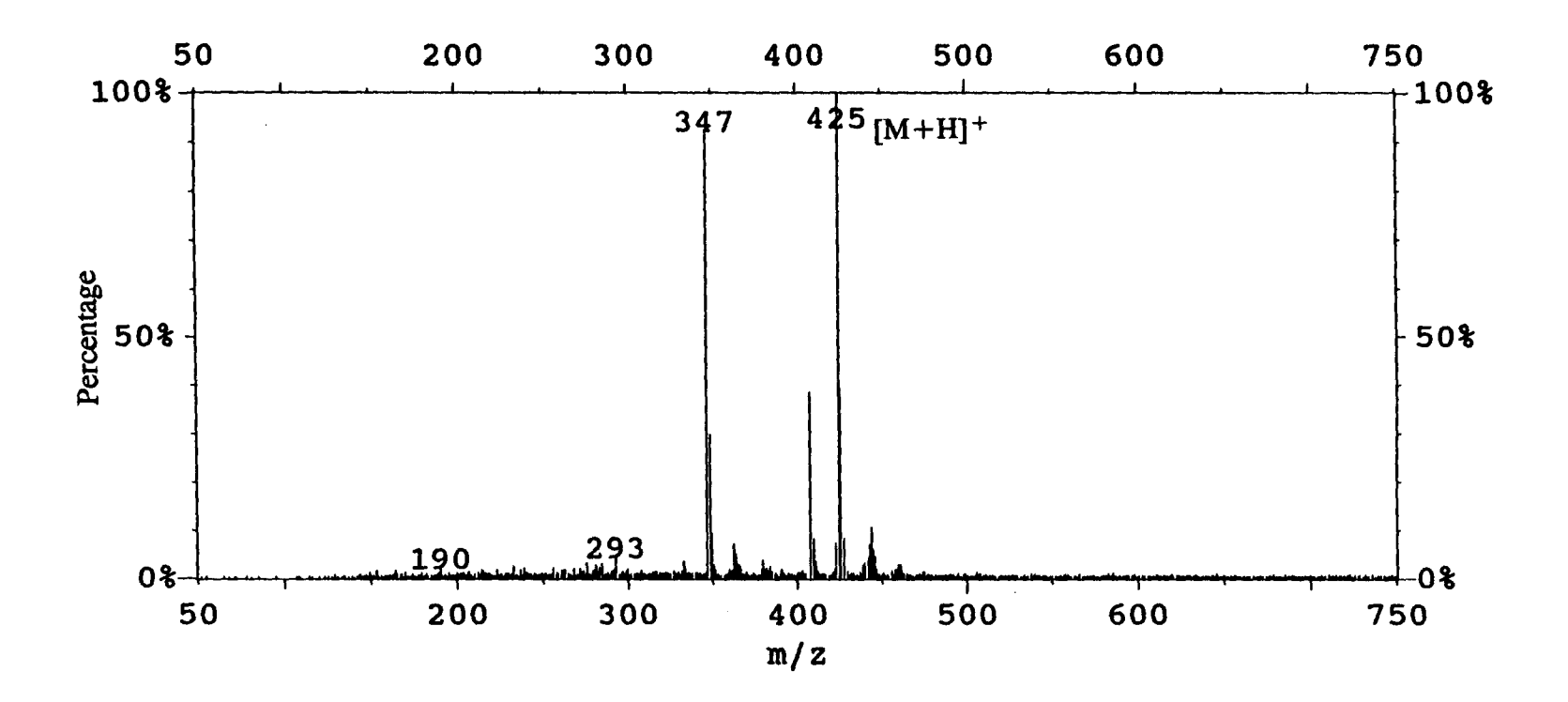


Fig. 42. Low resolution DCI mass spectrum of semi-synthetic apo-12-fucoxanthinal (3) using NH3 as the reagent gas.

A low resolution DCI mass spectrum of the semi-synthetic apo-12-fucoxanthinal gave an [M+H]<sup>+</sup> peak at 425 (Fig. 42). High resolution DCI mass spectrometry gave a value for [M+H]<sup>+</sup> of 425.2670 (deviation = -2.1 ppm). These results are in good agreement with the mass spectrometry results for the natural apo-12-fucoxanthinal (Appendix E, Fig. E3; Table 2). In both of these materials, one of the major fragment ions shown in the low resolution DCI mass spectrum was at an m/z value of 347. This peak can be explained by the loss of water and acetic acid from the molecule, as shown in Figure 43.

Fig. 43. Fragmentation pattern of apo-12-fucoxanthinal (3), explaining the peak at 347 in the DCI mass spectrum.

Apo-12-fucoxanthinal was the most unstable of the four apo-fucoxanthinoids isolated in this study. When exposed to light, there were rapid interconversions

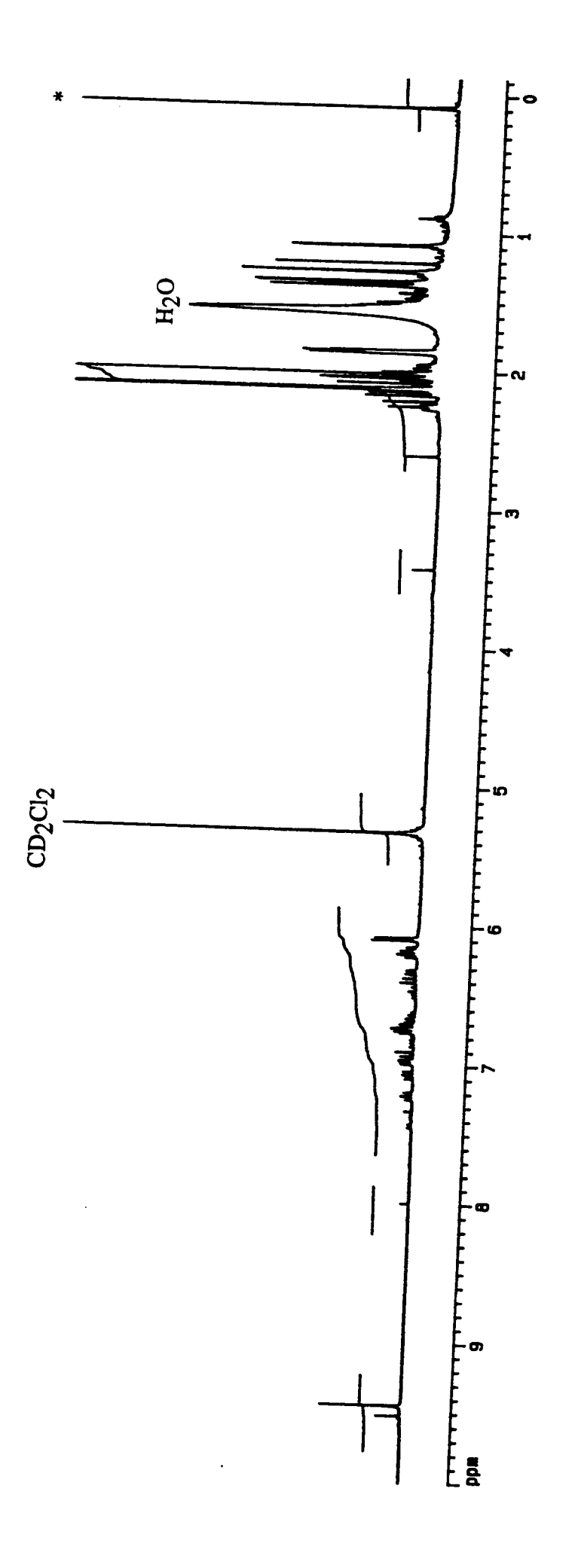


Fig. 44. Proton nmr (500 MHz) spectrum of semi-synthetic apo-12-fucoxanthinal (3) in CD<sub>2</sub>Cl<sub>2</sub>. \* denotes impurities.

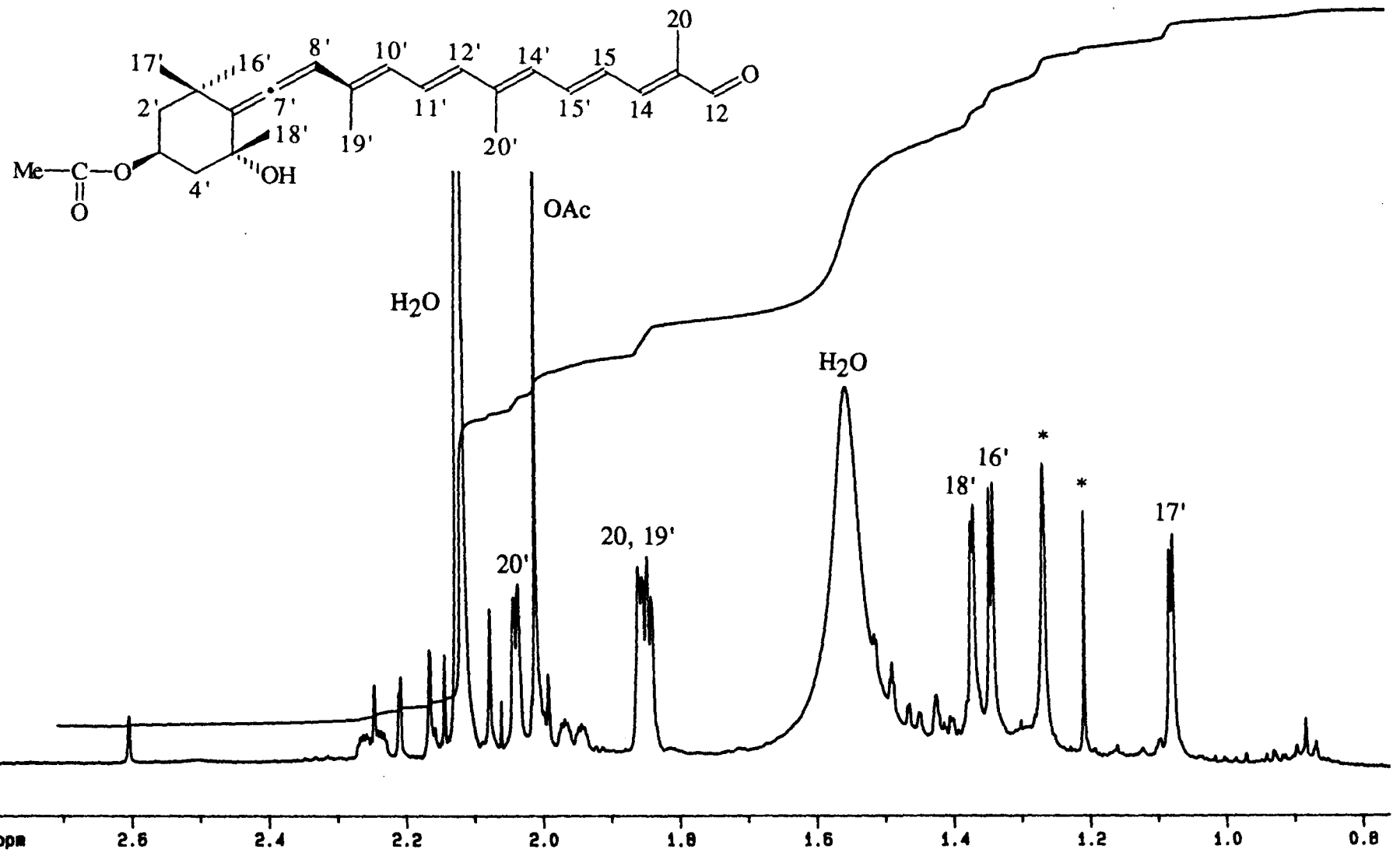


Fig. 45. Expansion of the proton nmr (500 MHz) spectrum of semi-synthetic apo-12-fucoxanthinal (3) in CD<sub>2</sub>Cl<sub>2</sub>. showing resonances from the methyl groups. \* denotes minor impurities. Note the doubling of the methyl peaks due to the presence of the cis isomer.

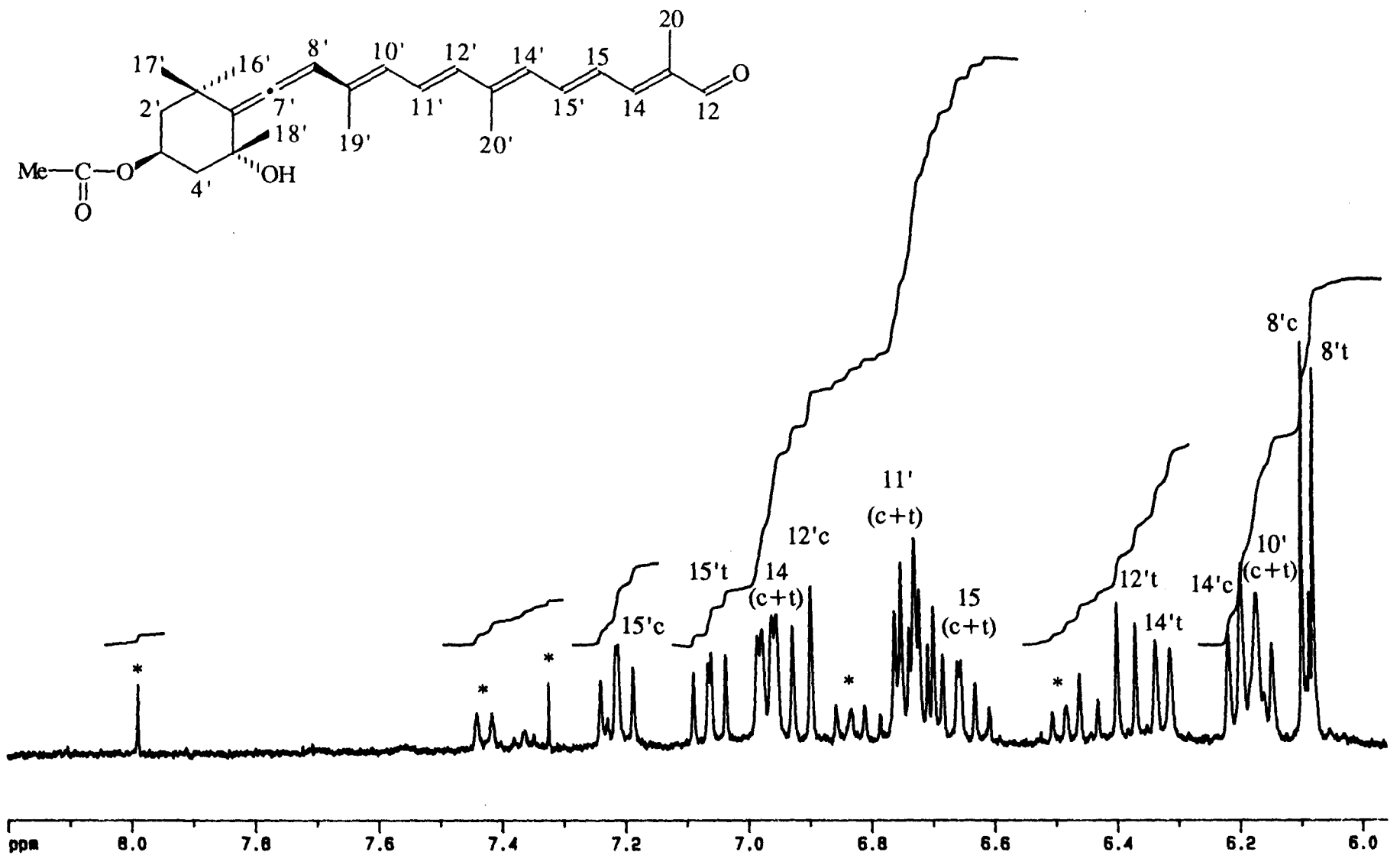


Fig. 46. Expansion of the proton nmr (500 MHz) spectrum of semi-synthetic apo-12-fucoxanthinal (3) in CD<sub>2</sub>Cl<sub>2</sub>. showing olefinic protons. \* denotes impurities (probably cis-trans isomers of compound (3)); t = resonances from the all trans compound; c = resonances from the major mono-cis compound (probably 13 cis).

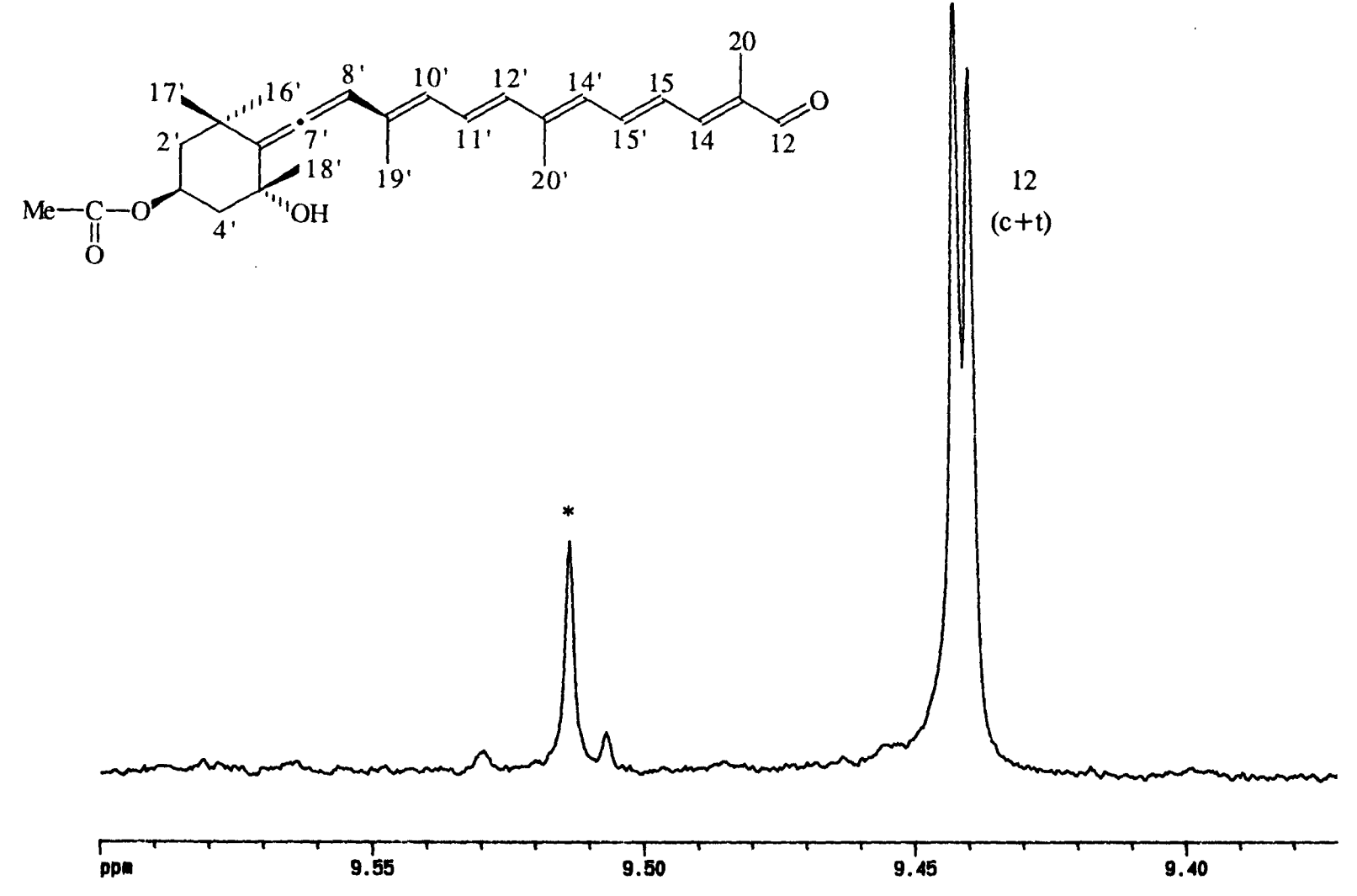


Fig. 47. Expansion of the proton nmr (500 MHz) spectrum of semi-synthetic apo-12-fucoxanthinal (3) in CD<sub>2</sub>Cl<sub>2</sub>. showing the aldehyde proton. \* denotes impurities (probably cis-trans isomers of compound (3)); t = resonances from the all trans compound; c = resonances from the major mono-cis compound (probably 13 cis).

between the cis and trans forms of this molecule. This resulted in a rather complicated proton nmr spectrum. However, proton assignments were made based on nmr data from semi-synthetic apo-13'-fucoxanthinone and literature values for all trans and 13-cis  $\beta$ -apo-12'-carotenal (Vetter *et al.*, 1971). The proton nmr spectrum of apo-12-fucoxanthinal indicated that there was an approximately 1.33: 1 ratio of the all trans compound and one mono-cis compound. For each compound, there were seven methyl groups, eight olefinic protons, one aldehyde proton, one methine proton, and four methylene protons (Figs. 44 - 47). Assignments for the all trans compound are shown in Table 4. Assignments of the all trans and mono-cis (probably 13-cis) olefinic protons by comparison with the all trans and 13-cis  $\beta$ -apo-12'-carotenal are listed in Table 7. The chemical shift values for the semi-synthetic all trans apo-12-fucoxanthinal protons match those for the natural apo-12-fucoxanthinal (Tables 3 and 4).

**Table 7.** Comparison of proton chemical shifts of the all trans and 13-cis forms of apo-12-fucoxanthinal and  $\beta$ -apo-12'-carotenal (Vetter *et al.*, 1971).

Position	β-apo-12'-carotenal chemical shift (ppm) CDCl <sub>3</sub>		Position	apo-12-fuc chemical s CD <sub>2</sub>	hift (ppm)
	all trans	13'-cis	-	all trans	13-cis
8	6.14	6.17	8'	6.08	6.10
10	6.16	6.16	10'	≈ 6.15	≈ 6.15
11	6.79	6.78	11'	≈ 6.74	≈6.74
12	6.36	6.91	12'	6.38	6.91
14	6.29	6.22	14'	6.32	6.20
15	7.03	7.20	15'	7.06	7.20
15'	6.66	6.61	15	≈6.66	<b>≈</b> 6.66
14'	6.94	6.96	14	6.97	6.97
12'	9.45	9.46	12	9.44	9.44

The UV-vis spectrum of semi-synthetic apo-12-fucoxanthinal gave a  $\lambda_{max}$  of 407 nm in methanol (Appendix E, Fig. E20). This value corresponds very well with

the literature values (Table 5). Using Woodward's rules for calculating the  $\lambda_{max}$  of enones, the following values were calculated:

base value for an acyclic  $\alpha,\beta$ -unsaturated aldehyde:

210 nm

5 double bonds extending conjugation:

5 x 30 nm

150 nm

 $3 \gamma$  or higher alkyl groups:

3 x 18 nm

54 nm

total (in methanol):

414 nm

This calculated value agrees reasonably well with the observed value. Neither Woodward's rules for enones nor the Fieser-Kuhn rules for polyenes corrects for the presence of an allenic fuctionality in the chromophore. However, in this case, Woodward's rules calculated a value closer to the observed value than the Fieser-Kuhn rules (which calculated 393.7 nm). Woodward's rules generally produce good  $\lambda_{max}$  predictions for compounds with four conjugated double bonds or less. Thus the difference between the calculated and observed values may also be due to the inaccuracy of Woodward's rules in estimating the  $\lambda_{max}$  of a compound with more than four double bonds. There is a very strong "cis band" at 290 nm (Appendix E, Fig. E20) indicating the presence of a large amount of cis compound.

The IR spectrum of apo-12-fucoxanthinal (Appendix E, Fig. E24) showed stretching vibrations for an  $\alpha,\beta$ -unsaturated aldehyde, an acetate group, an allenic group, and a hydroxyl group, which corresponds with the proposed structure. These vibrational frequencies agreed with the results from Bonnett *et al.* (1969; Table 6).

## d) Apo-13'-fucoxanthinone (Fig. 48)

Fig. 48. Structure and numbering scheme for apo-13'-fucoxanthinone (4).

Low resolution DCI mass spectrometry of the semi-synthetic apo-13'fucoxanthinone gave an [M+H]<sup>+</sup> peak at 333 (Fig. 49). The high resolution DCI
mass spectrum generated a value for [M+H]<sup>+</sup> of 333.2056 (deviation = -1.0 ppm).
These results agree well with the mass spectrometry results for the natural apo-13'fucoxanthinone (Appendix E, Fig. E4; Table 2). The major fragment ion shown in the
low resolution DCI mass spectrum was at an m/z value of 255. This peak can be
explained by the loss of water and acetic acid from the molecule, as shown in Figure
50.

Apo-13'-fucoxanthinone is a novel compound. The proton assignments for this compound were made based on data from the proton and  $^{1}\text{H-}^{1}\text{H}$  COSY nmr's, and by comparison with the literature values for the three previous apo-fucoxanthinoids. The stereochemistry shown is based on the known stereochemistry for fucoxanthin, as this compound is related to fucoxanthin. The proton nmr spectrum showed six methyl groups, four olefinic protons, one methine, and four methylene protons (Figs. 51 - 53; Table 4). The chemical shift values for these protons match those for the natural apo-13'-fucoxanthinone (Tables 3 and 4). The relationships between these protons were determined by the  $^{1}\text{H-}^{1}\text{H}$  COSY nmr experiment (Figs. 54 - 55). The olefinic proton H-11' formed an AMX coupling pattern with the protons H-10' and H-12'. The methylene protons at position 2' showed both geminal coupling and coupling to the

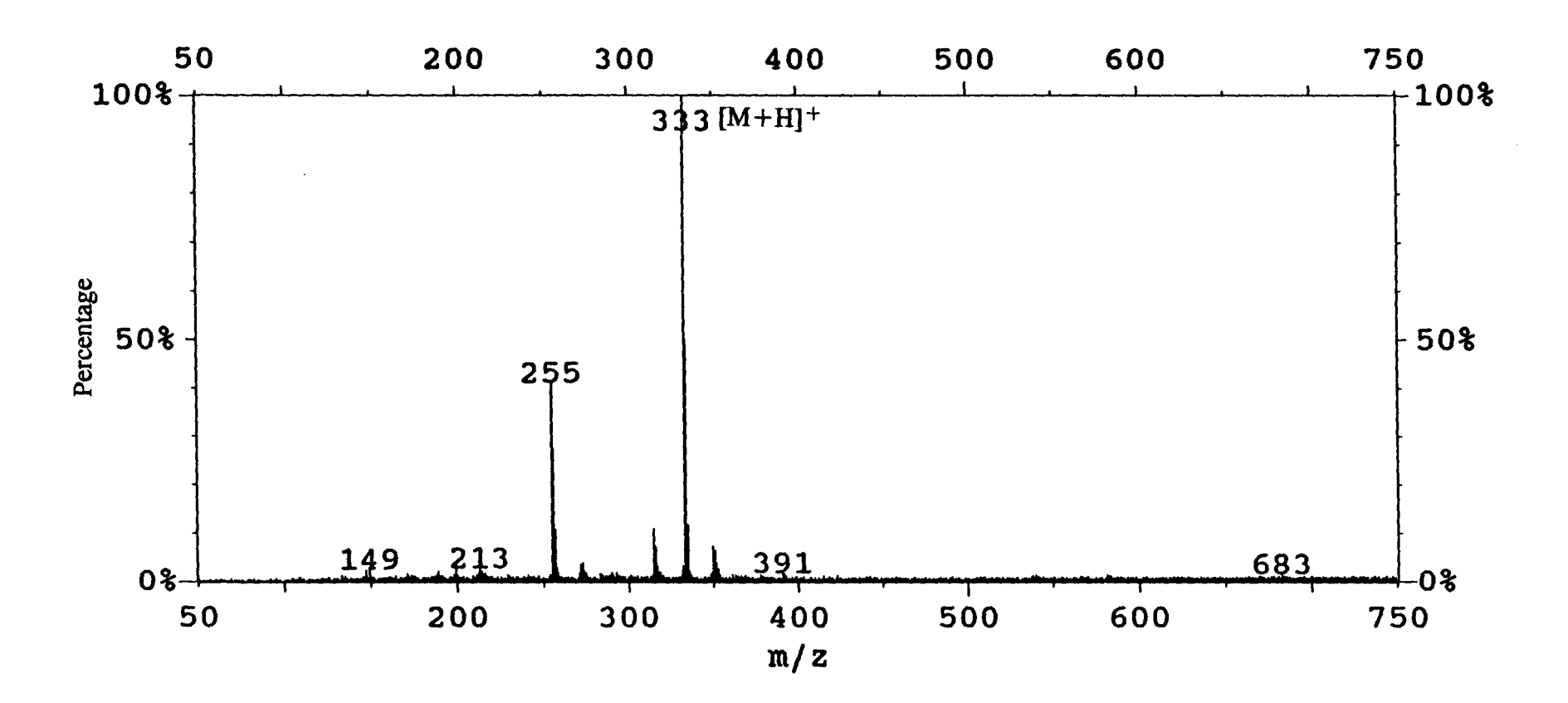


Fig. 49. Low resolution DCI mass spectrum of semi-synthetic apo-13'-fucoxanthinone (4) using NH<sub>3</sub> as the reagent gas.

Fig. 50. Fragmentation pattern of apo-13'-fucoxanthinone (4), explaining the peak at 255 in the DCI mass spectrum.

methine proton, H-3'. The geminally coupled methylene protons, H-4'a and H-4'b, were also coupled to H-3'. Allylic coupling of the olefinic protons with methyl protons was observed between the methyl protons at position 19' and the H-10' methine.

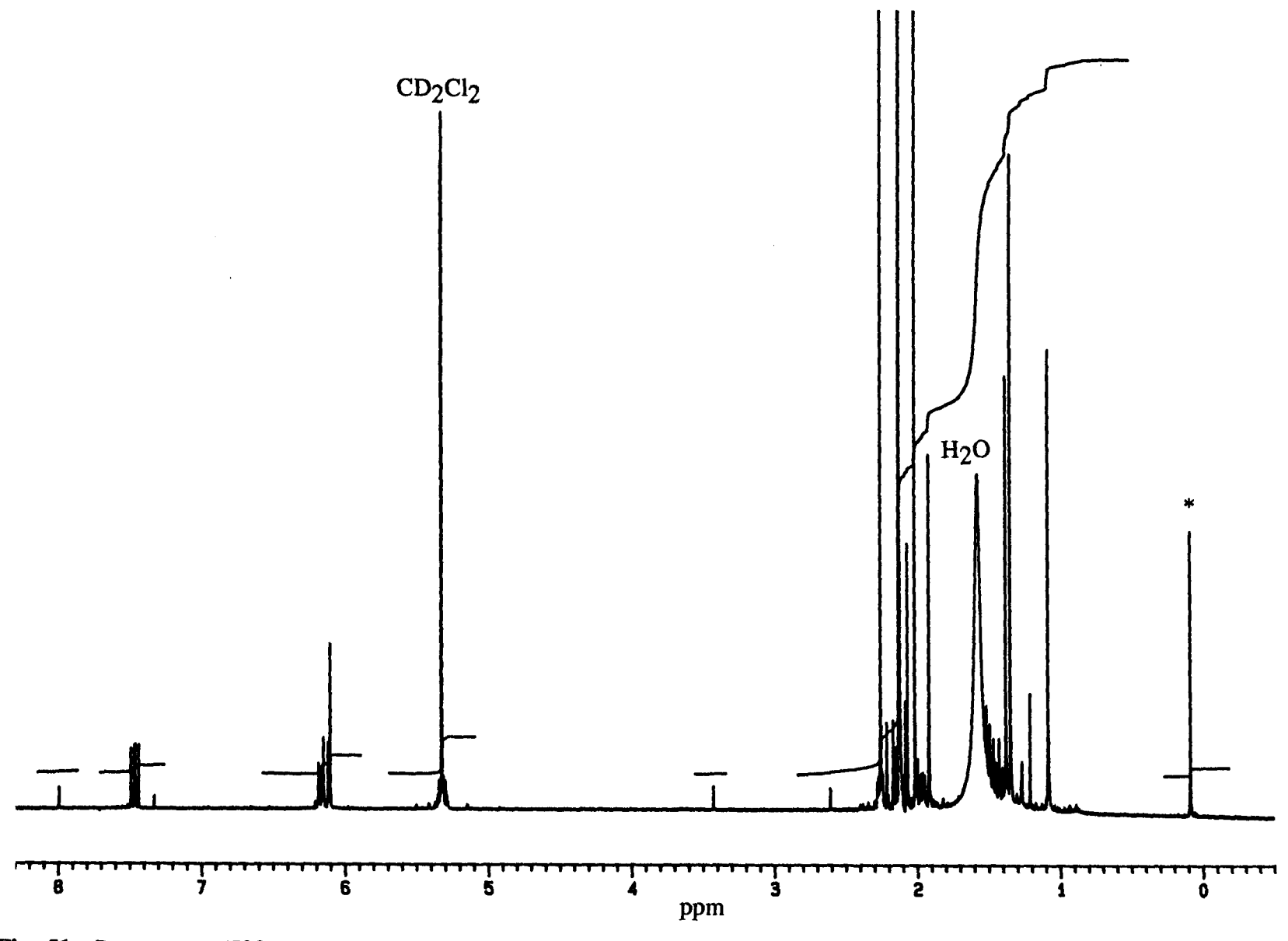


Fig. 51. Proton nmr (500 MHz) spectrum of semi-synthetic apo-13'-fucoxanthinone (4) in CD<sub>2</sub>Cl<sub>2</sub>. \* denotes minor grease impurities.

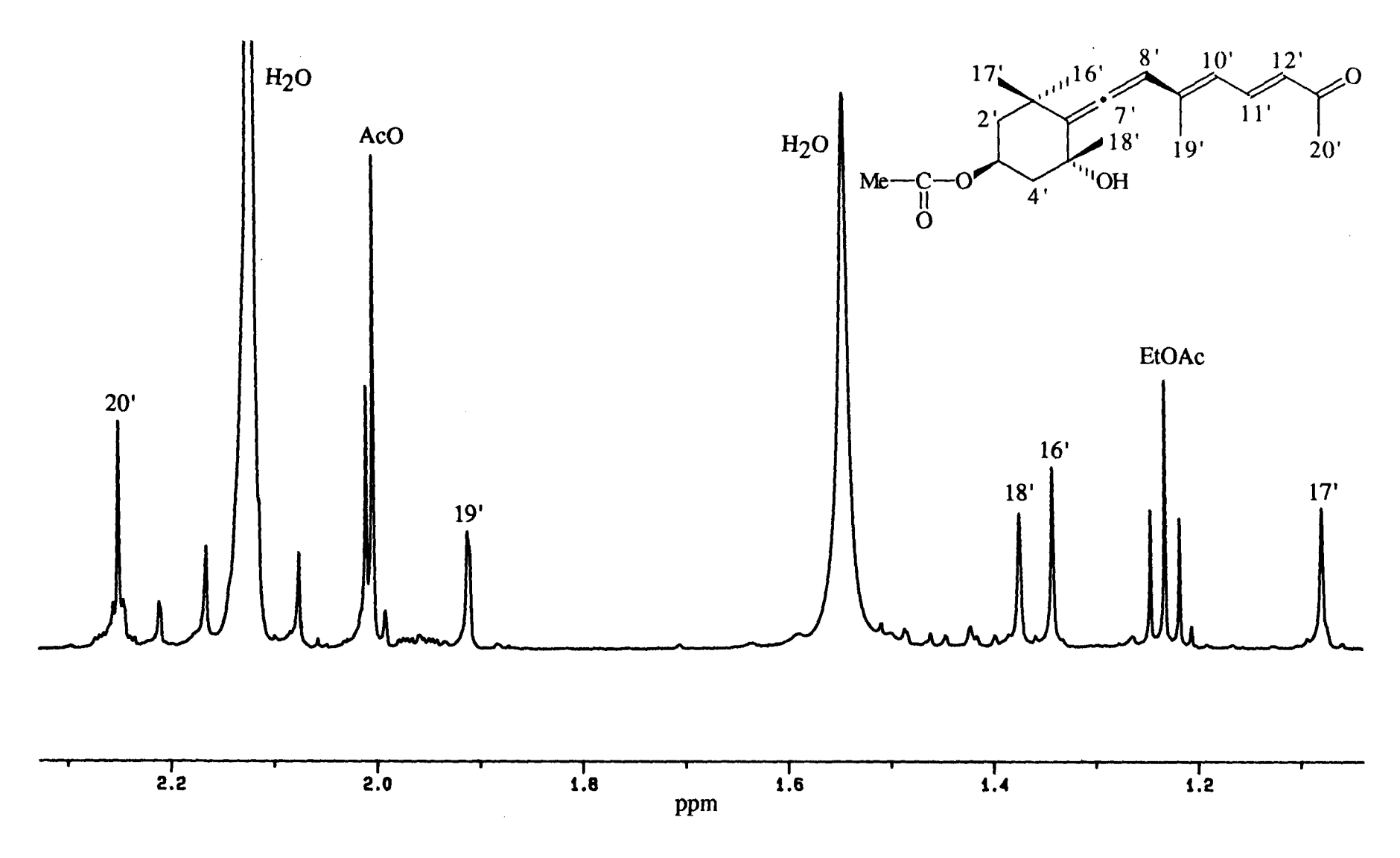


Fig. 52. Expansion of the proton nmr (500 MHz) spectrum of semi-synthetic apo-13'-fucoxanthinone (4) in CD<sub>2</sub>Cl<sub>2</sub> showing resonances from the methyl groups.

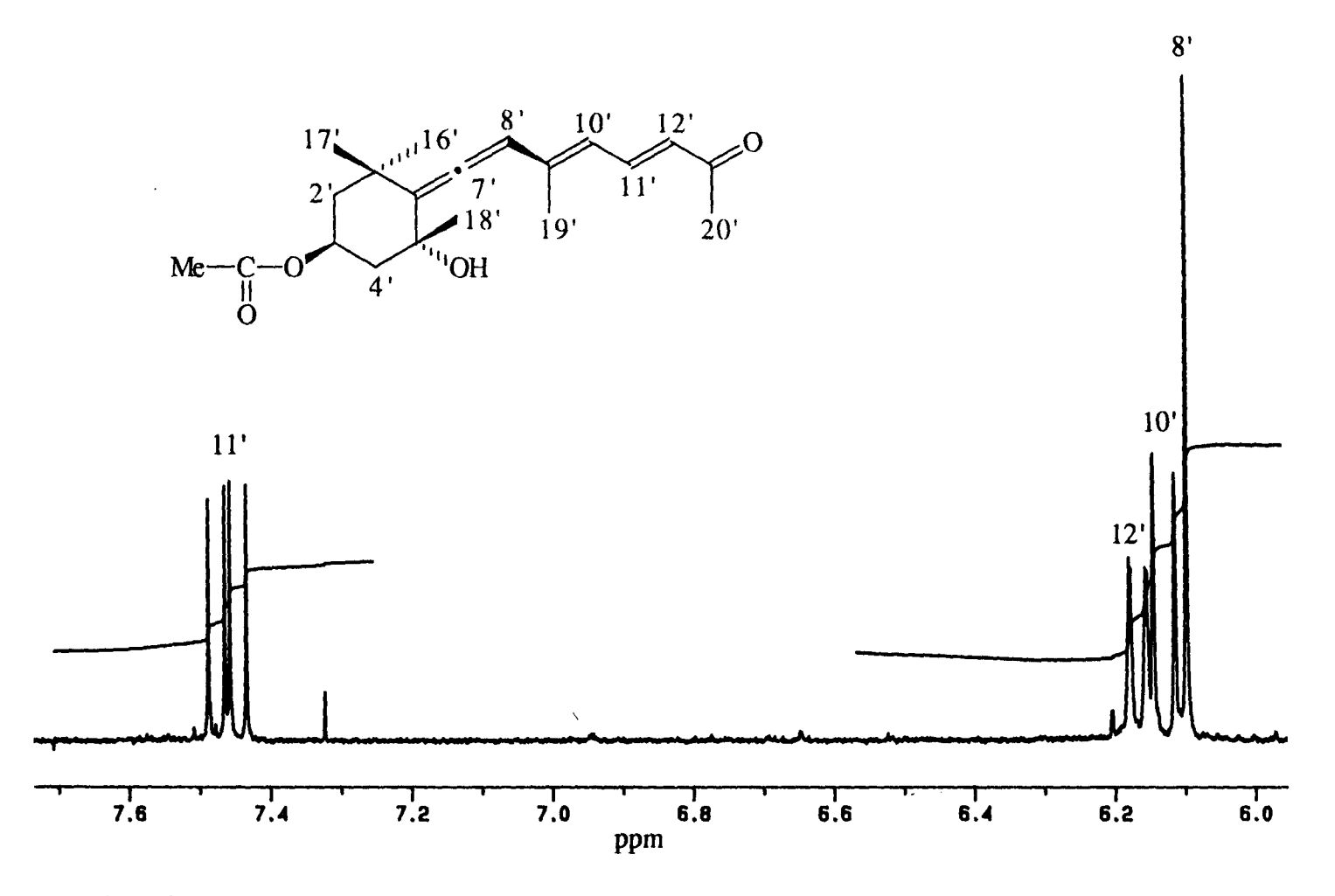


Fig. 53. Expansion of the proton nmr (500 MHz) spectrum of semi-synthetic apo-13'-fucoxanthinone (4) in CD<sub>2</sub>Cl<sub>2</sub> showing olefinic protons.

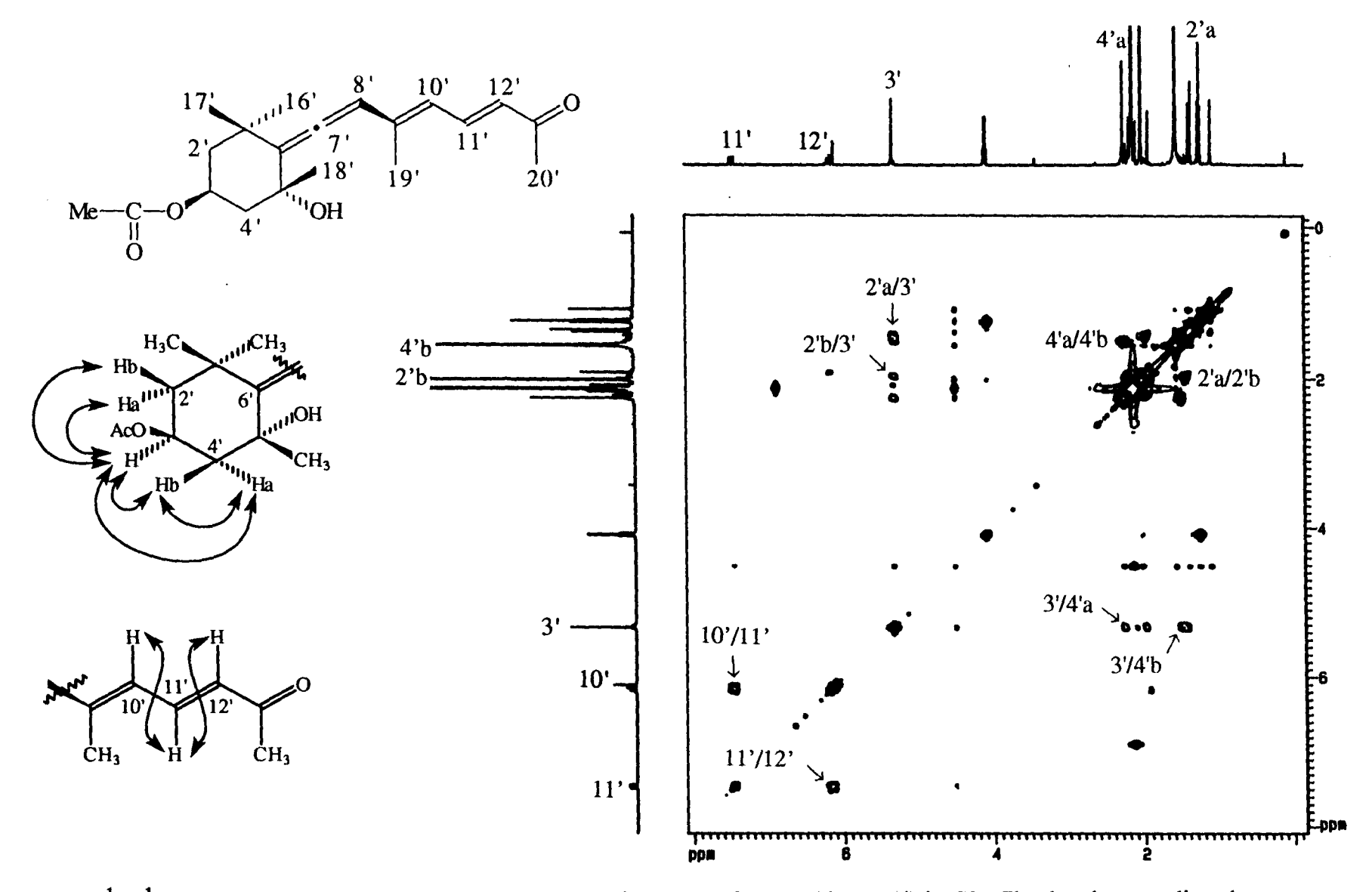


Fig. 54. <sup>1</sup>H-<sup>1</sup>H COSY (500 MHz) spectrum of semi-synthetic apo-13'-fucoxanthinone (4) in CD<sub>2</sub>Cl<sub>2</sub> showing couplings between olefinic protons and couplings between ring protons.

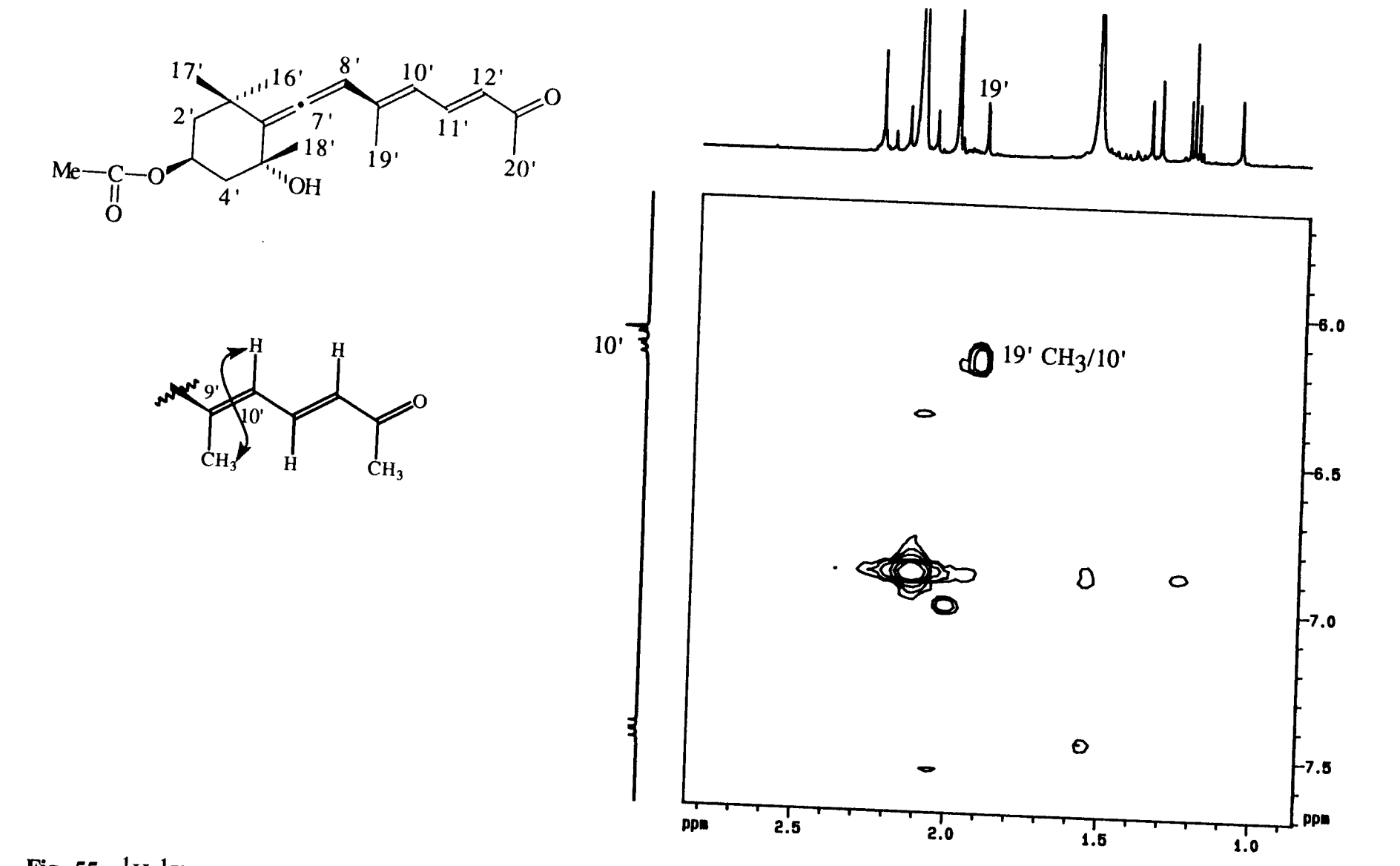


Fig. 55. <sup>1</sup>H-<sup>1</sup>H COSY (500 MHz) spectrum of semi-synthetic apo-13'-fucoxanthinone (4) in CD<sub>2</sub>Cl<sub>2</sub> showing allylic couplings.

The UV-vis spectrum of semi-synthetic apo-13'-fucoxanthinone gave a  $\lambda_{max}$  of 329 nm in methanol (Appendix F, Fig. F21). Using Woodward's rules for calculating the  $\lambda_{max}$  of enones, the following values were calculated:

base value for an acyclic  $\alpha,\beta$ -unsaturated ketone: 215 nm

2 double bonds extending conjugation:

2 x 30 nm 60 nm

 $2 \gamma$  or higher alkyl groups:

2 x 18 nm <u>36 nm</u>

total (in methanol): 311 nm

This calculated value is somewhat lower than the observed value. This is probably due to the allenic functionality in the molecule which is not corrected for by Woodward's rules. The Fieser-Kuhn rules calculated an even lower theoretical  $\lambda_{max}$  (300.8 nm).

The IR spectrum of apo-13'-fucoxanthinone (Appendix E, Fig. E25; Table 6) showed stretching vibrations for an  $\alpha,\beta$ -unsaturated ketone, an acetate group, an allenic group, and a hydroxyl group, which corresponds with the proposed structure.

### iii. Bioassay Results for Semi-synthetic Compounds

The four semi-synthetic apo-fucoxanthinoids were quantitatively bioassayed using the copepod *Tigriopus californicus*. The IC<sub>50</sub> (concentration of compound which inhibits the fecal pellet production rate by 50%) values ranged from 20.2 to 2.2 ppm. The details of this work will be discussed in Chapter 4. Clearly, these four compounds behave as feeding deterrents at very low levels, and are responsible, at least in part, for the feeding deterrent activity of the crude cellular extract from *Phaeodactylum* tricornutum.

### D. General Discussion and Conclusions

The marine diatom *Phaeodactylum tricornutum* was shown to elicit feeding deterrent activity in the copepod *Tigriopus californicus* (Chapter 2). However, the compounds responsible for this activity were unknown. Using a feeding deterrent bioassay based on fecal pellet production by *T. californicus* (Chapter 2), this activity was traced through a chemical isolation scheme, and four compounds were purified which had feeding deterrent activity.

Spectroscopic methods (UV-vis, IR, and nmr spectroscopy and mass spectrometry) were used to tentatively identify these compounds as apo-10'-fucoxanthinal, apo-12'-fucoxanthinal, apo-12-fucoxanthinal, and apo-13'-fucoxanthinone. However, as is often the case with bioactive materials, these compounds were only present in trace amounts, and there was not enough material to do the exhaustive spectroscopy needed to confirm these identifications. Furthermore, these compounds were associated with contaminants which may have been responsible for the feeding deterrent activity.

These compounds appeared to be derived from the carotenoid pigment fucoxanthin by oxidative cleavage. Fucoxanthin is a major pigment in both diatoms and macroscopic brown algae. In order to confirm the identification of the four feeding deterrent compounds, these compounds were prepared semi-synthetically (Bonnett et al., 1969) from fucoxanthin purified from the brown macroalga Fucus distichus. It was believed that any impurities in the semi-synthetic preparations would be different from impurities in the natural material isolated from the diatom Phaeodactylum tricornutum.

Spectroscopic examination of the semi-synthetic compounds found them to be identical to the natural compounds. A thorough study of these compounds using nmr techniques, and comparison with data from the literature (Bonnett *et al.*, 1969)

conclusively identified three of the compounds as apo-10'-fucoxanthinal, apo-12'-fucoxanthinal, and apo-12-fucoxanthinal. The fourth compound was identified as apo-13'-fucoxanthinone based on its proton and <sup>1</sup>H-<sup>1</sup>H COSY nmr spectra. Bioassays showed all four semi-synthetic compounds to be feeding deterrents at very low levels (2 - 20 ppm).

Although these apo-fucoxanthinoids have been made synthetically in the laboratory (Bonnett et al., 1969), they have never been isolated as natural products, nor have they been tested for biological activity. Apo-13'-fucoxanthinone is a novel compound, and has not been described in the literature before, as either a synthetic or natural product. Furthermore, advancements in nmr technology have allowed a more complete assignment of the proton spectra of these molecules than was done by Bonnett et al. (1969). These four compounds are the first feeding deterrent compounds to be isolated from marine phytoplankton using a bioassay specifically designed to detect chemicals responsible for feeding deterrent activity.

As mentioned previously, these compounds appear to be related to fucoxanthin, the major carotenoid pigment in diatoms. Although the diatoms *Thalassiosira* pseudonana and *Phaeodactylum tricornutum* were bioassayed for feeding deterrent activity, only *P. tricornutum* deterred feeding (Chapter 2), and this activity was traced by bioassay-guided chemical fractionation to the four compounds described above. As both diatoms produce fucoxanthin, one would expect to find apo-fucoxanthinoid feeding deterrents in both species if they were being produced enzymatically from fucoxanthin by an enzyme system common to diatoms. In fact, apo-fucoxanthinoids are produced by both *P. tricornutum* and *T. pseudonana* (Chapter 6). However, *P. tricornutum* produces these compounds in much greater quantities than *T. pseudonana*, thus explaining why *P. tricornutum* has a strong feeding deterrent activity while *T. pseudonana* does not. Carotenoids can be oxidized *in vivo* by various oxidative enzymes. In higher plants, one of the main oxidative enzymes, lipoxygenase, catalyzes

the oxidation of unsaturated fatty acids by molecular oxygen to form fatty acid hydroperoxides. It has been suggested by Gross (1991) that these hydroperoxides may, in turn, oxidize carotenoids to apo-carotenoids. It is possible that a similar system could exist in diatoms. The factors which induce or inhibit the activity of such an enzyme would vary from species to species, as is obviously the case for *T. pseudonana* and *P. tricornutum*.

Apo-13'-fucoxanthinone is very closely related to the grasshopper ketone (Fig. 56) isolated from the grasshopper *Romalea microptera* (Meinwald *et al.*, 1968), differing only in having a somewhat longer olefinic chain and one acetylated hydroxyl group. Grasshopper ketone appeared to be produced by the degradation of fucoxanthin-like carotenoids in the grasshopper's diet. This compound had a repellent effect on ants and possibly other predators; thus there is a precedent for the feeding deterrent nature of some apo-carotenoids. In terms of energetics, it would be quite logical to produce a deterrent compound from an abundant pre-existing material. Thus, it seems likely that the diatom *Phaeodactylum tricornutum* does produce apocarotenoids from fucoxanthin, and these compounds function as feeding deterrents to grazers.

Fig. 56. Comparison of the structures of apo-13'-fucoxanthinone (4) and grasshopper ketone (Meinwald *et al.*, 1968).

### Chapter 4

# Observations on Lethal and Sub-lethal Effects of Apo-fucoxanthinoids on the Copepod Tigriopus californicus

#### A. Introduction

Bioactive compounds, such as the apo-fucoxanthinoids isolated and identified from the diatom *Phaeodactylum tricornutum*, can have both lethal and sub-lethal (e.g. feeding deterrence) effects on other organisms (Chapters 2 and 3). Quantitative bioassays can be performed in which the test organisms are exposed to increasing concentrations of the compound of interest, and various parameters, such as feeding rate, swimming speed and survivorship, are measured. These experiments can determine the concentration at which a compound produces a measurable effect in the test organism (Hubert, 1984; Reish and Oshida, 1987).

Quantitative bioassays were performed in this research for two main reasons:

- 1) it was necessary to prove that the semi-synthetic apo-fucoxanthinoids (Chapter 3) did indeed have feeding deterrent activity. Since these semi-synthetic compounds are identical to the natural compounds isolated from the cellular extract of *Phaeodactylum tricornutum* (Chapter 3), then this would prove that the feeding deterrent activity of the cellar extract was due, at least in part, to the apo-fucoxanthinoid compounds.
- 2) it was necessary to determine the effective concentrations of the apofucoxanthinoids in order to determine if they existed in the natural environment at concentrations high enough to produce feeding deterrence.

Therefore, various concentrations of apo-10'-fucoxanthinal, apo-12'-fucoxanthinal, apo-12-fucoxanthinal, and apo-13'-fucoxanthinane were tested on the copepod *Tigriopus californicus*. Two parameters were observed: the fecal pellet production rate

and the percentage of copepods which survived after 24 h. From these observations, the concentration at which there was a 50% inhibition of the fecal pellet production rate  $(IC_{50})$  and the concentration at which there was a 50% mortality  $(LC_{50})$  were calculated.

#### **B.** Materials and Methods

Samples of the semi-synthetic apo-fucoxanthinoids were quantitatively bioassayed as follows. A weighed amount of dried material to be bioassayed was dissolved in 1 ml of autoclaved seawater and sonicated (1 min in bath sonicator at 60 Hz) to facilitate mixing. Five ml of an exponentially growing culture of the diatom *Thalassiosira pseudonana* was added to the dissolved cell extract. Clumps were removed from the cell culture prior to use in the bioassay by filtration (forced through a 200  $\mu$ m screen at a rate of  $\approx 50$  ml min<sup>-1</sup> using a syringe; repeated 4 times). This mixture was placed in a glass vial (volume  $\approx 7$  ml) and five male C6 copepods (*Tigriopus californicus*) were added. The vial was stoppered loosely with cotton wool, and placed in a wire rack. The wire rack held 15 vials. The assay was incubated for 24 h at 18°C with an irradiance of  $\approx 100 \ \mu$ mol m<sup>-2</sup> s<sup>-1</sup> and a L:D cycle of 18:6. Copepods were preconditioned in autoclaved seawater without food for 24 h prior to the bioassay.

Two separate experiments were run. In the first experiment, apo-10'-fucoxanthinal and apo-12'-fucoxanthinal were bioassayed. In the second experiment, apo-12-fucoxanthinal and apo-13'-fucoxanthinane were bioassayed. In each experiment, 5 concentrations of each compound were assayed, in addition to five controls (total number of samples in an experiment = 15). The controls contained 5 ml of live *Thalassiosira pseudonana* cells and 1 ml of autoclaved seawater.

At the end of 24 h, the number of live copepods and the number of fecal pellets in each sample were enumerated. In each of the samples containing an apofucoxanthinoid compound, 10 fecal pellets (or less if the total number of pellets in that sample was less than 10) were selected at random and their dimensions measured. Fecal pellet volume was calculated using the equation  $V = \pi r^2 h$ . In each of the two experiments, 10 fecal pellets from each of two control samples (total pellets = 20 per experiment) were also measured.

## C. Results and Discussion

In each of the following sections, results will be illustrated graphically using only apo-12'-fucoxanthinal. The results shown for this compound are typical for the other three compounds.

# i. Fecal Pellet Volume

The volumes of fecal pellets from copepods fed a diet of *Thalassiosira* pseudonana mixed with varying amounts of feeding deterrent compounds were measured to determine whether feeding deterrent concentration had any effect on fecal pellet size (Appendix F, Tables F1 and F2). For all four apo-fucoxanthinoids, a slight decrease in fecal pellet volume was observed with increasing concentration of feeding deterrent (Fig. 57). However, due to the large variations in fecal pellet size, this decrease was not statistically different from a line representing constant fecal pellet size. In addition, copepods given high concentrations of apo-fucoxanthinoid feeding deterrents produced pellets which were irregularly formed, small, and reddish in color, as well as producing a number of "ghost pellets" (empty fecal pellet membranes).

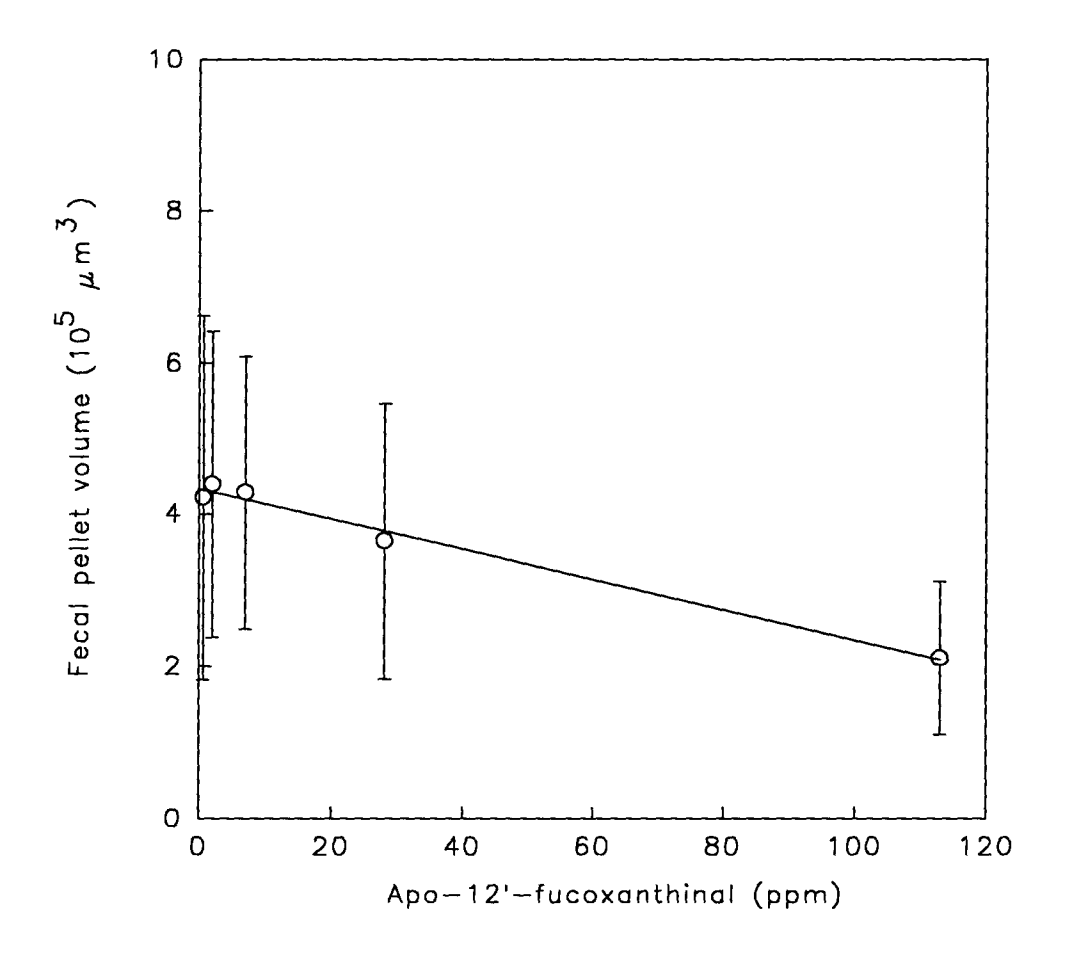


Fig. 57. Decrease in fecal pellet volume of the copepod *Tigriopus californicus* when given increasing amounts of the compound apo-12'-fucoxanthinal. Error bars  $= \pm 1$  SD.

# ii. Fecal Pellet Count

The number of fecal pellets produced by *Tigriopus californicus* on diets containing varying amounts of feeding deterrent compounds was observed (Appendix F, Tables F3 and F4). The number of fecal pellets decreased as the concentration of feeding deterrent compound increased for all four apo-fucoxanthinoids.

The fecal pellet production rate (pellets h<sup>-1</sup> copepod<sup>-1</sup>) was calculated from the fecal pellet count for each sample. A curve was fit to each of the four data sets using the program Sigmaplot 5.0. These curves were of the general equation:

$$F = F_m * e^{-kc^a}$$

where c = the concentration of the feeding deterrent (ppm)

F = fecal pellet production rate (pellets  $h^{-1}$ )

 $F_m$  = the maximum fecal pellet production rate (pellets  $h^{-1}$ )

= the average value for the control (c = 0)

k, a = constants

This equation makes the following assumptions:

- 1)  $F \rightarrow Fm$  when  $c \rightarrow 0$
- 2)  $F \rightarrow 0$  when  $c \rightarrow \infty$ .

Figure 58 shows this equation fitted to data from the quantitative bioassays for apo-12'-fucoxanthinal. Producing an equation for each data set allows bioassay results from a sample containing an unknown amount of an apo-fucoxanthinoid to be used to calculate the concentration of the apo-fucoxanthinoid. Table 8 lists the fitting parameters for each of the four apo-fucoxanthinoids tested.

**Table 8.** Constants for the equation  $F = F_m * e^{-kc^a}$  when fitted to the data sets for each of the four apo-fucoxanthinoid compounds.

Compound Type	Compound	Fm	k	a
Epoxide	Apo-10'-fucoxanthinal	1.09	0.59	0.20
	Apo-12'-fucoxanthinal	1.09	0.45	0.39
Allenic	Apo-12-fucoxanthinal	1.76	0.12	0.91
	Apo-13'-fucoxanthinone	1.76	1.30 x 10 <sup>-6</sup>	4.39

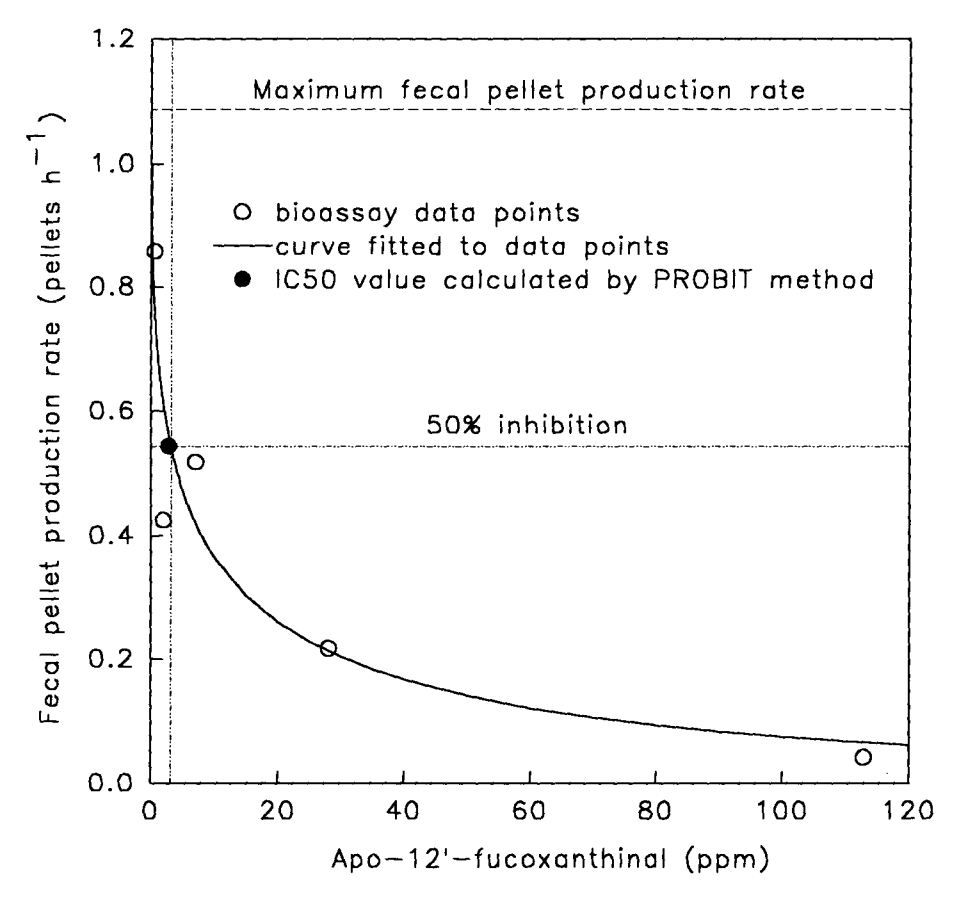


Fig. 58. Decrease in fecal pellet production rate of the copepod *Tigriopus californicus* when given increasing amounts of the compound apo-12'-fucoxanthinal. The IC<sub>50</sub> value, as calculated by the PROBIT method, is shown.

The IC<sub>50</sub> (concentration at which fecal pellet production rate was inhibited by 50%) values were calculated by the PROBIT method (Appendix G; Hubert, 1984). These values ranged from 1.84 to 20.0 ppm (Table 9). Therefore, the apofucoxanthinoids act as feeding deterrents at very low concentrations. From these results, one can see that longer chain compounds are more active than shorter chain compounds. Of the two compounds containing the epoxide functionality, apo-10'-fucoxanthinal, the compound with the longest chain length, acts as a feeding deterrent at a lower concentration than apo-12'-fucoxanthinal, the shorter chain length compound. Likewise, of the two compounds containing the allenic functionality, the longer chain length compound apo-12-fucoxanthinal is more active than the shorter

chain length compound apo-13'-fucoxanthinone. Thus, there is a structure/function relationship for the feeding deterrent activity of the apo-fucoxanthinoids.

**Table 9.** IC<sub>50</sub> values and standard deviations calculated from the fecal pellet production rate data for the four apo-fucoxanthinoids using the PROBIT method. a, b = calculated parameters from the PROBIT method (Appendix G);  $r^2$  = coefficient of determination (a measure of how well the data fits the PROBIT line).

Compound Type	Compound	a	b	IC <sub>50</sub> (ppm)	σ	r <sup>2</sup>
Epoxide	Apo-10'-fucoxanthinal	3.96	0.46	1.84	1.53	0.49
	Apo-12'-fucoxanthinal	2.52	1.01	2.87	0.10	0.90
Allenic	Apo-12-fucoxanthinal	0.59	1.60	5.75	0.04	0.98
	Apo-13'-fucoxanthinone	2.08	0.88	20.0	0.14	0.53

## iii. Total Fecal Pellet Volume

The total volume of fecal material produced in a given sample was determined by multiplying the total number of fecal pellets produced in that sample by the average fecal pellet volume for that sample. This total fecal pellet volume was then converted into a rate (fecal volume h<sup>-1</sup> copepod<sup>-1</sup>), and the effect of varying concentrations of apo-fucoxanthinoid feeding deterrents on this rate was observed (Appendix F, Tables F5 and F6). As in the previous studies, increasing concentrations of feeding deterrents had a negative impact on the feeding of *Tigriopus californicus*, and this was reflected by decreases in the fecal volume production rate.

The four apo-fucoxanthinoid data sets were fit to the same equation as used before (Fig. 59) except that total fecal volume was considered instead of fecal pellet number. Table 10 lists the fitting parameters for each of the four apo-fucoxanthinoids tested.

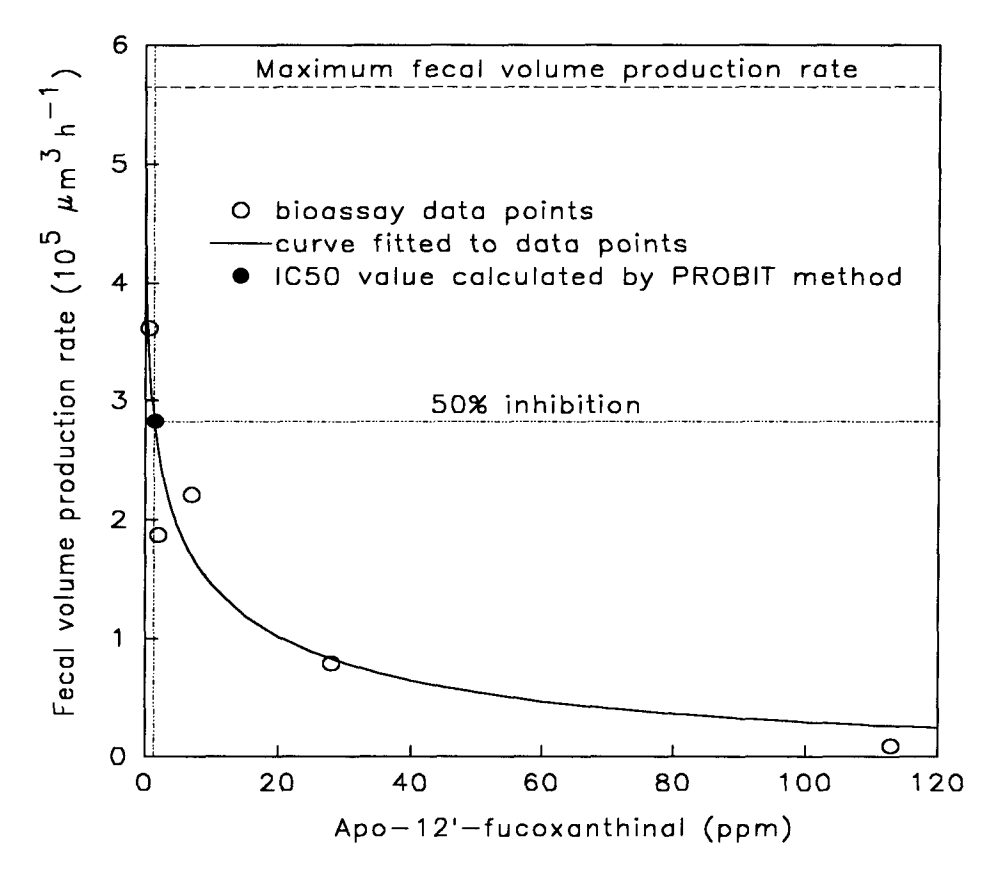


Fig. 59. Decrease in fecal volume production rate of the copepod *Tigriopus* californicus when given increasing amounts of the compound apo-12'-fucoxanthinal. The IC<sub>50</sub> value, as calculated by the PROBIT method, is shown.

**Table 10.** Constants for the equation  $F = F_m * e^{-kc^a}$  when fitted to the data sets for each of the four apo-fucoxanthinoid compounds.

Compound Type	Compound	$F_{\mathbf{m}}$	k	a
Epoxide	Apo-10'-fucoxanthinal	5.65	0.92	0.17
•	Apo-12'-fucoxanthinal	5.65	0.63	0.34
Allenic	Apo-12-fucoxanthinal	9.15	0.34	0.90
	Apo-13'-fucoxanthinone	9.15	5.91x10 <sup>-8</sup>	5.54

The IC<sub>50</sub> (concentration at which fecal volume production rate was inhibited by 50%) values were calculated by the PROBIT method (Appendix G; Hubert, 1984). These values ranged from 0.40 to 7.93 ppm (Table 11), and reflected the IC<sub>50</sub> values calculated from the fecal pellet production rate. Again, longer chain compounds were active at lower concentrations that shorter chain compounds. However, this method is considered less accurate for predicting the IC<sub>50</sub> values than the fecal pellet production rate method because it relies on an average fecal pellet volume calculated from only 10 fecal pellets.

Table 11. IC<sub>50</sub> values and standard deviations calculated from the fecal volume production rate data for the four apo-fucoxanthinoids using the PROBIT method. a, b = calculated parameters from the PROBIT method (Appendix G);  $r^2$  = coefficient of determination (a measure of how well the data fits the PROBIT line).

Compound Type	Compound	a	b	IC <sub>50</sub> (ppm)	σ	r <sup>2</sup>
Epoxide	Apo-10'-fucoxanthinal	4.06	0.58	0.40	0.51	0.55
	Apo-12'-fucoxanthinal	2.83	1.00	1.48	0.10	0.90
Allenic	Apo-12-fucoxanthinal	2.09	1.37	1.34	0.05	0.91
	Apo-13'-fucoxanthinone	1.92	1.06	7.93	0.09	0.49

## iv. Lethal Concentrations

The lethal effects of high concentrations of feeding deterrents were observed for two compounds, apo-10'-fucoxanthinal and apo-12'-fucoxanthinal. Of the four semi-synthetic compounds, only these two were produced in high enough yields (Chapter 3) so that enough material was available for assays at concentrations at which mortality was observed. As expected, increasing concentrations of the feeding deterrents produced increasing mortality (Appendix F, Table F7).

The two data sets were fit to the equation:

$$S = 100*e^{-kc^a}$$

where  $S = percentage$  of subjects which survived at the end of 24 h

 $c = concentration$  of feeding deterrent compound (ppm)

 $k$ ,  $a = constants$ 

This equation makes the following assumptions:

1) 
$$S \rightarrow 100$$
 when  $c \rightarrow 0$ 

2) 
$$S \rightarrow 0$$
 when  $c \rightarrow \infty$ .

Figure 60 shows the data set and the fitted line for apo-12'-fucoxanthinal. Table 12 lists the fitting parameters for the two apo-fucoxanthinoids tested.

**Table 12.** Constants for the equation  $S = 100 *e^{-kc^a}$  when fitted to the data sets for the two apo-fucoxanthinoid compounds tested for lethal effects.

k	a
6.61x10 <sup>-3</sup>	1.07
1.14x10 <sup>-8</sup>	5.04

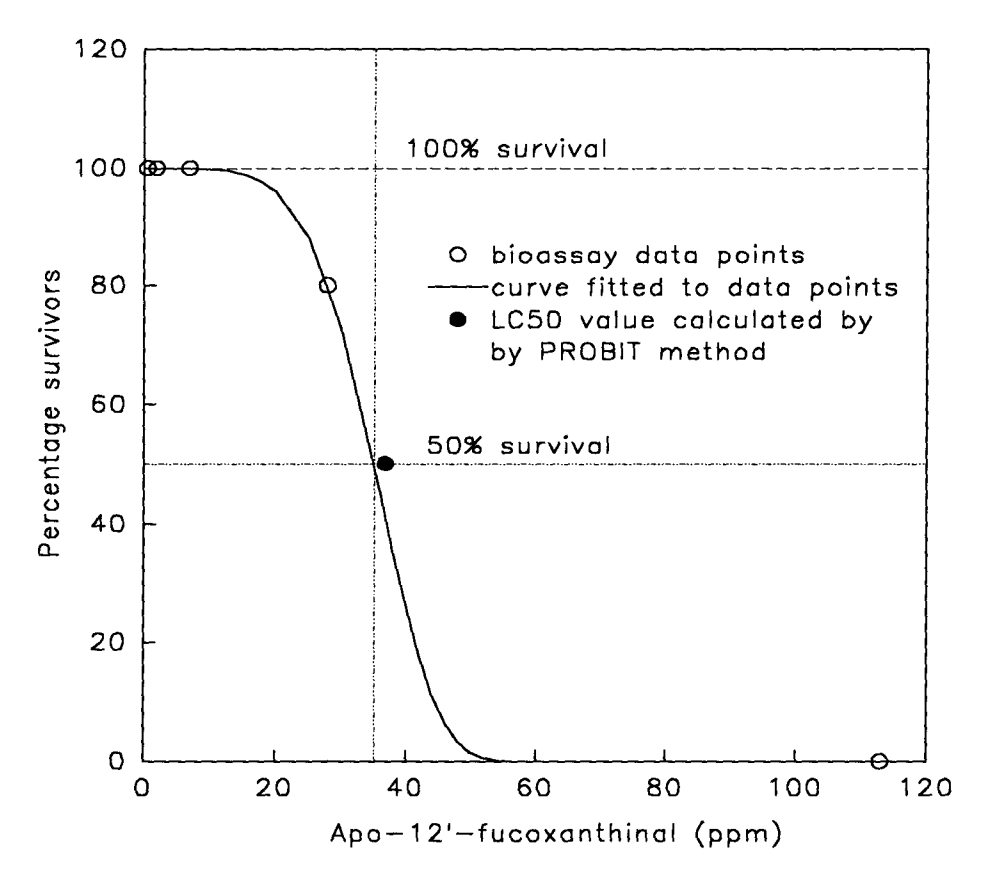


Fig. 60. Increased mortality of the copepod *Tigriopus californicus* when given increasing amounts of the compound apo-12'-fucoxanthinal. The LC<sub>50</sub> value, as calculated by the PROBIT method, is shown.

The LC<sub>50</sub> (concentration at which the mortality rate was 50%) values were calculated by the PROBIT method (Appendix G; Hubert, 1984). These values ranged between 36.9 and 337 ppm (Table 13). Unlike the IC<sub>50</sub> values, the shorter chain compound (apo-12'-fucoxanthinal) was toxic at lower concentrations than the longer chain compound (apo-10'-fucoxanthinal). This may be due to the fact that the modes of action for feeding inhibition may be quite different from those for lethality.

**Table 13.** LC<sub>50</sub> values and standard deviations calculated for apo-10'-fucoxanthinal and apo-12'-fucoxanthinal using the PROBIT method. a, b = calculated parameters from the PROBIT method (Appendix G);  $r^2 = coefficient$  of determination (a measure of how well the data fits the PROBIT line).

Compound	a	b	LC <sub>50</sub> (ppm)	σ	r <sup>2</sup>
Apo-10'-fucoxanthinal	2.86	0.47	337	1.32	0.46
Apo-12'-fucoxanthinal	1.44	1.00	36.9	0.10	0.65

# D. General Discussion and Conclusions

The lethal and sub-lethal effects of the apo-fucoxanthinoids were observed using the copepod *Tigriopus californicus*. The use of quantitative bioassays allowed the minimum concentrations at which either feeding deterrent or lethal effects were observed to be determined. From this data, IC<sub>50</sub> (feeding deterrent effect) and LC<sub>50</sub> (lethal effect) values were calculated.

All four apo-fucoxanthinoid compounds tested displayed feeding deterrent activity. This conclusively proved that the feeding deterrent activity in *Phaeodactylum tricornutum* cellular extracts was due, at least in part, to these four compounds, since the semi-synthetic compounds used in these tests were identical to the compounds isolated from *P. tricornutum* (Chapter 3).

When Tigriopus californicus was fed a diet of Thalassiosira pseudonana cells mixed with varying amounts of feeding deterrent compound, both the fecal pellet number and the total fecal pellet volume showed a decrease with increased concentrations of feeding deterrent. The IC50 values were calculated using either the fecal pellet or fecal volume production rate. Both methods produced similar results, however it was felt that the fecal pellet production rate was more accurate, as it didn't depend on an average fecal pellet volume (it was too time consuming to measure the

volume of every fecal pellet). The IC<sub>50</sub> values calculated from the fecal pellet production rate ranged from 1.84 to 20.0 ppm. Therefore, apo-fucoxanthinoids are capable of acting as feeding deterrents at very low concentrations.

The structure of the apo-fucoxanthinoids appeared to have an effect on their function. Longer chain compounds (such as apo-10'-fucoxanthinal) had a greater feeding deterrent activity than shorter chain compounds (such as apo-12'-fucoxanthinal). There are two possible explanations for this:

- 1) the receptor site to which these compounds bind in order to produce deterred feeding may bind more strongly to longer chain compounds.
- 2) longer chain compounds are more lipophilic than shorter chain compounds, and can penetrate membranes more readily. Thus, they may be able to reach intracellular receptor sites better than shorter chain compounds.

An equation of the form  $F = F_m * e^{-kc^a}$  was fitted to each of the data sets. This provides a very useful tool for future studies. A sample containing an unknown amount of an apo-fucoxanthinoid feeding deterrent can be bioassayed, and the results of this bioassay (F) can be used to calculate the concentration (c) of the feeding deterrent in the bioassay.

At high concentrations, the apo-fucoxanthinoids can have lethal effects. Both apo-10'-fucoxanthinal and apo-12'-fucoxanthinal produced lethal effects, with LC<sub>50</sub> values which ranged from 36.9 to 337 ppm. In contrast to the feeding deterrent effect, the shorter chain compound was more active than the longer chain compound. This suggests that the modes of action for the feeding deterrent effect and the lethal effect are quite different.

This study shows how the simple procedure of quantitative bioassays can be used to increase understanding of lethal and sub-lethal responses, concentration effects, and modes of action. It also allows compounds which are suspected to be bioactive to

be conclusively tested in a controlled situation. Thus, quantitative bioassays form one more tool in the arsenal necessary to solve complex ecological problems.

# Chapter 5

# Development of an High Performance Liquid Chromatography Technique for Quantitative Analyses of Apo-fucoxanthinoids

## A. Introduction

The concentrations of apo-fucoxanthinoid feeding deterrents can be determined by quantitative bioassays (Chapter 4). However, the precision of quantitative bioassays is relatively low due to the natural variations in responses to feeding deterrents among the individual subjects in the bioassays. Furthermore, these feeding deterrent bioassays are very time consuming, as approximately a month is required to set up phytoplankton and copepod cultures, and each quantitative bioassay takes a week to perform.

High performance liquid chromatography (HPLC, Chapter 3) is a very powerful technique for separation, identification, and quantification of compounds. As HPLC depends strictly on physical/chemical factors to quantify compounds, and these factors have a low level of natural variability compared to the variability of organisms, the precision of this technique is much greater than that for quantitative bioassays.

Analysis of a sample using HPLC is very rapid, requiring approximately 2 h to set up equipment and equilibrate the HPLC column, and as little as 20 min to assay a sample. Therefore, an HPLC method capable of quantifying apo-fucoxanthinoids would be a very useful tool in further studies of these compounds.

All four apo-fucoxanthinoid compounds isolated have strong UV-vis absorptions (Chapter 3) which are characteristic of these compounds, and which are readily detected using a spectrophotometer, an instrument commonly coupled to an HPLC in order to detect compounds eluting from the HPLC column. In this study, the apofucoxanthinoids were detected using a photo-diode array (PDA) detector. This is

simply a spectrophotometer capable of recording an entire UV-vis spectrum instantaneously (Chapter 3). Thus, a complete UV-vis spectrum can be taken for each compound eluting from the HPLC column. Using the data collected from such a system, compounds can be:

- 1) identified by their characteristic elution times and UV-vis spectra.
- 2) quantified by integration of the area under the elution peak at a given wavelength.

An excellent HPLC system for the analysis of chlorophylls and carotenoids has been developed by Wright *et al.* (1991). This system has been modified slightly for use in detecting apo-fucoxanthinoids.

## **B.** Materials and Methods

# i. Sample Preparation

A cellular extract was prepared from the diatom *Phaeodactylum tricornutum* as described in Chapter 2. A known amount of this dried methanolic extract was dissolved in 10 ml of water/methanol (80:20) and applied to a C-18 sep-pak. The sep-pak was rinsed with 20 ml water, and retained pigments were eluted with 10 ml ethyl acetate. The ethyl acetate was evaporated under a stream of nitrogen gas. Just prior to injection on the HPLC column, the sample was redissolved in 0.8 ml of methanol and 0.2 ml of water.

Samples containing known amounts of semi-synthetic apo-fucoxanthinoids were used as standards. These standards were dissolved in 0.8 ml methanol and 0.2 ml water just prior to injection on the HPLC column.

# ii. HPLC Method

The HPLC method used in this research was a modified version of the one developed by Wright *et al.* (1991). The solvent system was as follows:

solvent A: 80:20 methanol: 0.5 M ammonium acetate (aq.; pH 7.2 v/v)

solvent B: 90:10 acetonitrile (210 nm UV cut-off grade): water (v/v)

solvent C: ethyl acetate (HPLC grade)

The HPLC was operated in gradient mode (the solvent system composition underwent programmed changes over the course of a run). The program used is shown in Table 14.

**Table 14.** Program for the HPLC solvent system gradient used for quantifying apofucoxanthinoids.

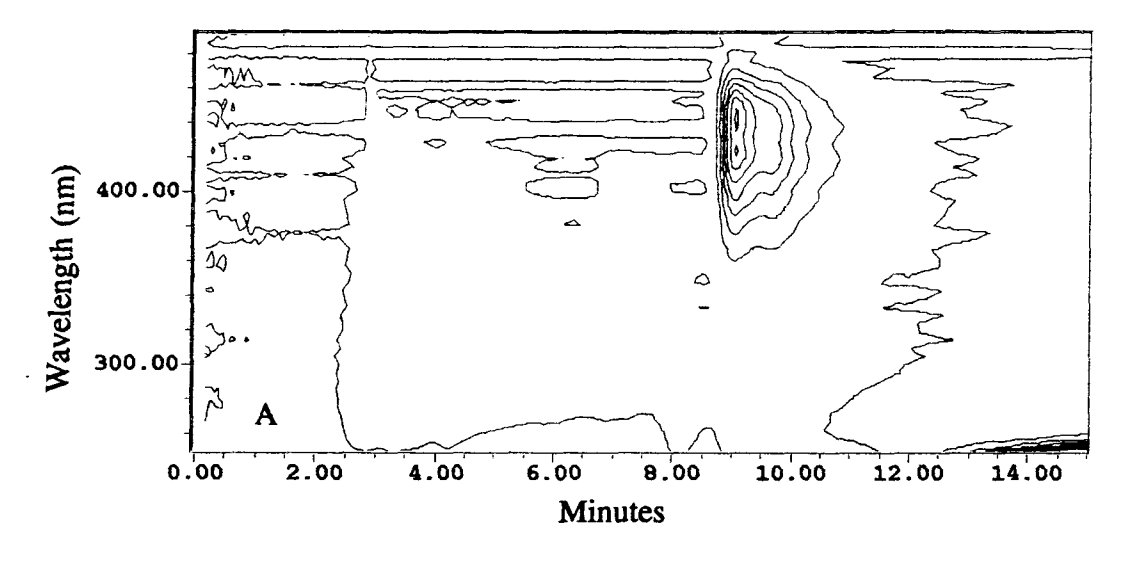
Time (min)	Flow rate (ml min <sup>-1</sup> )	% A	% B	% C	Conditions
0	1.0	100	0	0	Injection
4	1.0	0	100	0	Linear gradient
18	1.0	0	20	80	Linear gradient
21	1.0	0	100	0	Linear gradient
24	1.0	100	0	0	Linear gradient
35	1.0	100	0	0	Equilibration
36	0	100	0	0	Shut down;
					linear gradient

The HPLC system used was a Waters HPLC with a PDA detector. The column was an Econsil C-18, 5  $\mu$ m (1 = 250 mm, I.D. = 4.6 mm) reverse phase column. The injection volume for all samples was 25  $\mu$ l. Data was processed on an IBM-type 486 computer using Water's Millenium software.

## C. Results and Discussion

## i. Standards

Apo-10'-fucoxanthinal, apo-12'-fucoxanthinal, apo-12-fucoxanthinal, and apo-13'-fucoxanthinone were run individually using the previously described HPLC method. Figures 61 - 64 show the data from the HPLC/PDA system for each of these compounds. The retention times and absorbance wavelengths are specific to and characteristic of each of these compounds. Note that each broad peak has at least one major shoulder. These shoulders result from the presence of cis-trans isomers (Chapter 3). The major peak is probably the all trans compound, and the shoulder is probably the 13-cis isomer. It is very difficult to isolate pure trans compounds, and once isolated, the trans compounds undergo cis-trans isomerization as soon as they are exposed to light. As this isomerization is believed to occur in the natural seawater environment, and thus both cis and trans isomers play a role in feeding deterrent effects, no further efforts were made to separate cis-trans isomers. For calculation purposes, the area under the peak included the "cis" shoulder, as all previous absorbance measurements also included cis compounds. Table 15 lists retention times and absorbance maxima for all for compounds. The peak height (V) and peak area (V s) normalized to 1  $\mu$ g of compound are also given. Due to the very limited amounts of pure apo-fucoxanthinoids available, a calibration curve was not done, and all calculations were based on the HPLC response at a single concentration (assuming a linear response with increasing concentration). The error resulting from this assumption was quite small in comparison to the errors resulting from sample preparation.



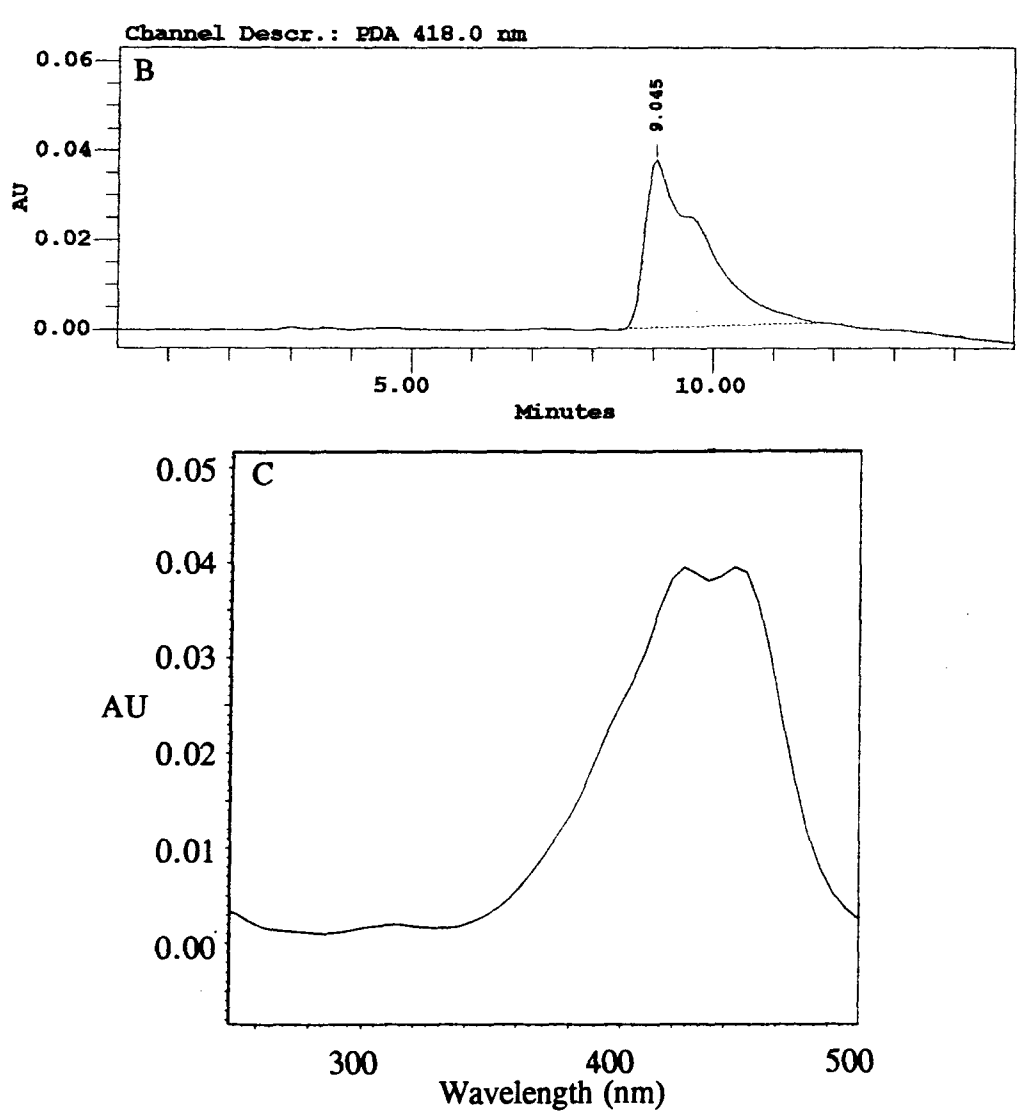
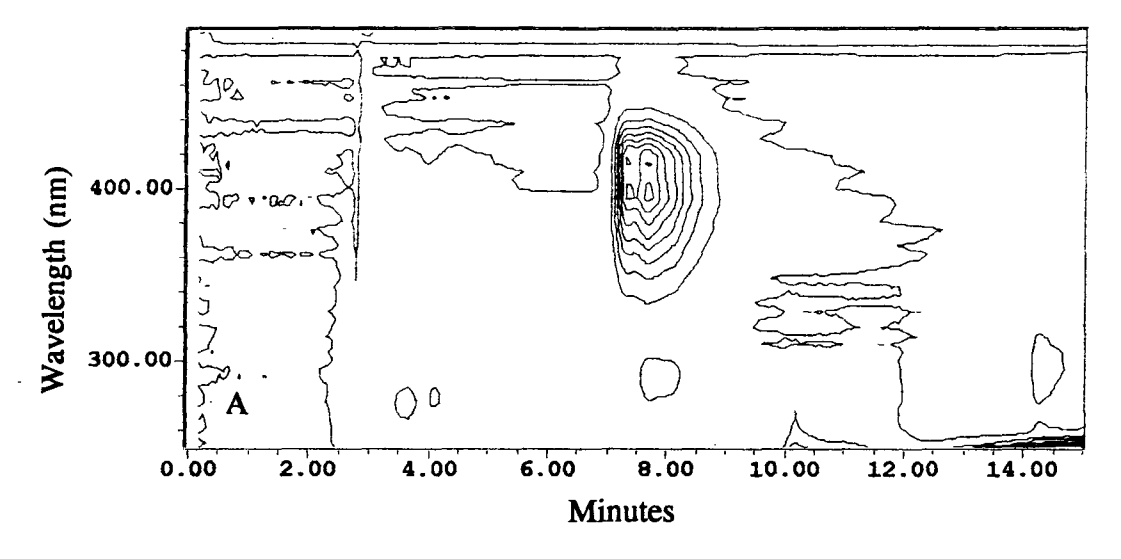


Fig. 61. Data generated by the HPLC/photo-diode array detector system for the apo-10'-fucoxanthinal standard. A. Contour plot. B. Chromatogram at 418 nm showing peak at 9.045 min. C. UV-vis spectrum of peak at 9.045 min.



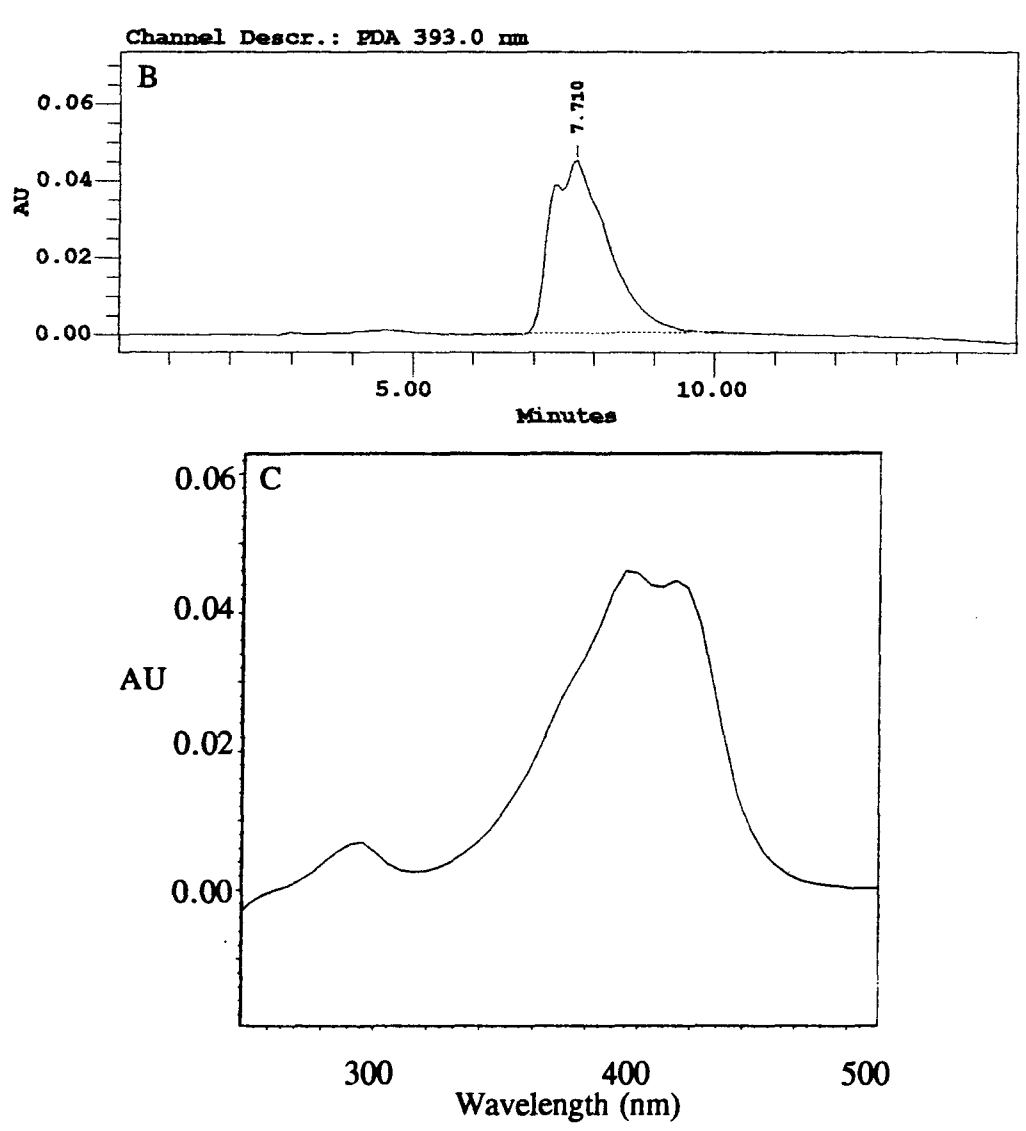
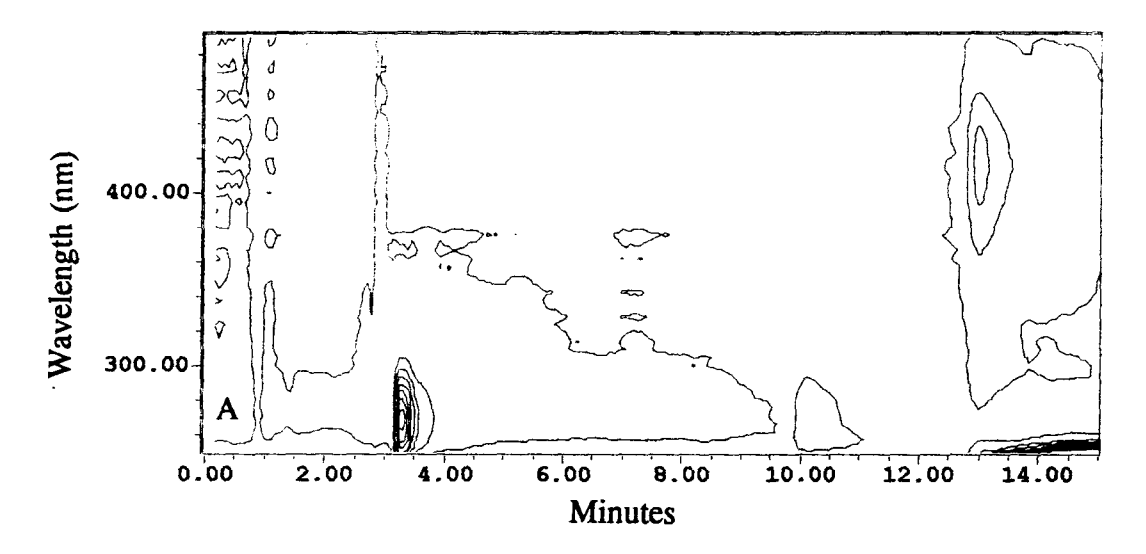


Fig. 62. Data generated by the HPLC/photo-diode array detector system for the apo-12'-fucoxanthinal standard. A. Contour plot. B. Chromatogram at 393 nm showing peak at 7.710 min. C. UV-vis spectrum of peak at 7.710 min.



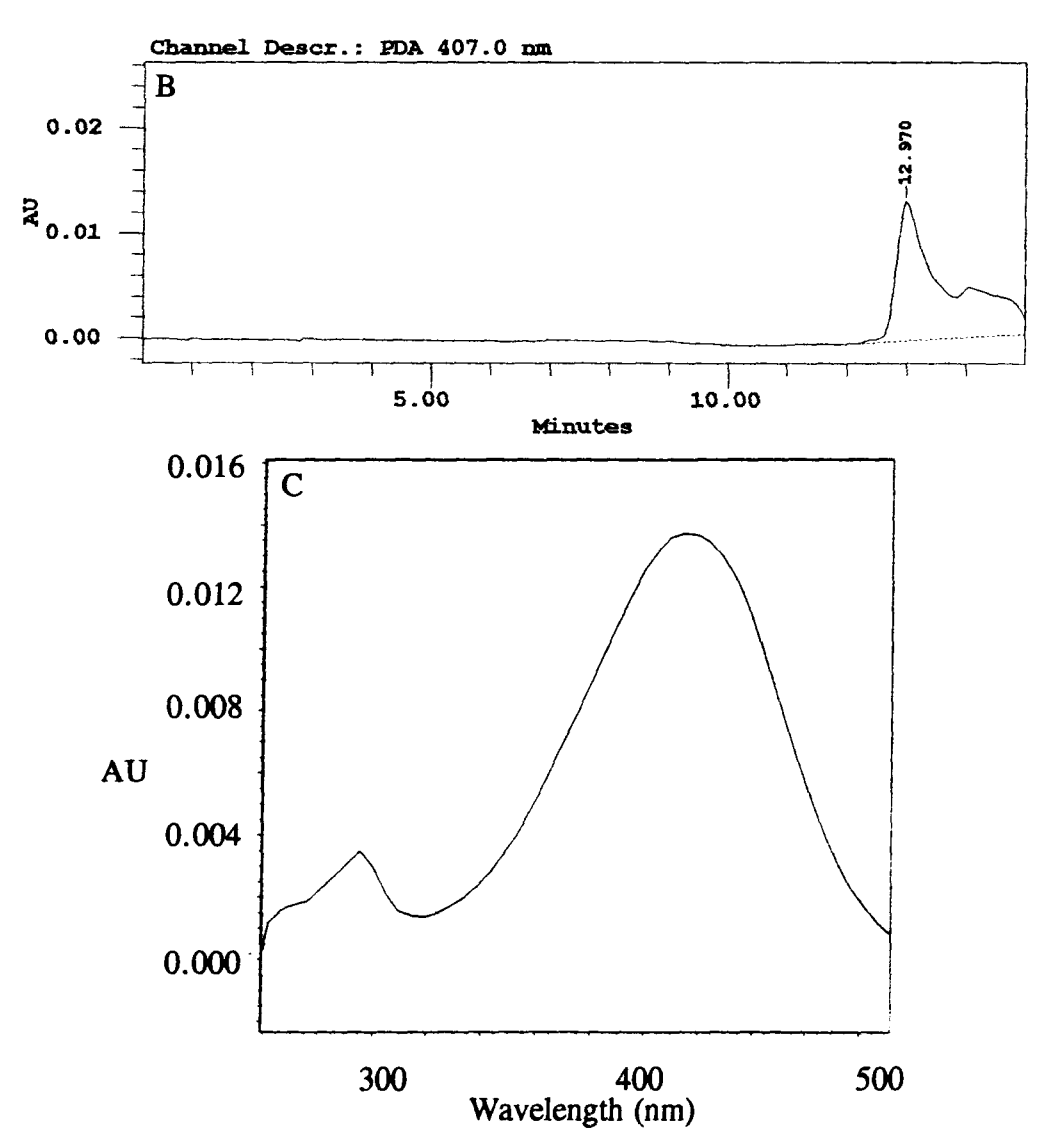
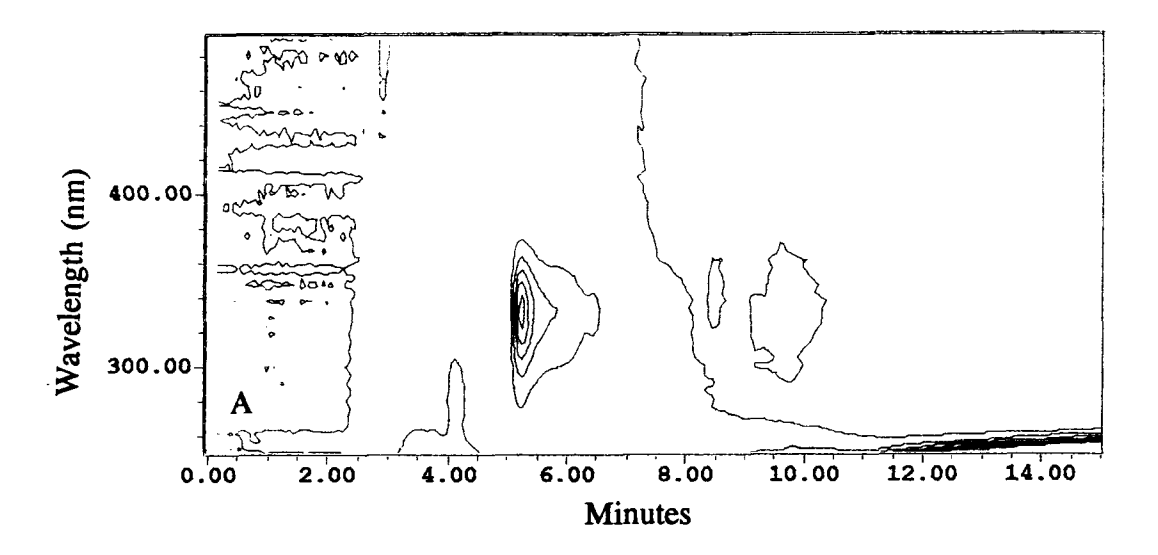


Fig. 63. Data generated by the HPLC/photo-diode array detector system for the apo-12-fucoxanthinal standard. A. Contour plot. B. Chromatogram at 407 nm showing peak at 12.970 min. C. UV-vis spectrum of peak at 12.970 min.



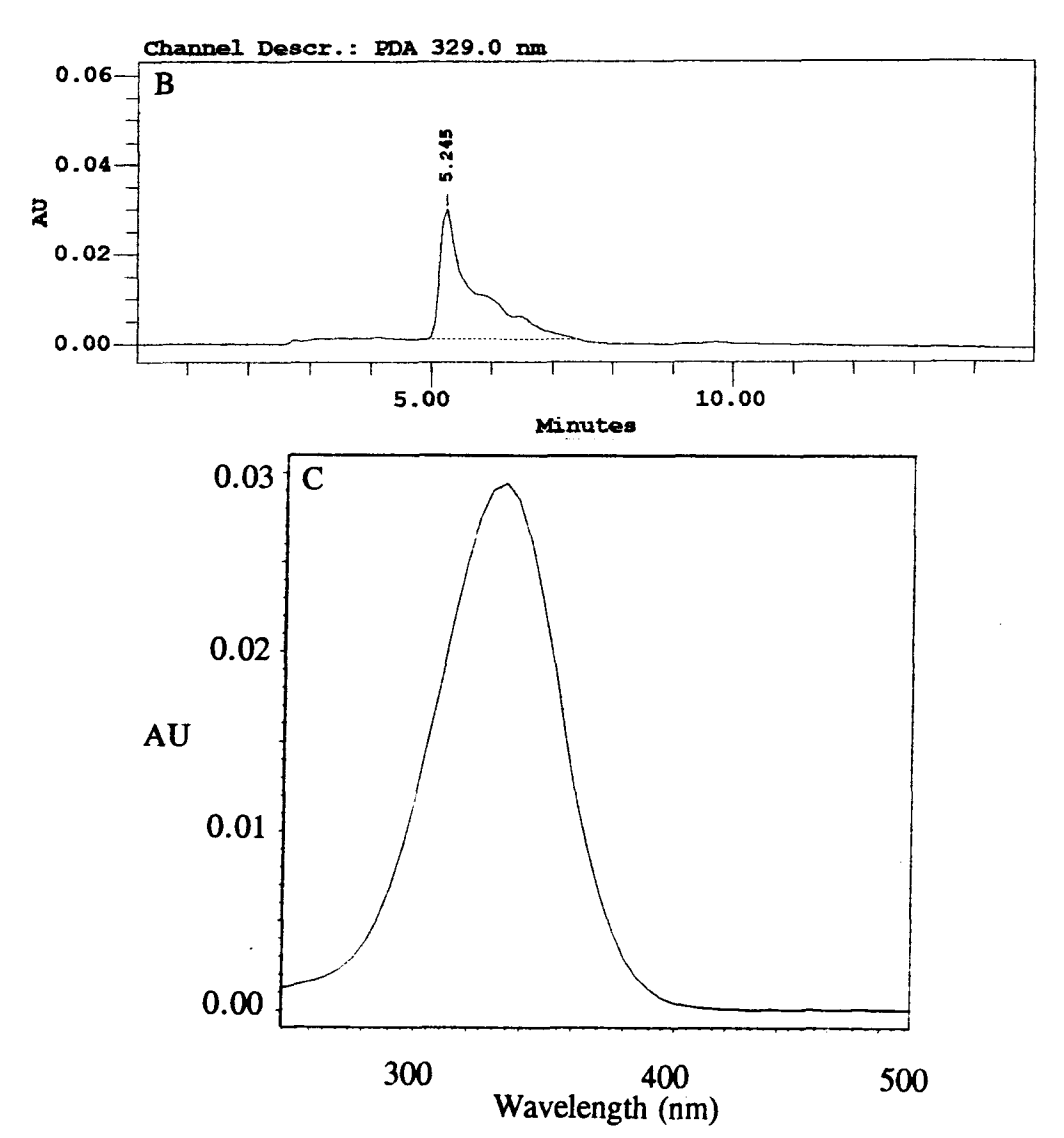


Fig. 64. Data generated by the HPLC/photo-diode array detector system for the apo-13'-fucoxanthinone standard. A. Contour plot. B. Chromatogram at 329 nm showing peak at 5.245 min. C. UV-vis spectrum of peak at 5.245 min.

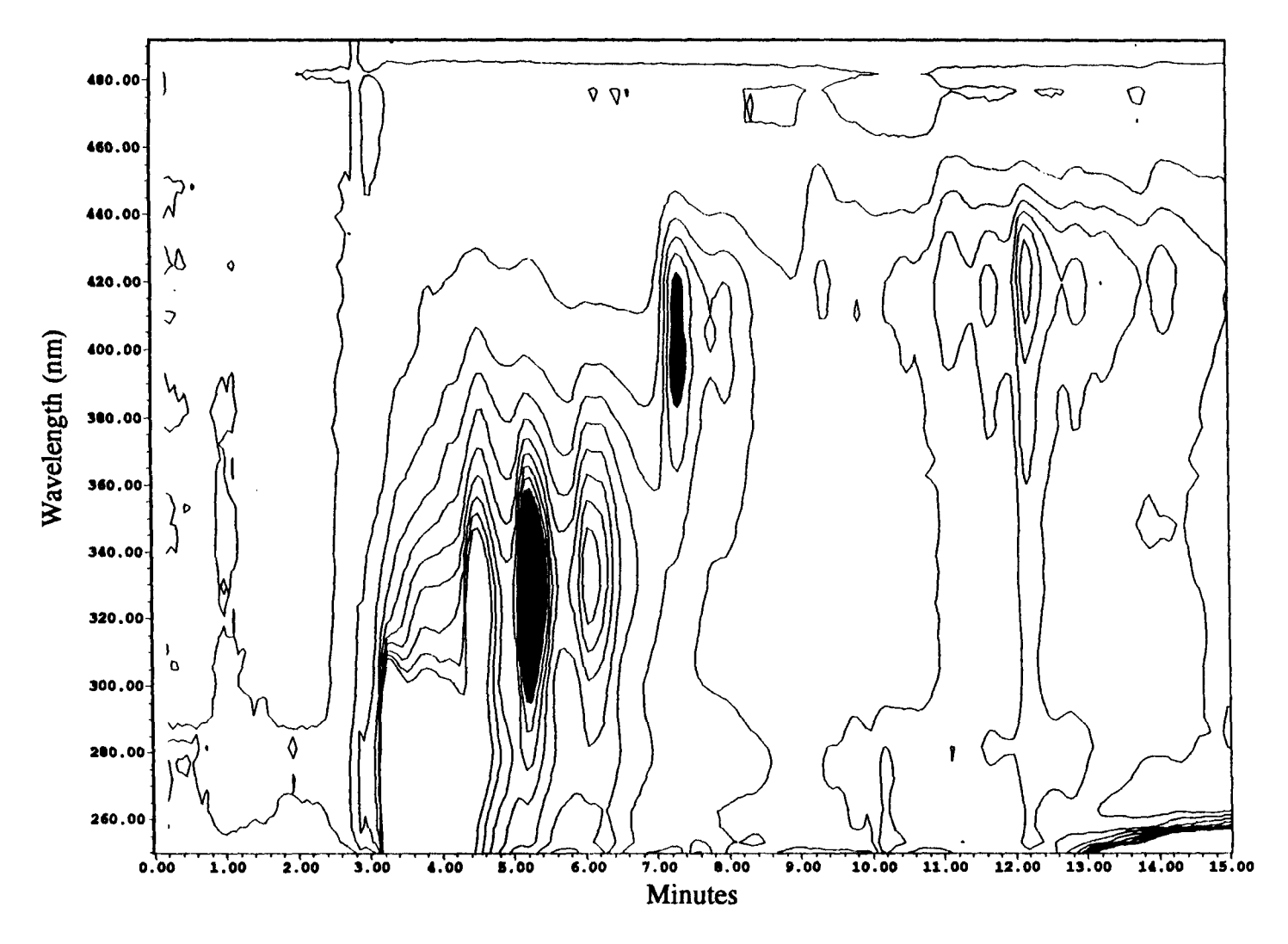


Fig. 65. Data from HPLC/photo-diode array detector for crude cellular extract from *Phaeodactylum tricornutum*. Shaded areas indicate two peaks identified as apo-13'-fucoxanthinone (at 5.240 min) and apo-12'-fucoxanthinal (at 7.307 min) respectively.

# ii. Analysis of Crude Cellular Extract from Phaeodactylum tricornutum

A sample of crude cellular extract from *Phaeodactylum tricornutum* was analyzed using quantitative HPLC to determine if this method could detect and quantify apo-fucoxanthinoids in a mixture of other carotenoid and chlorophyll pigments. Figure 65 shows a contour plot of the region of interest for apo-fucoxanthinoid analysis. Although they have not been shown here, fucoxanthin elutes at 16.440 min and chlorophyll  $\underline{a}$  elutes at 21.307 min, so this system could quantify these compounds as well. By comparison with the standards (Table 16), two apo-fucoxanthinoid compounds were identified and quantified. In the 25  $\mu$ l injection volume of crude cellular extract, there was 17.8 ng of apo-12'-fucoxanthinal and 140 ng of apo-13'-fucoxanthinone.

**Table 15.** Data on apo-fucoxanthinoid standards for quantitative HPLC assays. V = volts; s = seconds; V s = volt seconds = peak area as given by the photo-diode array detector.

	Apo-10'- fucoxanthinal	Apo-12'- fucoxanthinal	Apo-12- fucoxanthinal	Apo-13'- fucoxanthinone
Retention time (min):				
major peak:	9.045	7.710	12.970	5.245
shoulder:	9.578	7.310	14.037	-
Observed peaks (nm):	424, 445	395, 418	417	333
Wavelength for analysis (nm);	418	393	407	329
Peak height (V, normalized to 1 $\mu$ g):	0.0849	0.0718	0.0327	0.0653
Peak area (V s, normalized to 1 $\mu$ g):	5.68	4.76	1.97	2.61

**Table 16.** Comparison of HPLC data from apo-fucoxanthinoids in a crude cellular extract from *Phaeodactylum tricornutum* with HPLC data from standards.

	Retention time (min)	Observed Peaks (nm)
Apo-12'-fucoxanthinal, standard	7.310, 7.710	395, 418
Apo-12'-fucoxanthinal, crude	7.307	398, 417
Apo-13'-fucoxanthinone, standard	5.245	333
Apo-13'-fucoxanthinone, crude	5.240	330

## D. General Discussion and Conclusions

Previous studies (Chapter 4) have shown that it is possible to quantify apofucoxanthinoid feeding deterrents using a feeding deterrent bioassay. However, this method is quite slow and has low precision due to the natural variability of the animals used in the bioassay. A rapid, precise method for detecting apo-fucoxanthinoid compounds has been developed based on an analytical HPLC method developed by Wright *et al.* (1991).

This new HPLC method can separate, detect, and quantify apo-10'-fucoxanthinal, apo-12'-fucoxanthinal, apo-12-fucoxanthinal, and apo-13'-fucoxanthinone. Semi-synthetic standards of these four compounds were run to calibrate the system. Coupling a photo-diode array detector to the HPLC system has further increased the power of this system. Using the HPLC/PDA system, the apo-fucoxanthinoids can be identified not only by their retention times, but also by their characteristic UV-vis absorptions. This system was able to detect apo-12'-fucoxanthinal and apo-13'-fucoxanthinone at ng levels in a crude cellular extract from *Phaeodactylum tricornutum*.

A new analytical HPLC method was developed for measuring apofucoxanthinoid feeding deterrent concentrations in crude cellular extracts from phytoplankton. This method is rapid and requires little preparation time. Therefore, it should be a valuable tool for future studies on the factors affecting production of apofucoxanthinoid feeding deterrents by phytoplankton such as the diatom *Phaeodactylum tricornutum*.

# Chapter 6

Comparison of Quantitative Bioassays and HPLC Analysis as Methods for

Detecting Apo-fucoxanthinoid Feeding Deterrents - A Preliminary Study of Biotic

and Abiotic Apo-fucoxanthinoid Production

## A. Introduction

A quantitative bioassay has been developed for detecting and measuring feeding deterrent activities in crude cellular extracts from phytoplankton (Chapters 2 and 4). In the diatom *Phaeodactylum tricornutum*, several apo-fucoxanthinoid compounds were found to be responsible for feeding deterrent activity (Chapter 3). This led to the development of an analytical HPLC method for detecting and quantifying the individual apo-fucoxanthinoid compounds in the crude cellular extract (Chapter 5). In order to bring this research full circle, and to better understand the role of apo-fucoxanthinoids as feeding deterrents, several questions remain to be answered:

- 1) Is there agreement between the analytical HPLC and quantitative bioassay techniques on the total amount of feeding deterrent compounds in an extract?
- 2) At what point during the growth cycle of a culture are feeding deterrents produced?
- 3) Are apo-fucoxanthinoids simply abiotic degradation products of fucoxanthin? The analytical HPLC method developed for detecting apo-fucoxanthinoids can be used to determine the concentrations of four compounds: apo-10'-fucoxanthinal, apo-12'-fucoxanthinal, apo-12-fucoxanthinal, and apo-13'-fucoxanthinone. Using the equations derived during the IC<sub>50</sub> calculations (Chapter 4), these analytical results can be converted into a predicted fecal pellet production rate. This rate can then be compared with the observed rate from a quantitative bioassay performed on the same

sample. This comparison will determine if the concentrations of the four apofucoxanthinoids are a good predictor of total feeding deterrent activity in a cell extract.

Two theories have been proposed to explain the production of feeding deterrents by phytoplankton. Huntley (1986) proposed that the production of feeding deterrents allowed slow growing species, such as dinoflagellates, to attain bloom concentrations. This theory would predict that maximum production of feeding deterrents should occur during the logarithmic phase of growth when the phytoplankton are actively growing. A second theory for the production of feeding deterrents is that they are produced when the phytoplankton cells are stressed by an environmental limitation, are no longer actively growing, and are therefore susceptible to grazing pressure (Hansen *et al.*, 1992). Using this theory, production of feeding deterrents would be expected to increase during the senescent phase of phytoplankton growth, and would be correlated with a limiting factor (e.g. nutrient limitation). Thus, the time at which feeding deterrents are produced during the cell growth cycle is important in determining the ecological significance of these deterrents.

These theories also apply to the production of phycotoxins (which may act as feeding deterrents), antibiotics, and allelopathic compounds. There is evidence to support both of these theories. Boyer et al. (1985, 1986) showed that PSP toxins from dinoflagellates Alexandrium tamarense (= Protogonyaulax tamarensis) and Alexandrium (=Protogonyaulax) catenella were found in greatest concentrations during the exponential phase of growth. However, cells from cultures of senescent Chlamydomonas sp. produced lower filtering and ingestion rates in the rotifer Brachionus plicatilis than cells from exponential phase cultures of this flagellate (Chotiyaputta and Hirayama, 1978). Wilson (1979) found that cell-free medium from cultures of lsochrysis galbana, another flagellate, which were collapsing or declining inhibited the feeding of oyster larvae Ostrea edulis, whereas I. galbana cell-free medium from cultures just entering stationary phase stimulated grazing. The

dinoflagellate *Prorocentrum minimum* was shown to produce the antibiotic β-diketone in a single "pulse" during stationary phase (Trick *et al.*, 1984). The PSP-producing dinoflagellate *A. tamarense* had increased toxin production in stationary phase when growth was limited (Hansen, 1989). *Pseudonitzschia* (= *Nitzschia*) *pungens*, a diatom, produced domoic acid (responsible for amnesic shellfish poisoning) only in post-exponential phase (Subba Rao *et al.*, 1990). Even autoinhibitor production displays this pattern, as *Skeletonema costatum* was shown to produce increased amounts of autoinhibitor during stationary phase (Imada *et al.*, 1991). However, as this autoinhibitor also inhibited the growth of a number of species of phytoplankton, the role of its production was probably the inhibition of competing species, not self-inhibition. Thus, the production of protective compounds by phytoplankton during specific times in the growth cycle is well documented.

The nature of the stresses to which a phytoplankton cell is exposed is also important in controlling the production of these protective compounds. In particular, limitation of cell growth by a nutrient such as phosphate has been well researched. Trick et al. (1984) showed that phosphate-limited cultures of Prorocentrum minimum produced twice as much  $\beta$ -diketone than nitrogen-limited cultures. Alexandrium tamarense (= Protogonyaulax tamarensis) and Alexandrium (= Protogonyaulax) catenella both produced more PSP toxins under phosphate limitation (Boyer et al., 1985, 1987). Reguera and Oshima (1990) found that high N:P ratios (phosphate limitation) produced increased PSP toxins in the dinoflagellate Gymnodinium catenatum. The flagellates Chrysochromulina polylepis and Prymnesium patelliferum also showed increased toxin production when phosphate-limited (Carlsson, 1990; Larsen et al., 1993). Therefore, it is important not only to observe when a protective substance is being produced, but the nature of the environmental conditions which may be responsible for this production.

Based on a review of this research, it was decided that an appropriate preliminary study of the production of apo-fucoxanthinoid feeding deterrents by *Phaeodactylum tricornutum* would be to observe this production during a cell growth cycle in which the limiting factor was phosphate.

The apo-fucoxanthinoids isolated during this research appear to be derived from the abundant diatom pigment fucoxanthin by oxidative cleavage. Thus, it could be possible that these compounds are produced abiotically in the natural environment in the presence of light and oxygen. A study by Milborrow (1974) states that the yield of xanthoxin (a growth inhibitor produced by higher plants analogous to apo-10'-fucoxanthinal) from violaxanthin (a xanthophyll pigment analogous to fucoxanthin) is so low and light intensities required for photolysis so high, that such a method of production is unlikely. To determine if the apo-fucoxanthinoids were produced abiotically, an experiment was designed where fucoxanthin was incubated in seawater in the presence of light and oxygen, and the accumulation of degradation products was observed.

## **B.** Material and Methods

# i. Phytoplankton Cultures

Cultures of the diatoms *Thalassiosira pseudonana* and *Phaeodactylum* tricornutum were grown and harvested to yield cellular extracts suitable for quantitative bioassays and HPLC analysis. Culturing conditions were the same as those described in Chapter 2 with the following changes. Cultures were grown under continuous irradiance ( $\approx 224 \ \mu \text{mol m}^{-2} \text{ s}^{-1}$ ), bubbled with air filtered through GF/F filters, and stirred at  $\approx 60 \text{ rpm}$ .

Three 12 L cultures were grown simultaneously. Space limitations in the water-cooled tank used for culturing permitted only three cultures to be grown in a single

experiment. Therefore, two replicate *Phaeodactylum tricornutum* cultures and only one *Thalassiosira pseudonana* (control) culture were used.

Culture growth was measured by *in vivo* fluorescence. Cell densities were determined microscopically. Cell volumes were calculated from microscopic measurements of dimensions of cells preserved in Lugol's iodine solution.

The initial and final culture pH's were measured using a Radiometer PHM62 standard pH meter. Initial and final nitrate and phosphate concentrations were measured using a Technicon Autoanalyzer.

Phytoplankton cells were harvested by gentle filtration (<50 mm Hg) through a GF/F glass fiber filter. This filter was placed in a grinding tube and cellular extracts of the phytoplankton cells were obtained by grinding the harvested cells in methanol and rinsing the cell debris repeatedly in methanol until all pigments were removed. This methanolic extract was filtered through a GF/F glass fiber filter to remove remaining cell debris. The methanolic extract then underwent rotary evaporation to yield a dry solid. This solid was dissolved in 7.0 ml of methanol, and 1.0 ml aliquots of this solution were quantitatively transferred to 7 glass vials (volume  $\approx$  7 ml). These samples were dried under a stream of nitrogen gas and stored at -16°C. Exposure of samples to light was avoided as much as possible during these procedures.

The extracellular material was collected by passing the filtrate from the harvested cells through two C-18 sep-paks connected in series. The sep-paks were then rinsed with 20 ml of water, and the retained compounds were eluted with 20 ml of ethyl acetate. The ethyl acetate was evaporated under a stream of nitrogen gas and the dried sample was stored at -16°C. Exposure of samples to light was avoided as much as possible during these procedures.

## ii. Bioassay Procedure

The samples of crude cell extract in the glass vials were quantitatively bioassayed as described in Chapter 4 with the following changes. Two male C6 copepods (*Tigriopus californicus*) were added to the bioassay mixture in each vial. Six replicates were done for each culture sample (e.g. six of the seven vials, each containing 1/7th of the total crude cellular extract for each sample, were used in the bioassay). The assay was incubated for 23 - 23.5 h at 18°C with an irradiance of  $\approx 100 \ \mu \text{mol m}^{-2} \text{ s}^{-1}$  and a L:D cycle of 18:6.

# iii. HPLC Analysis

Cellular and extracellular samples were prepared for HPLC analysis as follows. The cellular extract from one of the seven vials (e.g. 1/7th of the total cellular extract from a sample) was dissolved in 10 ml of water/methanol (80:20) and applied to a C-18 sep-pak. The sep-pak was rinsed with 20 ml water, and retained pigments were eluted with 10 ml ethyl acetate. The ethyl acetate was evaporated under a stream of nitrogen gas. Just prior to injection on the HPLC column, the sample was redissolved in 0.8 ml of methanol and 0.2 ml of water. The extracellular extract was processed in the same manner. The HPLC method used for the analysis of the samples is described in Chapter 5.

## iv. Fucoxanthin Incubation Experiment

Fucoxanthin was incubated in the presence of light and oxygen to determine if apo-fucoxanthinoids could be produced abiotically under these conditions. Fucoxanthin was isolated by the method described by Haugen and Liaaen-Jensen (1989) from *Fucus distichus* collected from Copper Cove, West Vancouver, British Columbia on March 6, 1993. Twenty-eight mg of pure fucoxanthin was suspended in 500 ml of ES enriched (Harrison *et al.*, 1980) natural seawater. This mixture was incubated in a 1 L flask for

6.75 d at 19°C with continuous irradiance of  $\approx$  224  $\mu$ mol m<sup>-2</sup> s<sup>-1</sup>. The solution was vigorously bubbled with air filter through a GF/F filter and stirred at 60 rpm.

Four times over the course of the incubation 50 ml of solution was removed from the flask and passed through a C-18 sep-pak. The sep-pak was rinsed with 20 ml of water, and retained compounds were eluted with 20 ml of ethyl acetate. The ethyl acetate was evaporated under a stream of nitrogen gas and the dried sample was stored at -16°C. Exposure of samples to light was avoided as much as possible during these procedures. Just prior to injection on the HPLC column, the sample was redissolved in 0.8 ml of methanol and 0.2 ml of water. The HPLC system used for analysis of these samples is the same as the one described above.

## C. Results and Discussion

## i. Phytoplankton Cultures

One culture of *Thalassiosira pseudonana* (#1) and two cultures of *Phaeodactylum tricornutum* (#2 and #3) were grown and harvested to yield cellular extracts suitable for quantitative bioassays and HPLC analysis. Each culture was harvested at three points during the growth cycle (Fig. 66). The first harvest time was at mid-logarithmic phase (M,  $\approx$  2 days after culture inoculation), the second was at late-logarithmic/early senescence phase (L,  $\approx$  4 days after culture inoculation), and the third was at senescence phase (S,  $\approx$  6 days after culture inoculation) (Appendix H, Tables H1 - H4).

The pH, nitrate concentration, and phosphate concentration were measured before the culture was inoculated and again at the end of 6 days (Appendix H, Tables H1 - H3) in order to determine which factors were limiting. The pH was constant during the experiment for all cultures, which indicates that there was no carbon limitation experienced by any of the cultures (which would have resulted in an increase

in pH due to a decrease in dissolved CO<sub>2</sub>). The final N:P ratios of the medium were 111, 3830, and 493 for cultures #1, #2, and #3 respectively. The cellular N:P ratio for *Thalassiosira pseudonana* is 33, and for *Phaeodactylum tricornutum* it is 37 (Harrison et al., 1990). Therefore both diatoms were phosphate-limited. Culture #2 was considerably more phosphate-limited than culture #3. As a result, these two P. tricornutum cultures may not be good replicates.

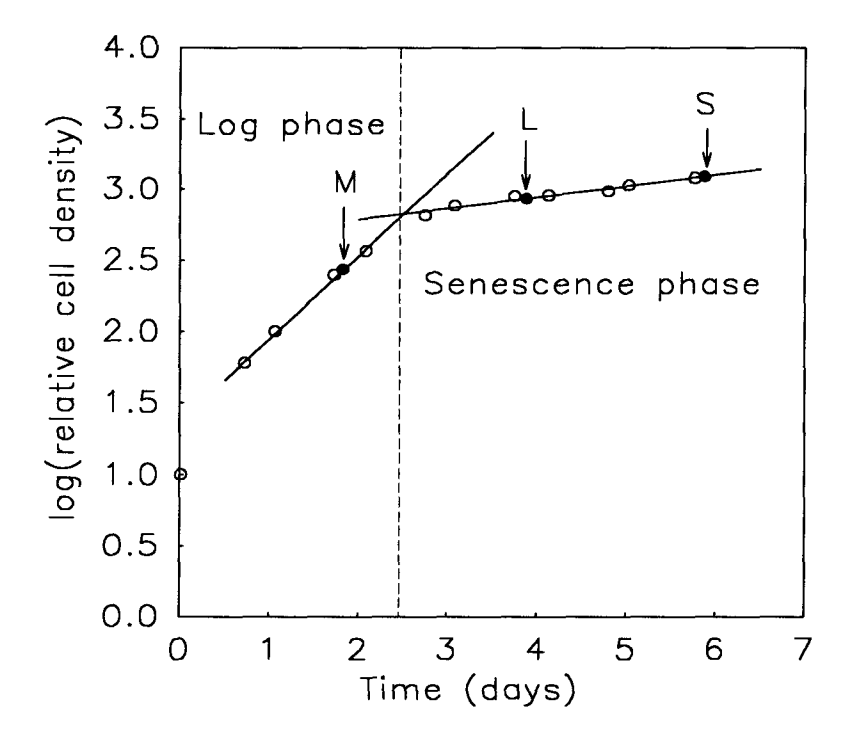


Fig. 66. Growth curve for *Phaeodactylum tricornutum* (culture #2). The dashed line indicates the time at which the culture changed from logarithmic growth to senescence phase. The culture was harvested three times for analysis as shown. M = mid-log phase; L = late log/early senescence phase; S = senescence phase.

The cell volumes were calculated for both phytoplankton species (Appendix I). Thalassiosira pseudonana had a cell volume of  $163 \mu m^3$ . Using a Coulter Counter (model TAII), the cell volume of T. pseudonana has been previously measured as 41.5 - 70.4  $\mu m$  (Thompson et al., 1991; Thompson, 1991). However, it has been shown

experimentally that the Coulter Counter volume  $\approx 0.45*$  (optically determined volume) due to a "shape factor" (the Coulter Counter calculates volumes of cells assuming the cells are spherical, which is usually not the case) and inaccurate optical measurements (error of  $< 0.5 \, \mu m$ ; Montagnes and Berges, 1993). Thus an optically determined cell volume of 163  $\mu m^3$  is equivalent to a Coulter Counter volume of  $\approx 73 \, \mu m^3$ . This value is reasonably close to the values given by Thompson *et al.* (1991). The dimensions of *T. pseudonana* were optically determined to be  $7 \, \mu m \times 6 \, \mu m$ . The dimensions given in the literature for *T. pseudonana* are  $5 \, \mu m \times 3 \, \mu m$  (Rublee and Gallegos, 1989). Thus the *T. pseudonana* used in this study was slightly larger than the *T. pseudonana* observed by Rublee and Gallegos (1989). Since no selenium was added to the culture medium in which these cells were grown, this increase in cell size may have been due to mild selenium limitation, which causes elongation of cells.

Phaeodactylum tricornutum had dimensions of 20  $\mu$ m x 2.9  $\mu$ m for the fusiform cells and an arm length of 7  $\mu$ m for the triradiate cells. The literature values for P. tricornutum give the dimensions of the fusiform cells as 25 -35  $\mu$ m x 3 - 5  $\mu$ m and the arm length of the triradiate cells as 6 - 8  $\mu$ m (Hendley, 1964). Thus the P. tricornutum used in this study was reasonably close in size to the observed sizes for P. tricornutum in the literature. The optically determined cell volume of P. tricornutum was 37  $\mu$ m<sup>3</sup> (Appendix I). The overall length of P. tricornutum was much greater than that of T. pseudonana, but most of this length was taken up by spines, which have negligible volume. In terms of volume, T. pseudonana was approximately 4.5 times bigger than P. tricornutum.

## ii. Comparison of Quantitative Bioassays and HPLC Analysis

The relative apo-12'-fucoxanthinal concentration expected to be present in the bioassay medium was calculated based on the concentrations of each of the apo-fucoxanthinoids in the sample as measured by the HPLC, and on the relative feeding

deterrent activities of each of the apo-fucoxanthinoids as determined by their IC<sub>50</sub> values (e.g. 1 ppm apo-13'-fucoxanthinone = 0.14 ppm apo-12'-fucoxanthinal). This relative apo-12'-fucoxanthinal concentration in the bioassay (Cb) was used to calculate the predicted fecal pellet production rate (Fp) using the equations developed from the IC<sub>50</sub> experiments in Chapter 4 (Appendix K, Table K1; Appendix L, Table L1). This predicted rate was compared to the observed fecal pellet production rate (Fb) from the bioassay of that sample (Fig. 67).

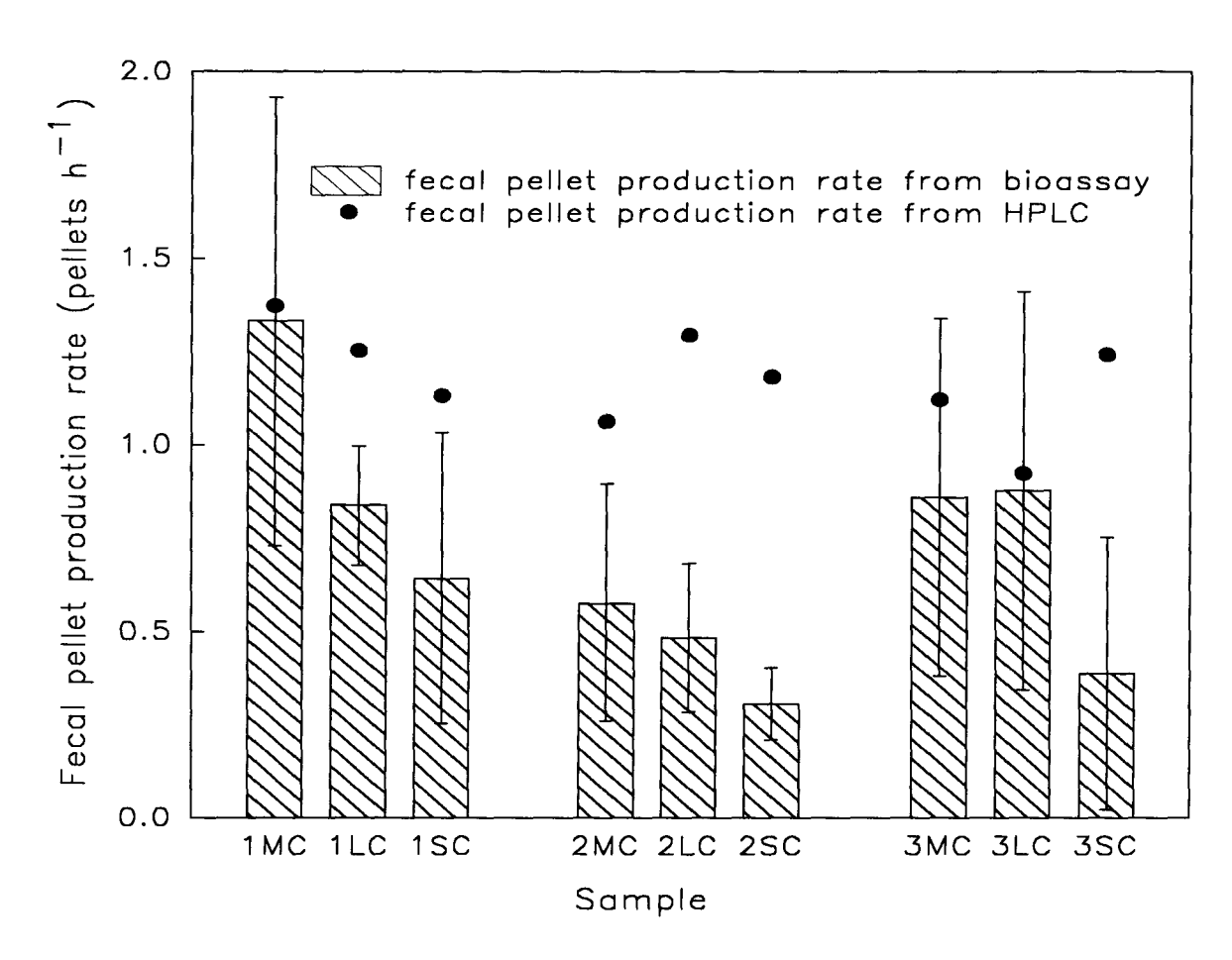


Fig. 67. Comparison of predicted fecal pellet production rates (Fp) from HPLC analysis of samples with observed fecal pellet production rates (Fb) from the bioassay. Comparisons are shown for 3 cultures (1, 2, 3) at 3 times (M, L, S). Culture 1 was *Thalassiosira pseudonana* and cultures 2 and 3 were *Phaeodactylum tricornutum*. M = mid-log phase; L = late log/early senescence phase; S = senescence phase. Error bars are 1 SD (n=6) from bioassay replicates.

This comparison of bioassay results with HPLC results indicated that the predicted fecal pellet production rate calculated from the HPLC data consistently overestimated the observed fecal pellet production rate from the bioassay. Closer examination of the data showed a small overestimation for 1LC, 1SC, and 2MC, and a much larger overestimation for 2LC, 2SC, and 3SC. This overestimation was probably due to a combination of two problems:

- 1) there may have been one or more additional active compounds in the crude extract which have not been identified.
- 2) the relative activities of the apo-fucoxanthinoids in the crude cellular extracts may have been different from those measured in the IC<sub>50</sub> experiments using pure compounds. This may have been due to:
  - a) inaccurate measurements of the activities of the apo-fucoxanthinoid compounds in the IC<sub>50</sub> experiments
  - b) inaccurate measurements of the total activity in the crude cellular extracts using the quantitative bioassay
  - c) altered solubility behaviors of compounds in the crude extract.
  - d) a synergistic effect between apo-fucoxanthinoids.

The three dimensional data sets generated by the HPLC/PDA system contained UV-vis information on all the compounds in the crude extracts. These data sets were rechecked to see if there were any additional signals for compounds which had UV-vis spectra characteristic of apo-fucoxanthinoids. This search discovered a compound, unknown #1, which had a retention time of 13.2 min and a  $\lambda_{max}$  of 439 nm. The peak shape was characteristic of an allenic apo-fucoxanthinoid. These values were very similar to those of the allenic compound apo-12-fucoxanthinal (retention time = 12.97 min;  $\lambda_{max} = 417$  nm). This compound was tentatively identified as apo-10-fucoxanthinal (same structure as apo-12-fucoxanthinal, but with 8 conjugated double

bonds instead of 7). The  $\lambda_{max}$  for this compound as calculated by Woodward's rules for enones was 444 nm, which agreed quite well with the observed value.

The feeding deterrent activity of apo-10-fucoxanthinal was assumed to be the same as for apo-12-fucoxanthinal. Therefore, based on the IC<sub>50</sub> experiments, the relative activities of apo-12'-fucoxanthinal: apo-13'-fucoxanthinone: apo-10-fucoxanthinal was 1:0.14:0.50. These values were then used to calculate new predicted fecal pellet production rates (Fp) based on the HPLC results. However, a comparison of these Fp values with the observed fecal pellet production rates (Fb) from the bioassays showed that the HPLC results were still underestimating the degree of feeding deterrent activity in the crude samples. Further examination of the HPLC/PDA data sets did not provide any evidence of more apo-fucoxanthinoid compounds present in the crude samples.

In a final attempt to relate the HPLC and bioassay results, the assumption was made that the relative activities of the apo-fucoxanthinoids as measured by the IC50 experiments did not agree with the relative activities of the apo-fucoxanthinoids in the crude extracts as measured by the quantitative bioassays (due to the reasons listed above). A model was used to answer the question: If the relative activities of apo-12'-fucoxanthinal: apo-13'-fucoxanthinone: apo-10-fucoxanthinal are 1: a: b, then what are the values of "a" and "b" such that the predicted fecal pellet production rate (Fp) from the HPLC results is equal to the observed fecal pellet production rate (Fb)? The model iteratively adjusted "a" and "b" until the values calculated for Fp fell within the  $\alpha=0.05$  confidence intervals of Fb (Appendix L). The relative activities calculated by this model were 1: 11: 0.23. The results from this model are shown in Figure 68. Therefore, it appears that the activity of the crude cellular extracts was due to three compounds, apo-10-fucoxanthinal, apo-12'-fucoxanthinal, and apo-13'-fucoxanthinone (note that no apo-10'-fucoxanthinal or apo-12-fucoxanthinal were detected by HPLC in the samples). The results from the model showed that the relative activities for

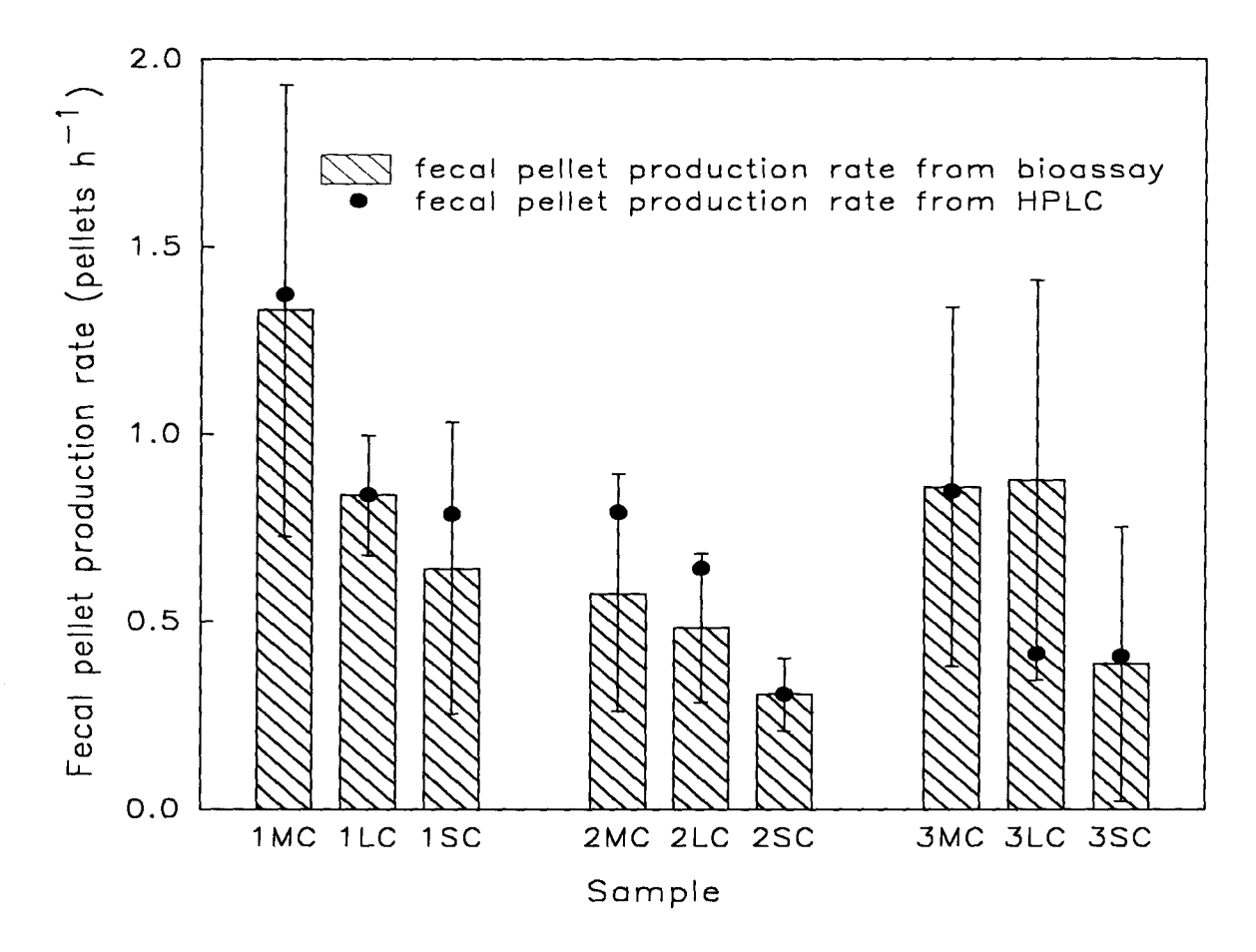


Fig. 68. Comparison of predicted fecal pellet production rates (Fp), calculated using a model (described in Appendix L) and the results from HPLC analysis of samples, with observed fecal pellet production rates (Fb) from the bioassay. Comparisons are shown for 3 cultures (1, 2, 3) at 3 times (M, L, S). Culture 1 was Thalassiosira pseudonana and cultures 2 and 3 were Phaeodactylum tricornutum. M = mid-log phase; L = late log/early senescence phase; S = senescence phase. Error bars are 1 SD (n=6) from bioassay replicates.

apo-12'-fucoxanthinal and apo-10-fucoxanthinal were very similar to the measured relative activities from the IC<sub>50</sub> experiments (model prediction was 1:0.23 as compared to the measured relative activity of 1:0.5, assuming apo-10-fucoxanthinal and apo-12-fucoxanthinal have the same activity). However, the model prediction of the relative activity of apo-13'-fucoxanthinane was markedly different from the measured relative activity (model prediction was 11 as compared to a measured value of 0.14). The calculation of the IC<sub>50</sub> value for this compound may be suspect since

the  $r^2$  (coefficient of determination) value for the fit of the data to the PROBIT line used to calculate the IC<sub>50</sub> value was 0.53, indicating a very poor line fit to the data.

# iii. Quantitative Feeding Deterrent Bioassays

Quantitative feeding deterrent bioassays were performed on three cultures (one *Thalassiosira pseudonana* culture and two *Phaeodactylum tricornutum* cultures) at three times throughout the growth cycle in order to determine if culture age affected feeding deterrent production. The raw data for these bioassays is shown in Appendix J, Table J1. Analysis of variance calculations were performed on the untransformed fecal pellet production rates (Appendix J, Table J3). All three samples taken from senescent cultures (both *T. pseudonana* and *P. tricornutum*) were significantly lower than the control (no cell extract). In addition, all three samples from culture #2 of *P. tricornutum* were also significantly lower than the control, as well as being significantly lower than the sample from the logarithmic phase of culture #1 (*T. pseudonana*). The feeding deterrent activity from the *T. pseudonana* culture was unexpected, as this diatom had been previously shown not to produce a feeding deterrent. However, the increase in feeding deterrent activity in senescent cultures, and the increased feeding deterrent activity in the most phosphate-limited culture (#2) agree well with work from other researchers (Introduction).

Using the equations developed from the IC<sub>50</sub> experiments, and correcting the results for cell number and cell volume, the bioassay data can be transformed into relative intracellular apo-12'-fucoxanthinal concentrations (Appendix J, Table J2). The results from the two *Phaeodactylum tricornutum* cultures were then averaged, and these average values were compared with the values for the *Thalassiosira pseudonana* cultures (Fig. 69). Statistical differences were determined using one-tailed t-tests (Appendix J, Table J4). Results from the t-tests showed that the relative intracellular apo-12'-fucoxanthinal concentration (Cc) of the sample from the senescence phase of

the *P. tricornutum* cultures was marginally significantly higher than both a Cc value of  $0 \ (\alpha = 0.077)$  and the Cc value for the senescent culture of *T. pseudonana* ( $\alpha = 0.086$ ). As well, a t-test between the L and S samples of the *P. tricornutum* cultures gave  $\alpha = 0.10$ . Therefore, *P. tricornutum* had a higher Cc value than *T. pseudonana* when both cultures were compared during their senescence phases, and the Cc value increased slightly as the culture aged.

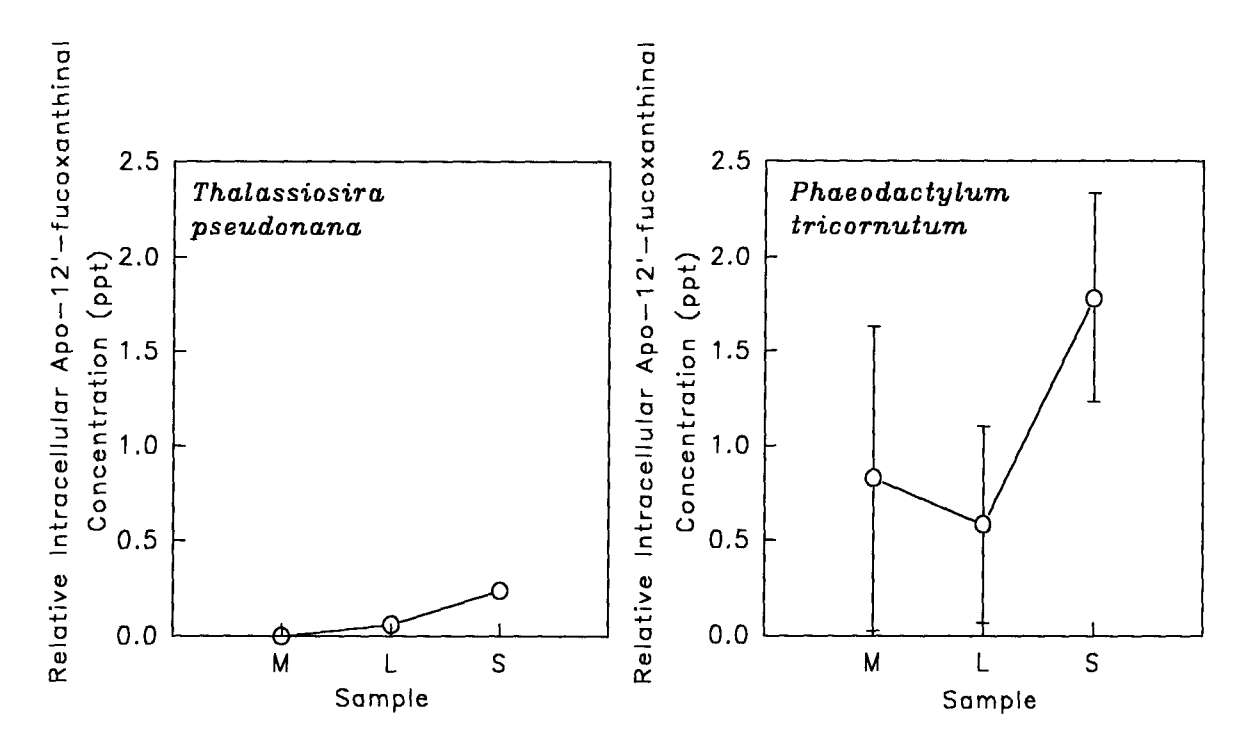
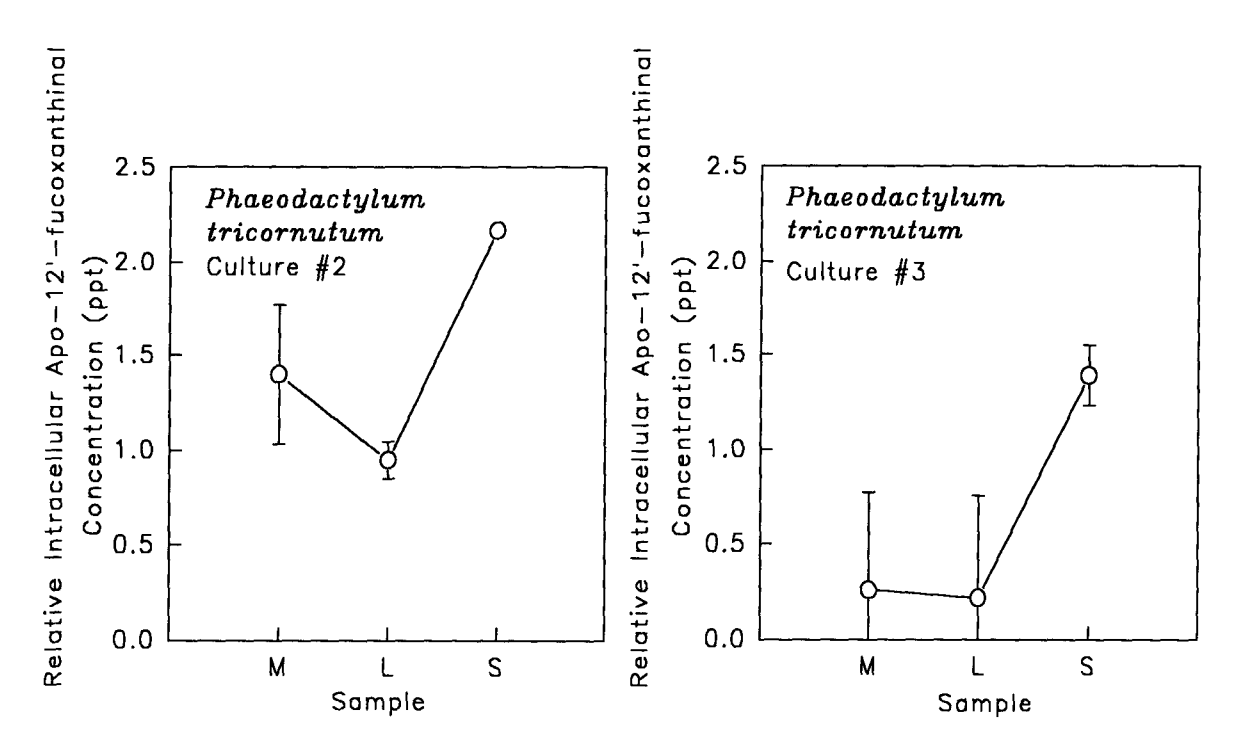


Fig. 69. Comparison of the average relative intracellular apo-12'-fucoxanthinal concentrations from *Phaeodactylum tricornutum* and *Thalassiosira pseudonana*. Error bars are  $\pm$  1 SD. No error bars are shown on data from the *T. pseudonana* culture as it was not replicated.

As the degree of phosphate limitation varied between the two *Phaeodactylum* tricornutum cultures, it was useful to look at the separate results from these two cultures (Fig. 70). Note that the highest values for both occurred during the senescence phase, and that the value for culture #2 was higher than that for culture #3. Since

culture #2 was the most phosphate-limited, it would appear that increased phosphate limitation produced increased apo-fucoxanthinoid production.



**Fig. 70.** Comparison of the average relative intracellular apo-12'-fucoxanthinal concentrations for the two *Phaeodactylum tricornutum* cultures. Error bars are estimated from the relative error in the bioassays as there was no replication of these samples.

# iv. HPLC Analysis of Intracellular Apo-fucoxanthinoids

The intracellular concentrations of fucoxanthin, apo-10-fucoxanthinal, apo-12'-fucoxanthinal, and apo-13'-fucoxanthinal were calculated from the HPLC data (Appendix K, Tables K1 - K4; Fig. 71). No apo-10'-fucoxanthinal or apo-12-fucoxanthinal was observed in these samples. The reason for this was uncertain, but it was possible that the different conditions under which the cultures used for isolation and identification of these two compounds (Chapter 3) were grown (e.g. day/night cycle vs. continuous light) may be responsible. Note the large error bars on samples taken at the late log/early senescence period in the growth cycle of *Phaeodactylum* 

tricornutum. The time at which these samples were taken was very close to the time when the cells changed from log phase cell physiology to senescence phase cell physiology. Since culture #2 was more phosphate-limited than culture #3, it entered the senescence phase first. Therefore, when the samples were taken at L, culture #2 was in a senescent state while culture #3 was still in a growth phase. Since the two cultures were in quite different states at this point, they had different intracellular concentrations of fucoxanthin and apo-fucoxanthinoids, hence the large deviation around the average value at L.

One-tailed t-tests were used to compare the intracellular concentrations from *Phaeodactylum tricornutum* and *Thalassiosira pseudonana* (Appendix K, Table K5). The intracellular fucoxanthin concentrations of *P. tricornutum* were significantly higher than those of *T. pseudonana* at both the M ( $\alpha = 0.0005$ ) and S ( $\alpha = 0.000891$ ) phases. Apo-12'-fucoxanthinal and apo-13'-fucoxanthinal showed an unexpected pattern. Both of these compounds were significantly higher in *P. tricornutum* only during the logarithmic phase of growth ( $\alpha = 0.0684$  for apo-12'-fucoxanthinal and  $\alpha = 0.0405$  for apo-13'-fucoxanthinone). However, apo-10'-fucoxanthinal showed the opposite pattern, with the *P. tricornutum* samples being significantly higher than the *T. pseudonana* samples during the senescence phase. As the *P. tricornutum* cell extracts showed the greatest feeding deterrent activity in the senescence phase samples, most of this activity must be a result of apo-10-fucoxanthinal.

The relative intracellular apo-12'-fucoxanthinal concentration (Cc) was calculated from the HPLC data using the values for the relative activities, a and b, which were calculated from the model developed during the comparison of HPLC results with bioassay results (Appendix L, Table L2; Fig. 72). As in the previous results, the error bars on the samples taken at time L were very large due to the fact that cultures #2 and #3 were not in the same state at this point in time.

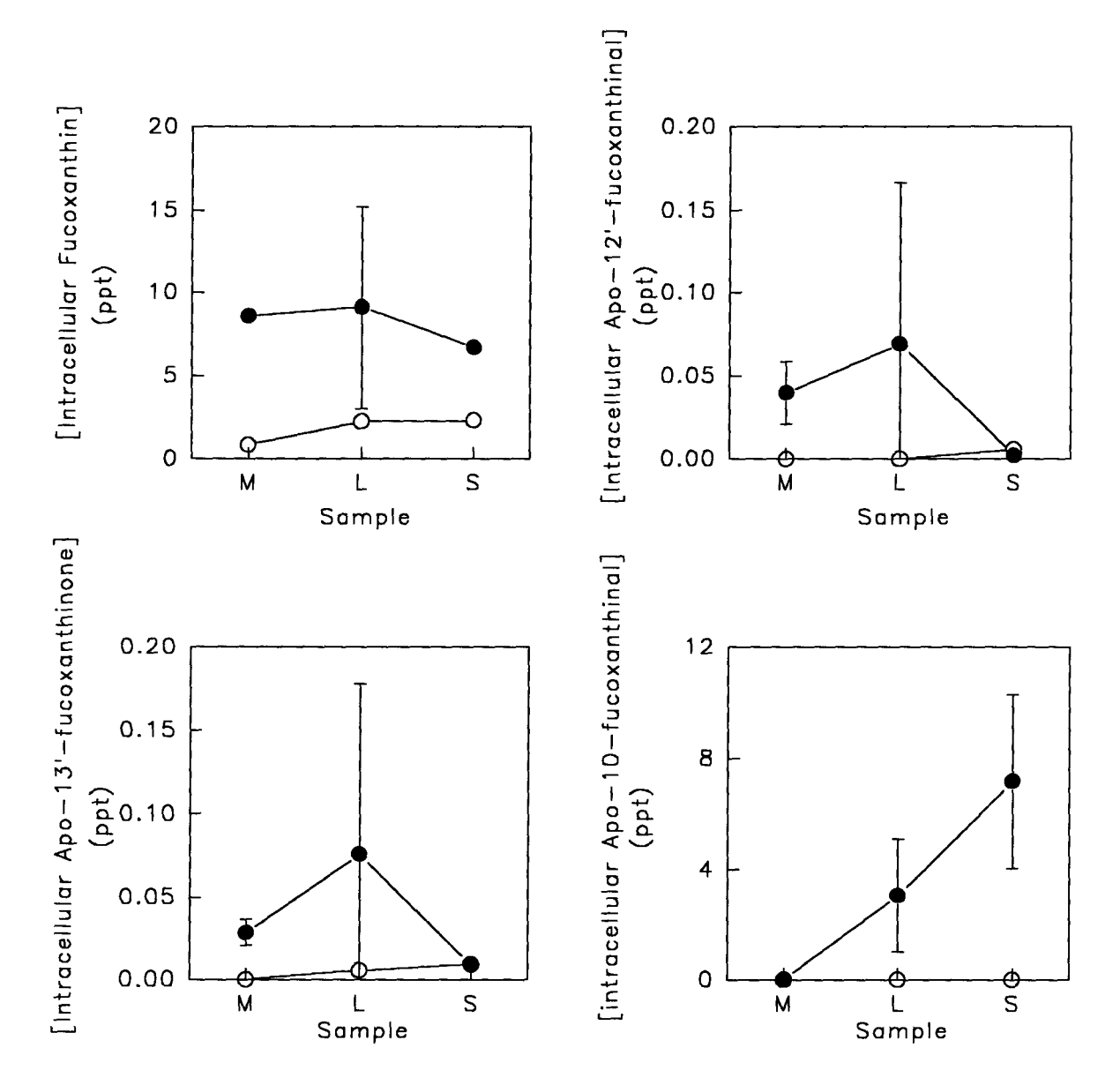


Fig. 71. Comparison of the average intracellular concentrations of fucoxanthin, apo-10-fucoxanthinal, apo-12'-fucoxanthinal, and apo-13'-fucoxanthinone from Phaeodactylum tricornutum (filled circles) and Thalassiosira pseudonana (open circles). Error bars are  $\pm$  1 SD. No error bars are shown on data from the T. pseudonana culture as it was not replicated.

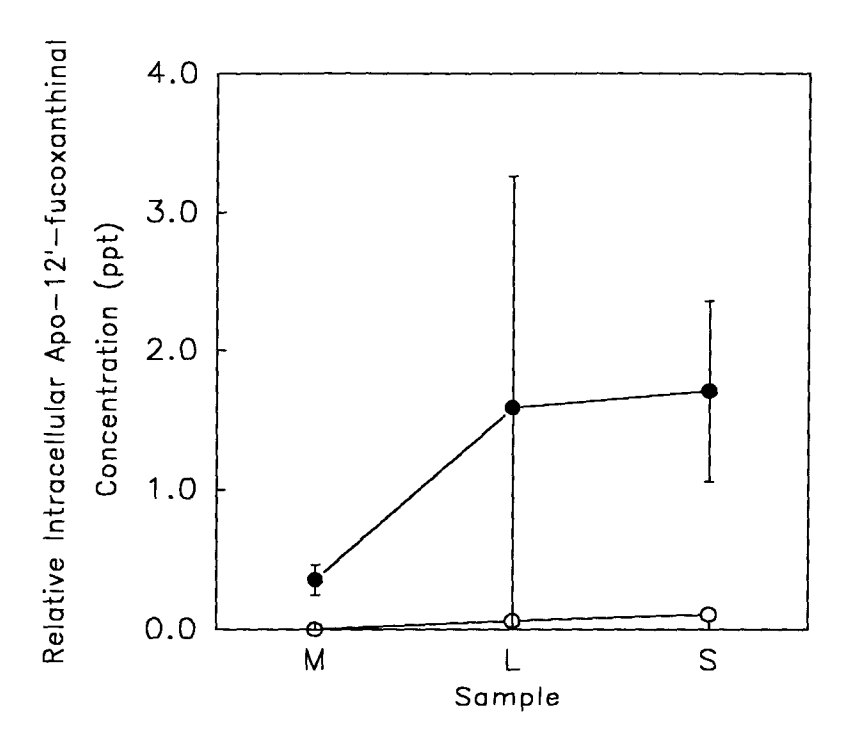


Fig. 72. Comparison of the average relative intracellular apo-12'-fucoxanthinal concentration from *Phaeodactylum tricornutum* (filled circles) and *Thalassiosira pseudonana* (open circles). Error bars are  $\pm$  1 SD. No error bars are shown on data from the *T. pseudonana* culture as it was not replicated.

One-tailed t-tests were used to compare the results from *Phaeodactylum* tricornutum and *Thalassiosira pseudonana* (Appendix L, Table L3). The *P.* tricornutum cultures had significantly higher Cc values than the *T. pseudonana* culture during both log phase ( $\alpha = 0.0430$ ) and senescence phase ( $\alpha = 0.0547$ ). This reflects the higher levels of apo-12'-fucoxanthinal and apo-13'-fucoxanthinal during log phase and the higher levels of apo-10-fucoxanthinal during senescence phase. There was a slightly significant increase in Cc concentration from log phase to senescence phase in *P. tricornutum* ( $\alpha = 0.107$ ) which agreed with the previous observations that senescence phase samples had higher feeding deterrent activity.

The maximum Cc concentration reached by *Phaeodactylum tricornutum* was 2.17 ppt. This was 1000 times greater than the IC<sub>50</sub> value range of 1.84 - 20.0 ppm for the apo-fucoxanthinoids as calculated in Chapter 4. Therefore, if an organism, such as the copepod *Tigriopus californicus*, was exposed to an intracellular concentration of 2.17 ppt while handling/breaking/ingesting *P. tricornutum* cells, it would experience significant feeding inhibition.

# v. HPLC Analysis of Extracellular Apo-fucoxanthinoids

The extracellular material from the *Phaeodactylum tricornutum* and *Thalassiosira pseudonana* cultures was analyzed using the HPLC/PDA method. No apo-10-fucoxanthinal, apo-10'-fucoxanthinal, apo-12-fucoxanthinal, apo-12'-fucoxanthinal, or apo-13'-fucoxanthinane was detected in any of the extracellular samples (Appendix K, Table K1). Thus, one would expect the extracellular filtrate to have no feeding deterrent activity. However, this disagreed with research results from Thompson *et al.* (1993), who showed that *P. tricornutum* filtrate decreased ingestion rate of plastic beads in oyster larvae. There were four possible explanations for this:

- these compounds may have been present in the extracellular medium at levels below the HPLC detection limit due to cell lysis or breakage during harvesting procedures. The oyster larvae may be sensitive to the apofucoxanthinoids at these low levels.
- 2) the methods used to concentrate the samples for HPLC analysis may degrade some of the apo-fucoxanthinoids. If these compounds were present at very low levels, this degradation may be enough to reduce the levels to zero.
- 3) the age and condition of the culture may affect the amount of apofucoxanthinoids released extracellularly. The cultures in the Thompson et al. (1993) study may have been in a different physiological state than the

- cultures in this study, and thus may have been releasing more extracellular apo-fucoxanthinoids.
- 4) there may have been an additional class of feeding deterrent compounds released extracellularly which were not detected by HPLC.

Fucoxanthin was present in the extracellular samples (Appendix K, Table K6). This fucoxanthin was probably released from cell breakage during the harvesting procedures or from natural cell lysis. However, no definite trends were seen in the data, either by culture or by age.

### v. Fucoxanthin Incubation Experiment

Pure fucoxanthin was incubated in for approximately 7 days in seawater with continuous irradiance and bubbling with air in order to determine if apofucoxanthinoids could be produced abiotically from fucoxanthin in the presence of light and oxygen. However, HPLC analysis showed no detectable amounts of apo-10-fucoxanthinal, apo-10'-fucoxanthinal, apo-12-fucoxanthinal, apo-12'-fucoxanthinal, or apo-13'-fucoxanthinone. Therefore, these compounds were not produced abiotically from fucoxanthin in the presence of light and oxygen, and under phytoplankton culturing conditions.

Fucoxanthin did degrade over 7 days, as the amount of fucoxanthin present in solution was reduced by 23% (Fig. 73). Several degradation products accumulated (peaks #1, #2, and #3), but none of them appeared to be apo-fucoxanthinoids of the type associated with feeding deterrent activity.

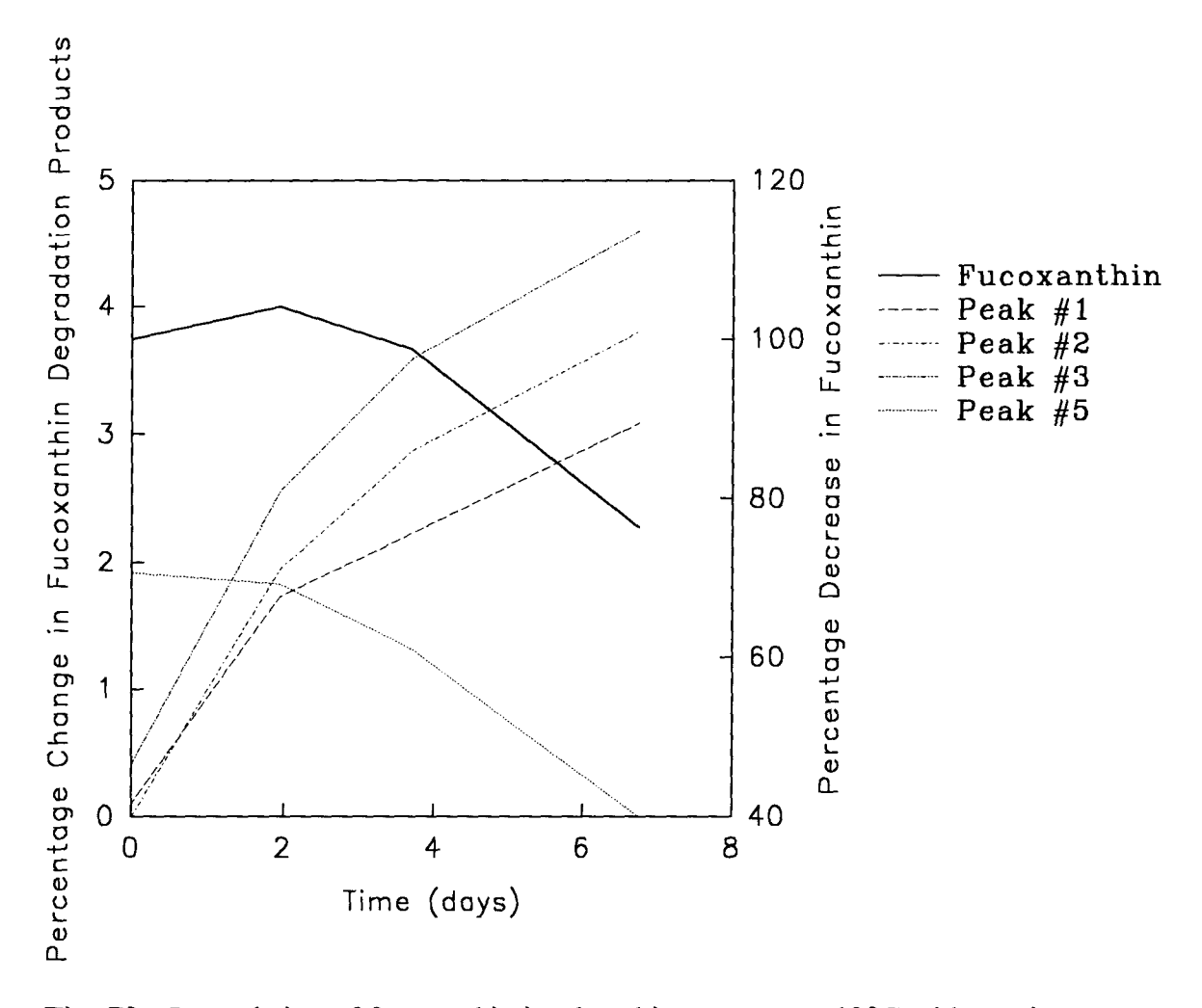


Fig. 73. Degradation of fucoxanthin incubated in seawater at 19°C with continuous irradiance of  $\approx 224 \ \mu \text{mol m}^{-2} \text{ s}^{-1}$ .

# D. General Discussion and Conclusions

An attempt has been made to integrate the production of feeding deterrents by *Phaeodactylum tricornutum* with the concentrations and feeding deterrent activities of apo-fucoxanthinoids. The HPLC method for detecting apo-fucoxanthinoids and the quantitative bioassay for measuring feeding deterrent activity were compared. Both of these methods were then used to observe the effects of culture age on the production of feeding deterrent compounds. In addition, the HPLC method was used to study the abiotic production of apo-fucoxanthinoids.

The HPLC method was found to underestimate the feeding deterrent activity in crude samples. This was due to two problems. There was at least one more apofucoxanthinoid in the crude samples which had not been previously identified. This compound, identified as apo-10-fucoxanthinal, was produced only by *Phaeodactylum* tricornutum, and appeared to be responsible for most of the feeding deterrent activity in senescent cultures. It is possible that there may have been other types of feeding deterrent compounds present as well. Secondly, given the assumption that there were no other feeding deterrent compounds in addition to the apo-fucoxanthinoids present in the crude cell extract, the relative activity of apo-13'-fucoxanthinone appeared to be much greater in the crude samples than was measured in the IC50 experiments. This apparent increase in activity may be due to an inaccurate measurement of the activity in the IC<sub>50</sub> experiment (the data fit very poorly to the PROBIT line used to calculate the IC<sub>50</sub> value), an inaccurate measurement of the activity of the crude cellular extracts using the quantitative bioassays, an altered solubility behavior of the compound in the crude extract, or a synergistic effects between the apo-fucoxanthinoid compounds (or other compounds in the crude mixture).

Both *Thalassiosira pseudonana* and *Phaeodactylum tricornutum* had feeding deterrent activity as measured by the quantitative bioassay, and both contained apofucoxanthinoids. However, extracts from *P. tricornutum* were more active than those from *T. pseudonana*, and *P. tricornutum* expressed feeding deterrent activity throughout its growth cycle, while *T. pseudonana* only had feeding deterrent activity during senescence. This production of apo-fucoxanthinoid compounds may be a phenomenon common to all diatoms, with the level of production being dependent on species (probably species-specific enzymes which have variable levels of activity).

Both diatom species showed increased total apo-fucoxanthinoid production during senescence. This production may be a function of cessation of active growth and the start of cell aging. Thus this process might be analogous to the increase in

carotenoid degradation products in aging tissues (e.g. leaves) of higher plants (Gross, 1991).

In *Phaeodactylum tricornutum*, an increase in total apo-fucoxanthinoid production during senescence was seen with increased phosphate limitation. This agrees with observed increases in other biologically active compounds in phytoplankton under phosphate limitation (Trick *et al.*, 1984; Boyer *et al.* 1985, 1987; Reguera and Oshima, 1990; Carlsson, 1990). From an ecological viewpoint, the production of feeding deterrent compounds during senescence should prevent overgrazing of the phytoplankton population during a period of time when they are unable to outgrow the grazing pressures.

Apo-fucoxanthinoids do not appear to be produced abiotically. This agrees with Milborrow (1974), who believed that the production of biologically active materials by photolysis of carotenoids was too inefficient to account for observed biological activity. Thus, the apo-fucoxanthinoids from diatoms must be produced by enzymatic oxidative cleavage of fucoxanthin, possibly using an enzyme such as lipoxgenase (Gross, 1991).

Apo-fucoxanthinoids produced by diatoms act as feeding deterrents. This production may be a process universal to all diatoms, although the degree to which it occurs may be species dependent. This process is enzymatic, and appears to be related to culture aging and phosphate limitation, which are factors that govern the production of other biologically active compounds by phytoplankton. The results from this research are preliminary, and more studies on the physiology of feeding deterrent production by diatoms need to be done. In addition, this work has raised a number of questions for which only suggested answers have been given, and more in depth studies must be performed in order to validate these conjectures.

#### Chapter 7

# General Discussion, Conclusions, and Future Directions

#### A. Conclusions

The purpose of this research was to develop a series of methodologies which would probe the production of feeding deterrents by phytoplankton. With these new techniques, the understanding of the nature and function of feeding deterrent compounds could be increased. Thus, this work was only a preliminary study, an attempt to find new methods which would allow further studies in this field of research. The initial findings from this work should bring some new insights into the study of biologically active compounds produced by phytoplankton and the interaction of phytoplankton with other organisms in their environment via these compounds. With this in mind, the following conclusions can be drawn from this body of research:

- 1) A feeding deterrent bioassay was developed using the copepod *Tigriopus* californicus. This bioassay was simple, rapid, cost-efficient, reliable and accurate, and was designed to be used to guide chemical fractionation in order to isolate a feeding deterrent compound. Using this bioassay, feeding deterrent activity was detected in the dinoflagellate *Gonyaulax grindleyi* and the diatom *Phaeodactylum tricornutum*.
- 2) The feeding deterrent activity in *Phaeodactylum tricornutum* was traced to four compounds: apo-10'-fucoxanthinal, apo-12'-fucoxanthinal, apo-12-fucoxanthinal, and apo-13'-fucoxanthinane. These compounds were isolated by chromatographic techniques and conclusively identified using various spectroscopic means.

- The IC<sub>50</sub> values of the pure apo-fucoxanthinoid compounds were determined, and ranged from 1.84 - 20.0 ppm.
- 4) The LC<sub>50</sub> values of apo-10'-fucoxanthinal and apo-12'-fucoxanthinal were determined, and ranged between 37 and 337 ppm.
- 5) An HPLC/PDA method was developed to quantify the apo-fucoxanthinoids. Using this method, a fifth apo-fucoxanthinoid compound, apo-10-fucoxanthinal, was identified.
- 6) Given the assumption that there were no other feeding deterrent compounds in addition to the apo-fucoxanthinoids, the relative activity of apo-13'-fucoxanthinone appeared to be much greater in the crude cellular extracts than was measured in the IC50 experiment. This may be due to an inaccurate measurement of the activity in the IC50 experiment, an inaccurate measurement of the activity in the crude cellular extracts using the quantitative bioassays, an altered solubility behavior of the compound in the crude extract, or a synergistic effect between compounds.
- 7) The apo-fucoxanthinoids are produced enzymatically in two diatoms, Phaeodactylum tricornutum and Thalassiosira pseudonana. The production of apo-fucoxanthinoids may be a process common to all diatoms, however the degree of production is species-specific, as P. tricornutum produces a greater amount of these compounds than T. pseudonana.
- 8) The production of total intracellular apo-fucoxanthinoids appeared to increase with culture age and degree of phosphate limitation.
- 9) The concentration of total intracellular apo-fucoxanthinoids in *Phaeodactylum* tricornutum was 1000 times higher than the concentration in solution necessary to produce a 50% inhibition of fecal pellet production in the copepod *Tigriopus californicus*.

#### **B.** General Discussion

# i. Ecological Implications

Based on the above conclusions, several general statements can be made. It appears that aging diatom cells enzymatically produce apo-fucoxanthinoid compounds intracellularly. Certain diatoms produce more of these apo-fucoxanthinoid compounds than others. In Phaeodactylum tricornutum, the intracellular concentration of these apo-fucoxanthinoids is high enough to act as a feeding deterrent for grazers when the cells are ingested. An increase in the intracellular feeding deterrent concentration in a cell would not increase the fitness of an individual cell (as the cell must be consumed in order to deter the predator), but it would decrease the predation on the entire population of cells. If it is assumed that all the phytoplankton cells in a bloom are clones originating from one individual through asexual fission, then the bloom can be considered a multicellular individual. Therefore, if a single cell containing an intracellular feeding deterrent is ingested, and this results in deterred predation on the entire population (all genetically identical to the sacrificed cell), then the production of intracellular feeding deterrents will increase the fitness of the "multicellular" bloom. Since all the cells in the bloom are genetically identical, increased fitness of the bloom will increase the fitness of the founder cell of the bloom (Hansen, 1989).

Apo-fucoxanthinoids may also be released into the "phycosphere" surrounding the cell or be bound onto the surface of the cell. Compounds closely associated with the cell surface would not be distinguishable from intracellular compounds using the methods developed in this research. However, contact chemoreception by grazers, followed by subsequent particle rejection could reduce grazing of the phytoplankton cells without ingestion of the cells. Thus predation could be deterred without sacrificing individual cells (Targett and Ward, 1991).

The bioassay organism, *Tigriopus californicus*, is a very hardy, tidepooldwelling harpacticoid copepod. It is not commonly associated with phytoplankton blooms. However, if a deterrent compound produces a response in an hardy organism, it is likely to have a much stronger effect on more sensitive organisms. The effects of apo-fucoxanthinoids on other species of zooplankton need to be examined further. However, if some species are more sensitive to apo-fucoxanthinoids than *T. californicus*, then low levels of apo-fucoxanthinoids may have a significant impact on some grazers in the natural environment.

Although *Phaeodactylum tricornutum* is not an important bloom-forming species in the marine environment, this research suggests that the production of apofucoxanthinoid compounds may be common to all diatoms, and may be of ecological significance in natural blooms of diatoms entering senescence. Diatoms which produce larger amounts of apo-fucoxanthinoids may have a competitive edge in certain ecological situations (e.g. under conditions of nutrient limitation when grazing pressures are high). If the presence of these apo-fucoxanthinoid feeding deterrents causes grazers to selectively prey on certain phytoplankton species and not others, then the production of apo-fucoxanthinoids may play an important role in phytoplankton species succession.

# ii. Commercial Applications

The results of this research may be of commercial value. In mariculture, where phytoplankton are used as a food source for organisms such as oyster larvae, it is important to know which species of phytoplankton are good food sources. This work clearly indicates that *Phaeodactylum tricornutum* is a poor choice. As well, any diatom cultures entering senescence may be of reduced value as a food source if they produce apo-fucoxanthinoids. Attempting to grow commercially important invertebrates using phytoplankton which produce feeding deterrents would lead to decreased growth rates

and increased mortality in the mariculture species, which would reduce the net profit of the "crop". A better understanding of which species produce feeding deterrents and what factors affect the production of these feeding deterrents would improve culturing practices in mariculture.

# C. Future Research Questions

Any research generates as many questions as it answers. This work is no exception. Many of the results from this work are preliminary in nature and still need to be verified, while other areas have been left unstudied. Questions in three of the more interesting areas for future research are listed below:

- 1) Feeding deterrents from dinoflagellates:
  - What is the nature of the feeding deterrent produced by the dinoflagellate Gonyaulax grindleyi? Is this feeding deterrent the same type of compound as the apo-fucoxanthinoids, or is it a neurotoxic compound, as suggested by Sykes and Huntley (1987)? If it is a neurotoxin, is it related to the PSP toxins produced by some dinoflagellates? Are the well known phycotoxins in fact feeding deterrent compounds?
- 2) Apo-fucoxanthinoids produced by diatoms:

Is the production of apo-fucoxanthinoids a general phenomenon common to all diatoms, or is it specific to only a few? Do all senescent cells produce feeding deterrents? What effects do apo-fucoxanthinoids have on various species of zooplankton? What is the ecological significance of apo-fucoxanthinoid production by diatoms? Are there synergistic effects between apo-fucoxanthinoids?

3) Physiological studies of apo-fucoxanthinoid production:

What affects do nitrate and silicate limitation have on apo-fucoxanthinoid production by *Phaeodactylum tricornutum*? What affects do variations in irradiance and temperature have on this production?

From these questions, it can be seen that there is a need to screen more phytoplankton species, both diatoms and dinoflagellates, as well as others. In species shown to produce feeding deterrents, such as *Gonyaulax grindleyi*, the feeding deterrents need to be isolated and their structures characterized. Finally, in species in which the nature of the feeding deterrent in known, such as *Phaeodactylum tricornutum*, the physiology of production needs to be studied in more detail. However, now that several new tools have been developed for this type of research, these studies should be somewhat easier.

# **Literature Cited**

- Ayukai, T., Nishizawa, S. (1986). Defecation rate as a possible measure of ingestion rate of *Calanus pacificus pacificus* (Copepoda: Calanoida). Bull. Plank. Soc. Jap. 33: 3-10.
- Ali, R.M. (1970). The influence of suspension density and temperature on the filtration rate of *Hiatella arctica*. Mar. Biol. 6: 291-302.
- Andersen, R.J., LeBlanc, M.J., Sum, F.W. (1980). 1-(2,6,6-trimethyl-4-hydroxycyclohexenyl)-1,3-butanedione, an extracellular metabolite from the dinoflagellate *Prorocentrum minimum*. J. Org. Chem. 45: 1169-1170.
- Andersen, R.J., Luu, H.A., Chen, D.Z.X., Holmes, C.F.B., Kent, M.L., LeBlanc,
  M., Taylor, F.J.R., Williams, D.E. (1993). Chemical and biological evidence links microcystins to salmon 'netpen liver disease'. Toxicon 31: 1315-1323.
- Baden, D.G. (1989). Brevetoxins: unique polyether dinoflagellate toxins. FASEB Journal 3: 1807-1817.
- Bautista, B., Harris, R.P., Tranter, P.R.G., Harbour, D. (1992). *In situ* copepod feeding and grazing rates during a spring bloom dominated by *Phaeocystis* sp. in the English Channel. J. Plank. Res. 12: 691-703.
- Bell, W.H., Mitchell, R. (1972). Chemotactic and growth responses of marine bacteria to algal extracellular products. Biol. Bull. 143: 265-277.
- Benn, R., Gunther, H. (1983). Modern pulse methods in high resolution NMR spectroscopy. Agnew. Chem. Int. Ed. Eng. 22: 350-380.
- Berges, J.A., Virtanen, C. (1993). Expanding the capabilities of laboratory instruments using built-in microprocessors and serial interfaces: adapting an LKB Ultraspec II UV spectrophotometer for scanning and enzyme kinetic analyses. Comput. Biol. Med. 23: 131-141.
- Bishop, O.N. (1983). Statistics for biology: a practical guide for the experimental biologist. Longman, Harlow, Essex, 205 pp.
- Bonnett, R., Mallams, A.K., Spark, A.A., Tee, J.L., Weedon, B.C.L., McCormick, A. (1969). Carotenoids and related compounds. Part XX. Structure and reactions of fucoxanthin. J. Chem. Soc. C 3: 429-454.
- Bose, A.K. (1965). Proton nuclear magnetic resonance spectroscopy. In: S.K. Freeman (ed.) Interpretive spectroscopy. Reinhold Publ. Corp., New York, NY, p. 211-219.

- Boyer, G.L., Sullivan, J.J., Andersen, R.J., Harrison, P.J., Taylor, F.J.R. (1985). Toxin production in three isolates of *Protogonyaulax* sp. In: D.M. Anderson, A.W. White, D.G. Baden (eds.) Toxic dinoflagellates. Elsevier, New York, NY, p. 281-286.
- Boyer, G.L., Sullivan, J.J., Andersen, R.J., Harrison, P.J., Taylor, F.J.R. (1987). Effects of nutrient limitation on toxin production and composition in the marine dinoflagellate *Protogonyaulax tamarensis*. Mar. Biol. 96: 123-128.
- Boyer, G.L., Sullivan, J.J., Andersen, R.J., Taylor, F.J.R., Harrison, P.J., Cembella, A.D. (1986). Use of high-performance liquid chromatography to investigate the production of paralytic shellfish toxins by *Protogonyaulax* spp. in culture. Mar. Biol. 93: 361-369.
- Burkholder, P.R., Burkholder, L.M., Almodovar, L.R. (1960). Antibiotic activity of some marine algae of Puerto Rico. Bot. Mar. 2: 149-156.
- Burton, R.S., Feldman, M.W., Curtsinger, J.W. (1979). Population genetics of *Tigriopus californicus* (Copepoda Harpacticoida): I. Population structure along the central California coast. Mar. Ecol. Prog. Ser. 1: 29-39.
- Carlsson, P., Graneli, E., Olsson, P. (1990). Grazer elimination through poisoning: one of the mechanisms behind *Chrysochromulina polylepis* blooms? In: E. Graneli *et al.* (eds.) Toxic marine phytoplankton. Elsevier, New York, NY, p. 116-122.
- Carmichael, W.W. (1986). Algal toxins. Adv. Bot. Res. 12: 47-101.
- Carmichael, W.W., Gorham, P.R. (1981). The mosaic nature of toxic blooms of cyanobacteria. In: W.W. Carmichael (ed.) The water environment: algal toxins and health. Plenum, New York, NY, p. 161-171.
- Carmichael, W.W., Mahmood, N.A. (1984). Toxins from freshwater cyanobacteria. In: E.P. Ragelis (ed.) Seafood toxins. Am. Chem. Soc., Wash., p. 377-389.
- Carmichael, W.W., Beasley, V., Bunner, D.L., Eloff, J.N., Falconer, I., Gorham, P., Harada, K-I., Krishnamurthy, T., Yu, M.-J., Moore, R.E., Rinehart, K.L., Runneger, M., Skulberg, O.M., Watanabe, M. (1988a). Naming of cyclic heptapeptide toxins of cyanobacteria (blue-green algae). Toxicon 26: 971-973.
- Carmichael, W.W., Eschedor, J.T., Patterson, G.M.L., Moore, R.E. (1988b). Toxicity and partial structure of a hepatotoxic peptide produced by the cyanobacterium *Nodularia spumigena* Mertens emend. L575 from New Zealand. Appl. Environ. Microbiol. 54: 2257-2263.

- Chen, D.Z.X., Boland, M.P., Smillie, M.A., Klix, H., Ptak, C., Andersen, R.J., Holmes, C.F.B. (1993). Identification of protein phosphatase inhibitors of the microcystin class in the marine environment. Toxicon, accepted June 1993.
- Chotiyaputta, C., Hirayama, K. (1978). Food selectivity of the rotifer *Brachionus* plicatilis feeding on phytoplankton. Mar. Biol. 45: 105-111.
- Craigie, J.S., McLachlan, J. (1964). Excretion of colored ultraviolet-absorbing substances by marine algae. Can. J. Bot. 42: 23-33.
- DeMott, W.R., Zhang, Q.-X., Carmichael, W.W. (1991). Effects of toxic cyanobacteria and purified toxins on the survival and feeding of a copepod and three species of *Daphnia*. Limnol. Oceanogr. 36: 1346-1357.
- De Pauw, N., Persoone, G. (1988). Micro-algae for aquaculture. In: M.A. Borowitzka and L.J. Borowitzka (eds.) Micro-algal biotechnology. Cambridge University Press, New York, NY, p. 197-221.
- Dethier, M.N. (1980). Tidepools as refuges: Predation and the limits of the harpacticoid copepod *Tigriopus californicus* (Baker). J. Exp. Mar. Biol. Ecol. 42: 99-111.
- Devlin, J.P., Edwards, O.E., Gorham, P.R., Hunter, N.R., Pike, R.K., Stavric, B. (1977). Anatoxin-A, a toxic alkaloid from *Anabaena flos-aquae* NRC-44h. Can. J. Chem. 55: 1367-1371.
- Draper, C., Gainey, L., Shumway, S., Shapiro, L. (1990). Effects of *Aureococcus anophagefferens* ("brown tide") on the lateral cilia of 5 species of bivalve molluscs. In: E. Graneli *et al.* (eds.) Toxic marine phytoplankton. Elsevier, New York, NY, p. 128-131.
- Droop, M.R., Elson, G.R. (1966). Are pelagic diatoms free from bacteria? Nature, Lond. 211: 1096-1097.
- Egloff, D.A. (1986). Effects of *Olisthodiscus luteus* on the feeding and reproduction of the marine rotifer *Synchaeta cecilia*. J. Plankton Res. 8: 263-274.
- Epifanio, C.E., Valenti, C.C., Turk, C.L. (1981). A comparison of *Phaeodactylum tricornutum* and *Thalassiosira pseudonana* as foods for the oyster, *Crassostrea virginica*. Aquaculture 23: 347-353.
- Fattorusso, E., Piattelli, M. (1980). Amino acids from marine algae. In: Schuer, P.J. (ed.) Marine natural products. Academic Press, New York, NY, Vol. 3, p. 105-107.
- Forbes, W.F. (1965). Ultraviolet spectroscopy. In: S.K. Freeman (ed.) Interpretive spectroscopy. Reinhold Publ. Corp., New York, NY, p. 1-2.

- Frost, B.W. (1972). Effects of the size and concentration of food particles on the feeding behavior of the marine planktonic copepod, *Calanus pacificus*. Limnol. Oceanogr. 17: 805-815.
- Frost, B.W. (1977). Feeding behavior of *Calanus pacificus* in mixtures of food particles. Limnol. Oceanogr. 22: 472-491.
- Gentien, P, Arzul, G. (1990a). A theoretical case of competition based on the ectocrine production by *Gyrodinium* cf. *aureolum*. In: E. Graneli *et al*. (eds.) Toxic marine phytoplankton. Elsevier, New York, NY, p. 161-164.
- Gentien, P., Arzul, G. (1990b). Exotoxin production by *Gyrodinium* cf. *aureolum* (Dinophyceae). J. mar. biol. Ass. U.K. 70: 571-581.
- Gill, C.W., Harris, R.P. (1987). Behavioural responses of the copepods *Calanus helgolandicus* and *Temora longicornis* to dinoflagellate diets. J. mar. biol. Ass. U.K. 67: 785-801.
- Gross, J. (1991). Pigments in vegetables: chlorophylls and carotenoids. Van Nostrand Reinhold, New York, NY, p. 75-99.
- Guillard, R.R.L. and Hellebust, J.A. (1971). Growth and the production of extracellular substances by two strains of *Phaeocystis pouchetii*. J. Phycol. 7: 330-338.
- Hansen, P.J. (1989). The red tide dinoflagellate *Alexandrium tamarense*: effects on behaviour and growth of a tintinnid ciliate. Mar. Ecol. Prog. Ser. 53: 105-116.
- Hansen. P.J., Cembella, A.D., Moestrup, O. (1992). The marine dinoflagellate *Alexandrium ostenfeldii*: paralytic shellfish toxin concentration, composition, and toxicity to a tintinnid ciliate. J. Phycol. 28: 597-603.
- Harris, R.P. (1982). Comparison of the feeding behavior of *Calanus* and *Pseudocalanus* in two experimentally manipulated enclosed ecosystems. J. mar. biol. Ass. UK 62: 71-91.
- Harrison, A.G. (1992). Chemical ionization mass spectrometry. CRC press, Inc., Florida, 208 pp.
- Harrison, P.J., Thompson, P.A., Calderwood, G.S. (1990). Effects of nutrient and light limitation on the biochemical composition of phytoplankton. J. Appl. Phycol. 2: 45-56.
- Harrison, P.J., Waters, R.E., Taylor, F.J.R. (1980). A broad spectrum artificial seawater medium for coastal and open ocean phytoplankton. J. Phycol. 16: 28-35.

- Haugan, J.A., Liaaen-Jensen, S. (1989). Improved isolation procedures for fucoxanthin. Phytochemistry 28: 2797-2798.
- Hendley, I.N. (1964). An introductory account of the smaller algae of British coastal waters. Part V: Bacillariophyceae (diatoms). Her Majesty's Stationary Office, London, pp. 269-270.
- Huber, C.S. (1972). The crystal structure and absolute configuration of 2,9-diacetyl-9-azabi-cyclo[4.2.1]-non-2-ene. Acta Crystallog. Sect. B 28: 2577-2582.
- Hubert, J.J. (1984). Bioassay. Kendall/Hunt Publishing Company, Dubuque, Iowa, p. 50-62.
- Hughes, E.O., Gorham, P.R., Zehnder, A. (1958). Toxicity of a unialgal culture of *Microcystis aeroginosa*. Can. J. Microbiol. 4: 225-236.
- Huntley, M.E. (1982). Yellow water in La Jolla Bay, California, July 1980. II. Supression of zooplankton grazing. J. Exp. Mar. Biol. Ecol. 63: 81-91.
- Huntley, M.E., Barthel, K.-G., Star, J.L. (1983). Particle rejection by *Calanus* pacificus: discrimination between similarly sized particles. Mar. Biol. 74: 151-160.
- Huntley, M., Sykes, P., Rohan, S., and Marin, V. (1986). Chemically-mediated rejection of dinoflagellate prey by the copepods *Calanus pacificus* and *Paracalanus parvus*: mechanism, occurrence and significance. Mar. Ecol. Prog. Ser. 28: 105-120.
- Imada, N., Kobayashi, K., Tahara, K., Oshima, Y. (1991). Production of an autoinhibitor by *Skeletonema costatum* and its effect on the growth of other phytoplankton. Nippon Suisan Gakkaishi 57: 2285-2290.
- Ishibashi, M., Ohizumi, Y., Hamashima, M., Nakamura, H., Hirata, Y., Sasaki, T., Kobayashi, J. (1987). Amphidinolide-B, a novel macrolide with potent antineoplastic activity from the marine dinoflagellate *Amphidinium* sp. J. Chem. Soc., Chem. Commun. 1127-1129.
- Ives, J.D. (1987). Possible mechanisms underlying copepod grazing responses to levels of toxicity in red tide dinoflagellates. J. Exp. Mar. Biol. Ecol. 112: 131-145.
- Jones, A.K., Cannon, R.C. (1986). The release of micro-algal photosynthate and associated bacterial uptake and heterotrophic growth. Br. phycol. J. 21: 341-358.
- Kemp, W. (1986). NMR in chemistry. A multinuclear introduction. MacMillan Education Ltd., London, 240 pp.

- Kobayashi, J., Ishibashi, M., Nakamura, H., Ohizumi, Y., Yamasu, T., Sasaki, T., Hirata, Y. (1986). Amphidinolide-A, a novel antineoplastic macrolide from the marine dinoflagellate *Amphidinium* sp. Tetrahedron Let. 27: 5755-5758.
- Kobayashi, J., Ishibashi, M., Wälchli, M.R., Nakamura, H., Hirata, Y., Sasaki, T., Ohizumi, Y. (1988) Amphidinolide C: the first 25-membered macrocyclic lactone with potent antineoplastic activity from the cultured dinoflagellate *Amphidinium* sp. J. Am. Chem. Soc. 110: 490-494.
- Lampitt, R.S., Noji, T., von Bodungen, B. (1990). What happens to zooplankton faecal pellets? Implications for material flux. Mar. Biol. 104: 15-23.
- Larsen, A., Eikrem, W., Paasche, E. (1993). Growth and toxicity in *Prymnesium* patelliferum (Prymnesiophyceae) isolated from Norwegian waters. Can. J. Bot. 71: 1357-1362.
- Leadbeater, B. (1969). A fine structural study of *Olisthodiscus luteus* Carter. Br. Phycol. J. 4: 3-17.
- Loeblich, III, A.R. (1975). A seawater medium for dinoflagellates and the nutrition of *Cachonina niei*. J. Phycol. 11: 80-86.
- Lux, H. (1965). Barium Manganate (VII). In: G. Brauer (ed.) Handbook of preparative inorganic chemistry. Academic Press, New York, NY, p. 1462.
- Meinwald, J., Erickson, K., Hartshorn, M., Meinwald, Y.C., Eisner, T. (1968).

  Defensive mechanisms of arthropods. XXIII. An allenic sesquiterpenoid from the grasshopper *Romalea microptera*. Tetrahedron Let. 25: 2959-2962.
- Milborrow, B.V. (1974). The chemistry and physiology of abscisic acid. Ann. Rev. Plant Physiol. 25: 259-307.
- Montagnes, D.J.S., Berges, J.A. (1993). Estimating carbon, nitrogen, protein and chlorophyll <u>a</u> from cell volume in marine phytoplankton: a comparison of optical and electronic particle counting techniques and the effects of fixation with Lugol's iodine. Abstract, ASLO and SWS 1993 Annual Meetings, University of Alberta, Edmonton, Alberta.
- Mullin, M. (1963). Some factors affecting the feeding of marine copepods of the genus *Calanus*. Limnol. Oceanogr. 8: 239-250.
- Murakami, M., Makabe, K., Yamaguchi, K., Konosu, S., Wälchli, M.R. (1988). Goniodomin A, a novel polyether macrolide from the dinoflagellate *Goniodoma pseudogoniaulax*. Tetrahedron Let. 29: 1149-1152.

- Murata, M., Sano, M., Iwashita, T., Naoki, H., Yasumoto, T. (1986). The structure of pectenotoxin-3, a new constituent of diarrhetic shellfish toxins. Agric. Biol. Chem. 50: 2693-2695.
- Murata, M., Kumagai, M., Lee, J.S., Yasumoto, T. (1987). Isolation and structure of yessotoxin, a novel polyether compound implicated in diarrhetic shellfish poisoning. Tetrahedron Let. 28: 5869-5872.
- Murata, M., Legrand, A.M., Ishibashi, Y., Yasumoto, T. (1989). Structures of ciguatoxin and its congener. Am. Chem. Soc. 111: 8929-8931.
- Murata, M., Naoki, H., Iwashita, T., Matsunaga, S., Sasaki, M., Yokoyama, A., Yasumoto, T. (1993). Structure of maitotoxin. J. Am. Chem. Soc. 115: 2060-2062.
- Nagai, H., Murata, M., Torigoe, K., Satake, M., Yasumoto, T. (1992). Gambieric acids, new potent antifungal substances with unprecedented polyether structures from a marine dinoflagellate *Gambierdiscus toxicus*. J. Org. Chem. 57: 5448-5453.
- Ohfune, Y., Tomita, M. (1982). Total synthesis of (-)-domoic acid. A revision of the original structure. J. Am. Chem. Soc. 104: 3511-3513.
- Ogata, T., Kodama, M., Komaru, K., Sakamoto, S., Sato, S., Simidu, U. (1990). Production of paralytic shellfish toxins by bacteria isolated from toxic dinoflagellates. In: E. Graneli *et al.* (eds.) Toxic marine phytoplankton. Elsevier, New York, NY, p. 311-315.
- Parsons, T., LeBrasseur, R., Fulton, J.D. (1967). Some observations on the dependence of zooplankton grazing on the cell size and concentration of phytoplankton blooms. J. Oceanogr. Soc. Japan. 23: 10-17.
- Pavia, D.L., Lampman, G.M., Kriz, G.S. Jr. (1979). Introduction to spectroscopy: a guide for students of organic chemistry. Saunders College, Philadelphia, 367 pp.
- Pesando, D. (1972). Etude chimique et structurale d'une substance lipidique antibiotique produite par une diatomee marine: *Asterionella japonica*. Rev. Int. Oceanogr. med. 25: 49-69.
- Pratt, R., Daniels, T.C., Eiler, J.J., Gunnison, J.B., Kummler, W.D., Oneto, J.R., Spoehr, H.A., Hardin, G.J., Milner, H.W., Smith, J.H.C., Strain, H.H. (1944). Chlorellin, an antibacterial substance from *Chlorella*. Science 49: 351-352.

- Reeve, M.R., Walter, M.A., Darcy, K., Ikeda, T. (1977). Evaluation of potential indicators of sub-lethal toxic stress on marine zooplankton (feeding, fecundity, respiration, and excretion): controlled ecosystem pollution experiment. Bull. Mar. Sci. 27: 105-113.
- Reguera, B., Oshima, Y. (1990). Responses of *Gymnodinium catenatum* to increasing levels of nitrate: growth patterns and toxicity. In: E. Graneli *et al.* (eds.) Toxic marine phytoplankton. Elsevier, New York, NY, p. 316-319.
- Reish, D.L., Oshida, P.S. (1987). Manual of methods in aquatic environmental research, part 10: short-term static bioassays. FAO Fisheries Technical Paper 247, Food and Agricultural Organization of the United Nations, Rome, 62 pp.
- Rinehart, K.L., Harada, K-I., Namikoshi, M., Chen, C., Harvis, C.A., Munro, M.H.G., Blunt, J.W., Mulligan, P.E., Beasely, V.R., Dahlem, A.M., Carmichael, W.W. (1988). Nodularin, microcystin and the configuration of ADDA. J. Am. Chem. Soc. 110: 8557-8558.
- Rublee, P.A., Gallegos, C.L. (1989). Use of fluorescently labelled algae (FLA) to estimate microzooplankton grazing. Mar. Ecol. Prog. Ser. 51: 221-227.
- Runge, J.A. (1980). Effects of hunger and season on the feeding behavior of *Calanus pacificus*. Limnol. Oceanogr. 26: 134-145.
- Satake, M., Murata, M., Yasumoto, T. (1993). Gambierol: a new toxic polyether compound isolated from the marine dinoflagellate *Gambierdiscus toxicus*. J. Am. Chem. Soc. 115: 361-362.
- Schantz, E.J. (1960). Biochemical studies on paralytic shellfish poisons. Ann. N.Y. Acad. Sci. 89: 843-855.
- Schantz, E.J., Mold, J.D., Stanger, D.W., Shavel, J., Riel, F.J., Bowden, J.P., Lynch, J.M., Wyler, R.S., Reigel, B., Sommer, H. (1957). Paralytic shellfish poison VI. A procedure for the isolation and purification of the poison from toxic clams and mussel tissues. J. Am. Chem. Soc. 78: 5230-5235.
- Schantz, E.J., Lynch, J.M., Vayvada, G., Matsumoto, K., Rapoport, H. (1966). The purification and characterization of the poison produced by *Gonyaulax catenella* in axenic culture. Biochemistry 5: 1191-1195.
- Schantz, E.J., Ghazarossian, V.E., Schnoes, H.K., Strong, F.M., Springer, J.P., Pezzanite, J.O., Clardy, J. (1975). The structure of saxitoxin. J. Am. Chem. Soc. 97: 1238-1239.

- Schulman, L.S., Roszell, L.E., Mende, T.J., King, R.W., Baden, D.G. (1990). A new polyether toxin from Florida's red tide dinoflagellate *Ptychodiscus brevis*. In: E. Graneli *et al.* (eds.) Toxic marine phytoplankton. Elsevier, New York, NY, p. 407-412.
- Scutt, J.E. (1964). Autoinhibitor production by *Chlorella vulgaris*. Am. J. Bot. 51: 581-584.
- Sharma, G.M., Michaels, L., Burkholder, P.R. (1968). Goniodomin, a new antibiotic from a dinoflagellate. J. Antibiotics 21: 659-664.
- Sherr, E. B., Sherr, B. F., McDaniel, J. (1991). Clearance rates of < 6 mm fluorescently labeled algae (FLA) by estuarine protozoa: potential grazing impact of flagellates and ciliates. Mar. Ecol. Prog. Ser. 69: 81-92.
- Shumway, S.E. (1990). A review of the effects of algal blooms on shellfish and aquaculture. J. World Aquacult. Soc. 21: 65-104.
- Sieburth, J.McN. (1959a). Gastrointestinal microflora of Antarctic birds. J. Bact. 77: 521-531.
- Sieburth, J.McN. (1959b). Antibacterial activity of Antarctic marine phytoplankton. Limnol. Oceanogr. 4: 419-424.
- Sieburth, J.McN. (1960). Acrylic acid, an "antibiotic" principle in *Phaeocystis* blooms in Antarctic waters. Science 132: 676-677.
- Sieburth, J.McN. (1961). Antibiotic properties of acrylic acid, a factor in the gastrointestinal antibiosis of polar marine animals. J. Bact. 82: 72-79.
- Sieburth, J. McN. (1965). Role of algae in controlling bacterial populations in estuarine waters. In: Pollutions marines par les microorganismes et les produits petroliers (Symposium de Monaco, Avril 1964). Commission Internationale pour l'exploration Scientifique de la Mar Mediteranee, Paris, p. 217-233.
- Sieburth, J.McN. (1968). The influence of algal antibiosis on the ecology of marine microorganisms. In: M.R. Droop and E.J. Fergusson-Wood (eds.) Advances in microbiology of the sea. Academic Press, London, p. 63-94.
- Skoog, D.A. (1985). Principles of instrumental analysis. Third edition. Saunders College Publ., Toronto, 879 pp.
- Sokal, R.R., Rohlf, F.J. (1987). Introduction to biostatistics. W.H. Freeman and Company, New York, NY, 363 pp.
- Spoehr, H.A., Smith, J.H.C., Strain, H.H., Milner, H.W., Hardin, G.J. (1949). Fatty acid antibacterials from plants. Carnegie Inst. Wash. Publ. 589: 1-67.

- Stevens, A.N. (1987). NMR spectroscopy: application to metabolic research. In: V.R. McCready, M. Leach, and P.J. Ell (eds.) Functional studies using NMR. Springer-Verlag, New York, NY, p. 61-63.
- Stoecker, D., Guillard, R.R.L., Kavee, R.M. (1981). Selective predation by *Favella ehrenbergii* (Tintinnia) on and among dinoflagellates. Biol. Bull. 160: 136-145.
- Subba Rao, D.V., de Freitas, A.S.W., Quilliam, M.A., Pocklington, R., Bates, S.S. (1990). Rates of production of domoic acid, a neurotoxic amino acid in the pennate marine diatom *Nitzschia pungens*. In: E. Graneli *et al.* (eds.) Toxic marine phytoplankton. Elsevier, New York, NY, p. 413-417.
- Sullivan, D.S., Bisalputra, T. (1980). The morphology of a harpacticoid copepod gut: a review and synthesis. J. Morphology 164: 89-105.
- Sykes, P.F., Huntley, M.E. (1987). Acute physiological reactions of *Calanus* pacificus to selected dinoflagellates: direct observations. Mar. Biol. 94: 19-24.
- Tabachnick, B.G., Fidell, L.S. (1983). Using multivariate statistics. Harper & Row Publishers, New York, NY, 509 pp.
- Taber, D.F. (1982). TLC mesh column chromatography. J. Org. Chem. 47: 1351-1352.
- Tachibana, K., Scheuer, P.J., Tsukitani, Y., Kikuchi, H., Van Engen, D., Clardy, J., Gopichand, Y., Schmitz, F.J. (1981). Okadaic acid, a cytotoxic polyether from two marine sponges of the genus *Halichondria*. J. Am. Chem. Soc. 103: 2469-2471.
- Targett, N.M., Ward, J.E. (1991). Bioactive microalgal metabolites: mediation of subtle ecological interactions in phytophagous suspension-feeding marine invertebrates. Bioorg. Mar. Chem. 4: 91-118.
- Taylor, F.J.R. (1990). Red tides, brown tides and other harmful algal blooms: the view into the 1990's. In: E. Graneli *et al.* (eds.) Toxic marine phytoplankton. Elsevier, New York, NY, p. 527-533.
- Taylor, R.D., Ikawa, M., Sasner, J.J.Jr., Thurburg, F.P., Anderson, K.K. (1974). Occurrence of choline esters in the marine dinoflagellate *Amphidinium carteri*. J. Phycol. 10: 279-283.
- Thompson, P.A. (1991). The influence of irradiance, nitrogen limitation, and temperature on the biochemical composition of marine phytoplankton and their nutritional value to larval *Crassostrea gigas*. PhD. thesis, University of British Columbia, Vancouver, B.C., 183 pp.

- Thompson, P. A., Harrison, P. J., Whyte, J. N.C. (1990). Influence of irradiance on the fatty acid composition of phytoplankton. J. Phycol. 26: 278-288.
- Thompson, P.A., Harrison, P.J., Parslow, J.S. (1991). Influence of irradiance on cell volume and carbon quota for ten species of marine phytoplankton. J. Phycol. 27: 351-360.
- Thompson, P.A., Montagnes, D.J.S., Shaw, B.A., Harrison, P.J. (1993). The influence of three algal filtrates on the grazing rate of the larval oyster *Crassostrea gigas*. Aquaculture, accepted August, 1993.
- Thurburg, F.P., Sasner Jr., J.J. (1973). Biological activity of cell extract from the dinoflagellate *Amphidinium carteri*. Chesapeake Sci. 14: 48-69.
- Torigoe, K., Murata, M., Yasumoto, T., Iwashita, T. (1988). Prorocentrolide, a toxic nitrogenous macrocycle from a marine dinoflagellate, *Prorocentrum lima*. J. Am. Chem. Soc. 110: 7876-7877.
- Torigoe, K., Satake, M., Murata, M., Yasumoto, T., Hirota, H. (1992). Gambieric acids: unprecedented potent antifungal substances isolated from cultures of a marine dinoflagellate *Gambierdiscus toxicus*. J. Am. Chem. Soc. 114: 1102-1103.
- Trick, C.G., Harrison, P.J., Andersen, R.J. (1981). Extracellular secondary metabolite production by the marine dinoflagellate *Prorocentrum minimum* in culture. Can J. Fish. Aquat. Sci. 38: 864-867.
- Trick, C.G., Andersen, R.J., Harrison, P.J., (1984). Environmental factors influencing the production of an antibacterial metabolite from a marine dinoflagellate, *Prorocentrum minimum*. Can. J. Fish. Aquat. Sci. 41: 423-432.
- Tsuda, A., Nemoto, T. (1990). The effect of food concentration on the fecal pellet size of the marine copepod *Pseudocalanus newmani* Frost. Bull. Plank. Soc. Jap. 37: 83-90.
- Uye, S., Takamatsu, K. (1990). Feeding interactions between planktonic copepods and red-tide flagellates fron Japanese coastal waters. Mar. Ecol. Prog. Ser. 59: 97-107.
- Van Alstyne, K.L. (1986). Effects of phytoplankton taste and smell on feeding behavior of the copepod *Centropages hamatus*. Mar. Ecol. Prog. Ser. 34: 187-190.
- Verity, P.G., Stoecker, D. (1982). Effects of *Olisthodiscus luteus* on the growth and abundance of tintinnids. Mar. Biol. 72: 79-87.

- Vetter, W., Englert, G., Rigassi, N., Schwieter, U. (1971). IV. Spectroscopic methods. In: O. Isler (ed.) Carotenoids. Birkhäuser Verlag, Basel, p. 189-266.
- Waksman, S.A., Stokes, J.L., Butler, M.R. (1938). Relation of bacteria to diatoms in sea water. J. mar. biol. Ass. UK 22: 359-373.
- Wang, R., Shimuzu, Y. (1990). Bacillariolides I and II, a new type of cyclopentane eicosanoids from the diatom *Nitzschia pungens*. J. Chem. Soc., Chem. Commun. 413-414.
- Wangersky, P.J., Guillard, R.R.L. (1960). Low molecular weight organic base from the dinoflagellate *Amphidinum carteri*. Nature, Lond. 185: 689-690.
- Ward, E., Targett, N.M. (1989). Influence of marine microalgal metabolites on the feeding behavior of the blue mussel *Mytilus edulis*. Mar. Biol. 101: 313-321.
- Wilkinson, G.N. (1961). Statistical estimations in enzyme kinetics. Biochem. J. 80: 324-332.
- Wilson, J.H. (1979). Observation on the grazing rates and growth of *Ostrea edulis* L. larvae when fed algal cultures of different ages. J. exp. mar. Biol. Ecol. 38: 187-199.
- Wolfe, S., Ingold, C.F. (1983). Oxidation of organic compounds by zinc permanganate. J. Am. Chem. Soc. 105: 7755-7757.
- Wootton, L.S. (1989). Salt-flocculated organic material as a food source in estuarine food webs. M.Sc. thesis, University of British Columbia, Vancouver, B.C., 140 pp.
- Wright, J.L.C., Boyd, R.K., deFreitas, A.S.W., Falk, M., Foxall, R.A., Jamieson, W.D., Laycock, M.V., McCulloch, A.W., McInnes, A.G., Odense, P., Pathak, V.P., Quilliam, M.A., Ragan, M.A., Sim, P.G., Thibault, P., Walter, J.A., Gilgan, M., Richard, D.J.A., Dewar, D. (1989). Identification of domoic acid, a neuroexcitatory amino acid, in toxic mussels from eastern Prince Edward Island. Can. J. Chem. 67: 481-490.
- Wright, S.W., Jeffrey, S.W., Mantoura, R.F.C., Llewellyn, C.A., Bjørnland, T., Repeta, D., Welschmeyer, N. (1991). Improved HPLC method for the analysis of chlorophylls and carotenoids from marine phytoplankton. Mar. Ecol. Prog. Ser. 77: 183-196.
- Wüthrich, K. (1986). 2D NMR with biopolymers. In: E.M. Bradbury and C.A. Nicolini (eds.) NMR in the life sciences. Plenum Press, New York, NY, p. 11-22.

- Yasumoto, T. (1990). Marine microorganisms toxins an overview. In: Graneli *et al.* (eds.) Toxic marine phytoplankton. Elsevier, New York, NY, p. 3-8.
- Yasumoto, T., Nakajima, I., Bagnis, R., Adachi, R. (1977). Finding of a dinoflagellate as a likely culprit of ciguatera. Bull. Jap. Soc. Sci. Fish. 43: 1021-1026.
- Yasumoto, T., Murata, M., Oshima, Y., Matsumoto, G.K., Clardy, J. (1985). Diarrhetic shellfish toxins. Tetrahedron 41: 1019-1025.
- Yasumoto, T., Underdal, B., Aune, T., Hormazabal, V., Skulberg, O.M., Oshima, Y. (1990). Screening for hemolytic and ichthyotoxic components of *Chrysochromulina polylepis* and *Gyrodinium aureolum* from Norwegian coastal waters. In: Graneli *et al.* (eds.) Toxic marine phytoplankton. Elsevier, New York, NY, p. 3-8.
- Yokoyama, A., Murata, M., Oshima, Y., Iwashita, T., Yasumoto, T. (1988). Some chemical properties of maitotoxin, a putative calcium channel agonist isolated from a marine dinoflagellate. J. Biochem. 104: 184-187.

# Appendix A. <u>A Model Demonstrating the Use of Total Fecal Pellet Production as a Measure of Fecal Pellet Production Rate</u>

The following model demonstrates how measurements of the total fecal pellet production over a given interval can be used as a measure of decrease in fecal pellet production rate. Given the following assumptions:

- 1) food particles are not in limiting concentrations
- feeding deterrents slow ingestion (and hence egestion) rate, but do not completely stop feeding
- 3) gut fullness will eventually be reached regardless of the presence of feeding deterrents, and this level of saturation is constant for all experiments, then fecal pellet production rate can be modeled by the equation:

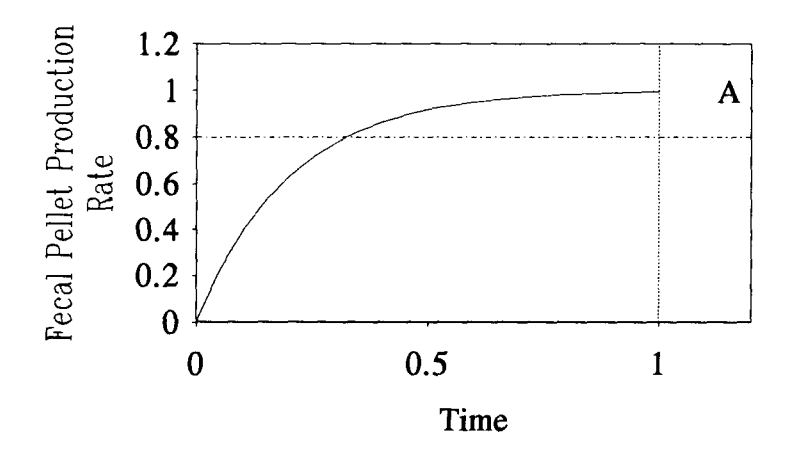
$$F = F_{\text{max}} (1 - e^{-bt})$$

where F = the fecal pellet production rate (fecal pellets  $h^{-1}$  copepod<sup>-1</sup>),  $F_{max}$  = the maximum fecal pellet production rate, b = a constant ( $h^{-1}$ ), and t = time (h). Fig. A1 shows two possible scenarios.

By integrating the area under the curve

$$\left(\int_{t1}^{t2} F_{max} (1 - e^{-bt}) dt\right) = \left[F_{max} t + \frac{F_{max} e^{-bt}}{b}\right]_{t1}^{t2}, \text{ which gives the total number of fecal}$$

pellets, and dividing it by the total elapsed time, one gets the average fecal pellet production rate over the time interval. For graph A, the control, this is equal to 0.80 fecal pellets/unit time. For graph B, this is equal to 0.37 fecal pellets/unit time. Thus, as  $\overline{F}_A > \overline{F}_B$ , it is possible to detect the decrease in fecal pellet production rate due to the presence of a feeding deterrent by counting the total number of fecal pellets produced in a given time.



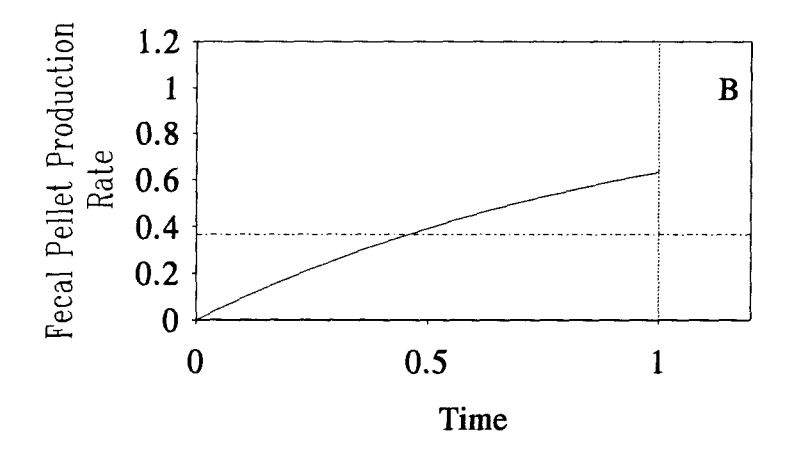


Fig. A1. Model for fecal pellet production rate. For simplicity,  $F_{max}$  and the total elapsed time are both equal to 1 unit. Graph A represents the control (no feeding deterrent), with b=5 (from equation for total number of fecal pellets). Graph B represents the affect of a feeding deterrent, with b=1. The area under the curve, from  $t_1=0$  to  $t_2=1$  (vertical line), is the total number of fecal pellets. The average fecal pellet production rate over this time interval is shown by the horizontal dotted line.

# Appendix B. Growth of Phytoplankton Cultures

**Table B1.** Growth of *Phaeodactylum tricornutum, Thalassiosira pseudonana*, and *Gonyaulax grindleyi* cultures at 19 °C with continuous irradiance of approximately 70  $\mu$ mol m<sup>-2</sup> s<sup>-1</sup>.

Species	Growth rate $(\mu)$ $(day^{-1})$	Time at which cultures entered senescence (days)	Maximum cell density (10 <sup>4</sup> cells·ml <sup>-1</sup> )
Phaeodactylum tricornutum	0.825	2.77	233
Thalassiosira pseudonana	1.57	2.08	74.8
Gonyaulax grindleyi	0.271	6.57	0.82

# Appendix C. Raw Data and Statistical Analysis for Feeding Deterrent Bioassays in Chapter 2

Tests for normality and homoscedasticity were done on all experimental data sets before ANOVA and t-tests were carried out. The assumption of normality was verified by calculating the skewness,

skewness = 
$$n^{\frac{1}{2}} \sum_{i=1}^{n} (y_i - \overline{y})^3 / [\sum_{i=1}^{n} (y_i - \overline{y})^2]^{\frac{3}{2}}$$
,

of the data set. The standard error for skewness =  $S_S = \sqrt{6/N}$ . The z-test for skewness = (skewness - 0)/Ss. If -2.58  $\leq$  z-test  $\leq$  2.58, then the data were normal (Tabachnick and Fidell, 1983). Homoscedasticity was verified by performing a two-tailed F-test on the variances of the data sets.  $F_S$  is the ratio of the greater variance over the lesser one, where  $F_S = S_1^2/S_2^2$ . The critical value is  $F_{\alpha/2[\nu_1,\nu_2]}$ , where  $\alpha$  is the accepted error level and the degrees of freedom are  $\nu_1 = n_1 - 1$ ,  $\nu_2 = n_2 - 1$  for the upper and lower variance respectively (Sokal and Rohlf, 1987).

Simple one-factor ANOVA's were performed using a program written in basic (based on Bishop, 1983). Two-factor ANOVA's and ANOVA's with unequal n were performed using the statistical package included with the program Microsoft Excel 4.0 for Windows.

**Table C1.** Raw data for the fecal pellet production rate of *Tigriopus californicus* over two different time intervals when presented with a diet of ground fish food.

Experiment	Replicates	Fecal pellets	Rate
Experiment	Replicates	r cear penets	(pellets h <sup>-1</sup> )
	<del></del>	<del></del>	(peners ii -)
Short term experiment			
(50.5 h)			
	1	53	1.1
	2	62	1.2
	3	45	0.89
	4	52	1.0
	5	52	1.0
Long term experiment			
(137 h)			
	1	102	0.74
	2	138	1.0
	3	131	0.96
	4	183	1.3
	5	167	1.2

Table C2. Statistical analysis of raw data from Table C1.

Statistic	Short term experiment	Long term experiment	
Mean rate (pellets h <sup>-1</sup> ):	1.1	1.1	
Standard deviation, S:	0.12	0.23	
Variance, S <sup>2</sup> :	0.014 0.054		
Skewness:	0.38	-0.065	
Z-test for normality:	0.35	-0.059	
Test for Homoscedasticity:			
F:	3.9		
$\nu_1$ :	4		
$\nu_2$ :	4		
α:	0.24		
One-way ANOVA			
(two-tailed):			
F:	0.0036		
df <sub>1</sub> :	1		
df <sub>2</sub> :	8		
α:	0.999		

**Table C3.** Raw data for the fecal pellet production rate of both untreated and antibiotic-treated *Tigriopus californicus* when presented with varying concentrations of *Thalassiosira pseudonana* cells. Each replicate consisted of two copepods incubated for 24 h.

Uı	ntreated Copepo	ods	Antibiotic-treated Copepods		
Initial cell	Fecal pellets	Rate	Initial cell	Fecal pellets	Rate
density		(pellets h <sup>-1</sup> )	density		(pellets h <sup>-1</sup> )
(cells ml <sup>-1</sup> )			(cells ml <sup>-1</sup> )		
489000	105	2.2	489000	105	2.2
48900	50	1.0	48900	80	1.7
4890	14	0.29	4890	2	0.04
489	3	0.06	489	5	0.10
48.9	6	0.13	48.9	5	0.10
4.89	1	0.02	4.89	7	0.15
498000	82	1.7	460000	75	1.6
498000	91	1.90	460000	95	2.0
398000	83	1.7	368000	86	1.8
398000	59	1.2	368000	86	1.8
299000	52	1.1	276000	86	1.8
299000	77	1.6	276000	82	1.7
199000	46	0.96	184000	56	1.2
199000	64	1.3	184000	94	2.0
99600	46	0.96	91900	15	0.31
99600	63	1.3	91900	103	2.2
49800	70	1.5	46000	73	1.5
49800	76	1.6	46000	68	1.4

Table C4. Statistical analysis of raw data from Table C3.

Statistic	Untreated copepods	Antibiotic-treated copepods
Wilkinson's regression:		
F <sub>max</sub> :	1.6	1.9
Standard error (F <sub>max</sub> ):	0.14	0.20
K <sub>c</sub> :	18000	21000
Standard error $(K_c)$ :	12000	15000
Standard deviation about	0.32	0.42
regression line, S:		
Variance, S <sup>2</sup> :	0.10	0.17
Skewness:	0.11	-1.5
Z-test for normality:	0.20	-2.6*
Test for Homoscedasticity:		
F:		1.7
ν <sub>1</sub> :		17
$v_2$ :		17
α:		0.30
t-tests (one-tailed):		
t-test for F <sub>max</sub> :		1.4
t-test for K <sub>c</sub> :		0.21
df:		14
$\alpha$ for $F_{max}$ :		0.09
$\alpha$ for $K_c$ :		0.25

<sup>\*</sup>Note that the data for the antibiotic-treated copepods are slightly skewed. As t-tests are relatively robust with respect to skewed data, and the degree of skewing was small, the raw data was analyzed without any transformations.

Table C5. Raw data for the egestion rate of *Tigriopus californicus* in response to treatments of copepods with antibiotics and treatments of ground fish food with cellular extracts from *Gonyaulax grindleyi*. The coated fish food was ≈ 20-23% cellular extract by weight. UU = untreated copepods fed uncoated fish food; UC = untreated copepods fed fish food coated with *G. grindleyi* cellular extract; AU = antibiotic-treated copepods fed uncoated fish food; AC = antibiotic-treated copepods fed fish food coated with *G. grindleyi* cellular extract.

Experiment	Replicates	Fecal pellets	Rate
			(pellets h <sup>-1</sup> )
UU (68.5 h)			
	1	41	0.60
	2	40	0.58
	3	67	0.98
	4	63	0.92
	5	41	0.60
	6	63	0.92
UC (68.5 h)			
	1	47	0.69
	2 3	57	0.83
	3	78	1.1
	4	96	1.4
	5	34	0.50
	6	97	1.4
AU (66.5 h)			
	1	101	1.5
	2	70	1.1
	2 3	108	1.6
	4 5	96	1.4
	5	100	1.5
	6	94	1.4
AC (66.5 h)			
	1	74	1.1
	2	69	1.0
	2 3	78	1.2
	4	47	0.71
	5	69	1.0
	6	69	1.0

Table C6. Statistical analysis of raw data from Table C5.

Statistic	UU	UC	AU	AC
Mean rate (pellets h <sup>-1</sup> ):	0.77	1.0	1.4	1.0
Standard deviation, S:	0.19	0.38	0.20	0.16
Variance, S <sup>2</sup> :	0.036	0.15	0.039	0.026
Skewness:	0.036	-0.052	-1.2	-1.3
Z-test for normality:	0.036	-0.052	-1.2	-1.3
Test for Homoscedasticity:				
$\nu_1; \ \nu_2:$		5;	5	
$F(UU,UC)$ ; $\alpha$ :		4.0;	0.16	
$F(UU,AU)$ ; $\alpha$ :		1.1;	0.96	
$F(UU,AC)$ ; $\alpha$ :		1.4;	0.78	
$F(UC,AU); \alpha$ :		3.8;	0.18	
$F(UC,AC)$ ; $\alpha$ :		5.6;	0.09	
$F(AU,AC)$ ; $\alpha$ :		1.5;	0.73	
Two-way ANOVA:				
df <sub>r</sub> :		1	l	
df <sub>c</sub> :		1	l	
$df_{\mathbf{I}}$ :		1	Į.	
df <sub>w</sub> :		2	0	
F (interaction); $\alpha$ :		9.8; (	0.005	
F (row=antibiotic vs. no		11; 0	.003	
antibiotic); $\alpha$ :				
F (column=uncoated vs.		0.79;	0.38	
coated fish food); $\alpha$ :				
Protected t-tests:				
LSD ( $p=0.05$ ; $df_W=20$ ):		0.3	30	
mean differences (UU-UC):		-0.	23	
mean differences (UU-AU):		-0.	66	
mean differences (UU-AC):		-0.	25	
mean differences (UC-AU):		-0.	43	
mean differences (UC-AC):		-0.	02	
mean differences (AU-AC):		0.4	<b>1</b> 1	
One-way ANOVA's:				
df <sub>1</sub> ; df <sub>2</sub> :		1;	10	
$F(UU,AU); \alpha$ :		35; <	0.001	
F (UC,AU); $\alpha$ :		6.0;	0.04	
F (AU,AC); $\alpha$ :		15; 0	.004	

Table C7. Raw data for the egestion rate of *Tigriopus californicus* in response to treatments of copepods with antibiotics and treatments of ground fish food with cellular extracts from *Thalassiosira pseudonana*. The coated fish food was ≈ 28% cellular extract by weight. UU = untreated copepods fed uncoated fish food; UC = untreated copepods fed fish food coated with *T. pseudonana* cellular extract; AU = antibiotic-treated copepods fed uncoated fish food; AC = antibiotic-treated copepods fed fish food coated with *T. pseudonana* cellular extract.

Experiment	Replicates	Fecal pellets	Rate
			(pellets h <sup>-1</sup> )
UU (64.75 h)			
	1	67	1.0
	2 3	49	0.76
		59	0.91
	4	50	0.77
	5	53	0.82
	6	60	0.93
UC (64.75 h)			
	1	68	1.1
	2	63	0.97
	3	64	0.99
	4	48	0.74
	5	50	0.77
	6	64	0.99
AU (72 h)			
	1	110	1.5
	2 3	76	1.1
		99	1.4
	4	85	1.2
	5	79	1.1
	6	82	1.1
AC (72 h)			
	1	<b>7</b> 9	1.1
	2	78	1.1
	2 3	74	1.0
	4	66	0.92
	5	81	1.1
	6	84	1.2

Table C8. Statistical analysis of raw data from Table C7.

Statistic	UU	UC	AU	AC
Mean rate (pellets h <sup>-1</sup> ):	0.87	0.92	1.2	1.1
Standard deviation, S:	0.11	0.13	0.18	0.088
Variance, S <sup>2</sup> :	0.011	0.017	0.034	0.0077
Skewness:	0.39	-0.58	0.77	-0.82
Z-test for normality:	0.39	-0.58	0.77	-0.82
Test for Homoscedasticity:				
$\nu_1; \ \nu_2:$		5;	5	
$F(UU,UC); \alpha$ :		1.5;	0.75	
$F(UU,AU); \alpha$ :		3.0;	0.30	
$F(UU,AC)$ ; $\alpha$ :		1.5;	0.73	
$F(UC,AU); \alpha:$		2.0;	0.47	
$F(UC,AC)$ ; $\alpha$ :		2.2;	0.45	
$F(AU,AC)$ ; $\alpha$ :		4.4;	0.14	
Two-way ANOVA:				
df <sub>r</sub> :		1	l	
df <sub>c</sub> :		1	l	
$df_{\mathbf{I}}$ :		1		
df <sub>w</sub> :		2	0	
F (interaction); $\alpha$ :		3.8;	0.07	
F (row=antibiotic vs. no		22; 0	.0001	
antibiotic); $\alpha$ :				
F (column=uncoated vs.		1.1;	0.31	
coated fish food); $\alpha$ :				
Protected t-tests:				
$LSD_{row}$ (p=0.05; df <sub>w</sub> =20):		0.	11	
row mean (untreated):		0.3	89	
row mean (antibiotic-treated):		1.	2	
difference in means (untreated		-0.	25	
<ul><li>antibiotic-treated):</li></ul>				
One-way ANOVA's:				
$df_1$ ; $df_2$ :		1;	22	
F (untreated vs. antibiotic-		20; <	0.001	
treated); $\alpha$ :				

Table C9. Raw data for the egestion rate of *Tigriopus californicus* in response to a diet of ground fish food coated with cellular extracts from *Thalassiosira* pseudonana and *Phaeodactylum tricornutum*. The coated fish food was ≈ 20% cellular extract by weight. ATP = antibiotic-treated copepods fed fish food coated with *T. pseudonana* cellular extract; APT = antibiotic-treated copepods fed fish food coated with *P. tricornutum* cellular extract.

Experiment	Replicates	Fecal pellets	Rate (pellets h <sup>-1</sup> )
ATP (74 h)			
, ,	1	86	1.2
	2	67	0.91
	3	80	1.1
	4	84	1.1
	5	64	0.86
	6	64	0.86
APT (74 h)			
	1	16	0.22
	2	10	0.14
	3	22	0.30
	4	27	0.36
	5	11	0.15
	6	20	0.27

Table C10. Statistical analysis of raw data from Table C9.

Statistic	ATP	APT	
Mean rate (pellets h <sup>-1</sup> ):	1.0	0.24	
Standard deviation, S:	0.14	0.089	
Variance, S <sup>2</sup> :	0.019	0.0079	
Skewness:	0.068	0.12	
Z-test for normality:	0.068	0.12	
Test for Homoscedasticity:			
$\nu_1; \nu_2:$	5; 5		
$F(ATP,APT); \alpha$ :	2.4; 0.40		
One-way ANOVA's:			
df <sub>1</sub> ; df <sub>2</sub> .	1:	1	
F (ATP, APT); $\alpha$ :	130; < 0.001		
<u> </u>			

**Table C11.** Raw data for the egestion rate of *Tigriopus californicus* when presented with a diet of live phytoplankton cells. ADTP = antibiotic-treated copepods fed live *Thalassiosira pseudonana* cells suspended in dissolved cellular extract from *T. pseudonana*; ADPT = antibiotic-treated copepods fed fed live *T. pseudonana* cells suspended in dissolved cellular extract from *Phaeodactylum tricornutum*.

Experiment	Replicates	Fecal pellets	Rate (pellets h <sup>-1</sup> )
ADTP			
(2 copepods, 22 h)			
	1	77	1.8
	2	101	2.3
	3	98	2.2
	4	65	1.5
	5	94	2.1
	6	66	1.5
ADPT			
(2 copepods, 22 h)			
	1	31	0.70
	2	13	0.30
	3	26	0.59
	4	28	0.64
	5	36	0.82
	6	21	0.48
	O	21	0.70

Table C12. Statistical analysis of raw data from Table C11.

Statistic	ADTP	ADPT
Mean rate (pellets h <sup>-1</sup> ):	1.9	0.59
Standard deviation, S:	0.37	0.18
Variance, S <sup>2</sup> :	0.14	0.033
Skewness:	-0.12	-0.43
Z-test for normality:	-0.12	-0.43
Test for Homoscedasticity:		
$\nu_1; \nu_2$ :	5; 5	
$F(ADTP,ADPT); \alpha:$	4.1; 0.16	
One-way ANOVA's:		
df <sub>1</sub> ; df <sub>2</sub> .	1:	10
F (ADTP, ADPT); $\alpha$ :	61; < 0.001	

Table C13. Raw data for the egestion rate of *Tigriopus californicus* when presented with a diet of live phytoplankton cells. ALTP = antibiotic-treated copepods fed live *Thalassiosira pseudonana* cells; ALPT = antibiotic-treated copepods fed fed live *Phaeodactylum tricornutum* cells. The cells were presented to the copepods at a density of 6 x 10<sup>5</sup> cells ml<sup>-1</sup>. Replicate 2 of the *T. pseudonana* series was anomalous (copepods were unhealthy) and was not used for data analysis.

Experiment	Replicates	Fecal pellets	Rate (pellets h <sup>-1</sup> )
ALTP	-		
(2 copepods, 19 h)			
	1	83	2.2
	2	16	0.42
	3	81	2.1
	4	85	2.2
	5	52	1.4
	6	96	2.5
ALPT			
(2 copepods, 19 h)			
	1	40	1.1
	2	39	1.0
	3	46	1.2
	4	43	1.1
	5	43	1.1
	6	38	1.0

Table C14. Statistical analysis of raw data from Table C13.

C4-4:-4:-	A T TOD	AT DO
Statistic	ALTP	ALPT
Mean rate (pellets h <sup>-1</sup> ):	2.1	1.1
Standard deviation, S:	0.43	0.079
Variance, S <sup>2</sup> :	0.19	0.0063
Skewness:	-1.0	0.29
Z-test for normality:	-0.92	0.29
Test for Homoscedasticity:		
$\nu_1;  \nu_2:$	4; 5	
$F(ALTP,ALPT); \alpha:$	30; 0.003*	
One-way ANOVA's:		
df <sub>1</sub> ; df <sub>2</sub> .	1; 9	
F (ALTP, ALPT); $\alpha$ :	32; 0.0003	
Mann-Whitney U test:		
n <sub>1</sub> ; n <sub>2</sub> :	6; 5	
$U_{S}; \alpha$ :	30; < 0.005	

<sup>\*</sup>The two data sets had significantly different variances. Several transformations (log, square root, arcsine) were applied to the data, but none produced variances which were not significantly different. Therefore, this data set does not meet the assumptions for ANOVA. As ANOVA is a robust statistical technique, the results of the ANOVA may still be valid, however a second nonparametric method (Mann-Whitney U test) was applied.

## Appendix D. Fecal Pellet Volume Measurements

**Table D1.** Measurements of diameter and length of fecal pellets from *Tigriopus* californicus on a diet of ground fish food. Pellet volume is calculated using the volume equation for a cylinder,  $V = \pi r^2 h$ .

$ \begin{array}{c ccccccccccccccccccccccccccccccccccc$	Commis	diamatan	lan ath		Samula.	diamatan	lanath	
1-1       43.8       219       3.30       4-1       54.8       110       2.58         1-2       32.9       131       1.11       4-2       32.9       153       1.30         1-3       32.9       131       1.11       4-3       43.8       153       2.31         1-4       43.8       142       2.14       4-4       43.8       164       2.47         1-5       54.8       175       4.12       4-5       43.8       186       2.80         1-6       32.9       65.7       0.557       4-6       32.9       131       1.11         1-7       43.8       98.6       1.48       4-7       43.8       175       2.64         1-8       43.8       110       1.65       4-8       32.9       230       1.95         1-9       43.8       76.7       1.15       4-9       43.8       110       1.65         1-10       43.8       120       1.81       4-10       54.8       219       5.16         2-1       54.8       120       2.84       5-1       43.8       208       3.13         2-2-2       32.9       175       1.48       5-2<	Sample	diameter	length	volume	Sample	diameter	length	volume
1-2     32.9     131     1.11     4-2     32.9     153     1.30       1-3     32.9     131     1.11     4-3     43.8     153     2.31       1-4     43.8     142     2.14     4-4     43.8     164     2.47       1-5     54.8     175     4.12     4-5     43.8     186     2.80       1-6     32.9     65.7     0.557     4-6     32.9     131     1.11       1-7     43.8     98.6     1.48     4-7     43.8     175     2.64       1-8     43.8     110     1.65     4-8     32.9     230     1.95       1-9     43.8     76.7     1.15     4-9     43.8     110     1.65       1-10     43.8     120     1.81     4-10     54.8     219     5.16       2-1     54.8     120     2.84     5-1     43.8     208     3.13       2-2     32.9     175     1.48     5-2     54.8     219     5.16       2-3     43.8     98.6     1.48     5-3     32.9     164     1.39       2-4     43.8     110     1.65     5-4     54.8     208     4.90       2-5 <td>1 1</td> <td><u> </u></td> <td>· · · · · · · · · · · · · · · · · · ·</td> <td></td> <td>4 1</td> <td></td> <td></td> <td></td>	1 1	<u> </u>	· · · · · · · · · · · · · · · · · · ·		4 1			
1-3       32.9       131       1.11       4-3       43.8       153       2.31         1-4       43.8       142       2.14       4-4       43.8       164       2.47         1-5       54.8       175       4.12       4-5       43.8       186       2.80         1-6       32.9       65.7       0.557       4-6       32.9       131       1.11         1-7       43.8       98.6       1.48       4-7       43.8       175       2.64         1-8       43.8       110       1.65       4-8       32.9       230       1.95         1-9       43.8       76.7       1.15       4-9       43.8       110       1.65         1-10       43.8       120       1.81       4-10       54.8       219       5.16         2-1       54.8       120       2.84       5-1       43.8       208       3.13         2-2       32.9       175       1.48       5-2       54.8       219       5.16         2-3       43.8       98.6       1.48       5-3       32.9       164       1.39         2-4       43.8       110       1.65       5-4 </td <td></td> <td></td> <td></td> <td></td> <td></td> <td></td> <td></td> <td></td>								
1-4       43.8       142       2.14       4-4       43.8       164       2.47         1-5       54.8       175       4.12       4-5       43.8       186       2.80         1-6       32.9       65.7       0.557       4-6       32.9       131       1.11         1-7       43.8       98.6       1.48       4-7       43.8       175       2.64         1-8       43.8       110       1.65       4-8       32.9       230       1.95         1-9       43.8       76.7       1.15       4-9       43.8       110       1.65         1-10       43.8       120       1.81       4-10       54.8       219       5.16         2-1       54.8       120       2.84       5-1       43.8       208       3.13         2-2       32.9       175       1.48       5-2       54.8       219       5.16         2-3       43.8       98.6       1.48       5-3       32.9       164       1.39         2-4       43.8       110       1.65       5-4       54.8       208       4.90         2-5       43.8       87.6       1.32       5-5<					H			
1-5       54.8       175       4.12       4-5       43.8       186       2.80         1-6       32.9       65.7       0.557       4-6       32.9       131       1.11         1-7       43.8       98.6       1.48       4-7       43.8       175       2.64         1-8       43.8       110       1.65       4-8       32.9       230       1.95         1-9       43.8       76.7       1.15       4-9       43.8       110       1.65         1-10       43.8       120       1.81       4-10       54.8       219       5.16         2-1       54.8       120       2.84       5-1       43.8       208       3.13         2-2       32.9       175       1.48       5-2       54.8       219       5.16         2-3       43.8       98.6       1.48       5-3       32.9       164       1.39         2-4       43.8       110       1.65       5-4       54.8       208       4.90         2-5       43.8       87.6       1.32       5-5       32.9       153       1.30         2-6       32.9       76.7       0.650       5-					i			
1-6       32.9       65.7       0.557       4-6       32.9       131       1.11         1-7       43.8       98.6       1.48       4-7       43.8       175       2.64         1-8       43.8       110       1.65       4-8       32.9       230       1.95         1-9       43.8       76.7       1.15       4-9       43.8       110       1.65         1-10       43.8       120       1.81       4-10       54.8       219       5.16         2-1       54.8       120       2.84       5-1       43.8       208       3.13         2-2       32.9       175       1.48       5-2       54.8       219       5.16         2-3       43.8       98.6       1.48       5-3       32.9       164       1.39         2-4       43.8       110       1.65       5-4       54.8       208       4.90         2-5       43.8       87.6       1.32       5-5       32.9       153       1.30         2-6       32.9       76.7       0.650       5-6       43.8       98.6       1.48         2-7       43.8       120       1.81       5								— <del>-</del>
1-7       43.8       98.6       1.48       4-7       43.8       175       2.64         1-8       43.8       110       1.65       4-8       32.9       230       1.95         1-9       43.8       76.7       1.15       4-9       43.8       110       1.65         1-10       43.8       120       1.81       4-10       54.8       219       5.16         2-1       54.8       120       2.84       5-1       43.8       208       3.13         2-2       32.9       175       1.48       5-2       54.8       219       5.16         2-3       43.8       98.6       1.48       5-3       32.9       164       1.39         2-4       43.8       110       1.65       5-4       54.8       208       4.90         2-5       43.8       87.6       1.32       5-5       32.9       153       1.30         2-6       32.9       76.7       0.650       5-6       43.8       98.6       1.48         2-7       43.8       120       1.81       5-7       54.8       186       4.38         2-8       32.9       87.6       0.742       5								
1-8       43.8       110       1.65       4-8       32.9       230       1.95         1-9       43.8       76.7       1.15       4-9       43.8       110       1.65         1-10       43.8       120       1.81       4-10       54.8       219       5.16         2-1       54.8       120       2.84       5-1       43.8       208       3.13         2-2       32.9       175       1.48       5-2       54.8       219       5.16         2-3       43.8       98.6       1.48       5-3       32.9       164       1.39         2-4       43.8       110       1.65       5-4       54.8       208       4.90         2-5       43.8       87.6       1.32       5-5       32.9       153       1.30         2-6       32.9       76.7       0.650       5-6       43.8       98.6       1.48         2-7       43.8       120       1.81       5-7       54.8       186       4.38         2-8       32.9       87.6       0.742       5-8       54.8       175       4.12         2-9       43.8       98.6       1.48       5								
1-9       43.8       76.7       1.15       4-9       43.8       110       1.65         1-10       43.8       120       1.81       4-10       54.8       219       5.16         2-1       54.8       120       2.84       5-1       43.8       208       3.13         2-2       32.9       175       1.48       5-2       54.8       219       5.16         2-3       43.8       98.6       1.48       5-3       32.9       164       1.39         2-4       43.8       110       1.65       5-4       54.8       208       4.90         2-5       43.8       87.6       1.32       5-5       32.9       153       1.30         2-6       32.9       76.7       0.650       5-6       43.8       98.6       1.48         2-7       43.8       120       1.81       5-7       54.8       186       4.38         2-8       32.9       87.6       0.742       5-8       54.8       175       4.12         2-9       43.8       98.6       1.48       5-9       32.9       120       1.02         2-20       32.9       110       0.928 <td< td=""><td>1-7</td><td>43.8</td><td></td><td></td><td>4-7</td><td>43.8</td><td>175</td><td>2.64</td></td<>	1-7	43.8			4-7	43.8	175	2.64
1-10       43.8       120       1.81       4-10       54.8       219       5.16         2-1       54.8       120       2.84       5-1       43.8       208       3.13         2-2       32.9       175       1.48       5-2       54.8       219       5.16         2-3       43.8       98.6       1.48       5-3       32.9       164       1.39         2-4       43.8       110       1.65       5-4       54.8       208       4.90         2-5       43.8       87.6       1.32       5-5       32.9       153       1.30         2-6       32.9       76.7       0.650       5-6       43.8       98.6       1.48         2-7       43.8       120       1.81       5-7       54.8       186       4.38         2-8       32.9       87.6       0.742       5-8       54.8       175       4.12         2-9       43.8       98.6       1.48       5-9       32.9       120       1.02         2-20       32.9       110       0.928       5-10       43.8       131       1.98         3-1       43.8       142       2.14 <td< td=""><td></td><td></td><td></td><td></td><td></td><td></td><td>230</td><td>1.95</td></td<>							230	1.95
2-1       54.8       120       2.84       5-1       43.8       208       3.13         2-2       32.9       175       1.48       5-2       54.8       219       5.16         2-3       43.8       98.6       1.48       5-3       32.9       164       1.39         2-4       43.8       110       1.65       5-4       54.8       208       4.90         2-5       43.8       87.6       1.32       5-5       32.9       153       1.30         2-6       32.9       76.7       0.650       5-6       43.8       98.6       1.48         2-7       43.8       120       1.81       5-7       54.8       186       4.38         2-8       32.9       87.6       0.742       5-8       54.8       175       4.12         2-9       43.8       98.6       1.48       5-9       32.9       120       1.02         2-20       32.9       110       0.928       5-10       43.8       131       1.98         3-1       43.8       142       2.14       6-1       43.8       142       2.14         3-2       65.7       186       6.31       6	1-9	43.8	76.7		4-9	43.8	110	1.65
2-2       32.9       175       1.48       5-2       54.8       219       5.16         2-3       43.8       98.6       1.48       5-3       32.9       164       1.39         2-4       43.8       110       1.65       5-4       54.8       208       4.90         2-5       43.8       87.6       1.32       5-5       32.9       153       1.30         2-6       32.9       76.7       0.650       5-6       43.8       98.6       1.48         2-7       43.8       120       1.81       5-7       54.8       186       4.38         2-8       32.9       87.6       0.742       5-8       54.8       175       4.12         2-9       43.8       98.6       1.48       5-9       32.9       120       1.02         2-20       32.9       110       0.928       5-10       43.8       131       1.98         3-1       43.8       142       2.14       6-1       43.8       142       2.14         3-2       65.7       186       6.31       6-2       43.8       153       2.31	1-10	43.8	120	1.81	4-10	54.8	219	5.16
2-3       43.8       98.6       1.48       5-3       32.9       164       1.39         2-4       43.8       110       1.65       5-4       54.8       208       4.90         2-5       43.8       87.6       1.32       5-5       32.9       153       1.30         2-6       32.9       76.7       0.650       5-6       43.8       98.6       1.48         2-7       43.8       120       1.81       5-7       54.8       186       4.38         2-8       32.9       87.6       0.742       5-8       54.8       175       4.12         2-9       43.8       98.6       1.48       5-9       32.9       120       1.02         2-20       32.9       110       0.928       5-10       43.8       131       1.98         3-1       43.8       142       2.14       6-1       43.8       142       2.14         3-2       65.7       186       6.31       6-2       43.8       153       2.31	2-1	54.8	120	2.84	5-1	43.8	208	3.13
2-4       43.8       110       1.65       5-4       54.8       208       4.90         2-5       43.8       87.6       1.32       5-5       32.9       153       1.30         2-6       32.9       76.7       0.650       5-6       43.8       98.6       1.48         2-7       43.8       120       1.81       5-7       54.8       186       4.38         2-8       32.9       87.6       0.742       5-8       54.8       175       4.12         2-9       43.8       98.6       1.48       5-9       32.9       120       1.02         2-20       32.9       110       0.928       5-10       43.8       131       1.98         3-1       43.8       142       2.14       6-1       43.8       142       2.14         3-2       65.7       186       6.31       6-2       43.8       153       2.31	2-2	32.9	175	1.48	5-2	54.8	219	5.16
2-5       43.8       87.6       1.32       5-5       32.9       153       1.30         2-6       32.9       76.7       0.650       5-6       43.8       98.6       1.48         2-7       43.8       120       1.81       5-7       54.8       186       4.38         2-8       32.9       87.6       0.742       5-8       54.8       175       4.12         2-9       43.8       98.6       1.48       5-9       32.9       120       1.02         2-20       32.9       110       0.928       5-10       43.8       131       1.98         3-1       43.8       142       2.14       6-1       43.8       142       2.14         3-2       65.7       186       6.31       6-2       43.8       153       2.31	2-3	43.8	98.6	1.48	5-3	32.9	164	1.39
2-6     32.9     76.7     0.650     5-6     43.8     98.6     1.48       2-7     43.8     120     1.81     5-7     54.8     186     4.38       2-8     32.9     87.6     0.742     5-8     54.8     175     4.12       2-9     43.8     98.6     1.48     5-9     32.9     120     1.02       2-20     32.9     110     0.928     5-10     43.8     131     1.98       3-1     43.8     142     2.14     6-1     43.8     142     2.14       3-2     65.7     186     6.31     6-2     43.8     153     2.31	2-4	43.8	110	1.65	5-4	54.8	208	4.90
2-7     43.8     120     1.81     5-7     54.8     186     4.38       2-8     32.9     87.6     0.742     5-8     54.8     175     4.12       2-9     43.8     98.6     1.48     5-9     32.9     120     1.02       2-20     32.9     110     0.928     5-10     43.8     131     1.98       3-1     43.8     142     2.14     6-1     43.8     142     2.14       3-2     65.7     186     6.31     6-2     43.8     153     2.31	2-5	43.8	87.6	1.32	5-5	32.9	153	1.30
2-8     32.9     87.6     0.742     5-8     54.8     175     4.12       2-9     43.8     98.6     1.48     5-9     32.9     120     1.02       2-20     32.9     110     0.928     5-10     43.8     131     1.98       3-1     43.8     142     2.14     6-1     43.8     142     2.14       3-2     65.7     186     6.31     6-2     43.8     153     2.31	2-6	32.9	76.7	0.650	5-6	43.8	98.6	1.48
2-9     43.8     98.6     1.48     5-9     32.9     120     1.02       2-20     32.9     110     0.928     5-10     43.8     131     1.98       3-1     43.8     142     2.14     6-1     43.8     142     2.14       3-2     65.7     186     6.31     6-2     43.8     153     2.31	2-7	43.8	120	1.81	5-7	54.8	186	4.38
2-20     32.9     110     0.928     5-10     43.8     131     1.98       3-1     43.8     142     2.14     6-1     43.8     142     2.14       3-2     65.7     186     6.31     6-2     43.8     153     2.31	2-8	32.9	87.6	0.742	5-8	54.8	175	4.12
3-1 43.8 142 2.14 6-1 43.8 142 2.14 3-2 65.7 186 6.31 6-2 43.8 153 2.31	2-9	43.8	98.6	1.48	5-9	32.9	120	1.02
3-2 65.7 186 6.31 6-2 43.8 153 2.31	2-20	32.9	110	0.928	5-10	43.8	131	1.98
i i i i i i i i i i i i i i i i i i i	3-1	43.8	142	2.14	6-1	43.8	142	2.14
3-3 43.8 131 1.98 6-3 54.8 142 3.35	3-2	65.7	186	6.31	6-2	43.8	153	2.31
	3-3	43.8	131	1.98	6-3	54.8	142	3.35
3-4 43.8 87.6 1.32 6-4 65.7 186 6.31	3-4	43.8	87.6	1.32	6-4	65.7	186	6.31
3-5 43.8 98.6 1.48 6-5 32.9 98.6 0.835	3-5	43.8	98.6	1.48	6-5	32.9	98.6	0.835
3-6 43.8 131 1.98 6-6 43.8 131 1.98	3-6			1.98	6-6	43.8	131	1.98
3-7 43.8 87.6 1.32 6-7 43.8 153 2.31				1.32				
3-8 32.9 76.7 0.650 6-8 43.8 110 1.65								
3-9 54.8 175 4.12 6-9 54.8 197 4.64								
3-10 43.8 131 1.98 6-10 32.9 110 0.928				1				

Average fecal pellet volume:  $2.26 \times 10^5 \mu m^3$ 

Appendix E. Spectroscopic Data for Apo-fucoxanthinoids

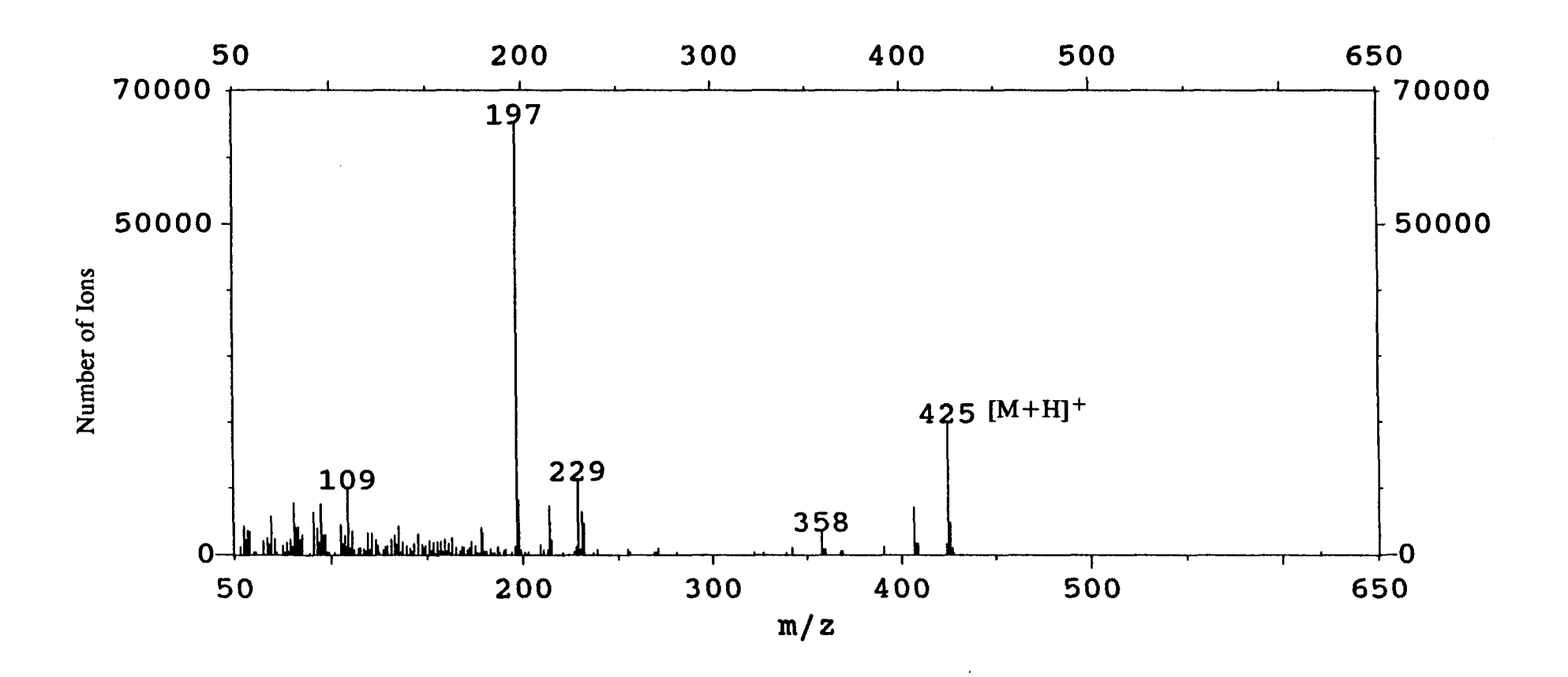


Fig. E1. Low resolution DCI mass spectrum of natural apo-10'-fucoxanthinal (1) using NH3 as the reagent gas.

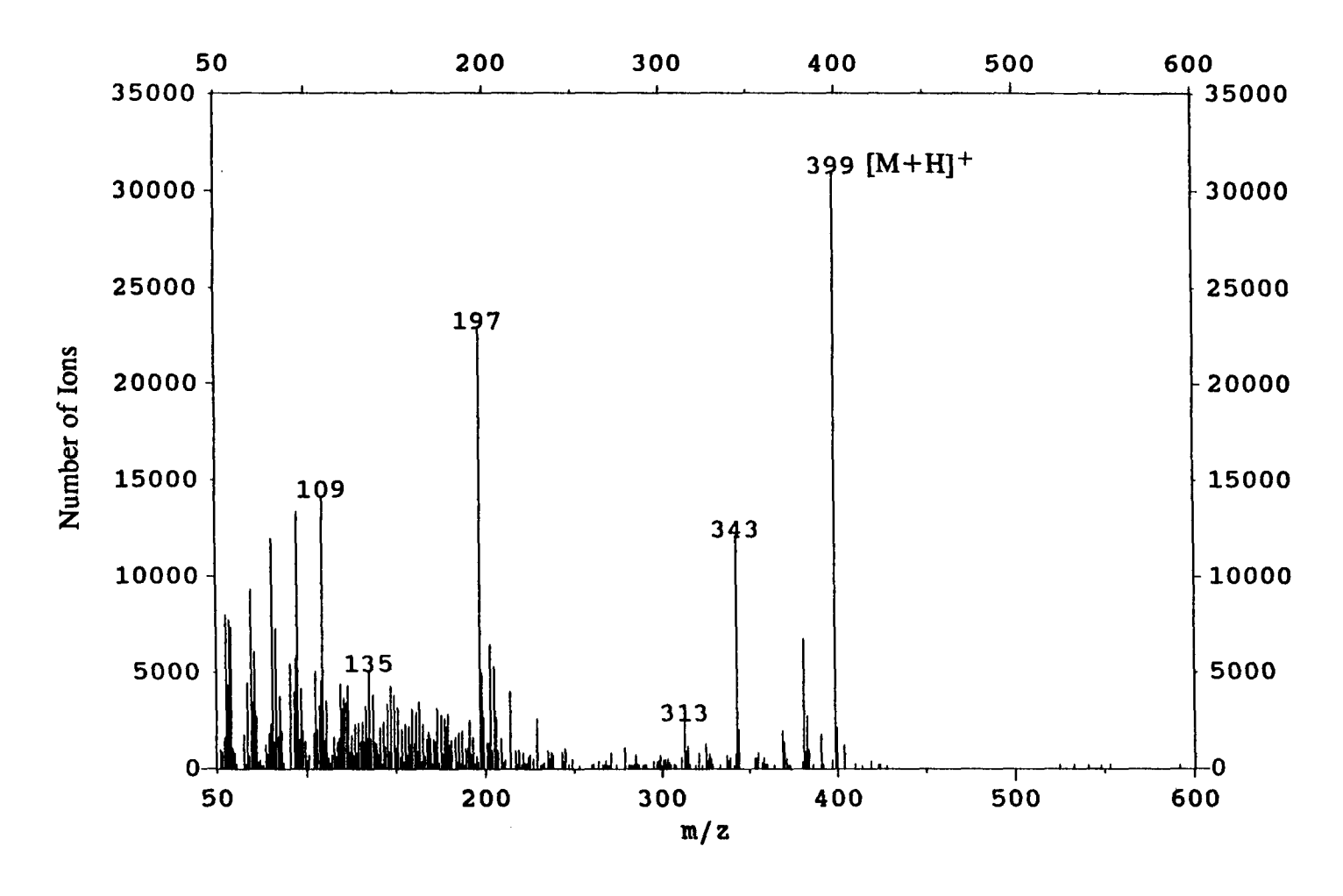


Fig. E2. Low resolution DCI mass spectrum of natural apo-12'-fucoxanthinal (2) using NH<sub>3</sub> as the reagent gas.

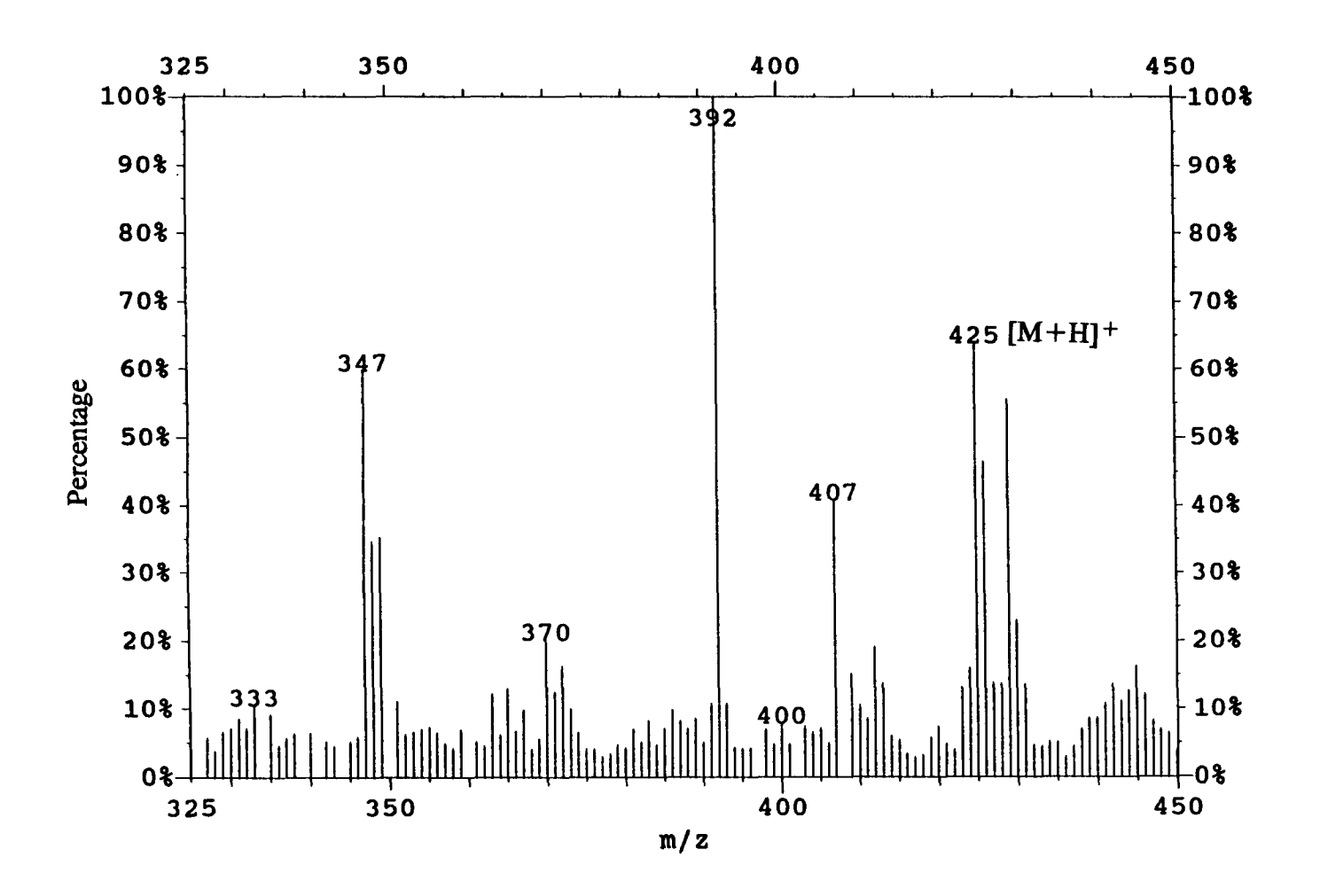


Fig. E3. Low resolution DCI mass spectrum of natural apo-12-fucoxanthinal (3) using NH3 as the reagent gas.

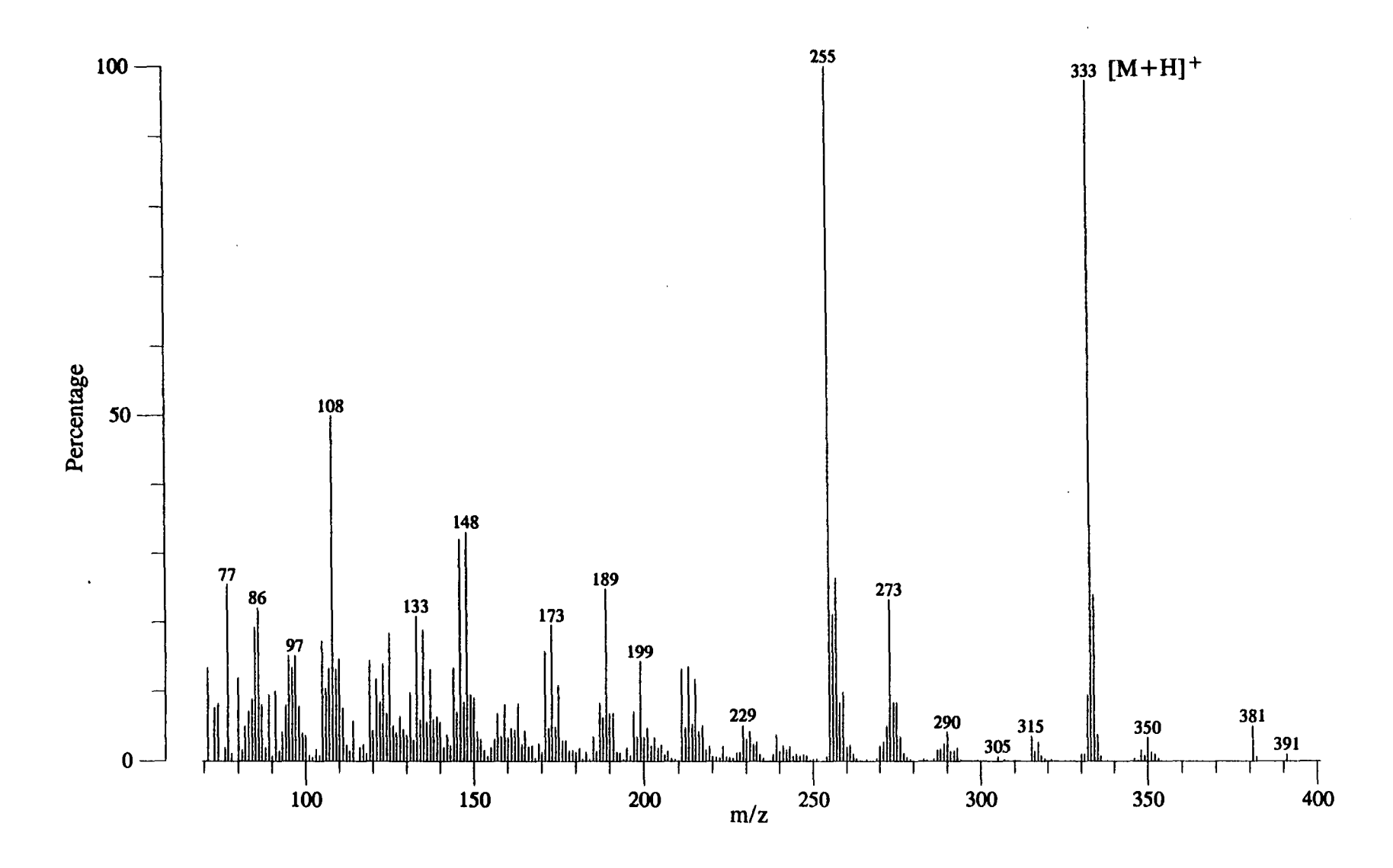


Fig. E4. Low resolution DCI mass spectrum of natural apo-13'-fucoxanthinone (4) using NH<sub>3</sub> as the reagent gas.



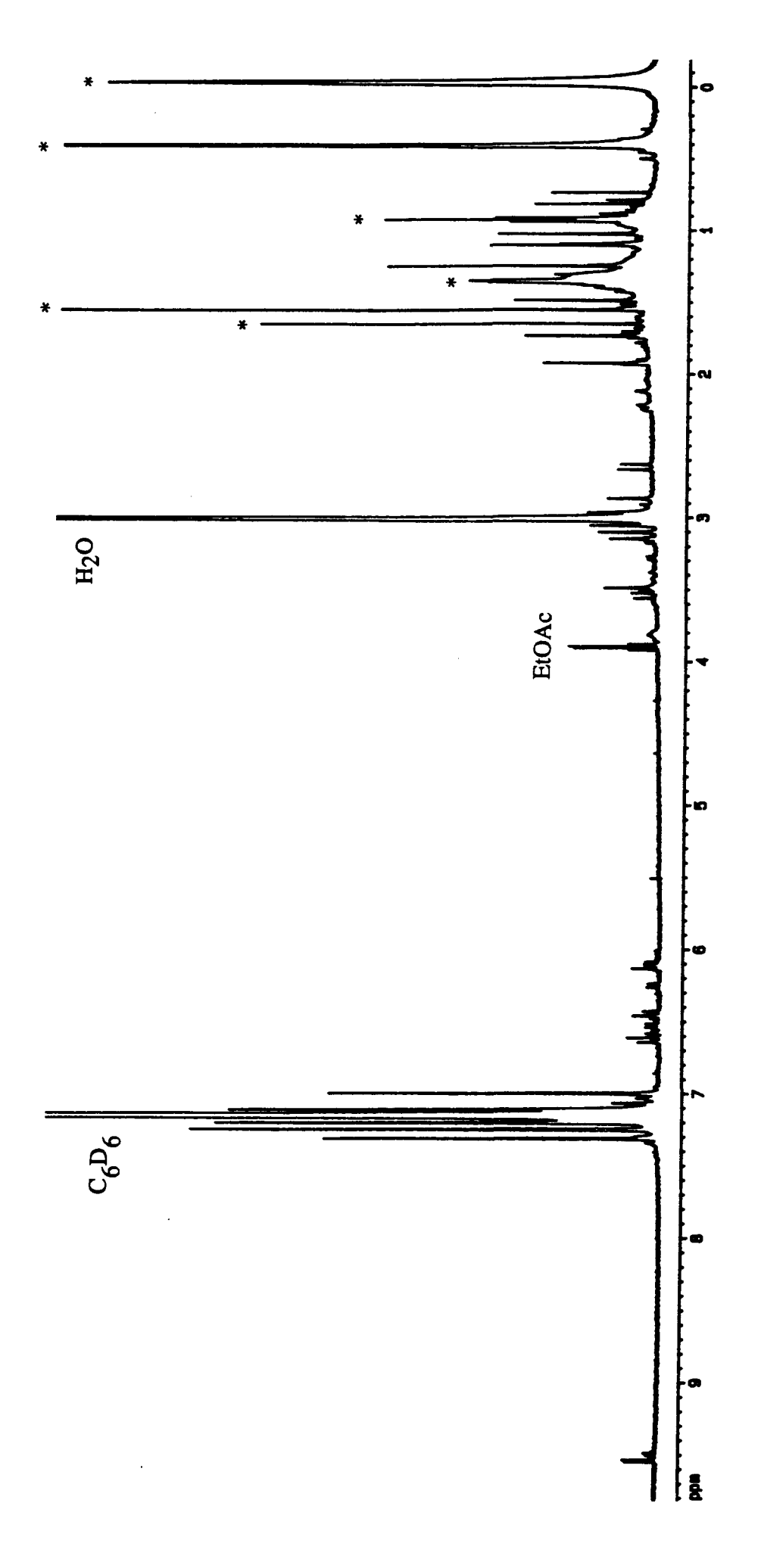


Fig. E5. Proton nmr (500 MHz) spectrum of natural apo-10'-fucoxanthinal (1) in C<sub>6</sub>D<sub>6</sub>. \* denotes impurities, probably grease or fatty acids.

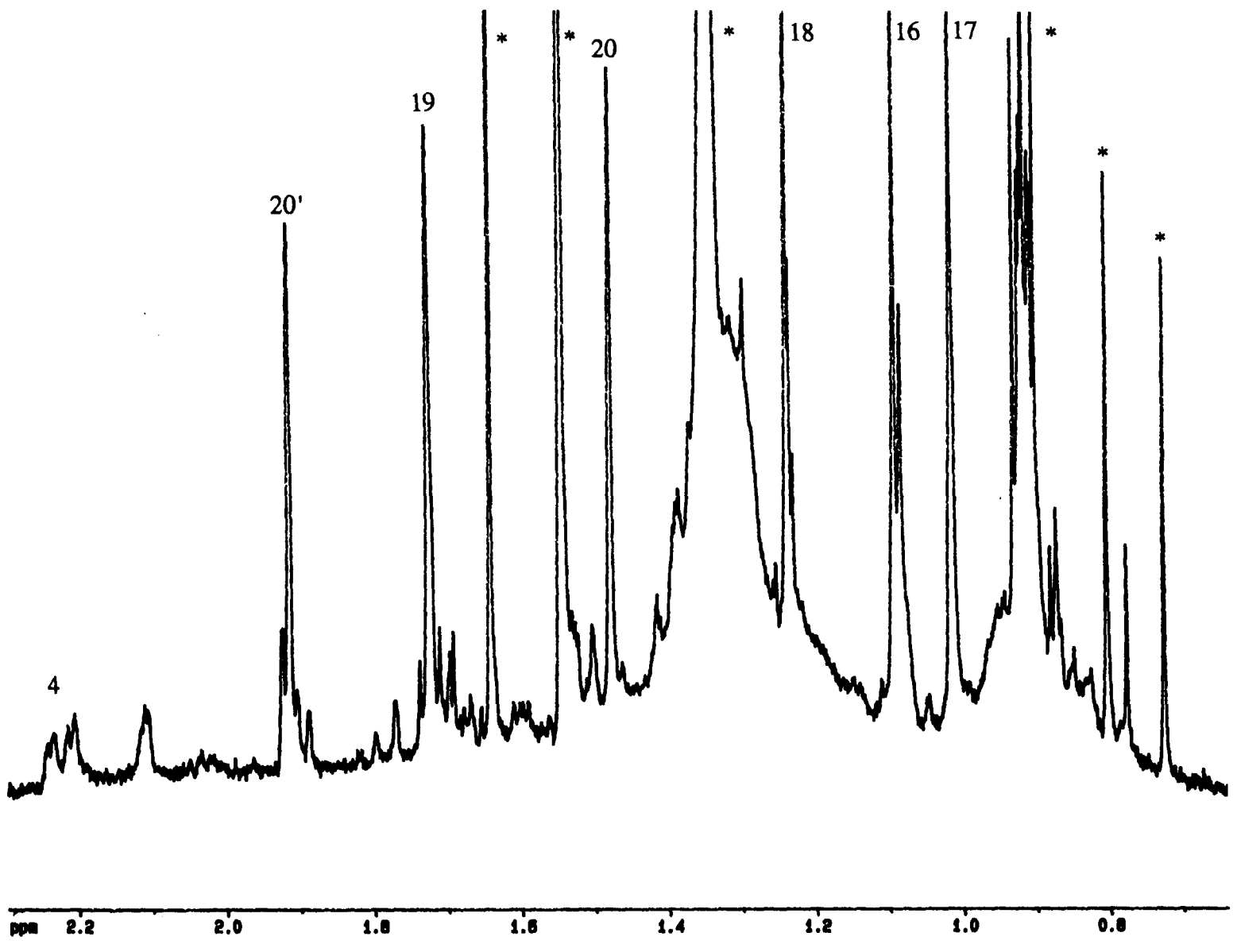


Fig. E6. Expansion of the proton nmr (500 MHz) spectrum of natural apo-10'-fucoxanthinal (1) in C<sub>6</sub>D<sub>6</sub>showing resonances from the methyl groups. \* denotes impurities, probably grease or fatty acids.

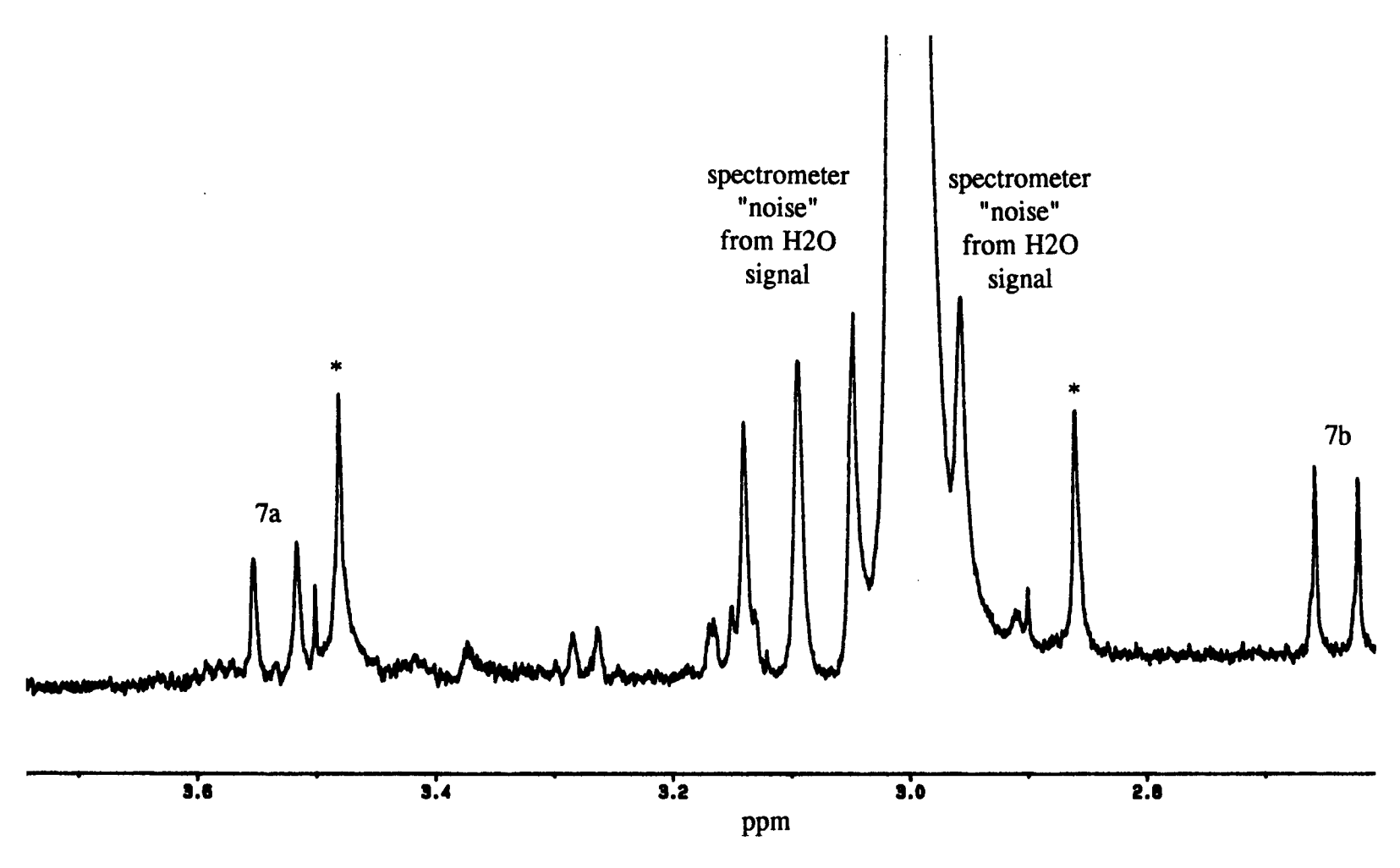
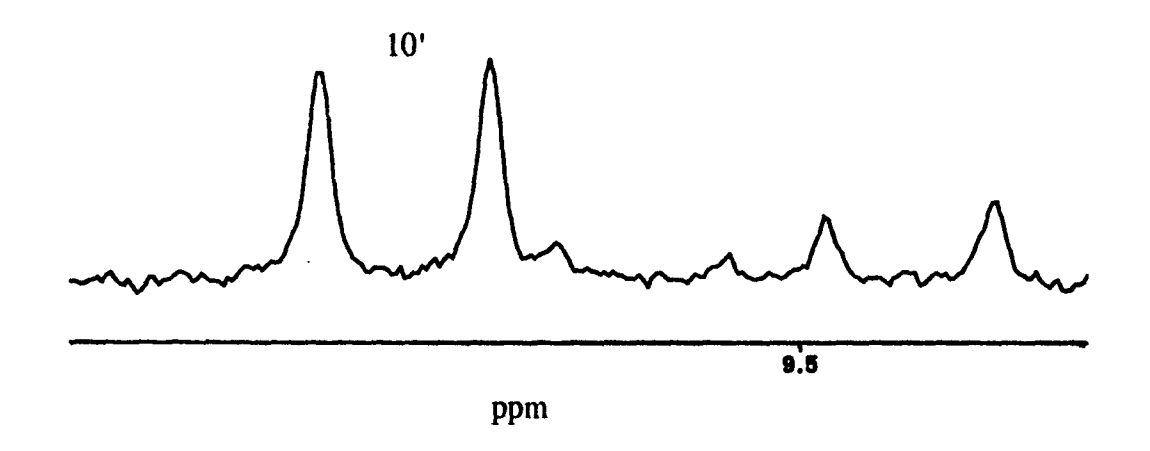


Fig. E7. Expansion of the proton nmr (500 MHz) spectrum of natural apo-10'-fucoxanthinal (1) in C<sub>6</sub>D<sub>6</sub> showing methylene protons at position 7. \* denotes minor impurities.



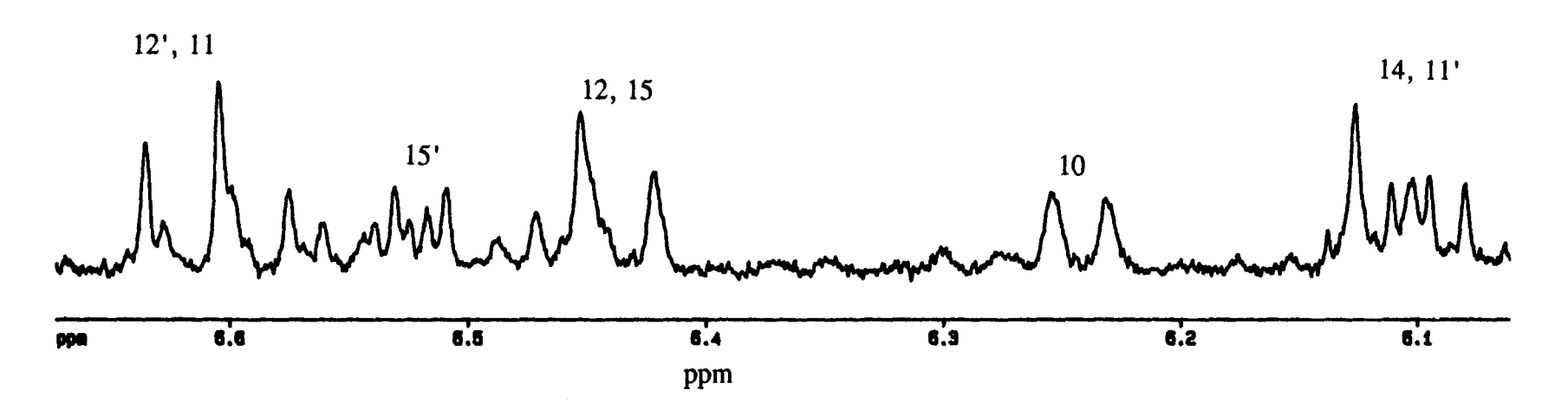


Fig. E8. Expansion of the proton nmr (500 MHz) spectrum of natural apo-10'-fucoxanthinal (1) in C<sub>6</sub>D<sub>6</sub> showing the olefinic protons and the aldehyde proton.

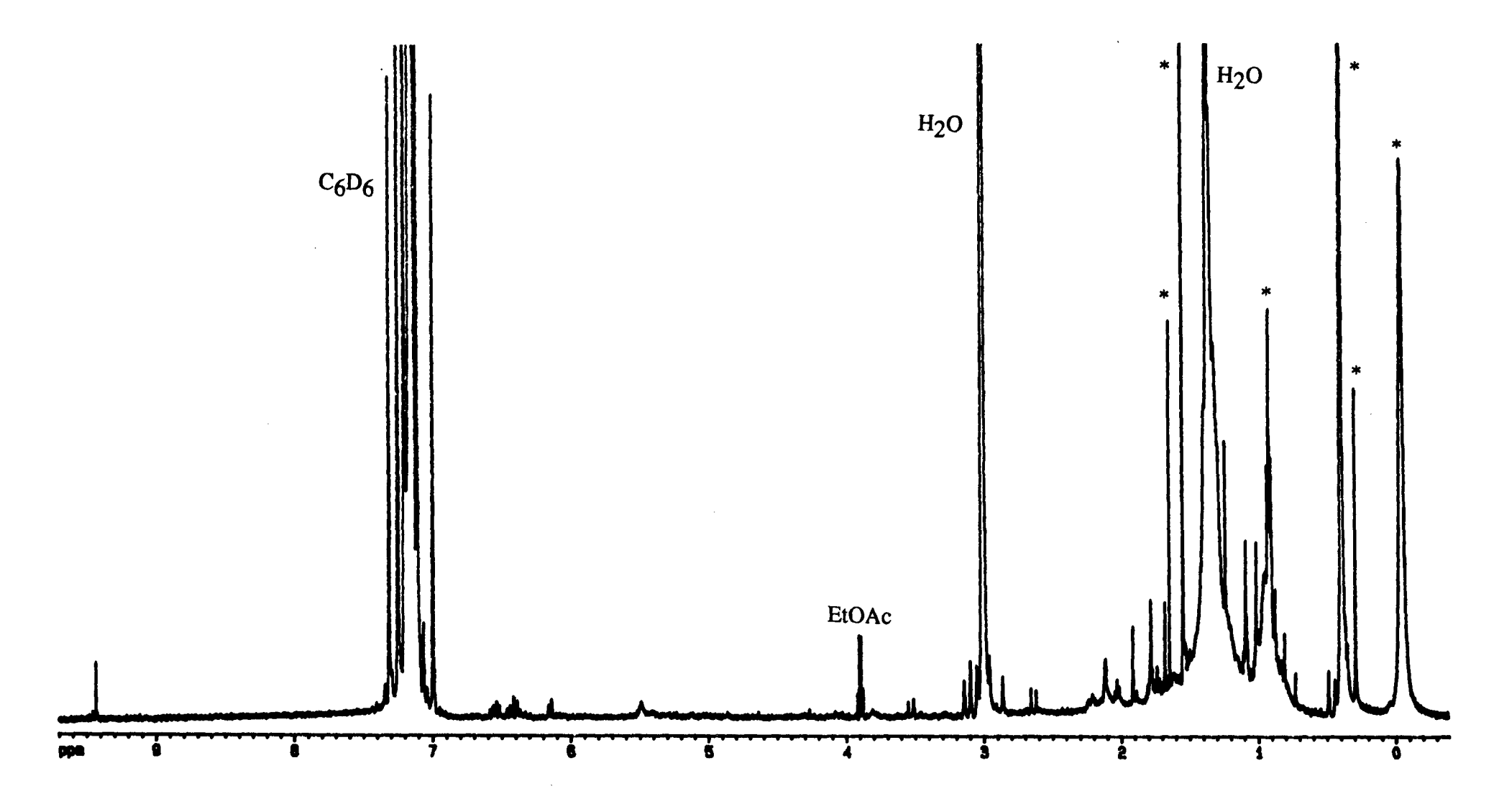


Fig. E9. Proton nmr (500 MHz) spectrum of natural apo-12'-fucoxanthinal (2) in C<sub>6</sub>D<sub>6</sub>. \* denotes impurities, probably grease or fatty acids.

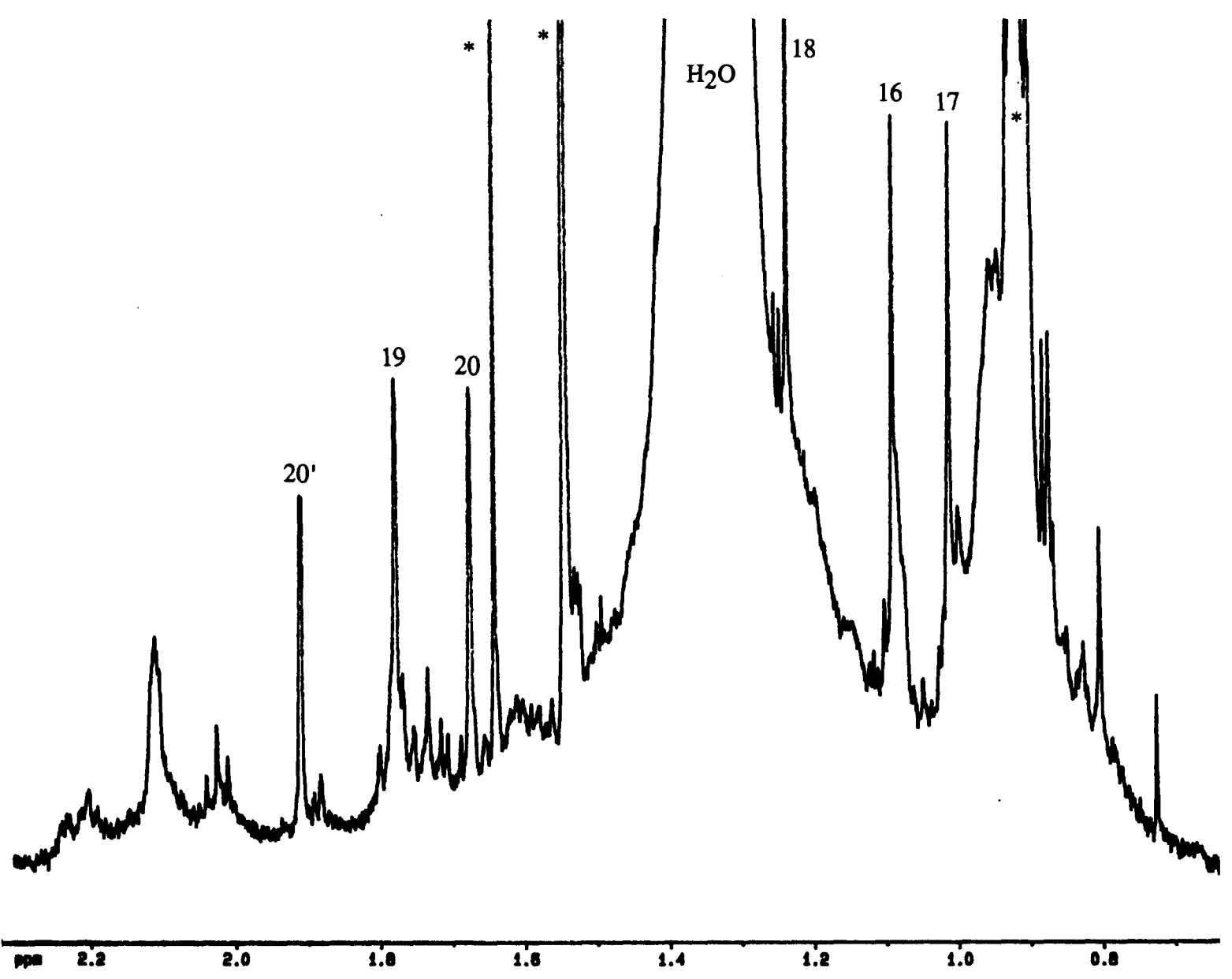


Fig. E10. Expansion of the proton nmr (500 MHz) spectrum of natural apo-12'-fucoxanthinal (2) in C<sub>6</sub>D<sub>6</sub> showing resonances from the methyl groups. \* denotes impurities, probably grease or fatty acids.

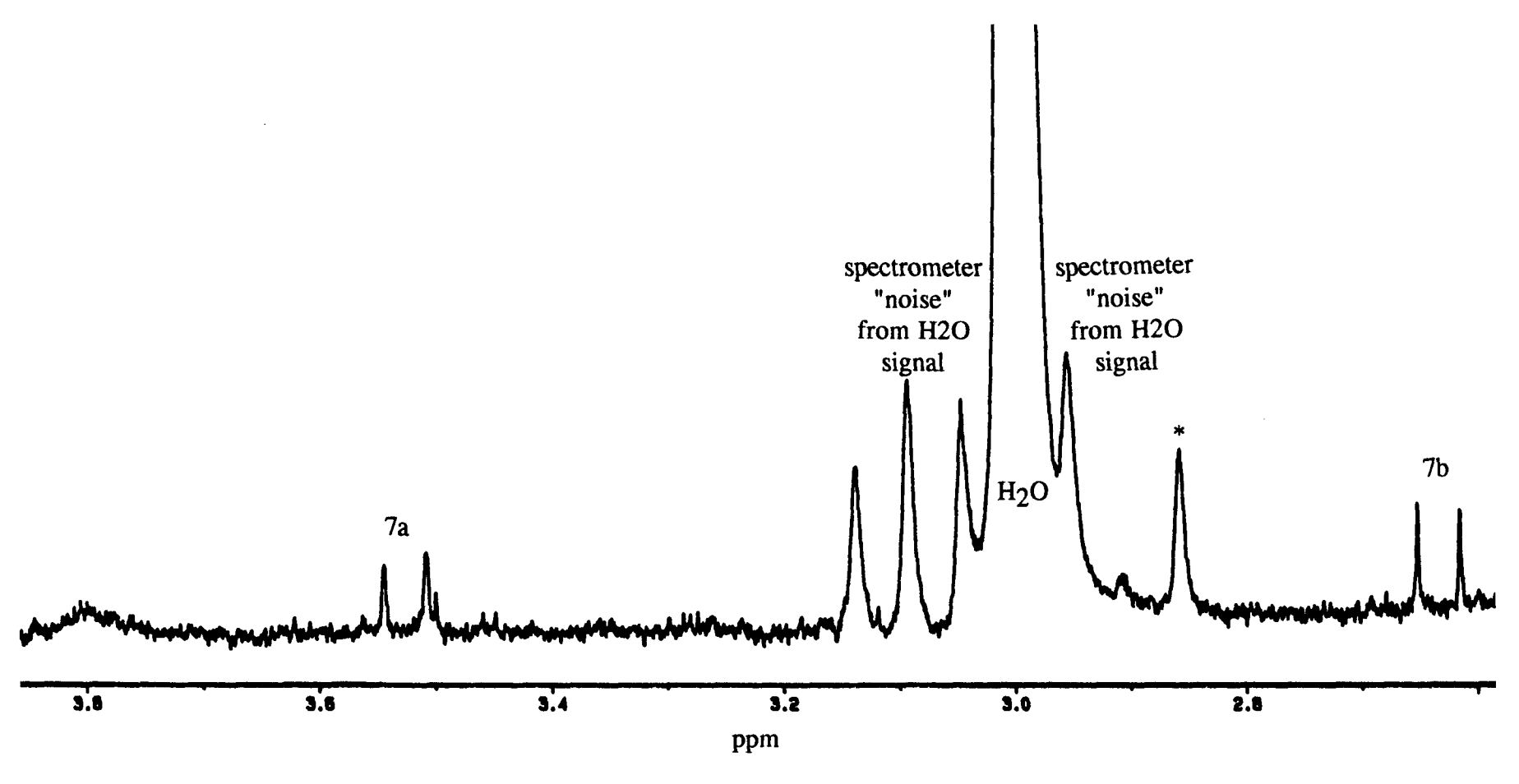
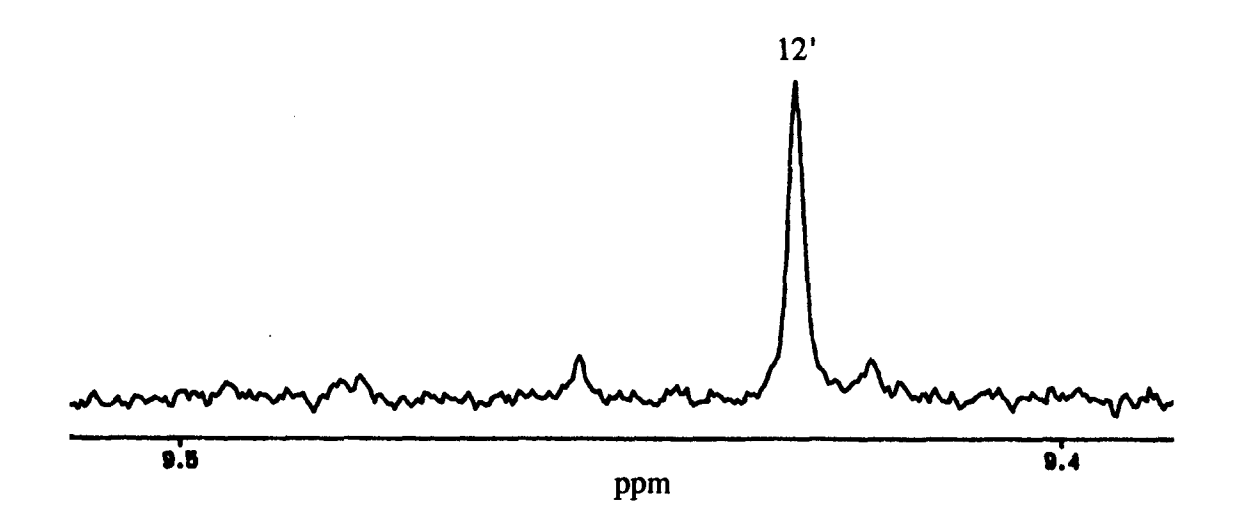


Fig. E11. Expansion of the proton nmr (500 MHz) spectrum of natural apo-12'-fucoxanthinal (2) in C<sub>6</sub>D<sub>6</sub> showing the methylene protons as position 7. \* denotes impurities.



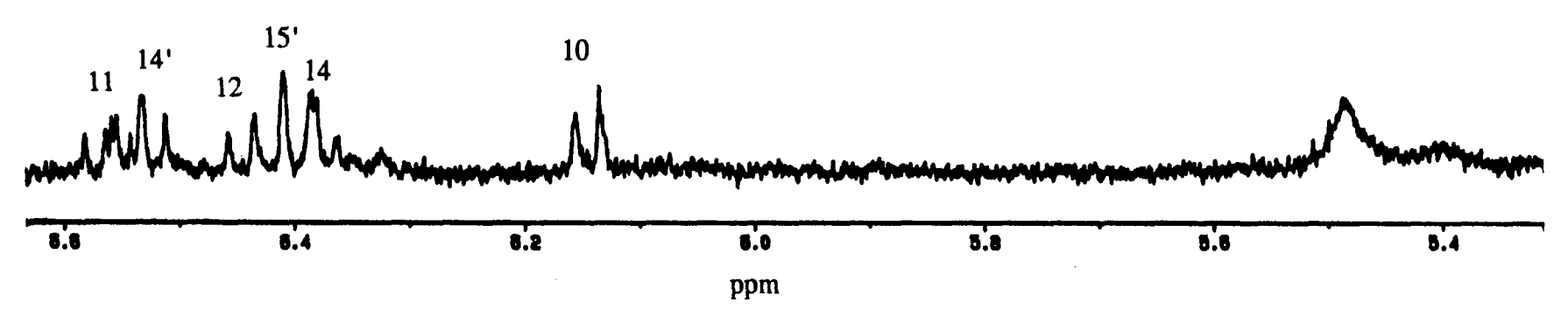


Fig. E12. Expansion of the proton nmr (500 MHz) spectrum of natural apo-12'-fucoxanthinal (2) in C<sub>6</sub>D<sub>6</sub> showing the olefinic protons and the aldehyde proton.

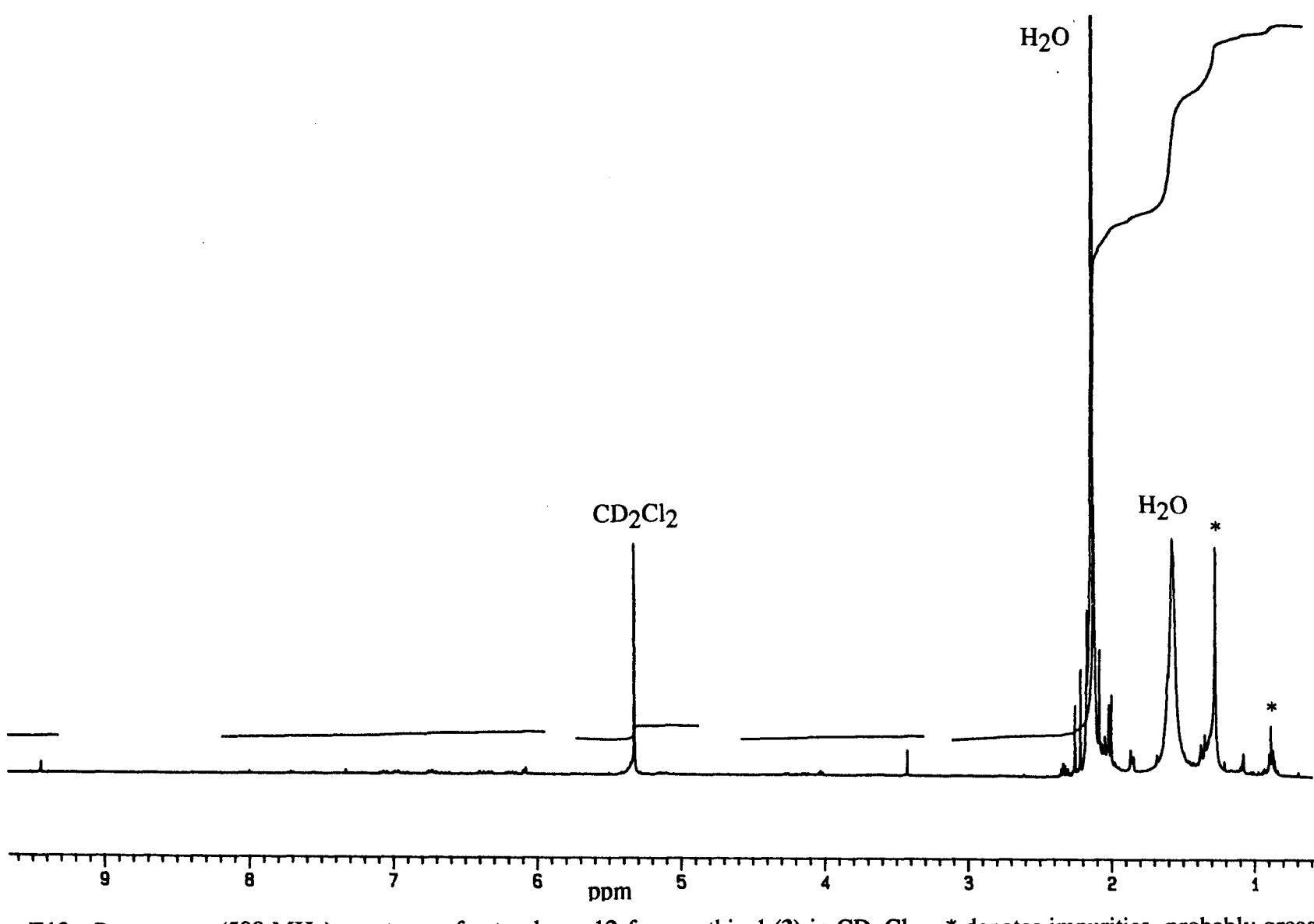


Fig. E13. Proton nmr (500 MHz) spectrum of natural apo-12-fucoxanthinal (3) in CD<sub>2</sub>Cl<sub>2</sub>. \* denotes impurities, probably grease or fatty acids.

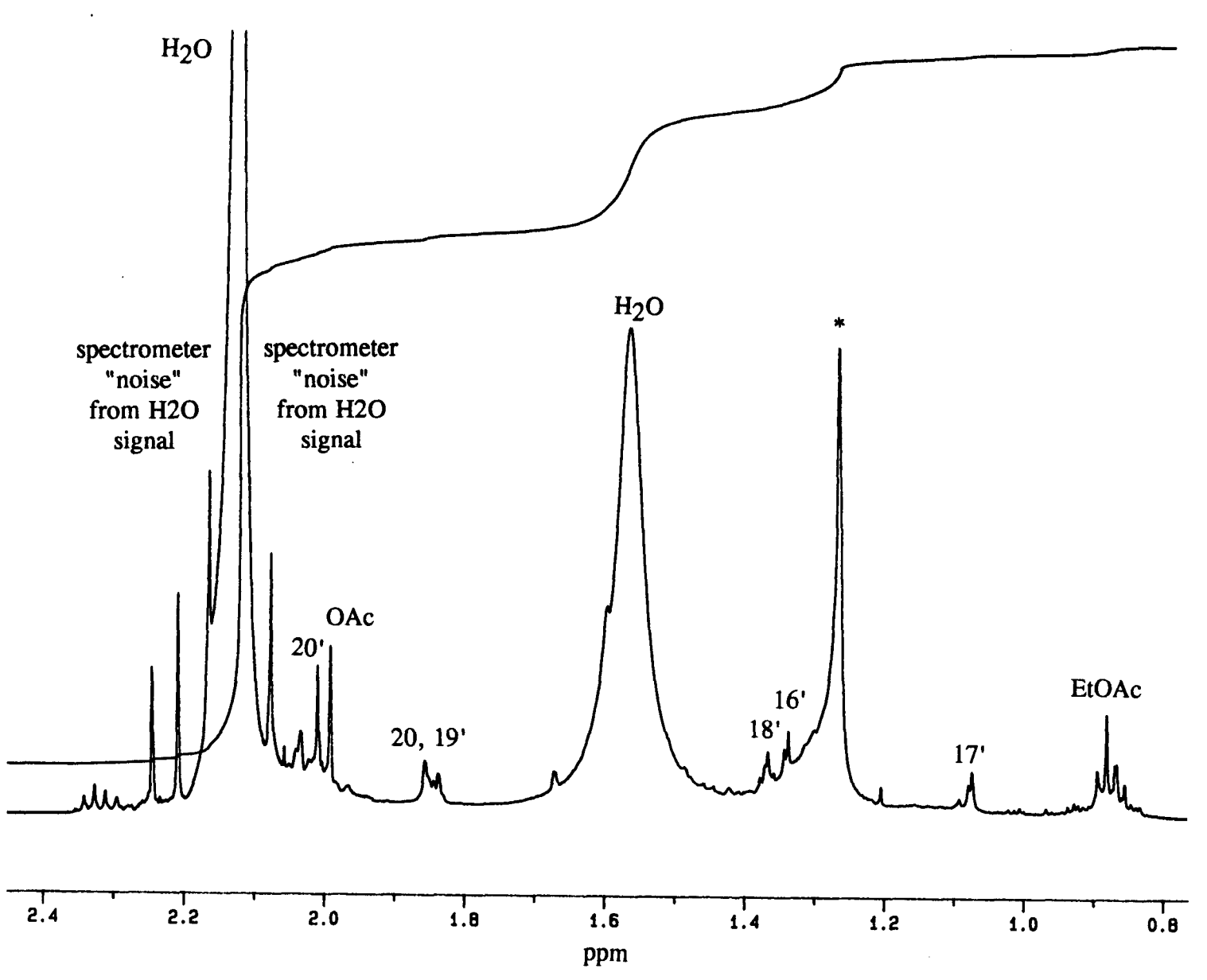


Fig. E14. Expansion of the proton nmr (500 MHz) spectrum of natural apo-12-fucoxanthinal (3) in CD<sub>2</sub>Cl<sub>2</sub> showing resonances from the methyl groups. \* denotes minor impurities, probably grease or fatty acids.

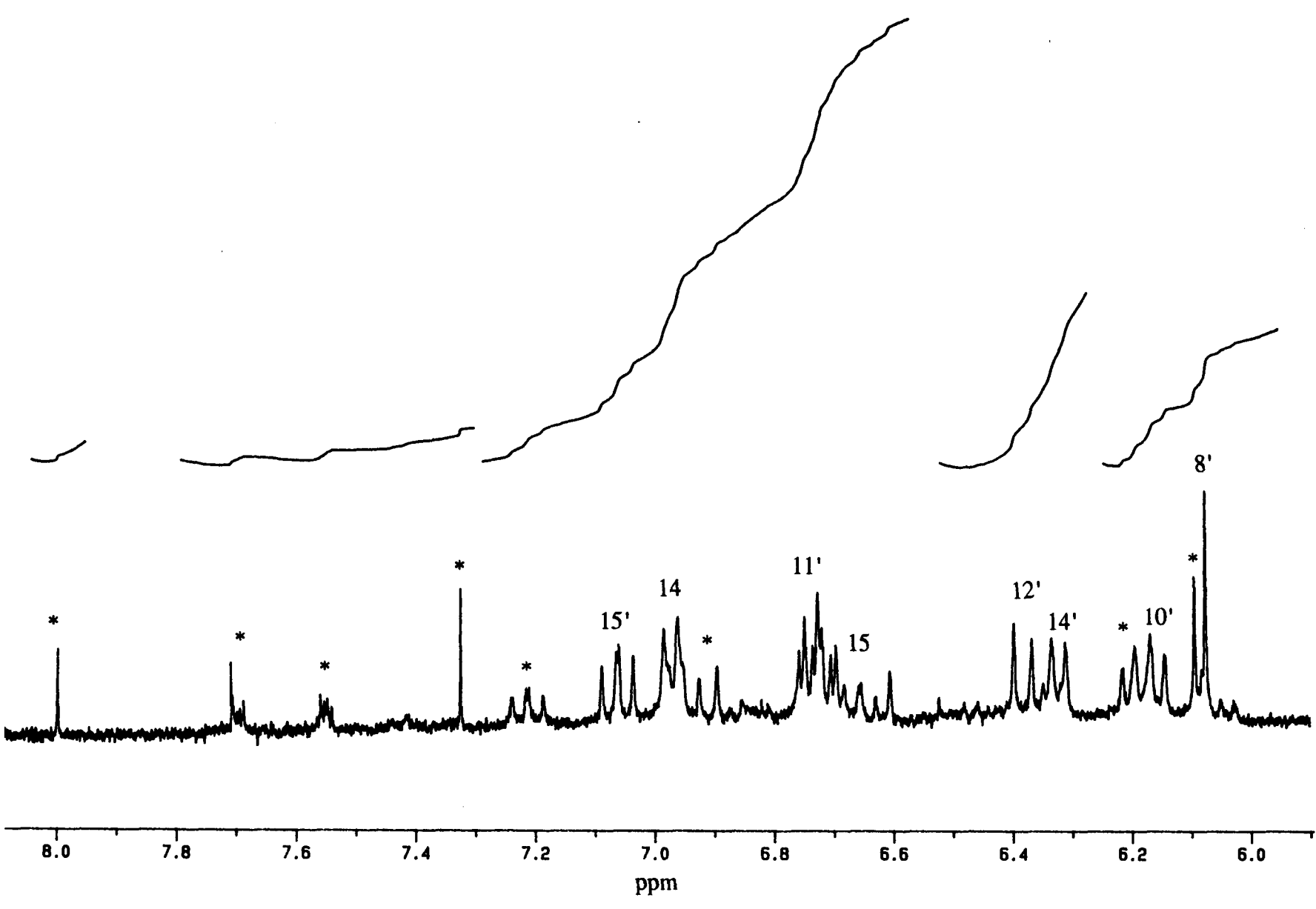


Fig. E15. Expansion of the proton nmr (500 MHz) spectrum of natural apo-12-fucoxanthinal (3) in CD<sub>2</sub>Cl<sub>2</sub> showing olefinic protons. \* denotes impurities (mostly cis-trans isomers of compound (3)).

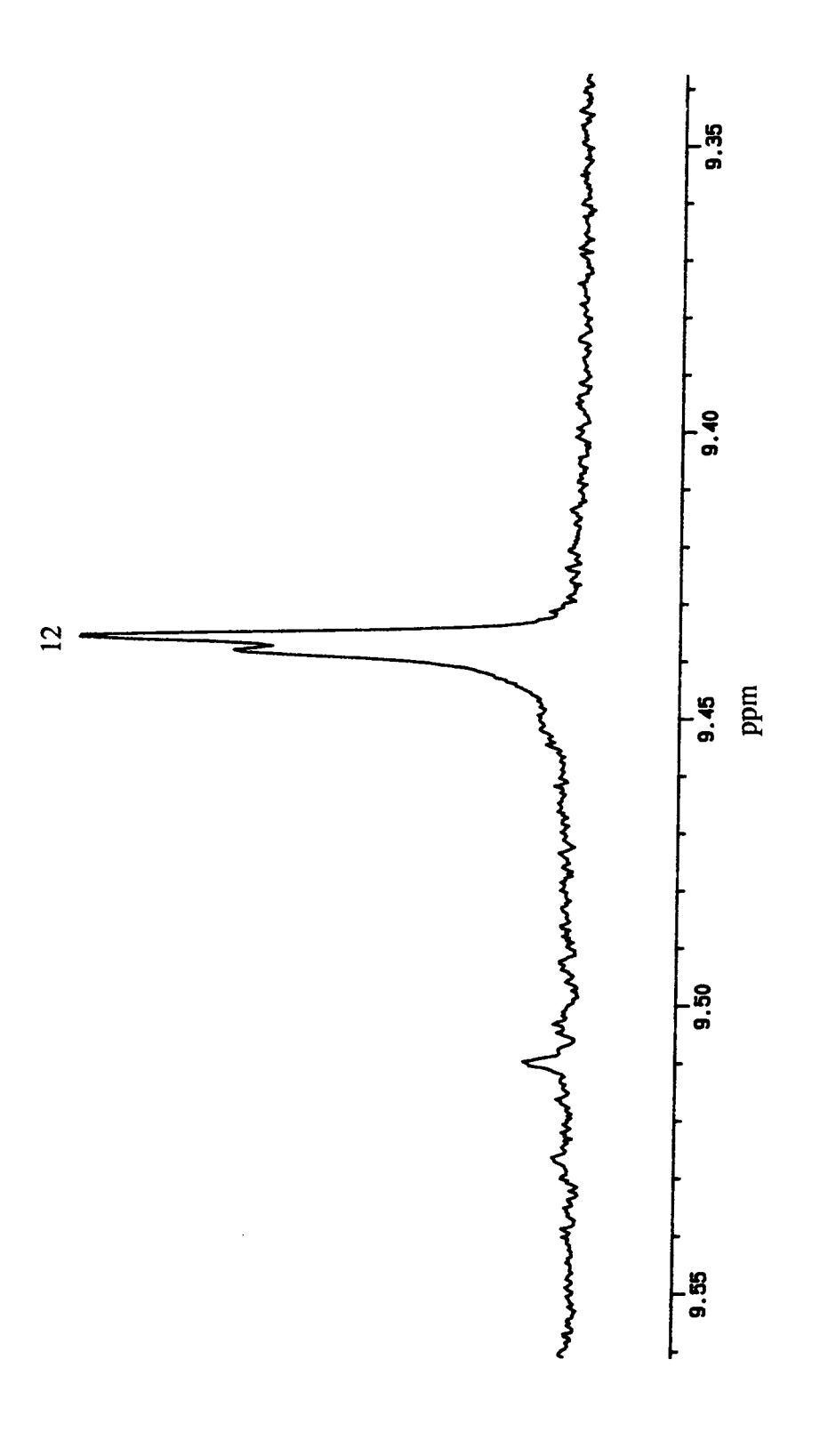


Fig. E16. Expansion of the proton nmr (500 MHz) spectrum of natural apo-12-fucoxanthinal (3) in CD<sub>2</sub>Cl<sub>2</sub> showing the aldehyde proton.

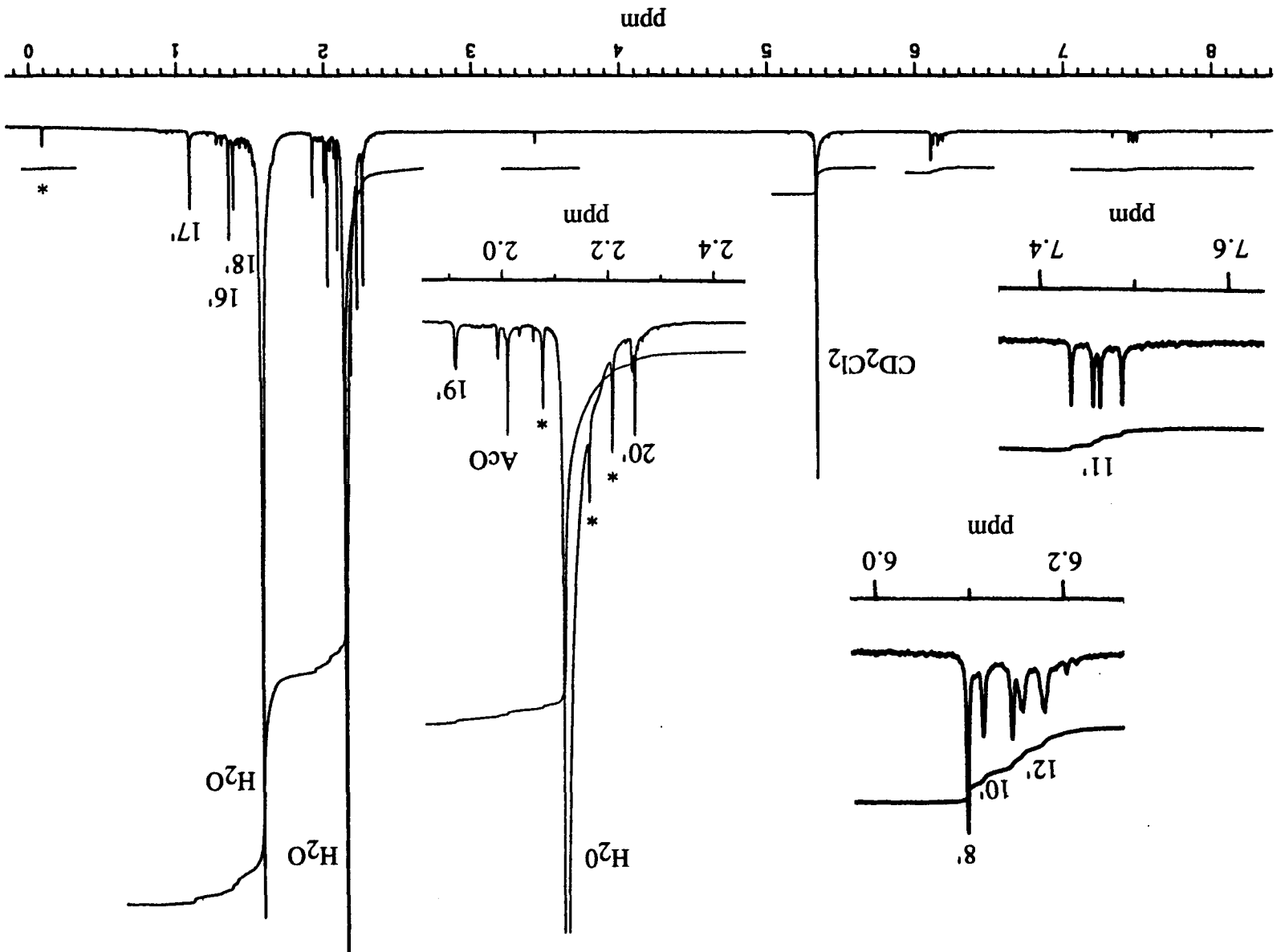


Fig. E17. Proton nmr (500 MHz) spectrum of natural apo-13'-fucoxanthinone (4) in CD<sub>2</sub>Cl<sub>2</sub>. \* denotes impurities, probably grease or fatty acids.

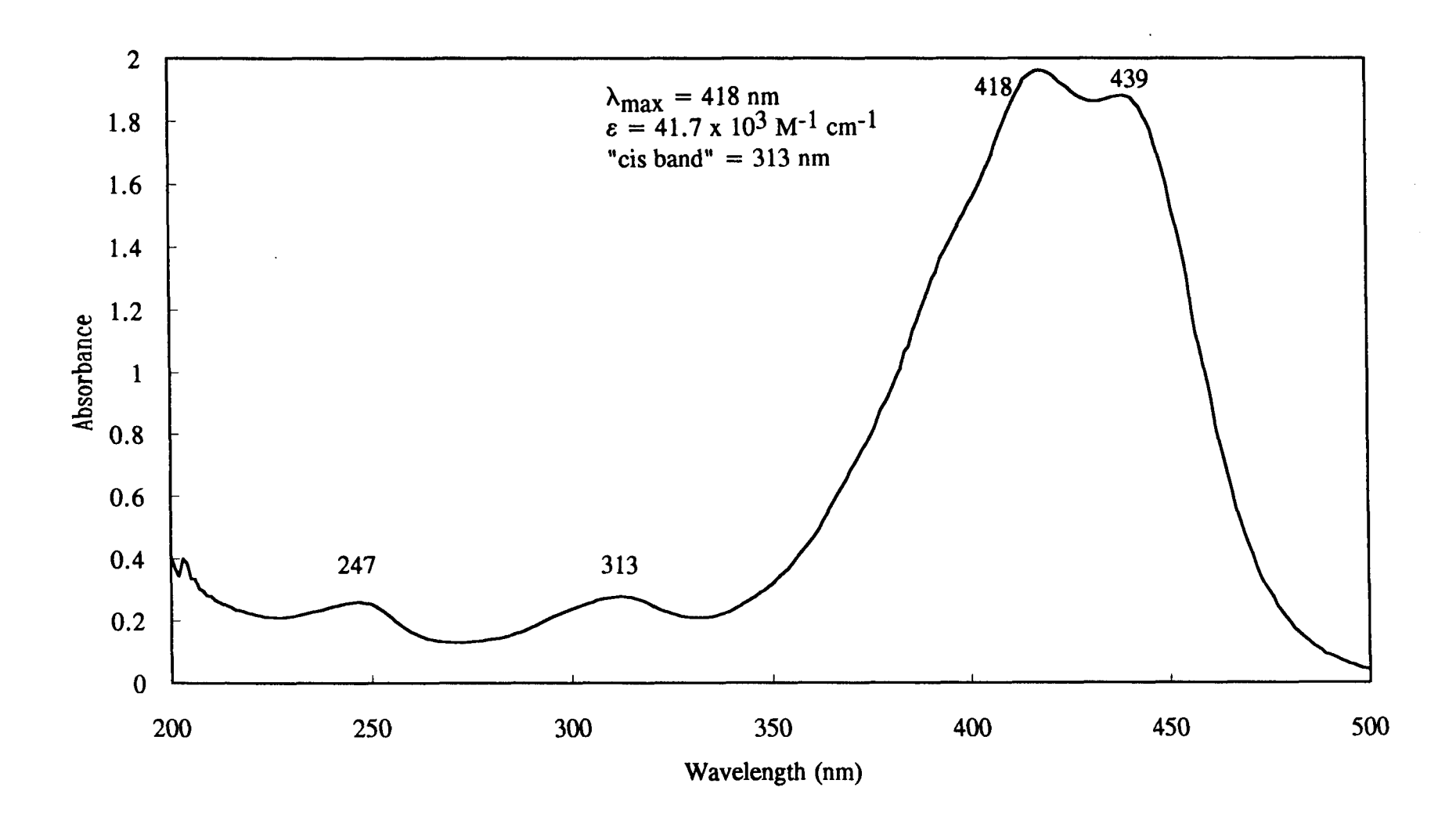


Fig. E18. Ultraviolet-visible spectrum of semi-synthetic apo-10'-fucoxanthinal (1) in methanol.

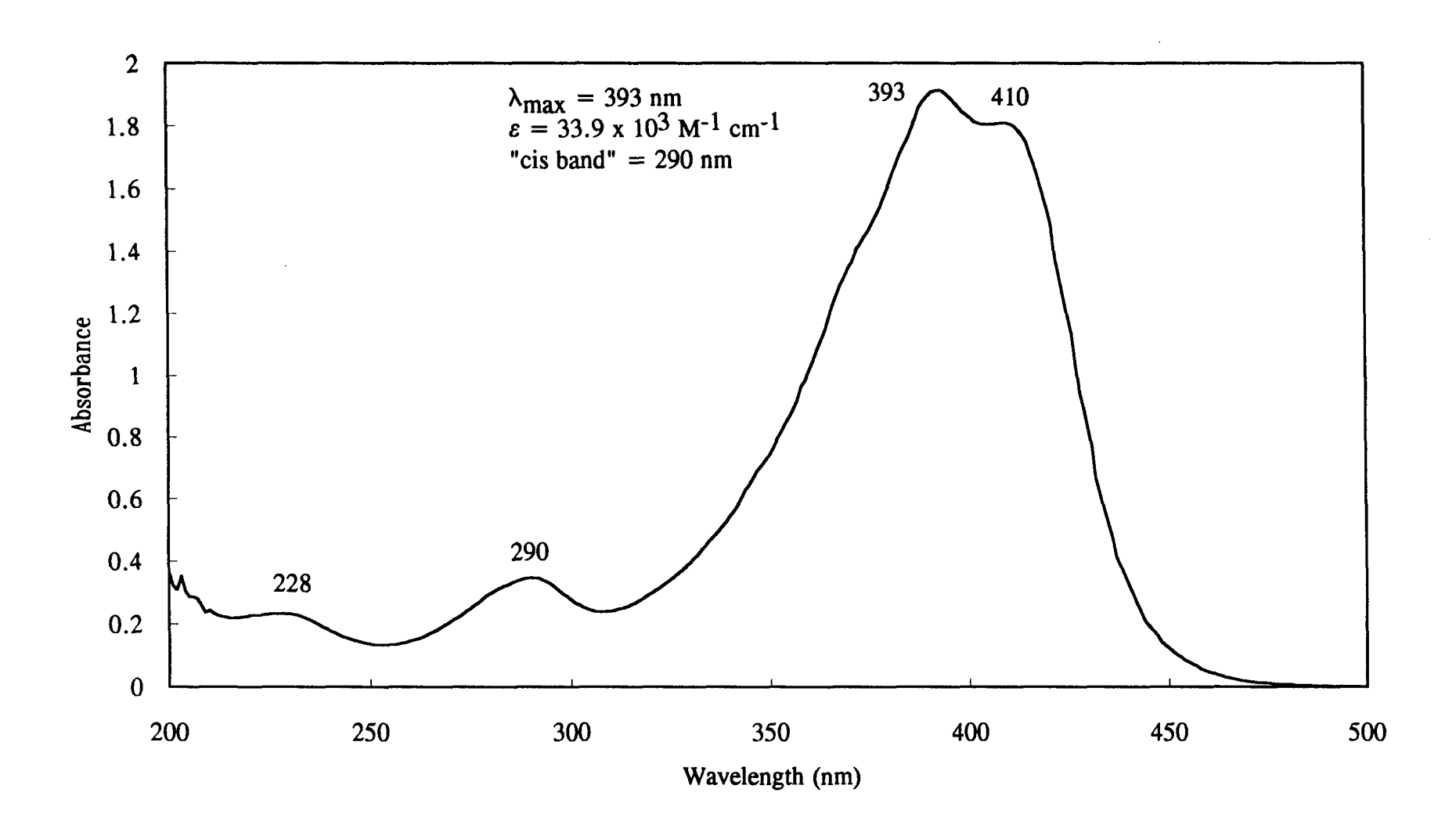


Fig. E19. Ultraviolet-visible spectrum of semi-synthetic apo-12'-fucoxanthinal (2) in methanol.

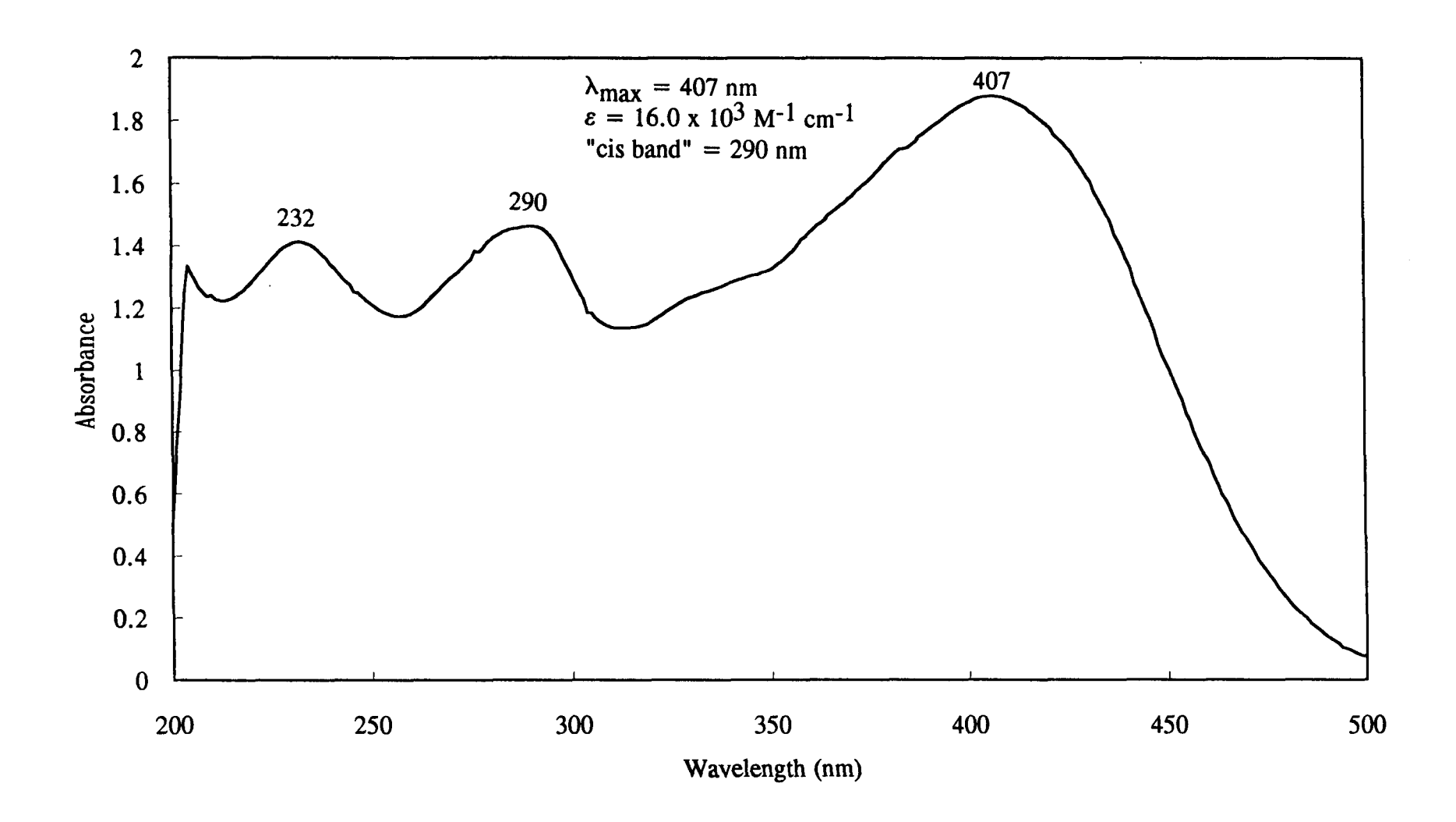


Fig. E20. Ultraviolet-visible spectrum of semi-synthetic apo-12-fucoxanthinal (3) in methanol.

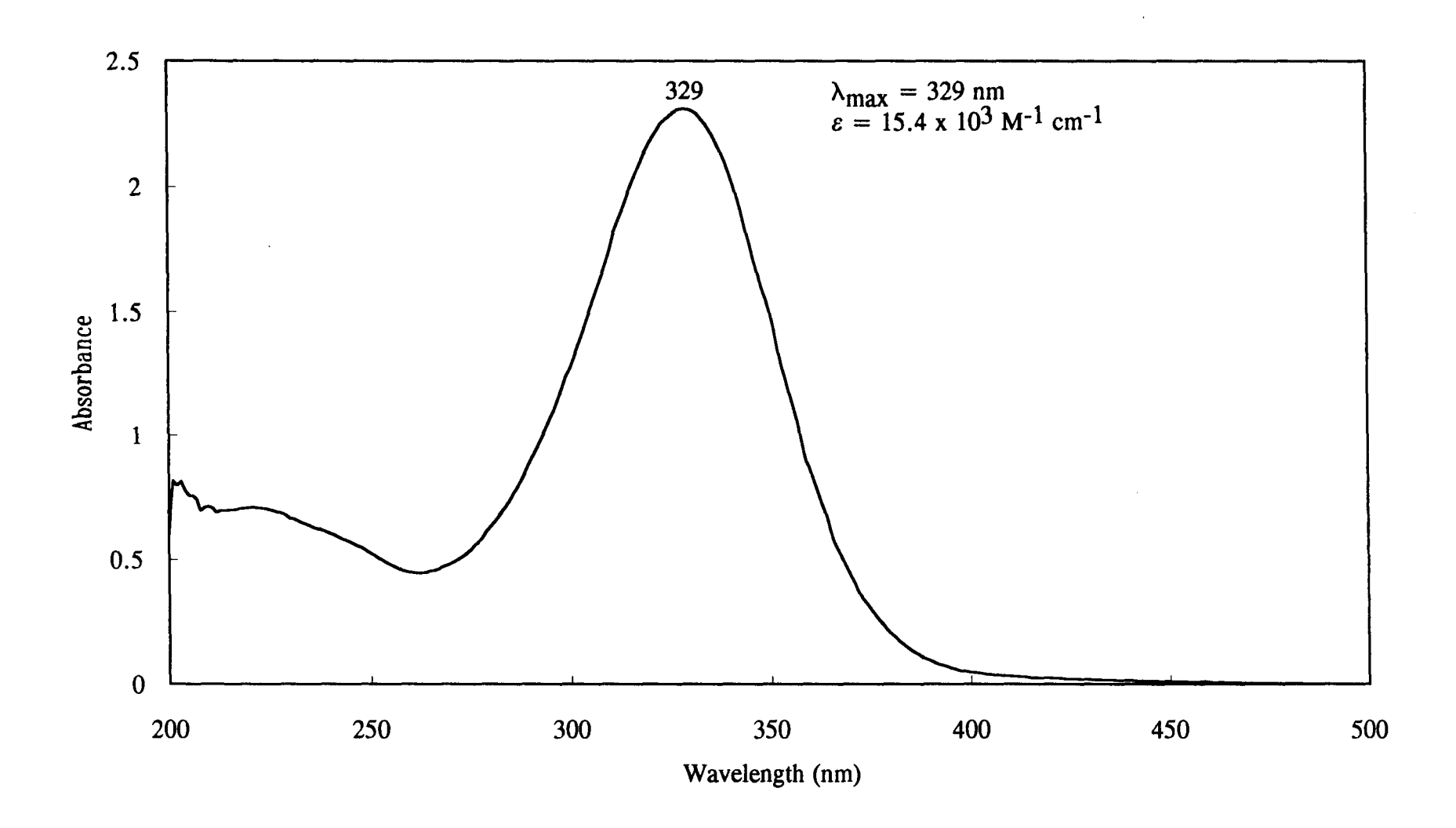


Fig. E21. Ultraviolet-visible spectrum of semi-synthetic apo-13'-fucoxanthinone (4) in methanol.

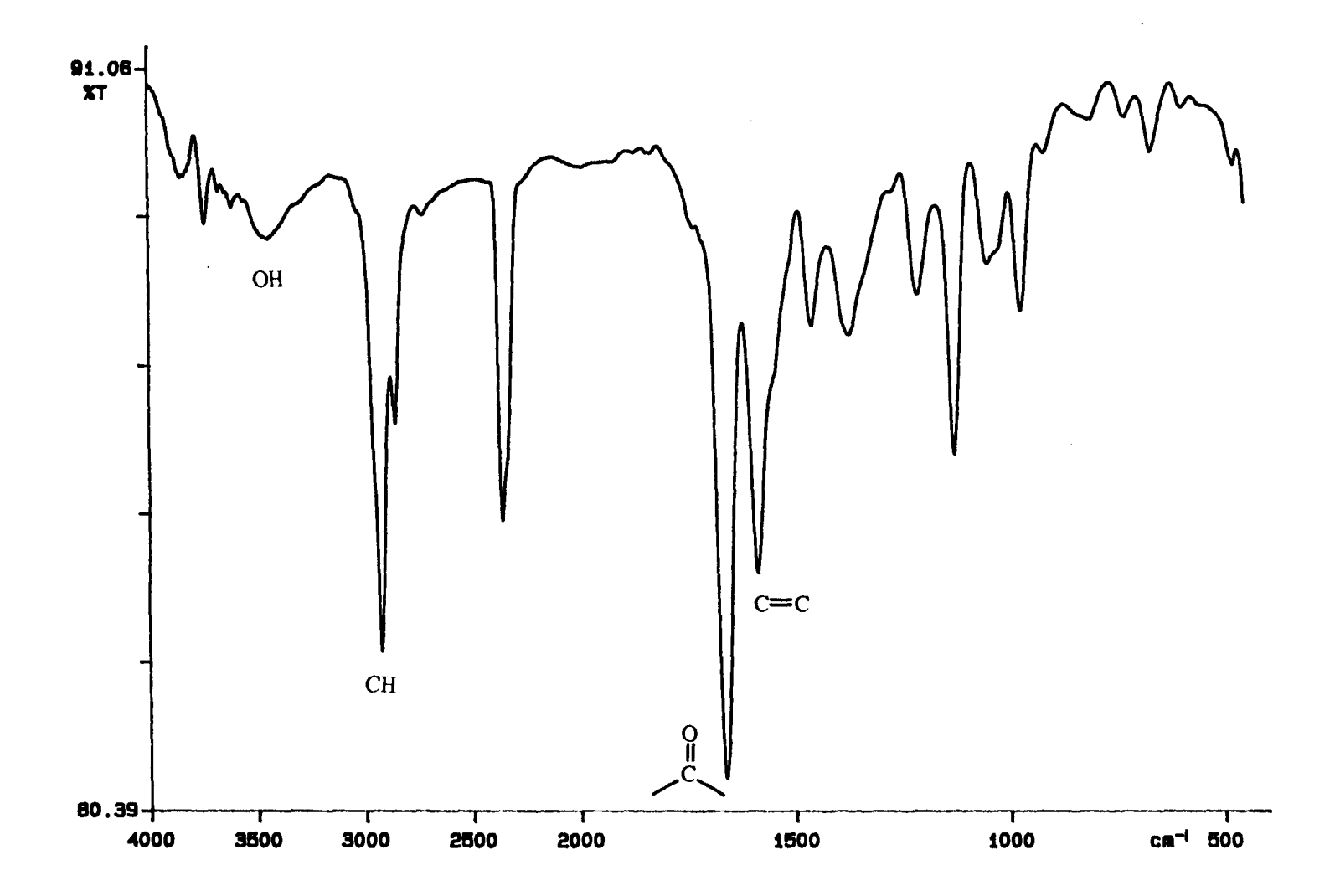


Fig. E22. Infrared spectrum of semi-synthetic apo-10'-fucoxanthinal (1) (film).

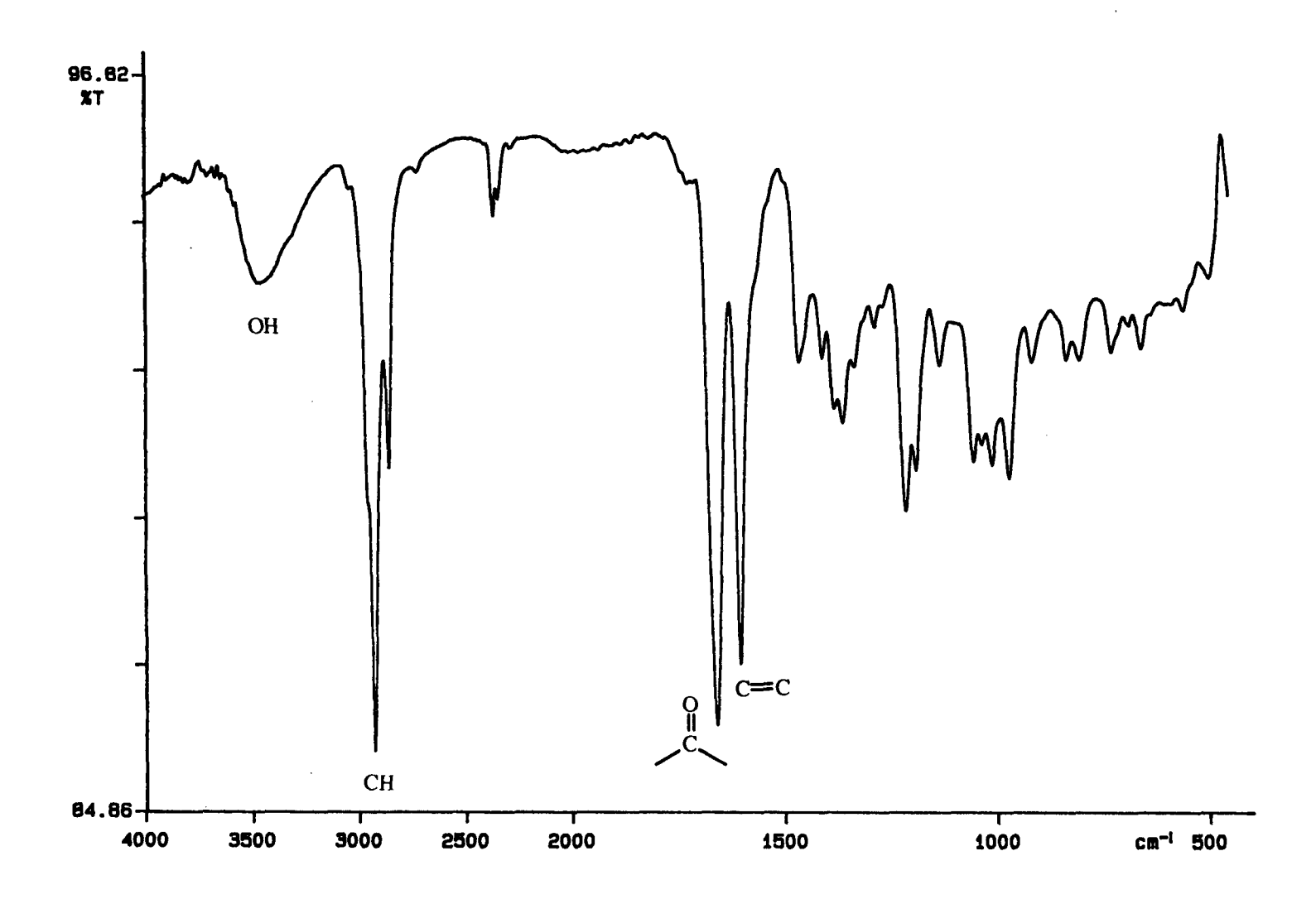


Fig. E23. Infrared spectrum of semi-synthetic apo-12'-fucoxanthinal (2) (film).

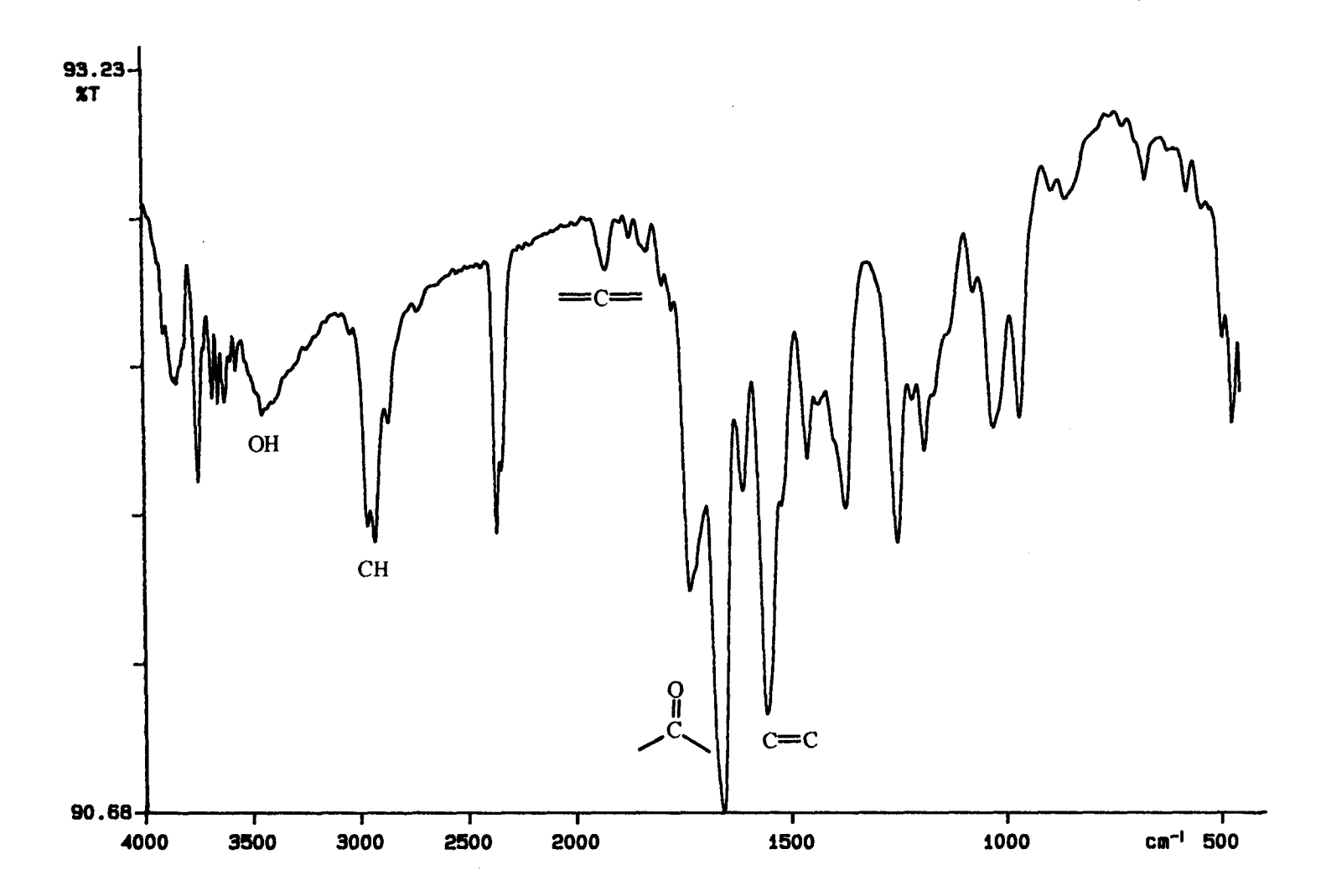


Fig. E24. Infrared spectrum of semi-synthetic apo-12-fucoxanthinal (3) (film).

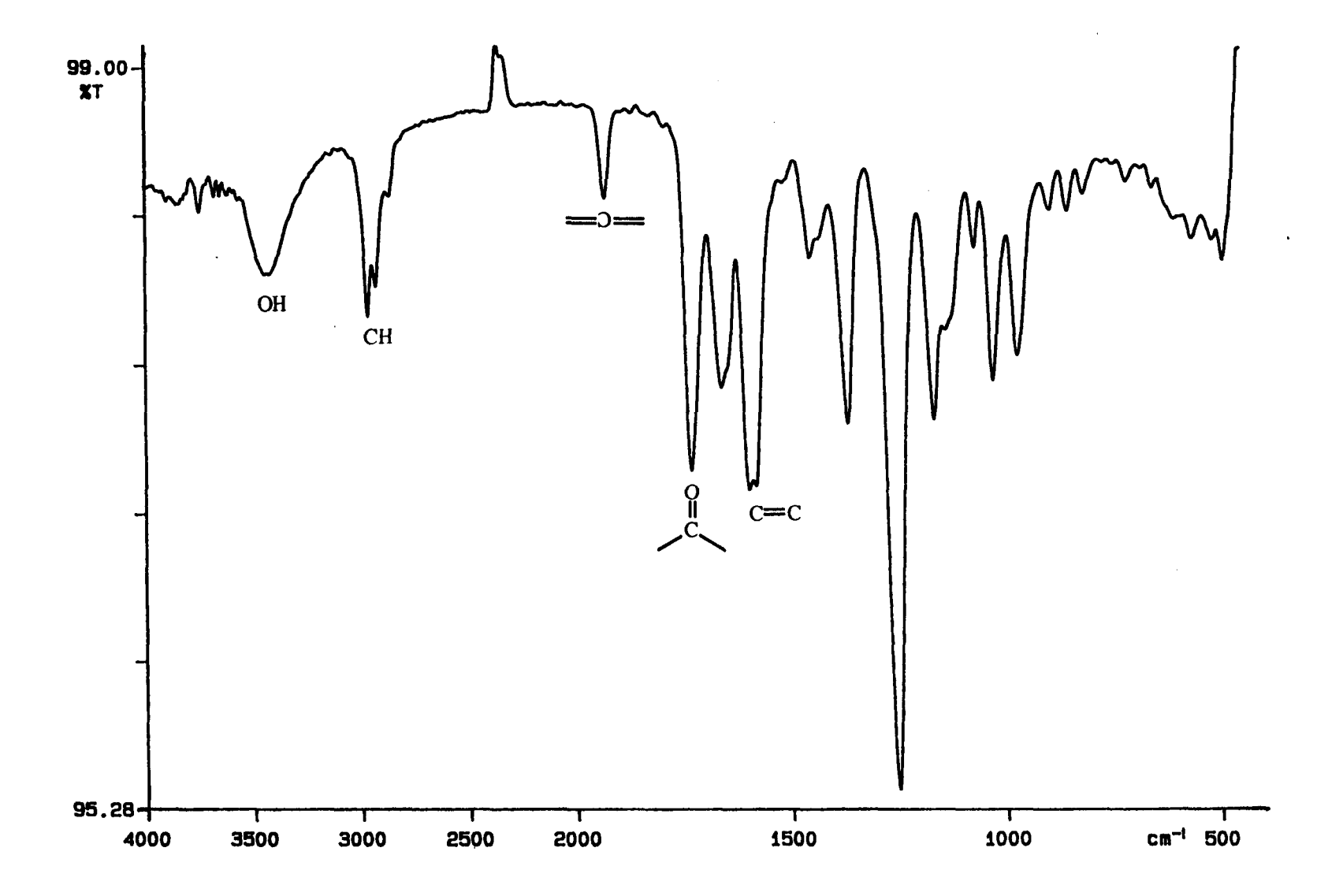


Fig. E25. Infrared spectrum of semi-synthetic apo-13'-fucoxanthinone (4) (film).

# Appendix F. Raw Data for Calculation of IC<sub>50</sub> and LC<sub>50</sub> Values in Chapter 4

Table F1. Measurements of fecal pellet volume ( $10^5 \mu m^3$ ) for *Tigriopus californicus* feeding on *Thalassiosira pseudonana* in the presence of various concentrations of apo-10'-fucoxanthinal or apo-12'-fucoxanthinal.

_		Concentration of	of apo-10'-fuco	xanthinal (ppm	1)
Replicate:	100	25	6	2	0.5
1	1.36	1.12	1.86	5.82	1.57
2	0.61	1.05	1.36	5.82	2.42
3	3.72	3.49	2.42	9.63	2.79
4	0.42	1.86	4.95	2.98	2.05
5	0.33	6.11	4.95	3.35	5.53
6	4.65	0.47	5.82	2.05	2.79
7	0.70	1.15	1.26	4.65	2.79
8	3.91	2.05	4.95	1.36	4.07
9	1.36	2.42	5.86	4.07	3.91
10	1.26	1.57	2.42	7.12	4.36
Average:	1.83	2.13	3.58	4.69	3.23
1 SD	1.62	1.64	1.88	2.50	1.21

	Concentration of apo-12'-fucoxanthinal (ppm)						
Replicate:	113	28	7	2	0.6		
1	2.23	1.47	1.78	4.65	1.68		
2	1.86	4.65	3.72	3.72	2.61		
3	1.68	6.11	4.95	4.36	5.53		
4	3.72	1.05	2.61	5.82	9.22		
5	1.05	3.17	5.24	2.23	6.11		
6	-	3.17	7.96	3.17	2.23		
7	-	4.95	3.17	4.95	6.11		
8	-	2.61	5.24	1.15	2.79		
9	-	6.40	5.24	5.53	2.98		
10	-	2.98	2.98	8.38	2.98		
Average:	2.11	3.65	4.29	4.40	4.22		
1 SD	1.00	1.82	1.80	2.02	2.40		
					_		

Table F1. Continued.

		ntrol		
	(no feeding deterrent)			
Replicate:	Sample 1	Sample 5		
1	5.82	7.27		
2	4.07	10.1		
3	4.95	3.54		
4	4.95	3.35		
5	6.70	5.24		
6	5.24	4.36		
7	4.95	4.28		
8	5.24	2.79		
9	2.61	6.11		
10	8.38	4.10		
Average:	5.29	5.11		
1 SD	1.52	2.21		
Average:	5.	20		
1 SD	0.	13		

**Table F2.** Measurements of fecal pellet volume ( $10^5 \mu m^3$ ) for *Tigriopus californicus* feeding on *Thalassiosira pseudonana* in the presence of various concentrations of apo-12-fucoxanthinal or apo-13'-fucoxanthinone.

_		Concentration (	of apo-12-fuco	xanthinal (ppm	1)
Replicate:	25	6	2	0.4	0.1
1	1.05	2.42	4.19	3.72	5.24
2	1.05	0.84	2.42	3.54	3.91
3	1.12	2.79	5.24	6.11	1.15
4	2.91	0.73	2.42	4.95	4.07
5	0.33	1.68	4.95	2.98	7.54
6	0.37	1.05	3.72	6.40	4.65
7	0.94	2.98	3.72	2.79	1.68
8	1.86	1.57	4.10	6.98	5.82
9	0.06	0.37	1.86	3.78	2.23
_10	1.30_	1.05_	3.35	5.53	8.38
Average:	1.10	1.55	3.60	4.68	4.47
1 SD	0.83	0.91	1.11	1.51	2.39

Table F2. Continued.

	C	oncentration of	f apo-13'-fucox	anthinone (ppi	n)
Replicate:	25	6	2	0.4	0.1
1	4.65	3.49	2.61	5.82	5.82
2	0.63	5.82	1.26	1.86	3.17
3	1.86	6.40	2.61	6.11	6.69
4	0.42	5.82	6.69	4.36	5.53
5	1.05	5.82	6.69	2.79	5.53
6	0.33	8.80	5.82	6.40	6.40
7	0.63	4.07	3.78	10.9	3.78
8	0.47	4.65	4.65	2.98	6.69
9	0.63	2.42	7.56	6.11	7.27
10	0.52	5.53	5.24	2.23	3.35
Average:	1.12	5.28	4.69	4.96	5.42
1 SD	1.32	1.76	2.08	2.72	1.48

	Control					
	(no feeding deterrent)					
Replicate:	Sample 1	Sample 5				
1	1.49	4.95				
2	2.91	6.28				
3	7.96	5.45				
4	2.79	6.69				
5	1.15	5.82				
6	2.23	5.53				
7	5.82	9.31				
8	6.69	9.22				
9	2.61	5.24				
10	7.56	4.36				
Average:	4.12	6.28				
1 SD	2.60	1.70				
Average:	5.	20				
1 SD	1.	53				

**Table F3.** Measurement of fecal pellet production rate (pellets h<sup>-1</sup> copepod<sup>-1</sup>) for *Tigriopus californicus* feeding on *Thalassiosira pseudonana* in the presence of various concentrations of apo-10'-fucoxanthinal or apo-12'-fucoxanthinal.

Concentration of apo-10'-fucoxanthinal (ppm)						
100	25	6	2	0.5		
17	39	84	74	55		
0.14	0.33	0.70	0.62	0.46		
Concentration of apo-12'-fucoxanthinal (ppm)						
113	28	7	2	0.6		
5	26	62	51	103		
0.04	0.22	0.52	0.43	0.86		
Co	ontrol replic	ates (no feed	ding deterre	nt)		
1	2	3	4	5		
154	132	131	113	122		
		130				
		1.09				
	100 17 0.14 Conc 113 5 0.04	100 25 17 39 0.14 0.33  Concentration of 113 28 5 26 0.04 0.22  Control replic 1 2	100     25     6       17     39     84       0.14     0.33     0.70       Concentration of apo-12'-fuctors       113     28     7       5     26     62       0.04     0.22     0.52       Control replicates (no feed 1)       1     2     3       154     132     131       130	100     25     6     2       17     39     84     74       0.14     0.33     0.70     0.62       Concentration of apo-12'-fucoxanthinal of apo-12		

**Table F4.** Measurements of fecal pellet production rate (pellets h<sup>-1</sup> copepod<sup>-1</sup>) for *Tigriopus californicus* feeding on *Thalassiosira pseudonana* in the presence of various concentrations of apo-12-fucoxanthinal or apo-13'-fucoxanthinone.

	Concentration of apo-12-fucoxanthinal (ppm)					
	25	6	2	0.4	0.1	
Fecal pellets	25	108	169	207	210	
Rate	0.21	0.90	1.41	1.73	1.75	
(pellets h <sup>-1</sup> copepod <sup>-1</sup> )						
	Concentration of apo-13'-fucoxanthinone (ppm)					
	25	6	2	0.4	0.1	
Fecal pellets	32	256	169	207	210	
Rate	0.27	2.13	1.80	1.72	1.83	
(pellets h <sup>-1</sup> copepod <sup>-1</sup> )						
	Co	ontrol replic	ates (no fee	ding deterre	nt)	
	1	2	3	4	5	
Fecal pellets	219	182	222	221	211	
Average:			211			
Rate			1.76			
(pellets h <sup>-1</sup> copepod <sup>-1</sup> )						

Table F5. Measurement of fecal volume production rate ( $10^5 \, \mu m^3 \, h^{-1}$  copepod<sup>-1</sup>) for *Tigriopus californicus* feeding on *Thalassiosira pseudonana* in the presence of various concentrations of apo-10'-fucoxanthinal or apo-12'-fucoxanthinal.

	Concentration of apo-10'-fucoxanthinal (ppm)				
	100	25	6	2	0.5
Rate $(10^5 \ \mu \text{m}^3 \ \text{h}^{-1} \ \text{copepod}^{-1})$	0.26	0.69	2.51	2.89	1.48
	Conc	entration of	apo-12'-fuc	oxanthinal (	(ppm)
	113	28	7	2	0.6
Rate (10 <sup>5</sup> μm <sup>3</sup> h <sup>-1</sup> copepod <sup>-1</sup> )	0.09	0.79	2.21	1.87	3.62
		Control (	no feeding	deterrent)	<del>- /s</del>
Average rate $(10^5 \mu \text{m}^3 \text{ h}^{-1} \text{ copepod}^{-1})$			5.65		

Table F6. Measurements of fecal volume production rate ( $10^5 \mu m^3 h^{-1}$  copepod<sup>-1</sup>) for *Tigriopus californicus* feeding on *Thalassiosira pseudonana* in the presence of various concentrations of apo-12-fucoxanthinal or apo-13'-fucoxanthinone.

	Concentration of apo-12-fucoxanthinal (ppm)					
	25	6	2	0.4	0.1	
Rate (10 <sup>5</sup> μm <sup>3</sup> h <sup>-1</sup> copepod <sup>-1</sup> )	0.23	1.39	5.07	8.07	7.82	
	Conce	ntration of a	apo-13'-fucc	exanthinone	(ppm)	
	25	6	2	0.4	0.1	
Rate $(10^5 \mu \text{m}^3 \text{ h}^{-1} \text{ copepod}^{-1})$	0.30	11.3	8.44	8.51	9.90	
		Control (	no feeding o	deterrent)		
Average rate $(10^5 \mu \text{m}^3 \text{ h}^{-1} \text{ copepod}^{-1})$			9.15			

**Table F7.** Percentage of *Tigriopus californicus* which survived at the end of 24 h when feeding on *Thalassiosira pseudonana* in the presence of various concentrations of apo-10'-fucoxanthinal or apo-12'-fucoxanthinal.

	Concentration of apo-10'-fucoxanthinal (ppm)						
	100	25	6	2	0.5		
Percentage survived	40	80	100	100	80		
	Concentration of apo-12'-fucoxanthinal (ppm)						
	113	28	7	2	0.6		
Percentage survived	0	80	100	100	100		

## Appendix G. Probit Method for Calculating IC<sub>50</sub> and LC<sub>50</sub> Values

(Hubert, 1984)

## i. IC<sub>50</sub> Value

#### **Definitions:**

c = concentration of feeding deterrent (ppm)

F = fecal pellet or fecal volume production rate (pellets  $h^{-1}$  or volume  $h^{-1}$ )

 $F_m$  = maximum fecal pellet or fecal volume production rate (pellets  $h^{-1}$  or volume  $h^{-1}$ )

= average fecal pellet or fecal volume production rate of control

#### Calculations:

$$X = log_{10}(100*c)$$

$$I = 100*[1-(F/F_m)]$$
if  $I \ge 100$ , then replace I with the value  $100*[1-(1/2n)]$ 
if  $I \le 0$ , then replace I with the value  $100*(1/2n)$ 
where  $n = number$  of subjects in the assay

Perform a least squares linear fit on X and Y

a = y-intercept

b = slope

 $r^2$  = correlation coefficient

Theory:

$$Y = [(X - \mu)/\sigma] + 5$$

where  $\mu = \text{mean}$ 

 $\sigma$  = standard deviation

Therefore:  $a = 5 - (\mu/\sigma)$ 

 $b = 1/\sigma$ 

In original units:

$$\sigma = (10^{1/b})/100$$

$$IC_{50} = (10^{((5-a)/b)})/100$$

## i. LC<sub>50</sub> Value

**Definitions:** 

c = concentration of feeding deterrent (ppm)

S = percentage of subjects surviving after 24 h

Calculations:

$$X = \log_{10}(100*c)$$

$$M = 100 - S$$

if  $M \ge 100$ , then replace M with the value 100\*[1-(1/2n)]

if  $M \le 0$ , then replace M with the value 100\*(1/2n)

where n = number of subjects in the assay

$$Y = PROBIT(M)$$

#### obtain value from PROBIT tables

Perform a least squares linear fit on X and Y

$$a = y$$
-intercept

$$b = slope$$

 $r^2$  = correlation coefficient

Theory:

$$Y = [(X - \mu)/\sigma] + 5$$

where 
$$\mu = \text{mean}$$

 $\sigma$  = standard deviation

Therefore: 
$$a = 5 - (\mu/\sigma)$$

$$b = 1/\sigma$$

In original units:

$$\sigma = (10^{1/b})/100$$

$$LC_{50} = (10^{((5-a)/b)})/100$$

# Appendix H. Growth of Phytoplankton Cultures

**Table H1.** Growth of *Thalassiosira pseudonana* (culture #1) at 19°C with continuous irradiance of 224  $\mu$ mol m<sup>-2</sup> s<sup>-1</sup>. Errors given are  $\pm$  1 SD.

Time (d)	Fluorescence	Cell numbers (cells ml <sup>-1</sup> )	Nitrate (μM)	Phosphate (µM)	pН	Harvest volume (ml)
0.00		<u>n = 5</u>	515	10.6	7.70	
0.02	0.44	_	-	-	7.70	_
0.73	2.66	_	_	_	_	_
1.06	5.92	_	_	_	_	_
1.73	13.8	_	_	-	_	_
1.75	-	$9.5 \times 10^5 \pm 2.3 \times 10^5$	-	-	-	4000
2.08	21.0	_	-	-	_	-
2.75	39.4	_	-	_	-	-
3.08	43.2	-	-	_	-	-
3.75	42.5	-	-	-	-	-
3.77	-	$1.8 \times 10^6 \pm 0.3 \times 10^6$	-	-	-	3000
4.13	44.0	_	-	-	-	-
4.79	38.5	-	_	-	-	_
5.02	39.0	-	-	-	_	_
5.77	39.4	_	-	-	-	-
5.79	-	$1.4 \times 10^6 \pm 0.5 \times 10^6$	165	1.49	7.75	3000

**Table H2.** Growth of *Phaeodactylum tricornutum* (culture #2) at 19°C with continuous irradiance of 224  $\mu$ mol m<sup>-2</sup>s<sup>-1</sup>. Errors given are  $\pm$  1 SD.

Time (d)	Fluorescence	Cell numbers (cells ml <sup>-1</sup> ) n = 5	Nitrate (µM)	Phosphate (µM)	рН	Harvest volume (ml)
0.00	-	-	527	12.1	7.65	-
0.02	1.01		-	-	-	-
0.73	5.99		-	-	-	-
1.06	10.1		-	-	-	_
1.73	25.0		_	-	-	-
1.83	-	$1.1 \times 10^6 \pm 0.1 \times 10^6$	-	~	-	4000
2.08	36.7		-	-	_	-
2.75	65.5		-	-	-	-
3.08	76.8		-	-	-	-
3.75	89.2		-	-	-	-
3.88	-	$3.5 \times 10^6 \pm 0.5 \times 10^6$	-	-	-	3000
4.13	90.6		-	-	-	-
4.79	97.3		-	-	-	-
5.02	107		-	-	-	-
5.77	120	_	-	-	-	-
5.96	-	$3.9 \times 10^6$ $\pm 0.6 \times 10^6$	85	0.02	7.77	3000

**Table H3.** Growth of *Phaeodactylum tricornutum* (culture #3) at 19°C with continuous irradiance of 224  $\mu$ mol m<sup>-2</sup>s<sup>-1</sup>. Errors given are  $\pm$  1 SD.

Time (d)	Fluorescence	Cell numbers (cells ml <sup>-1</sup> )	Nitrate (μM)	Phosphate (µM)	pН	Harvest volume (ml)
		n = 5	450	10.0	<del></del>	<del> </del>
0.00	-	-	453	10.0	7.69	-
0.02	0.675		-	~	-	-
0.73	4.84		-	-	-	-
1.06	8.09		-	-	-	-
1.73	20.9		-	-	-	-
1.98	-	$1.2 \times 10^6 \pm 0.2 \times 10^6$	-	-	-	4000
2.08	30.9		-	_	-	-
2.75	66.8		_	-	-	-
3.08	78.5		-	_	-	-
3.75	96.6		_	_	_	-
3.98	-	$1.7 \times 10^6 \pm 0.2 \times 10^6$	-	-	-	3000
4.13	98.1		_	_	-	_
4.79	108		-	-	_	_
5.02	124		_	-	_	_
5.77	130		_	_	_	_
5.96	-	$3.9 \times 10^6 \pm 0.3 \times 10^6$	53	0.11	7.74	3000

**Table H4.** Calculated growth constants from the data in Tables H1 - H3 for *Phaeodactylum tricornutum* and *Thalassiosira pseudonana*.

Species, culture	Growth rate $(\mu)$ $(day^{-1})$	Time at which cultures entered senescence (days)
Thalassiosira pseudonana, culture # 1	1.47	2.51
Phaeodactylum tricornutum, culture #2	1.34	2.46
Phaeodactylum tricornutum, culture #3	1.38	2.65

#### Appendix I. Calculation of Cell Volumes

**Table I1.** Cell dimensions for *Phaeodactylum tricornutum* and *Thalassiosira* pseudonana as measured with a microsope (n = 10). Errors shown are  $\pm 1$  SD.

Species	Dimension	Measurement (μm)
Thalassiosira pseudonana		
	height (h)	$7 \pm 1$
	diameter (d)	$6 \pm 1$
Phaeodactylum tricornutum		
triradiate	diameter (d)	$14 \pm 1$
fusiform	total length (3L)	$20 \pm 1$
	width (w)	$2.9 \pm 0.4$

#### **Cell Volume Calculations:**

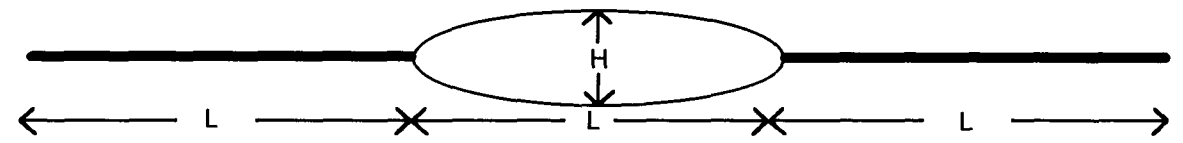
#### Thalassisira pseudonana:

Thalassiosira pseudonana was treated as a cylinder, and the cell volume was calculated using the equation  $V = \pi r^2 h$ . The diameter of the cell was measured as 5.54  $\mu$ m, hence radius was 2.77  $\mu$ m. The height of the cell was measured as 6.79  $\mu$ m. Therefore the volume was 163  $\mu$ m<sup>3</sup> = 163 fL

#### Phaeodactylum tricornutum:

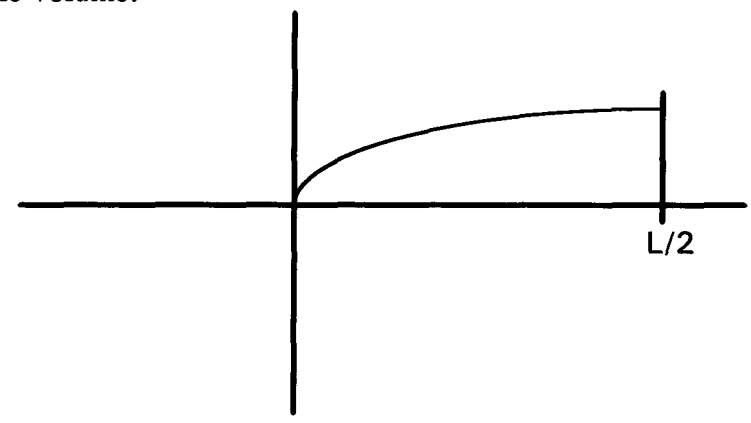
The volume was calculated for both the fusiform and the triradiate forms of *Phaeodactylum tricornutum*, and averaged based on a casual observation of a population consisting of 50% triradiates and 50% fusiforms.

For the fusiform form:



From measurements, H = 2.91  $\mu$ m and L = 6.65  $\mu$ m. The volume of the body of the cell was estimated using the volume generated by rotating the line y =  $\sqrt{x}$  around the

x-axis from 0 to L/2, and multiplying this volume by 2. The spines were assumed to have negligible volume.



The cross-section of this rotation was a circle of area  $\pi r^2 = \pi (\sqrt{x})^2 = \pi x$ . The volume was calculated by integration from 0 to L/2:

$$\frac{1}{2}V = \int_0^{L/2} \pi x dx = \pi (x^2/2) \Big|_0^{L/2}$$

Since L/2 = 3.32  $\mu$ m, then V = 34.7  $\mu$ m<sup>3</sup>. An average width,  $\overline{w}$ , of this shape can be calculated using a cylindrical estimate:

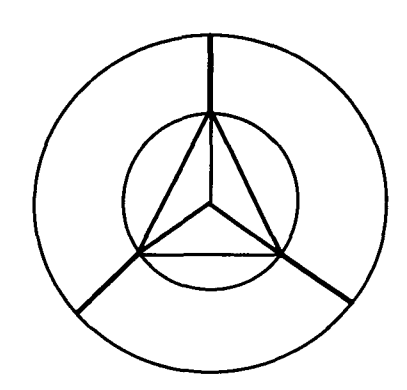
$$V = \pi r^{2}h$$

$$34.7 = \pi r^{2}(6.65)$$

$$r = 1.29 \ \mu m$$

Since  $\overline{w} = 2r$ , then  $\overline{w} = 2.58 \mu m$ .

The triradiate form can be represented by this diagram:



The volume of the spines was assumed negligible. The radius of the inner circle = 1/4d and spine length = 1/4 d. The area of the circumscribed equilateral triangle divided by the area of inner circle =  $(1.5)\cos 30^{\circ}/\pi$ . Since the area of the inner circle =  $\pi r^2$ , therefore:

(area of triangle)/
$$\pi r^2 = (1.5)\cos 30^\circ / \pi$$
  
area of triangle =  $(1.5)r^2\cos 30^\circ$ 

By measurements,  $d = 13.9 \mu m$ , therefore  $r = 3.46 \mu m$ . The area of the triangle =  $(1.5)(3.46)^2\cos 30^\circ = 15.6 \mu m^2$ . To get a volume, the average width of the fusiform form was used:

$$V = \overline{w}$$
 (area of triangle)  
 $V = (15.6)(2.58) = 40.2 \ \mu m^3$ 

Therefore, the average volume of *Phaeodactylum tricorntum* was  $(34.7 + 40.2)/2 = 37.4 \ \mu m^3 = 37.4 \ fL$ .

### Appendix J. Results from Feeding Deterrent Bioassays of Samples from a Thalassiosira pseudonana Culture (#1) and Two Phaeodactylum tricornutum Cultures (#2 and #3)

**Table J1.** Raw data from quantitative bioassays of samples from cultures #1, #2, and #3.

Sample	Fecal pellet counts	Incubation time (h)	Mean rate (pellets h <sup>-1</sup> )	Standard deviation
Control	33, 80, 48, 78, 82, (96)*	23.5	1.37	0.475
1MC	26, 37, 89, 60, 58, 96	23	1.33	0.601
1LC	34, 50, 31, 44, 39, 33	23	0.837	0.160
1SC	50, 40, 5, 11, 30, 41	23	0.641	0.390
2MC	15, 44, 43, 30, 13, 14	23	0.576	0.317
2LC	13, 34, 28, 14, 15, 29	23	0.482	0.200
2SC	17, 7, 13, 12, 20, 15	23	0.304	0.0972
3MC	63, 7, 67, 36, 42, 27	23.5	0.858	0.479
3LC	44, 57, 82, 27, 18, 19	23.5	0.876	0.534
3SC	22, 49, 22, 3, 7, 6	23.5	0.387	0.366

<sup>\*</sup> this replicate had 3 copepods instead of 2, and was not used in further analyses.

**Table J2**. Calculated values for the relative concentration of apo-12'-fucoxanthinal in the bioassay medium and in the intracellular fluid of the cell. The error values shown are estimates based on the variability of the bioassay results.

Sample	Relative apo-12'-	<b>Estimated</b>	Relative apo-12'-	<b>Estimated</b>
	fucoxanthinal	error of Cb	fucoxanthinal	error of Cc
	concentration in	due to	concentration in	due to
	bioassay, Cb	variability in	cell, Cc	variability in
	(ppm)	bioassay	(ppt)	bioassay
1MC	0.000944	2.74	0.0000640	0.186
1LC	1.28	0.727	0.0609	0.0347
1SC	3.89	1.77	0.239	0.109
2MC	5.47	1.44	1.40	0.368
2LC	8.87	0.911	0.948	0.0973
2SC	22.7	0.443	2.17	0.0425
3MC	1.11	2.18	0.261	0.510
3LC	0.993	2.44	0.219	0.536
3SC	14.5	1.67	1.39	0.160

Equations used in calculations for relative apo-12'-fucoxanthinal concentrations:

1) Rate:

(rate, pellets 
$$h^{-1}$$
) =  $\frac{\text{(fecal pellet count, pellets)}}{\text{(incubation time, h) * (number of copepods)}}$ 

2) Relative apo-12'-fucoxanthinal concentration in bioassay medium:

(Cb, ppm) = 
$$\frac{\ln \left( \frac{\text{(fecal pellet rate of test, pellets h}^{-1})}{\text{(fecal pellet rate of control, pellets h}^{-1})} \right)^{1/0.3892} -0.4456$$

3) Relative intracellular apo-12'-fucoxanthinal concentration:

(Cc, ppt) = 
$$\frac{\text{(Cb, ppm) * (bioassay volume = 6.0 ml) * (dilution factor = 7x10^9)}}{\text{(cell density, cells ml}^{-1}\text{) * (harvest volume, ml) * (cell volume, fL cell}^{-1}\text{)}}$$

Table J3. Pairwise comparisons of the fecal pellet production rates for samples from cultures #1, #2, and #3. As the sample variances were significantly different, an ANOVA analysis could not be applied to the entire data set. Each pair of samples was compared using an ANOVA on the raw, untransformed data (AU), an ANOVA on the log transformed raw data (AL), or a Mann-Whitney U test (MW), depending on the normality and variances of the sample data sets. S = samples were significantly the same; D = samples were significantly different.

	1MC	1LC	1SC	2MC	2LC	2SC	3МС	3LC	3SC
С	AU; S F=0.0144	MW; S U=24	AU; D F=7.76	AU; D F=10.9	AL; D F=17.4	AL; D F=41.4	AU; S F=3.09	AU; S F=2.53	AU; D F=15.0
1MC	$\alpha$ =0.907	α=0.075 MW; S	α=0.0212 AU; D	$\alpha = 0.00919$ AL; D	$\alpha = 0.00241$ AL; D	$\alpha = 1.20E-04$ AL; D	α=0.113 AU; S	α=0.146 AU; S	α=0.00380 AU; D
1LC		U = 25 $\alpha > 0.10$	F=5.49 $\alpha=0.0412$ MW; S	F=7.80 $\alpha=0.0190$ MW; S	F = 13.4 $\alpha = 0.00439$ AU; D	F=31.4 α=2.25E-04 AU; D	F=2.22 α=0.167 MW; D	F = 1.88 $\alpha = 0.200$ MW; S	F=10.7 $\alpha$ =0.00843 MW; D
ile			U=22.5 $\alpha > 0.10$	U=27.5 $\alpha=0.0875$	F=11.6 $\alpha=0.00677$	F=48.7 $\alpha=3.80E-05$	F=31.4 $\alpha=2.25E-04$	U=19 $\alpha > 0.10$	U=31 $\alpha=0.025$
1SC				AU; S F=0.101	MW; S U=23	MW; S U=25	AL; S F=0.464	AU; S F=0.755	AU; S F=1.36
2MC				$\alpha$ =0.757	α>0.10 AL; S F=0.169	α>0.10 AL; S F=4.01	α=0.511 AL; S F=0.608	α=0.405 AL; S F=1.33	α=0.270 AU; S F=0.919
2LC					$\alpha = 0.690$	$\alpha = 0.907$ AL; S	α=0.454 MW; S	$\alpha = 0.275$ AL; S	α=0.360 AU; S
200						F=3.56 $\alpha=0.0885$	$U=27$ $\alpha=0.10$	F = 2.83 $\alpha = 0.123$	$F=0.313$ $\alpha=0.588$
2SC							MW; D U=30.5 $\alpha$ =0.0313	AL; D F=10.6 α=0.00868	MW; S U=18.5 $\alpha > 0.10$
3MC							a 5,557.5	AU; S F=0.00366	AL; S F=3.40
3LC								$\alpha$ =0.953	$\alpha = 0.0952$ AU; S $F = 3.42$ $\alpha = 0.0941$

**Table J4.** Comparison of the average relative intracellular apo-12'-fucoxanthinal concentrations for the two *Phaeodactylum tricornutum* cultures (#2 and #3) with the control (Cc = 0) and with the *Thalassiosira pseudonana* culture (#1).

	Sample		
	M	L	S
Average:	0.828	0.583	1.78
Standard deviation:	0.802	0.516	0.553
t-tests with control:			
(Cc = 0)			
t (one-tailed):	1.46	1.60	4.56
$\alpha$ :	0.20	0.19	0.077
t-tests with culture #1:			
Comparison with:	1 <b>M</b>	1L	1 <b>S</b>
t (one-tailed):	1.46	1.43	3.95
α:	0.20	0.20	0.086
t-test between L and S:			
t (one-tailed):		3.07	
α:		0.10	

# Appendix K. Results from the HPLC Analysis of Samples from a *Thalassiosira* pseudonana Culture (#1) and Two Phaeodactylum tricornutum Cultures (#2 and #3)

**Table K1.** Raw data from analysis of culture samples for apo-fucoxanthinoids using the HPLC/PDA system.

	Peak heights $(\mu V)$					
Sample	Fuco.	Apo-10'	Apo-12'	Apo-12	Apo-13'	Unknown #1
1MC	454831	0	0	0	0	0
1ME	5668	0	0	0	0	0
1LC	1688338	0	0	0	1140	0
1LE	2170	0	0	0	0	0
1SC	1341524	0	974	0	1477	0
1SE	1421	0	0	0	0	0
2MC	1206136	0	2247	0	1315	0
2ME	2574	0	0	0	0	0
2LC	1604784	0	0	0	385	74511
2LE	2131	0	0	0	0	0
2SC	2517302	0	500	0	543	479692
2SE	1822	0	0	0	0	0
3MC	1314196	0	1212	0	960	0
3ME	1151	0	0	0	0	0
3LC	2185300	0	6763	0	6587	100801
3LE	1496	0	0	0	0	0
3SC	2502549	0	0	0	1215	254056
3SE	5638	0	0	0	0	0

**Table K2.** Retention times and absorbance maxima wavelengths for compounds of interest eluting from the HPLC.

Compound	Retention time (min)	Absorbance maxima (nm)
Apo-12'-fucoxanthinal	7.31	395 (max), 418
Apo-13'-fucoxanthinone	5.25	333 (max)
Fucoxanthin	14.8	448 (max), 467
Unknown #1	13.2	439 (max)

**Table K3.** Amounts of fucoxanthin and apo-fucoxanthinoids in the volume of sample injected onto the HPLC column.

	Amou	nt of compound i	n injection volur	ne (μg)
Sample	Fucoxanthin	Apo-12'	Apo-13'	Unknown #1
1MC	1.90	0	0	0
1LC	7.06	0	0.0175	0
1SC	5.61	0.0136	0.0226	0
2MC	5.05	0.0313	0.0201	0
2LC	6.71	0	0.00590	2.28
2SC	10.5	0.00696	0.00832	14.7
3MC	5.50	0.0169	0.0147	0
3LC	9.14	0.0942	0.101	3.08
3SC	10.5	0	0.0186	7.77

**Table K4.** Intracellular concentrations of fucoxanthin and apo-fucoxanthinoids based on the results from the HPLC analysis.

	Intracellular concentration (ppt)					
Sample	Fucoxanthin	Apo-12'	Apo-13'	Unknown #1		
1MC	0.860	0	0	0		
1LC	2.25	0	0.00555	0		
1SC	2.30	0.00555	0.00925	0		
2MC	8.58	0.0532	0.0342	0		
2LC	4.78	0	0.00420	1.62		
2SC	6.73	0.00445	0.00532	9.38		
3MC	8.57	0.0263	0.0229	0		
3LC	13.4	0.138	0.148	4.52		
3SC	6.69	0	0.0119	4.97		

**Table K5.** Comparison of the average intracellular concentrations of fucoxanthin and the apo-fucoxanthinoids for the two *Phaeodactylum tricornutum* cultures (#2 and #3) with the control (Cc = 0) and with the *Thalassiosira pseudonana* culture (#1).

Sample	Fucoxanthin	Apo-12'	Apo-13'	Unknown #1
M:				
mean	8.57	0.0398	0.0286	0
1 SD	0.00733	0.0190	0.00801	0
t-test with 1MC	2580	5.12	8.74	0
α	< 0.0005	0.0684	0.0405	1
t-test with $Cc=0$	2870	5.12	8.74	0
α	< 0.0005	0.0684	0.0405	1
L:				
mean	9.10	0.0691	0.0761	3.07
1 SD	6.10	0.0977	0.102	2.05
t-test with 1LC	2.75	1.73	1.70	3.67
α	> 0.1	> 0.1	> 0.1	0.0909
t-test with $Cc=0$	3.65	1.73	1.83	3.67
α	0.0912	> 0.1	> 0.1	0.0909
<b>S</b> :				
mean	6.71	0.00223	0.00861	7.17
1 SD	0.0280	0.00315	0.00465	3.12
t-test with 1SC	388	-2.58	-0.339	5.63
α	0.000891	> 0.1	> 0.1	0.0606
t-test with $Cc = 0$	589	1.73	4.53	5.63
α	0.000575	> 0.1	0.0776	0.0606

Equations for the calculation of the intracellular concentrations of fucoxanthin and apofucoxanthinoids:

1) Amounts of fucoxanthin and apo-fucoxanthinoids in the volume of sample injected onto the HPLC column:

$$(w_{12}^{-}, \mu g) = \frac{(\text{peak height of apo - 12'-fucoxanthinal}, \mu V) * 10^{-6}}{0.0718}$$

$$(w_{13}^{-}, \mu g) = \frac{(\text{peak height of apo - 13'-fucoxanthinone}, \mu V) * 10^{-6}}{0.0653}$$

$$(w_{0\#1}, \mu g) = \frac{(\text{peak height of unknown } \#1, \mu V) * 10^{-6}}{0.0327}$$

$$(w_f, \mu g) = \frac{(\text{peak height of fucoxanthin at 446 nm}, \mu V) * 10^{-6}}{0.239}$$

2) Intracellular concentrations of fucoxanthin and apo-fucoxanthinoids:

(Cc, ppt) = 
$$\frac{(w, \mu g) * (\text{dilution factor} = 280 \times 10^9)}{(\text{cell density, cells ml}^{-1}) * (\text{harvest volume, ml}) * (\text{cell volume, fL cell}^{-1})}$$

**Table K6.** Amounts of fucoxanthin present in the extracellular medium, expressed as amount "leaked" per cell.

Sample	Fucoxanthin in injection volume	Amount of fucoxanthin leaked	Leaked fucoxanthin as a percentage of
	(μg)	per cell	total intracellular
		(fg)	fucoxanthin
1ME	0.0237	1.75	1.25
1LE	0.00908	0.471	0.129
1SE	0.00595	0.396	0.106
2ME	0.0108	0.685	0.213
2LE	0.00892	0.238	0.133
2SE	0.00762	0.182	0.0724
3ME	0.00482	0.281	0.0876
3LE	0.00626	0.344	0.0685
3SE	0.0236	0.565	0.225

Equations used to calculate amount of fucoxanthin leaked per cell:

1) Amount of fucoxanthin in injection volume:

$$(w_f, \mu g) = \frac{(\text{peak height of fucoxanthin at 446 nm}, \mu V) * 10^{-6}}{0.239}$$

2) Amount of fucoxanthin leaked per cell:

(leakage per cell, fg) = 
$$\frac{(w_f, \mu g) * (\text{dilution factor} = 280 \times 10^9)}{(\text{cell density, cells ml}^{-1}) * (\text{harvest volume, ml})}$$

3) Leaked fucoxanthin as a percentage of total intracellular fucoxanthin:

(percentage leakage) = 
$$\frac{\text{(amount of fucoxanthin leaked per cell, fg)}}{\text{(amount of intracellular fucoxanthin, fg)}} * 100$$

# Appendix L. Comparison of the Results of the Quantitative Bioassays and the HPLC Method for Detecting Feeding Deterrents

Calculations for comparison of bioassay and HPLC methods:

1) Amount of compound in injection volume:

$$(w_{12}', \mu g) = \frac{(\text{peak height of apo - }12'\text{-fucoxanthinal}, \mu V) * 10^{-6}}{0.0718}$$

$$(w_{13}', \mu g) = \frac{(\text{peak height of apo - }13'\text{-fucoxanthinone}, \mu V) * 10^{-6}}{0.0653}$$

$$(w_{U\#1}, \mu g) = \frac{(\text{peak height of unknown }\#1, \mu V) * 10^{-6}}{0.0327}$$

Assumption: Unknown #1 is apo-10-fucoxanthinal (as identified by its UV-vis spectrum and retention time on the HPLC column) and will have similar absorption to apo-12-fucoxanthinal.

2) Relative concentration of apo-12'-fucoxanthinal in the bioassay:

(Cb, ppm) = 
$$[(w_{12}, \mu g) + a * (w_{13}, \mu g) + b * (w_{U#1}, \mu g)] * (dilution factor = 40/6)$$

3) Predicted fecal pellet production rate from HPLC results:

(Fp, pellets 
$$h^{-1}$$
) = Fc \* exp[- 0.4456 \* (Cb, ppm)<sup>0.3892</sup>]  
where Fc = fecal pellet production rate of the control = 1.37 pellets  $h^{-1}$ 

4) Comparison to results from quantitative bioassays using two-tailed t-tests:

$$t = \frac{[(Fb, pellets h^{-1}) - (Fp, pellets h^{-1})]}{sd / \sqrt{n}}$$

where Fb = fecal pellet production rate measured by the bioassay sd = standard deviation from the bioassay n = number of replicates in the bioassay

- 5) Minimizing t values:
  - a) while the constant b = 1, optimize the constant a such that  $|t_{1LC}| + |t_{1SC}| + |t_{2MC}| + |t_{3MC}|$  is a minimum

b) with a optimized, optimize b such that 
$$b \ge 0$$
 and  $|t_{21C}| + |t_{2SC}| + |t_{31C}| + |t_{3SC}|$  is a minimum

6) The optimized values are:

$$a = 11.0$$

$$b = 0.225$$

7) Therefore, assuming the  $IC_{50}$  value of apo-12'-fucoxanthinal is 2.87 ppm, the  $IC_{50}$  values calculated from the HPLC results are:

apo-12'-fucoxanthinal: 
$$IC_{50} = 2.87$$
 ppm

apo-13'-fucoxanthinone: 
$$IC_{50} = 0.262$$
 ppm

apo-10-fucoxanthinal: 
$$IC_{50} = 12.74$$
 ppm

8) Relative concentration of intracellular apo-12'-fucoxanthinal from HPLC results:

(Cc, ppt) = 
$$\frac{\text{(Cb, ppm)*(dilution factor } = 42 \times 10^9)}{\text{(cell density, cells ml}^{-1})*(\text{harvest volume, ml})*(\text{cell volume, fL cell}^{-1})}$$

Table L1. Comparison of the fecal pellet production rate calculated from the HPLC results (Fp) with the fecal pellet production rate measured by the quantitative bioassay (Fb). For this comparison, a = 2.87/20.00 (from IC<sub>50</sub> calculations, Chapter 4) and b = 0. At  $\alpha = 0.05$  and n = 6,  $|t_{crit}(two-tailed)| = 2.571$ .

Cb	Fp	t	Cc
(ppm)	(pellets h-1)		(ppt)
0	1.37	-0.163	0
0.0167	1.25	-6.30	0.000797
0.112	1.13	-3.07	0.00688
0.228	1.06	-3.77	0.0581
0.00564	1.29	-9.87	0.000603
0.0544	1.18	-22.1	0.00522
0.127	1.12	-1.33	0.0296
0.724	0.922	-0.211	0.159
0.0178	1.24	-5.74	0.00171
	(ppm) 0 0.0167 0.112 0.228 0.00564 0.0544 0.127 0.724	(ppm)         (pellets h-1)           0         1.37           0.0167         1.25           0.112         1.13           0.228         1.06           0.00564         1.29           0.0544         1.18           0.127         1.12           0.724         0.922	(ppm)         (pellets h-1)           0         1.37         -0.163           0.0167         1.25         -6.30           0.112         1.13         -3.07           0.228         1.06         -3.77           0.00564         1.29         -9.87           0.0544         1.18         -22.1           0.127         1.12         -1.33           0.724         0.922         -0.211

Table L2. Model used to explain underestimation of the feeding inhibition of the crude cellular extracts by the HPLC results. Optimization produced a=11.0 and b=0.225. At  $\alpha=0.05$  and n=6,  $|t_{crit}(two-tailed)|=2.571$ .

ည	(ppt)	0	0.0609	0.107	0.428	0.412	2.17	0.277	2.78	1.25
+		-0.163	0	-0.907	-1.67	-1.98	0	0.0499	2.12	-0.139
Fp	(pellets h-1)	1.37	0.837	0.786	0.792	0.643	0.304	0.848	0.413	0.407
ච	(mdd)	0	1.28	1.74	1.68	3.85	22.7	1.19	12.6	13.0
Sample		1MC	1LC	1SC	2MC	2LC	2SC	3MC	$3\Gamma$ C	3SC

**Table L3.** Comparison of the average relative intracellular concentrations of apo-12'-fucoxanthinal for the two *Phaeodactylum tricornutum* cultures (#2 and #3) with the control (Cc = 0) and with the *Thalassiosira pseudonana* culture (#1).

ample	
М:	
mean	0.353
1 SD	0.107
t-test with 1MC	8.10
α	0.0430
t-test with $Cc = 0$	8.10
$\alpha$	0.0430
t-test with S	-17.94
α	0.0418
• ••	
mean	1.59
1 SD	1.67
t-test with 1LC	2.25
$\alpha$	> 0.1
t-test with $Cc = 0$	2.33
$\alpha$	> 0.1
:	
mean	1.71
1 SD	0.65
t-test with 1SC	6.01
$\alpha$	0.0547
t-test with Cc=0	6.41
$\alpha$	0.0496
t-test with M	2.95
$\alpha$	0.107

#### Appendix M. Fucoxanthin Incubation Experiments

Table M1. Changes in peak areas ( $\mu V s = \mu V$ olt seconds) over time for samples from a 500 ml solution of fucoxanthin incubated in ES enriched (Harrison et al., 1980) seawater at 19°C with continuous irradiance of  $\approx 224 \ \mu mol \ m^{-2} \ s^{-1}$ . Absorbance was measured at 446 nm. No apo-10'-fucoxanthinal, apo-12'-fucoxanthinal, apo-12-fucoxanthinal, apo-13'-fucoxanthinone, or unknown #1 was present in these samples. Peaks #1, #2, and #3 are unidentified breakdown products of fucoxanthin. Peak #5 is probably a cis-trans isomer of fucoxanthin.

Time (days)	Peak #1 (μV s)	Peak #2 (μV s)	Peak #3 (μV s)	Peak #4 fucoxanthin (µV s)	Peak #5 (μV s)
0	196056	0	711743	171485739	3291935
1.958	3091413	3483758	4575414	178484762	3257799
3.708	3773224	4856831	6096454	169243738	2223169
6.75	4053281	4994634	6026110	131065021	0

**Table M2.** Peak areas of the fucoxanthin breakdown products measured as a percentage of fucoxanthin peak area.

Time (days)	Peak #1	Peak #2	Peak #3	Peak #5
0	0.11	0	0.42	1.92
1.958	1.73	1.95	2.56	1.83
3.708	2.23	2.87	3.60	1.31
6.75	3.09	3.81	4.60	0

The initial starting concentration of fucoxanthin was calculated from the weight of fucoxanthin added to solution. The initial concentration was 0.056 g L<sup>-1</sup>. The final concentration of fucoxanthin was estimated from a ratio of initial peak area of fucoxanthin to final peak area of fucoxanthin. The final concentration was 0.043 g L<sup>-1</sup>. Therefore, there was a 23% decrease in fucoxanthin over 7 days.

**Table M3.** HPLC data for five peaks observed during analysis of samples from the fucoxanthin incubation experiment.

Peak	HPLC retention time	Absorption maxima
	(min)	(nm)
1	10.9	334, 362, 380 (max), 406, 420
2	12.5	381, 400 (max), 424
3	13.3	380, 400 (max), 424
4	15.2	448 (max), 467
		[fucoxanthin]
5	17.2	417, 441 (max), 467